12-2021

Q-Griffithsin interactions and utility for the prevention and treatment of Mucosal infections.

Henry Nabeta
University of Louisville

12-2021

Q-Griffithsin interactions and utility for the prevention and treatment of Mucosal infections.

Henry Nabeta

Henry Nabeta

Q-GRIFFITHSIN INTERACTIONS AND UTILITY FOR THE PREVENTION AND TREATMENT OF MUCOSAL INFECTIONS

By

Henry Nabeta

MBChB., Makerere University, Kampala, Uganda, 2009

MSc., Makerere University, Kampala, Uganda, 2014

MS., University of Louisville, 2018

A Dissertation

Submitted to the Faculty of

The University of Louisville School of Medicine

In Partial Fulfilment of the Requirements

For the Degree of

Doctor of Philosophy

In Microbiology and Immunology

Department of Microbiology and Immunology

University of Louisville

Louisville, Kentucky, U.S.A

December 2021

Q-GRIFFITHSIN INTERACTIONS AND UTILITY FOR THE PREVENTION AND TREATMENT OF MUCOSAL INFECTIONS

By

Henry Nabeta

MBCh.B., Makerere University, Kampala, Uganda, 2009

M.S., Makerere University, Kampala, Uganda, 2014

M.S., University of Louisville, 2018

Date of Defense: September 30, 2021

A Dissertation Approved on November 9, 2021

By the following Dissertation Committee:

Kenneth E. Palmer, Ph.D.

Thomas C. Mitchell, Ph.D.

Pascale Alard, Ph.D.

Kevin Sokoloski, Ph.D.

Joh Joongho Ph.D.

Nobuyuki Matoba, Ph.D.

DEDICATION

This Dissertation is dedicated to my wife Vivian E. O. Nabeta, and kids Alvin Nabeta, Alexia Nabeta, and Austin Nabeta who have supported me and made the period of study worthwhile.

This work is also dedicated to my parents Henry and Prossy Batwaula, who have always inspired me to soar to greater heights.

Finally, this work is a constant reminder of the fortunate support, love, and encouragement from my siblings Grace Mark Tusubira, Frank Twayitibwa, Barbara Kisakye, Prossy Mirembe, and my niece Audrey Nicole Muzira.

ACKNOWLEDGEMENTS

I would like to thank my mentor, Dr. Kenneth Palmer, for his guidance, support and granting me the freedom to independently explore novel scientific ideas, more so in areas previously unchartered by the lab. For the countless consultations and problem-solving meetings, I am grateful for your calmness in dealing with any type of scenario/ situation, and always probing for my thoughts first. Thanks to my committee members: My co-mentor Dr. Mitchell for both the intriguing scientific discussions and life lessons shared; Dr. Alard, for always being available to guide me in my work, and being enthusiast about my findings; Dr. Sokoloski, for your help in designing experiments needed to better my results, and guidance in anticipating reviewer comments and planning beforehand; Dr. Joongho, for the opportunity to work in your lab during the early phase of figuring out what project I would pursue, and for the lab skills training provided; Dr. Matoba, for always asking the hard questions to stimulate deeper thinking, and providing statistical guidance to better present my data. Special appreciation goes to the late Prof. A. Bennet Jenson, for granting me the opportunity to work with his group/ lab during the start of my research, and for the professional advise shared. Finally, I would like to thank both current and former Palmer Lab members and collaborators Dr. Calvin Kouokam, Dr. Joshua Fuqua, Amanda Lasnik, Dr. Maryam Zahin, Dr. Divyasha Saxena, Dr. Lalit Batra, and Dr. Bomin Kim, who have provided a formidable support system and guided me throughout my years of study.

ABSTRACT

Q-GRIFFITHSIN INTERACTIONS AND UTILITY FOR THE PREVENTION AND TREATMENT OF MUCOSAL INFECTIONS

Henry Nabeta

September 30, 2021

Griffithsin (GRFT) is a carbohydrate binding agent (lectin) that was originally identified in the red alga *Griffithsia* sp. Q-Griffithsin (Q-GRFT) is an oxidation stable analog of GRFT. GRFT has demonstrated inhibitory activity against HIV-1, Coronaviruses, Hepatitis C, influenza and Ebola viruses. The broad-spectrum activity suggests the potential utility of this lectin in a wide range of viral infections. However, the lectin's activity in mucosal infections has not been extensively studied. Using *in vitro, ex vivo* and *in vivo* assays, we have demonstrated that Q-GRFT maintains the ability to bind glycosylated ligands following incubation in murine, macaque and human rectal fluids. Additionally, we demonstrated the first reported *in vitro* findings of antifungal activity by Q-GRFT. Furthermore, in murine prophylaxis and therapeutic infection models, Q-GRFT was efficacious against vaginal candidiasis. In response to the ongoing COVID-19 pandemic, we have demonstrated that in engineered human cornea and airway epithelia, repeated topical application resulted in Q-GRFT accumulation in mucosal tissues. In addition, in a human cadaver study, intranasal administration resulted in adequate drug dispersion on the nasal, nasopharyngeal and oropharyngeal cavities, with the drug detected in fluids collected from these anatomic sites. These findings support the development of a protocol for a Phase 1a first-in-human intranasal Q-GRFT administration to evaluate safety, tolerability, and pharmacokinetics of the drug product for pre-exposure prophylaxis against coronaviruses.

Altogether, these data demonstrated Q-GRFT's stability in the mucosal environment and support its incorporation in multipurpose STI prevention modalities

given the novel antifungal activity. Epithelial accumulation and ability to detect Q-GRFT in nasal specimens supports the feasibility of successfully performing the Phase 1a study and future drug development as a prophylaxis against coronaviruses.

TABLE OF CONTENTS

DEDICATION ii
ACKNOWLEDGEMENTS iv
ABSTRACT v
LIST OF TABLES viii
LIST OF FIGURES x
CHAPTER 1: INTRODUCTION AND BACKGROUND 1
INTRODUCTION 1
ENDOGENOUS LECTINS AND THEIR ROLES IN MUCOSAL INFECTIONS 2
EXOGENOUS LECTINS AND THEIR ROLES IN MUCOSAL INFECTIONS 21
CONCLUSION 29
CHAPTER 2: STABILITY OF Q-GRIFFITHSIN IN THE RECTAL MUCOSAL ENVIRONMENT 30
INTRODUCTION 30
MATERIALS AND METHODS 31
RESULTS 34
DISCUSSION 38
CHAPTER 3: IMPACT OF Q-GRFT ON THE GROWTH OF GUT AND RECTAL MICROBIOME, AND MYCOBIOME COMPONENTS 42
INTRODUCTION 42
MATERIALS AND METHODS 43
RESULTS 51
DISCUSSION 78
CHAPTER 4: EFFICACY AND IMMUNOLOGICAL CONSEQUENCE OF Q-GRFT IN VAGINAL CANDIDIASIS 84
INTRODUCTION 84
MATERIALS AND METHODS 86
RESULTS 89
DISCUSSION 99

CHAPTER 5: DEVELOPMENT OF Q-GRFT AS AN INTRANASAL SPRAY FOR BROAD-SPECTRUM CORONAVIRUSES PROPHYLAXIS 104
INTRODUCTION.....104
PRE-CLINICAL EXPERIMENTAL STUDY RESULTS 110
PHASE 1A CLINICAL STUDY PROTOCOL DESIGN.....117
DISCUSSION 134
CHAPTER 6: CONCLUSION AND FUTURE DIRECTIONS 137
REFERENCES 151
CURRICULUM VITAE.....188

LIST OF TABLES

Table 1.1 Endogenous lectins and their binding ligands on mucosal pathogens.....3

Table 1.2 GRFT effective concentrations to inhibit 50% virus infection (EC_{50}). 23

Table 1.3 Mucosal pathogen binding ligands for Griffithsin.....23

Table 2.1 Physicochemical properties of murine rectal fluids..... 35

Table 2.2 Physicochemical properties of human rectal fluids 36

Table 3.1 Sample and Barcode Information 50

Table 3.2 MIC_{50} results for Q-GRFT against *Chlamydia trachomatis* and *Neisseria gonorrhea*.....54

Table 3.3 Competition ELISA assay values (EC_{50} and 95% CI) for Q-GRFT binding to α-mannan, chitin and β-glucan. 60

Table 3.4 MIC_{50}s and MIC_{90}s of Q-GRFT against different *Candida* species.....67

Table 3.5 The top 20 down-regulated DEGs for 7.8 µM Q-GRFT treated *C. albicans* (1QG) vs non-treated control (VC) cells..... 71

Table 3.6 The top 20 down-regulated DEGs for 0.78 µM Q-GRFT treated *C. albicans* (2QG) vs non-treated control (VC) cells. 72

Table 3.7 The top 20 down-regulated DEGs for 7.8 µM Q-GRFT$^{lec\ neg}$ treated *C. albicans* (3QG) vs non-treated control (VC) cells. 73

Table 3.8 Comparison of differentially expressed genes following *C. albicans* growth at different conditions 76

Table 3. 9 Q-GRFT specific differentially expressed genes following *C. albicans* treatment for 4 hours at 37°C.....77

Table 5.1 *P*-values for EpiAirway tissues treatment with Q-GRFT. 111

Table 5.2 *P*-values for EpiAirway tissues treatment with Q-GRFT. 112

Table 5.3 Phase 1a study arms 119

Table 5.4 Schedule of Phase 1a study visits and evaluations 130

Table 5.5 Analysis of Safety Event Frequency for Arms of Size 12 (Q-GRFT nasal spray) 132

Table 5.6 Analysis of Safety Event Frequency for Arms of Size 6 (placebo spray). 133

Table 5.7 Analysis of safety event frequency for both arms of size 18.....134

LIST OF FIGURES

Figure 1.1 Sequence and structure of Griffithsin.....22

Figure 2.1 Stability of Q-GRFT in rectal fluids and seminal plasma.....37

Figure 3.1 Bioinformatics analysis workflow diagram 50

Figure 3.2 Q-GRFT inhibits HIV PsV QH069 replication..... 51

Figure 3.3 The effect of Q-GRFT on the growth of rectal microbiome (bacterial) components 53

Figure 3.4 Effect of on the growth of *C. albicans* 55

Figure 3.5 Q-GRFT binds to *C. albicans* 57

Figure 3.6 Q-GRFT binds to *C. albicans* cell wall 59

Figure 3.7 Effect of Q-GRFT on *C. albicans*' cell integrity and oxidative status 62

Figure 3. 8 *C. albicans* surface phenotype following treatment with Q-GRFT 64

Figure 3. 9 Impact of Q-GRFT on growth of non-*C. albicans* species 66

Figure 3. 10 *C. albicans* RNA expression profile following treatment with Q-GRFT 70

Figure 3.11 *C. albicans* RNA expression profile following treatment with Q-GRFT 73

Figure 3. 12 Top 20 enriched GO functions/ biological processes of DEGs with the adjusted P-values (FDR).....75

Figure 3. 13 Experimental plan to determine early RNA expression following *C. albicans* treatment at different conditions. 76

Figure 4. 1 Q-GRFT significantly inhibits vaginal fungal infection in a prophylaxis model of murine candidiasis. 91

Figure 4. 2 Efficacy of Q-GRFT in a murine model of vaginal candidiasis.....93

Figure 4.3 Q-GRFT treatment is associated with lower levels of vaginal inflammation in candidiasis.....97

Figure 4.4 Histological evaluation of vaginal candidiasis following treatment with Q-GRFT 99

Figure 5.1 Q-GRFT accumulation by dose in epithelial tissues following treatment 111

Figure 5.2 Q-GRFT does not affect basal expression of inflammatory cytokines in airway epithelium 113

Figure 5.3 Q-GRFT does not affect basal expression of inflammatory cytokines in cornea epithelium 114

Figure 5.4 Q-GRFT is detectable in the human nasal cavity, nasopharynx, and oropharynx 116

Figure 5.5 Q-GRFT is quantifiable in the human nasal cavity, nasopharynx, and oropharynx 117

Figure 5.6 Phase 1a study design 119

CHAPTER 1: INTRODUCTION AND BACKGROUND
THE ROLE OF LECTINS IN THE IMMUNE RESPONSE TO MUCOSAL INFECTIONS

INTRODUCTION

Lectins are proteins that recognize and interact with carbohydrate moieties (1). Endogenous lectins, encoded by the mammalian genome, include the collectin and galectin families. Collectins are collagenous C-type lectins (which require calcium for binding) and consist of a carbohydrate recognition domain (CRD) and a collagen-like domain. Examples include surfactant protein A (SP-A), surfactant protein D (SP-D) and mannose-binding lectin (MBL) (2, 3). Galectins consist of a CRD with β-sandwich fold and β-galactosidase-binding ability (4). Endogenous lectins play a major role in the innate immune system's recognition of microbial pathogens and commensal organisms. Presumably GRFT plays a similar role in its parent organism, a marine red alga of the genus *Griffithsia*. GRFT is a 25kDa domain swapped homodimer with a beta prism structure that has three binding sites recognizing oligomannose structures on either side of the homodimer, Figure 1.1 (5-9). GRFT displays an unusually potent antiviral activity against HIV-1 and some other viral pathogens *in vitro* (8, 10, 11).

There is a rising trend in *Candida* species isolated from human subjects that demonstrate resistance to antifungal agents (12). The *Candida* sp. cell wall comprises of mannose sugar moieties in α-mannan, that interact with GRFT (13). We have made a novel discovery of GRFT's ability to interact with several *Candida* species, inhibiting fungal growth (13). GRFT binds to glycan structures in coronaviruses envelope, inhibiting viral replication (10). In response to the ongoing COVID-19 pandemic, our laboratory is developing GRFT as a potential intranasal spray application to prevent coronaviruses transmission and infection.

This chapter reviews the role of both endogenous and exogenous lectins in mucosal infections. A summary of endogenous lectins and their major target molecules sugar binding specificity on mucosal pathogens is presented in Table 1.1. Binding targets of GRFT is summarized in Table 1.3.

ENDOGENOUS LECTINS AND THEIR ROLES IN MUCOSAL INFECTIONS

COLLECTINS: SP-A and SP-D

SP-A and SP-D are lung C-type lectins secreted into the alveolar fluid by type II alveolar epithelial cells (AEC), and into the airway lumen by submucosal- and Club cells (2). These lectins also immunoprotective in the trachea and nasal mucosa (14, 15), through their role as anti-infectious and immunomodulatory agents (16). By keeping the lungs free of infections and inflammation, SP-A and SP-D ensure effective gaseous exchange (16).

Numerous mechanisms have been proposed for the enhancement of pathogen clearance by lung collectins. These include: (i) Lung collectins binding simultaneously to bacteria and neutrophil extracellular traps (NET)-DNA, enhancing bacterial trapping by the NETs (17); (ii) Collectins' binding to and aggregating pathogens prevents cell entry, resulting in their removal through either mucocilliary clearance or phagocytosis by alveolar macrophages and neutrophils (2, 14, 18-20); (iii) Collectins upregulate the expression of microbial recognition receptors-mannose receptors and scavenger receptor SR-AI/II on the cell surface (21, 22); (iv) Collectins enhance the phagocytosis of complement-coated particles and Ig-G-opsonized microbes (18, 23, 24).

SP-A and SP-D are involved in critical processes in the lung immune response to pathogens, and recognize numerous respiratory microbes including viruses like respiratory syncytial virus, adenovirus, influenza A virus and coronaviruses; fungi like *Aspergillus fumigatus, Cryptococcus neoformans, Pneumocystis jiroveci*; bacteria like *Mycobacterium tuberculosis*, *Hemophilus influenzae* and *Pseudomonas aeruginosa*; helminths like *Nippostrongylus brasiliensis* and *Schistosoma* (14, 18, 20, 25-27).

Table 1. 1 Endogenous lectins and their binding ligands on mucosal pathogens.

Endogenous lectin	Pathogen	Binding ligand	Reference
Collectins			
SP-A, SP-D	*Pneumocystis* sp.	Major surface glycoprotein (MSG)	(28-30)
		Glycoprotein A (GpA)	(14, 30, 31)
	Nippostrongylus brasiliensis	Nonspecific	(25)
	Influenza A virus	Neuraminidase, HA_1 component of hemaglutinin	(32)
SP-A	*Aspergillus fumigatus*	Glycoproteins gp45, gp55	(33)
	Pseudomonas aeruginosa	Outer membrane protein OprH	(34)
	Hemophilus influenza type A	Major outer protein	(35)
	HIV-1	gp120	(36)
SP-D	SARS-CoV	Spike (S) protein	(37)
	Cryptococcus neoformans	Mannoprotein 1, glucuronoxylomannan	(38)
	Mycobacterium tuberculosis	Lipoarabinomannan (LAM)	(39)
	Schistosoma mansoni	Fucα1-3GalNAc, Fucα1-3GlcNAc	(27)
Galectins			
Gal-1, Gal-3	*Citrobacter rodentium*	Non-specific	(40)
	Trichomonas vaginalis	Lipophosphoglycan (LPG)	(41, 42)
Gal-1, Gal-9	*Helicobacter pylori*	Non-specific	(43)
Gal-1	*Chlamydia trachomatis*	Poly β-D-galactopyranosyl-(1-4)N-acetyl-D-glucosamine, β-1-6-N-acetylglucosamine	(44, 45)
	HIV-1	gp120, X4, X4R5, R5	(46)
Gal-3	*Cryptococcus neoformans*	-	(47)
	Paracoccidiodes brasiliensis	-	(48)
Gal-9	*Francisella novicida*	-	(49)
Mannose-binding lectin			
MBL	SARS-CoV	Spike (S) protein	(50)

Respiratory antiviral roles of SP-A and SP-D

Both SP-A and SP-D bind to human coronavirus 229E (HCoV-229E) virions in a dose-dependent manner (26). SP-D binds to the severe acute respiratory syndrome

(SARS-CoV) glycosylated spike (S) protein in a calcium-dependent fashion (37). Both SP-A and SP-D inhibited infection of human bronchial epithelial cells in a concentration-dependent manner, with SP-D demonstrating the greatest reduction in infection at similar concentrations of lectin used. However, the inhibitory impact of SP-A and SP-D on coronaviruses infection is likely dependent on the virus and pulmonary cell type being infected. This is because pre-treatment with SP-A, but not SP-D, significantly reduced infection of alveolar macrophages with HCoV-29E (26). Systemic SP-D levels have previously been shown to corelate with infectious lung injury (51, 52), and may be utilized as a biosignature of alveolar integrity in coronaviruses infection (53). In a study that enrolled participants with pulmonary infections, 16 patients who had been hospitalized with SARS-CoV type pneumonia exhibited significantly elevated serum SP-D levels (53). In addition, they demonstrated a significant correlation between serum SP-D and anti-SARS-CoV N protein IgG (53). Kerget et al., have proposed that SP-D may be a surrogate marker for predicting the course and planning treatment in COVID-19 (54). In their study, they identify that SARS-CoV-2 infection was associated with higher serum SP-D levels at admission, and among patients who developed macrophage activation syndrome and acute respiratory distress than those who did not. Similarly, Atsushi Saito et al. (55), have observed that serum SP-A and SP-D positively corelate with COVID-19 severity in SARS-CoV-2 pneumonia.

By binding to SARS-CoV-2, SP-A and SP-D may modulate the inflammatory response and/ or probably hinder human cell entry (16, 56). To support this hypothesis, studies with recombinant human SP-D (rfhSP-D) have demonstrated initial success in inhibiting cell entry and infection. In *in vitro* assays, rfhSP-D bound to S1 spike protein of SARS-CoV-2 in a dose-responsive manner, and protected HEK293T cells against infection with pseudotyped viral particles (57). Using human clinical samples, rfhSP-D inhibited the binding between the S1 subunit receptor binding domain of SARS-CoV-2 spike protein and human angiotensin converting enzyme-2 (hACE-2) receptor, attenuating viral infection and replication (58). These findings suggest the need for further exploration of the role of lung collectins as potential and/or surrogate diagnostic and therapeutic biosignatures for the severity and prognosis of COVID-19 in symptomatic patients.

SP-D uses its CRD to bind to mannosylated, *N*-linked carbohydrates on neuraminidase and the HA_1 component of hemagglutinin (HA) of Influenza A virus (IAV), mediating viral hemagglutination and infectivity (32). SP-A neutralizes IAV by interacting with the virus via its sialic acid residues in the CRD (59). Animal studies using mice deficient in SP-A and SP-D have demonstrated that when challenged intranasally with IAV, collectin-deficient mice developed more severe disease when compared to wild-type controls. In addition, SP-A and SP-D deficient mice displayed attenuated viral clearance, with increased production of proinflammatory cytokines in comparison to the controls (60, 61). Exogenous administration of the collectins in lungs of SP-A- and SP-D- deficient mice resulted in decreased epithelial injury, a lower viral load and attenuated production of proinflammatory cytokines like tumor necrosis factor (TNF), interleukin-6 (IL-6) and interferon gamma (IFN-ɤ) following challenge with IAV (62). However, because of differences in *N*-glycosylation patterns of viral HA, some pandemic pH1N1 strains are resistant to SP-A neutralization (63).

Unlike a complete SP-A molecule that provides protection against IAV, a recombinant/ truncated human surfactant protein A, rfhSP-A molecule was found to enhance pH1N1 and H3N2 infection of A549 lung epithelial cells (63). This was associated with increased transcription of proinflammatory cytokines TNF-α, IL-12, IL-6, IFN-α and Regulated upon Activation, Normal T Cell Expressed and Presumably Secreted (RANTES) (63). This response contrasts that observed with rfhSP-D, which upon binding HA reduced expression of proinflammatory cytokines (64). A therapeutic role of rfhSP-D has also been demonstrated by the ability to attenuate transduction of Madine Darby canine kidney (MDCK) cells by H1 + N1 pseudotyped lentivirus particles, hindering viral entry (64). Altogether, these results delineate that while still complex, further studies still need to be undertaken to better understand the full potential of SP-A, SP-D, and rfhSP-D for utility as therapeutics against IAV infection.

SP-A and SP-D interaction with respiratory fungal pathogens

Through its carbohydrate recognition domain, SP-D blocks immunoglobulin E (IgE)'s specific binding to *A. fumigatus*, enhancing fungal phagocytosis by human neutrophils and alveolar macrophages (33, 65). Interestingly, Madan et. al, (66) have also

demonstrated that SP-D protects against *A. fumigatus*-induced pulmonary hypersensitivity in mice. Similarly, Haczku et al. (51) found that SP-D levels in lung lavage fluids of BALB/c mice were elevated nine-fold during an allergic response to *A. fumigatus*-induced airway inflammation. Additionally, the elevated SP-D levels positively correlated with total serum IgE concentrations (51). Mice deficient in SP-D gene are generally more susceptible to invasive pulmonary aspergillosis (IPA) and display more severe disease symptoms compared to SP-A gene deficient rodents that are resistant to disease (67).

A. fumigatus secretes *N*-glycosylated fungal ligands gp45 and gp55, as glycoprotein antigens, which are recognized by SP-A. The secretory property and the ligands' recovery in culture filtrates has enabled their utility in aspergillosis immunodiagnostics (33). In developing anti-Aspergillosis respiratory therapeutic agents, Madan et al. have found that a recombinant protein containing an SP-D homotrimeric neck region and CRD domains (rSP-D), and purified human proteins when administered intranasally protect immunosuppressed mice from severe outcomes of lethal challenge with *A. fumigatus* conidia (68). Similarly, intranasal treatment with recombinant full-length (hSP-D) or truncated human SP-D (rhSP-D) improved survival in immunocompromised mice with IPA, reduced lung fungal growth and increased expression of TNF-alpha (TNF-α) and IFN-gamma (IFN-ɤ) in respiratory fluids. In addition, macrophage inflammatory protein-1 alpha (MIP-1α) was elevated in these fluids (69). These findings delineate the potential therapeutic benefits of recombinant forms of SP-D in protection against infection with *A. fumigatus* conidia (69).

SP-A binds to encapsulated and non-capsulated *Cryptococcus neoformans* yeast forms in a concentration dependent manner. In contrast to encapsulated strain binding, recognition of non-encapsulated variants did not enhance phagocytosis by monocyte-derived macrophages and human-alveolar macrophages (70). In a study by Giles et al., SP-A binding to *C. neoformans* is IgG dependent and subsequently inhibits alveolar macrophage IgG-mediated fungal phagocytosis (71). Using an inhalation challenge mouse model, they found that SP-A binding had no impact on host defense immune mechanisms against pulmonary *C. neoformans* infection. On the other hand, SP-D binds

to cryptococcal capsular components mannoprotein 1 and glucuronoxylomannan (38). Despite interactions with both encapsulated and non-encapsulated cryptococci, only non-encapsulated binding resulted in aggregation by SP-D (38). Geunes-Boyer et al. have demonstrated that SP-D facilitates *C. neoformans* infection *in vivo* (72). They found that SP-D -deficient mice are partially protected from infection, displaying a lower fungal burden compared to wild-type controls. Furthermore, in both *in vitro* and *in vivo* studies, SP-D binding protected yeast cells against macrophage-mediated destruction mechanisms and hydrogen peroxide-induced oxidative stress (72).

SP-A and SP-D bind the major surface glycoprotein (MSG), a predominant membrane protein rich in mannose residues, and used by *Pneumocystis* sp. to attach to alveolar epithelium (28). SP-D also binds to β-glucans found on cystic forms of *Pneumocystis* (29, 30). Interestingly, SP-A and SP-D demonstrate divergent outcomes upon interacting with *P. jiroveci*. Upon binding to the mannose-rich glycoprotein (GPA) in the cell wall, SP-D blocks *Pneumocystis*' interaction with macrophage mannose receptors, inhibiting phagocytosis (14, 30, 31). In contrast, SP-A binds to GPA and enhances *Pneumocystis*'s interaction with alveolar macrophages. In demonstrating this phenomenon, Atochina et al. found that mice lacking SP-A were more susceptible to *P. carinii* infection, and produced lower quantities of reactive oxygen-nitrogen species and proinflammatory cytokines compared to wild-type controls(73). It has been proposed that differences in the tertiary structure of these collectins may contribute to the contrasting outcomes despite binding to the same receptor (74).

Interaction of SP-A and SP-D with respiratory bacterial pathogens

Purified SP-D derived from healthy- human donor bronchoalveolar lavage fluids was demonstrated to bind *Mycobacterium tuberculosis*, resulting in bacterial agglutination (39). This binding was predominantly specific to lipoarabinomannan (LAM) and led to bacterial adherence to macrophages. Bacterial adherence to monocyte-derived macrophages was also significantly increased upon binding to SP-A. Similarly, Kazumi et al. have demonstrated that SP-D and SP-A bind to *Mycobacterium avium* in a concentration- dependent manner (75). Both collectins enhanced *M. avium* phagocytosis by rat alveolar- and human monocyte-derived macrophages. Upon binding, SP-A and SP-

D upregulated the expression of mannose receptors on monocyte-derived macrophages, enhancing phagocytosis. The alanine-and proline-rich antigenic (Apa) glycoprotein has also been identified as a binding target for SP-A on the *M. tuberculosis* cell wall. The binding is calcium-and mannose-dependent (76). However, the impact of binding to this receptor and its role on bacteria phagocytosis has not yet been explored or demonstrated.

A recombinant protein comprising of the neck-region and CRD of bovine SP-D was expressed in *E. coli* by Lim et al. (77). This protein displayed similar carbohydrate-binding specificity as the native protein and bound to lipopolysaccharides of *Pseudomonas aeruginosa* and *Klebsiella pneumoniae* (77). Using *Pseudomonsa aeruginosa* isolates from patients with cystic fibrosis, Qadi et al. identified outer membrane protein OprH as a ligand for SP-A (34). They demonstrated that phagocytic killing by macrophages was increased upon SP-A binding to OprH.

SP-A has also been shown to bind to the major outer membrane protein of *Hemophilus influenzae* type A in a calcium-dependent fashion. The resultant opsonization enhanced killing by alveolar macrophages in bactericidal assays (35). Distinct immune roles have been proposed for SP-A and SP-D during pulmonary infection with *Hemophilus influenza* (78). When challenged with *H. influenza* intratracheally, SP-D-deficient ($SP\text{-}D^{-/-}$) mice cleared infection, while SP-A -deficient ($SP\text{-}A^{-/-}$) animals demonstrated decreased bacterial killing. Mice deficient in either collectin demonstrated decreased bacteria uptake by macrophages and increased pulmonary inflammatory cell recruitment with inflammation-associated cytokines. However, a significantly greater production of oxidants, superoxide and hydrogen peroxide was associated with $SP\text{-}D^{-/-}$ -derived macrophages, while a lower production was associated with $SP\text{-}A^{-/-}$ -isolated macrophages, when compared to wild-type mice alveolar macrophages. It is likely that increased superoxides and peroxides contribute to *H. influenza* killing in $SP\text{-}D^{-/-}$ mice.

Anti-helminthic role of SP-A and SP-D in pulmonary infections

Using mice lacking SP-A, Minuutti et al. have shown that IL-4-dependent macrophage proliferation and activation in response to lung migratory helminth *Nippostrongylus brasiliensis* infection is enhanced by the collectin (79). SP-A was

associated with accelerated lung parasite clearance and lower pulmonary injury following *N. brasiliensis* infection. Type 2 immunity is enhanced by pulmonary epithelial responses, controlling nematode infections (25). Thawer et al. (25) have also demonstrated that SP-D concentrations are elevated in respiratory fluids following *N. brasiliensis* pulmonary infection. The host innate immune response to helminths was impaired in SP-$D^{-/-}$ mice, resulting in persistence of infection. Administering pulmonary SP-D prior to infection resulted in improved parasite clearance and enhanced expression of cells and cytokines modulating the type 2 immune responses, like IL-13 -producing type 2 innate lymphoid cells, increased markers of alternative activation of alveolar macrophages, and elevated IL-4 and IL-13. Additionally, when naïve mice received adoptively transferred alveolar macrophages from SP-D-treated helminth infected mice, there was evidence of enhanced immunity to *N. brasiliensis*. The enhanced parasitic killing was modulated by SP-D binding to the helminth via the CRD.

Fucosylated glycoconjugates Fucα1-3GalNAc and Fucα1-3GlcNAc are expressed on the surface of *Schistosoma mansoni*, a blood fluke that transiently resides in the lung during its life cycle and development (27). SP-D has been found to bind to *S. mansoni* cercariae and schistosomula via the CRD, in a calcium-dependent manner, during the pulmonary stage (27). However, the impact of this binding to worm elimination is yet to be extensively studied.

Interaction of SP-A and SP-D with genitourinary mucosal virus pathogens

Herpes simplex virus (HSV), human papillomavirus (HPV) and human immunodeficiency virus (HIV) are viral pathogens that may enter the human body via the genitourinary mucosa. SP-A and SP-D are expressed in genitourinary tissues including the vaginal epithelium, uterus, testis, prostate gland and kidneys (16, 80-82). These collectins may bind and neutralize viral pathogens, preventing entry and replication in the genitourinary mucosa.

Ujma et al., following findings that SP-A binds HPV16-PsV and impairs murine infection, have proposed the collectin's potential utility as a topical microbicide (83). They showed that phagocytosis of HPV16-PsV by RAW264.7 murine macrophages was enhanced by the HPV16-PsV/SP-A complex formed when SP-A bound pseudovirus

(PsV) particles. Interestingly, recombinant SP-D bound HPV16-PsV, albeit weakly and did not impact macrophage uptake. In a cervicovaginal challenge model, pre-incubation of HPV16-PsV with purified human SP-A significantly attenuated murine pseudoviral infection.

In binding assays, Iwaarden et. al demonstrated that SP-A recognized and interacted with HSV-1 via the carbohydrate moiety in a concentration- dependent manner (84). Additionally, in an *in vitro* study, SP-A, acting as an opsonin, enhanced phagocytosis (85), demonstrating the lectin's potential immune role in anti-HSV activity.

SP-A binds to the HIV envelope glycoprotein (gp120) in a calcium-dependent manner (36). However, a dual modulatory role of both infection attenuation and enhancement has been demonstrated upon SP-A interaction with different immune cells. By binding gp120, SP-A inhibited infection of CD4+ T cells by HIV strains Bal and IIIB. On the contrary, SP-A promoted gp120-dendritic cells (DCs) interaction, increased the uptake of viral particles and significantly enhanced virus transfer from DCs to CD4+ T cells (36). Similarly, SP-D inhibited HIV infectivity in *in vitro assays*, and enhanced viral binding and capture by immature monocyte derived dendritic cells (iMDDCs). Furthermore, lectin binding enhanced the transfer of HIV from iMDDCs to T-cell like line PM1 (86). Alistar et al. posit that following HIV binding at the CRD, SP-A and SP-D interact with other host receptors via the lectin's *N*-terminus (16). They further delineate that an engineered recombinant SP-A or SP-D molecule that is able to bind HIV, but devoid of the *N*-terminus would be effective in virus neutralization, while avoiding interaction with other immune cells (16), and impede transfer to lymphoid tissues (87). Indeed, Dodagatta et al. have reported a direct protein-protein interaction between rfhSP-D and Dendritic Cell-Specific Intercellular adhesion molecule-3-Grabbing Non-integrin (DC-SIGN) via C-type lectin domains (87). They demonstrated that SP-D and DC-SIGN compete for binding to HIV-1 gp120, and the recombinant lectin significantly attenuated HIV-1 transfer to activated peripheral blood monocytes. Given the paucity of data available, more studies are needed to investigate interactions between collectins- SP-A and SP-D, recombinant molecules- rfhSP-A and rfhSP-D, and HIV, and to establish their impact on infectivity and virus transfer to other immune cells (16).

GALECTINS

Galectins are animal lectins that share consensus amino acid sequences in the CRD and possess a high affinity for β-galactosides (88). The galectin family is classified based on the organization of CRD domains, namely:- (1) Prototype (galectins-1, -2, -5, -7, -10, -11, -13 and -14), consisting of monomers and homodimers of one CRD; (2) Tandem Repeat group (galectins -4, -6, -8, -9 and -12), a two-CRD type that consists of two distinct, yet homologous CRDs in a single polypeptide chain formation; (3) Chimeric type (galectin-3), consisting of a non-lectin proline component and glycine-rich short tandem repeats connected to a CRD (88, 89). Galectins are synthesized on cytosolic ribosomes and may be packaged and delivered to intracellular vesicles and compartments or secreted/ and translocated to the extracellular space (90, 91). Expression of these lectins varies from one cell type to another and may depend on the individual cell's activation status (91).

Antimicrobial properties of galectins in respiratory mucosal infections

Using both *in vitro* assays and murine influenza virus infection models, Yang et al. have demonstrated an innate immunity role for Gal-1 in respiratory viral pathogenesis (92). Gal-1 bound to IAV in a dose-dependent manner, and inhibited virus-induced hemagglutination activity *in vitro*. Additionally, Gal-1 protected MDCK cells from infection with various subtypes of IAV. Intranasal challenge with IAV resulted in enhanced Gal-1 expression in infected rodents. Furthermore, following infection, when mice treated intranasally with Gal-3 were compared with vehicle-treated controls, they had lower weight loss, a decreased viral burden, lower pulmonary inflammation, and better survival, despite challenge with a lethal dose of IAV. Similarly, Gal-1 -deficient mice had lower rates of survival after challenge with IAV compared to wild-type controls.

Following pulmonary *Francisella novicida* infection, a novel alarmin role for Gal-9 has been proposed, as the galectin enhances inflammation and modulates the immune response in the resultant sepsis (49). Pulmonary Gal-9 expression peaked at the onset of sepsis, was secreted extracellularly, and was associated with infiltration of lungs with neutrophils and inflammatory cytokines (TNF-α, IL-6) in response to infection. Gal-

9 response and disease modulation during *F. novicida* murine infection exhibited properties consistent with alarmin molecules. Upon infection, Gal-9 expression and extracellular secretion were enhanced, the galectin stimulated an increased inflammatory response to pathogens, while disease severity was attenuated in Gal-9 – deficient mice (49).

Fungal pathogens *Cryptococcus neoformans* and *Paracoccidioides brasiliensis* gain entry into the body via inhalation of infectious spores and conidia, respectively (93, 94). These fungal infections may manifest as pneumonia in susceptible immunocompromised individuals (47, 95). In *in vitro* experiments, Gal-3 binds to ligands in encapsulated *C. neoformans* strains and disrupts fungal viability of extracellular vesicles through lysis (47). In both human and murine disease, pulmonary Gal-3 levels are elevated following infection. Compared to wild-type controls, upon challenge with *C. neoformans*, mice deficient in Gal-3 were more susceptible to infection, displayed a higher fungal burden and succumbed to death earlier (47). Similarly, Gal-3 expression is enhanced in human and murine *P. brasiliensis* infection (48). The galectin impeded fungal growth through inhibition of budding and promoted denaturation and lysis of *P. brasiliensis* extracellular vesicles. In addition, Gal-3 enhanced macrophage internalization of extracellular vesicles (48).

Role of galectins in gastrointestinal mucosal infections

Galectin-1 (Gal-1) and galectin-3 (Gal-3) are significantly expressed in colonic mucosal epithelial cells (96, 97). While Gal-3 mediates pro-inflammatory activity like immune cell mobilization and maintenance, Gal -1 is anti-inflammatory, modulates regulatory T cell recruitment and attenuates the inflammatory response (97-99). These contrasting roles may be harnessed by the host to promote an inflammatory response to pathogens while maintaining an immune homeostatic state (40). Using a colonic mouse model of infection with the non-invasive *Citrobacter rodentium*, Curciarello et al. determined that Gal-1 and Gal-3 contributed only minimally to immunity against the gut pathogen (40). Upon challenge with *C. rodentium*, mice deficient in Gal-1 exhibited reduced macrophage and T cell responses. Bacterial challenge in Gal-3 deficient animals

was associated with delayed infection establishment, a prolonged duration of disease and delayed colonic migration of T cells, macrophages, and dendritic cells.

In a human study of patients with chronic gastritis and positive for *Helicobacter pylori*, Gal-3 and Gal-9 were significantly expressed in gastric epithelial mucosal cells, while Gal-1 was found in elevated amounts in the stroma (43). *H. pylori* infection was significantly associated with pro-inflammatory Gal-3 expression. Furthermore, expression of Gal-9, a galectin with immunomodulatory and regulatory functions was attenuated in epithelia of patients with chronic and chronic active gastritis. These data demonstrate that further studies are needed to explore and understand the mechanisms of galectins in modulation of gut mucosal infections.

Humoral mucosal immunity, largely driven by IgA is critical in the prevention of colonization and establishment of pathogenic gut mucosal infections (100). Gal-9 may modulate and contribute to the development of a mucosal adaptive immune response by IgA through communication with T helper 17 (Th17) cells (101). Liang et al. have demonstrated that following mucosal immunization, deficiency of Gal-9 in murine models is associated with an impaired gut mucosal antigen-specific IgA response (101). Immunized Gal-9 deficient mice exhibited an attenuated immune response to high dose cholera toxin (CT) and had lower rates of survival in comparison with wild-type controls. The paucity of lamina propria Th17 cells, attenuated *IL17* gene expression, and lower IgA in immunized Gal-9- deficient mice in comparison with wild-type controls, underscores the role of this galectin in the Th-17-IgA axis (101).

Interaction of galectins with genitourinary mucosal pathogens

Gal-1 and Gal-3, expressed by human cervical and vaginal epithelial cells, bind the protozoan parasite *Trichomonas vaginalis* via lipophosphoglycan (LPG), a glycoconjugate rich in galactose (41, 42). Interestingly, modulation of immunity by these galectins results in contrasting inflammatory responses, a feature that is exploited by the protozoan parasite for its survival (42). Gal-1 attenuates the proinflammatory response, resulting in reduced expression of phagocyte chemoattractant, IL-8, required to recruit immune cells that eliminate the parasite. In addition, Gal-1 suppresses the expression of Chemokine (C-C motif) ligand 20 (CCL20) and RANTES, chemokines that bridge the

innate immune response to adaptive immunity (42). Conversely, Gal-3 enhances the expression of chemokine IL-8 in the cervical-vagina environment. Moreover, in *in vivo* studies, *T. vaginalis* was observed to deplete Gal-3 from the extracellular milieu (42). Hence, the parasite manipulates and skews the immune response towards a Gal-1 predominant state, promoting its survival in cervico-vaginal tissues.

Endogenous, intracellularly expressed Gal-1 facilitates *Chlamydia trachomatis*-cervicovaginal host cell interactions, while promoting pathogen adhesion and immune evasion (44). Gal-1 interacts with *C. trachomatis* via numerous glycosylated ligands expressed on the bacteria surface including poly β-D-galactopyranosyl-(1-4)-*N*-acetyl-*D*-glucosamine [poly-LacNAc]-enriched glycan epitopes and β1-6-*N*-acetylglucosamine (β1-6GlcNAc)-branched complex *N*-glycans (44, 45). Furthermore, unlike the uniform diffuse pattern, upon cellular infection, Gal-1 redistributes to localize around chlamydial inclusion bodies. In HeLa cells, Gal-1 enhanced infection and formation of inclusion bodies. Similarly, exogenous addition of the lectin during vaginal challenge of wild type mice enhanced genital infection and promoted the formation of infectious bodies (44). These results demonstrate Gal-1's role in facilitating *C. trachomatis* infectivity.

The majority of HIV infections worldwide are sexually transmitted and occur across mucosal epithelial barriers (102). Gal-1 is significantly expressed by immune tissues and cells including lymphoid epithelial cells, activated B and T cells, macrophages, follicular dendritic cells and CD4+CD25+ T regulatory cells (103-105). In addition, T-helper subtype 1 (Th1) cells secrete substantial amounts of Gal-1 (55). CD4+ T cells, known to be highly susceptible to HIV-1 are localized in the lamina muscularis mucosae, a region where Gal-1 is highly expressed (106, 107). In fact, Gal-1, by crosslinking immune cell receptors (X4, X4R5 and R5) and glycoprotein 120 (Gp120) enhances the initial virus binding and adsorption kinetics (46), directly promoting HIV-1 infectivity of CD4+ T cells and macrophages (46, 106). Additionally, upon HIV-1 binding the T cell receptor, intracellular galectin-3 translocates to the virological synapse, co-localizing with G antigen (Gag), envelope (Env) and ALG-2-interacting protein X (Alix) proteins (108, 109). This interaction promotes HIV-1 transfer and augments virus transmission efficacy (108). Alix protein is critical in HIV-1 replication and working in

concert with the endosomal sorting complex required for transport (ESCRFT), stimulates virion propagation (109, 110). Moreover, Gal-3 enhances Alix-Gag association, an interaction that amplifies HIV-1 budding, promoting infectivity (109). Definitive studies will be imperative in establishing the potential efficacy and utility of galectin-blockade as a modality in the prevention of HIV-1 infection and transmission in murine and human subjects.

Role of galectins in ocular mucosal infections and immunity

The therapeutic potential and the ability of galectins to modulate the immune response, tolerance, and inflammation in immune privileged sites, including the eye (111-115), has been explored. Gal-1 may regulate the immune response via its immunosuppressive impact on T cells including T-cell adhesion to extracellular milieu, T-cell activation and Th1 cytokine release (114, 116-118). Gal-1's probable role in establishing immune privilege in the eye has been demonstrated by the lectin's secretion from retinal pigment epithelium, with the resultant suppression of T-cell activation (113, 114). Indeed, anti-retinal-Gal-1 antibodies (IgE, IgG and IgA) are significantly elevated in the sera of patients with infectious uveitis, including toxoplasmic retinochoroiditis, bacterial and retinochoroiditis (119). Moreover, the levels of these antibodies positively correlated with progression and poor outcome of disease. Galectin-1 is likely secreted into ocular tissues and aqueous humor in particular to perform an immunosuppressive role in response to ocular inflammation (120).

A glycocalyx coat, rich in transmembrane mucins containing *O*-linked carbohydrates, provides a protective barrier in the cornea and conjunctiva against pathogen adhesion and ocular infection (121, 122). Gal-3 binds to and cross-links mucins, including mucin1 (MUC1) and mucin16 (MUC16), in a carbohydrate-dependent manner (123, 124). Repression of galectin-3 biosynthesis in human ocular cornea epithelium impedes the tight intercellular junctions with a resultant loss of the protective barrier function (115). Interestingly, HSV-1 binds to and employs Gal-3 as an entry receptor into ocular tissues. By masking and impeding viral attachment to Gal-3 in the apical glycocalyx, corneal keratinocyte infection by herpesvirus is abrogated (125).

Undoubtedly, there is a promising therapeutic potential for galectins and /or galectin-inhibitory molecules in the treatment of ocular infections. However, this area is still not fully explored and will require more studies to be designed. Interestingly, initial studies have demonstrated the utility of Gal-1 in ocular herpetic lesions. Rajasagi et al. (126) have shown that following HSV-1 infection, recombinant Gal-1 diminished the severity of stromal keratitis, a chronic inflammatory lesion, and attenuated corneal neovascularization, pathologies that often result in blindness. Recombinant Gal-1 was associated with decreased corneal infiltration of proinflammatory cells and cytokines, and an increased production of immunosuppressive IL-10 and neovascularization-inhibitory molecules.

MANNOSE-BINDING LECTIN

Mannose-binding lectin (MBL) is a collectin produced mainly by hepatocytes and secreted into the systemic circulation (3). MBL activates the lectin complement pathway, enhances phagocytosis of microorganisms and modulates inflammation (127).

Role of MBL in fungal gastrointestinal mucosal infections

Complement activation occurs upon recognition of microorganisms through CRDs, that sense pathogen associated molecular patterns (PAMPs), that include pathogen associated glycan structures such as D-mannose, L-fucose and *N*-acetylglucosamine (128). These domains are expressed on the surface of microorganisms including *Candida albicans* (127, 129, 130). *C. albicans* is an opportunistic infection in the gastrointestinal tract and often results in invasive infection when epithelial and host immune functions are compromised or breached. MBL promotes *C. albicans*' opsonophagocytosis by neutrophils (131). Through the MBL-MBL-associated serine proteases (MASP) complex, MBL binds to C3b activating the complement system and opsonizing *C. albicans* (132). Following recognition by CR1 on the leukocyte surface, MBL may directly opsonize *C. albicans* (133). MBL expression is induced in response to *C. albicans* sensing in the gut and contributes to intestinal homeostasis and host defense (127). MBL has been identified as critical in the host's first line of defense against

invasive candidiasis, with a significant decrease in the lectin levels 2 days before positive blood cultures (131). In wild type mice, blocking MBL by feeding rodents with mannan resulted in increased *C. albicans* colonization. Furthermore, in MBL-deficient mice, dextran sodium sulfate-induced colitis promoted dissemination of *C. albicans* to kidneys and lungs, while deficient mice also predominantly expressed cytokines including IL-17 (127), a cytokine thought to be of little consequence in eliminating invasive candidiasis (134).

Impact of MBL on immunity and response to bacterial respiratory mucosal infections

There is vast literature about MBL binding to microorganisms and MBL-mediated complement activation following binding to mannan- coated polystyrene surfaces (132). The exact role of MBL in promoting phagocytosis has only recently been explored (132). Studies estimate that *MBL2* polymorphisms occur in about 5% of the population worldwide (135), with the associated MBL deficiency contributing to increased susceptibility to infections (136). Interestingly, polymorphism of MBL homozygous variant genotypes rs1800451 was associated with reduced pulmonary tuberculosis (PTB) risk, while that of allele rs5030737 demonstrated increased risk of PTB. Alleles rs1800450, rs7096206 and rs11003125 did not demonstrate any association with PTB susceptibility (137). Numerous publications describe a role for MBL in C3 deposition in *S. aureus* but scant data is available for the uptake of opsonized *S. aureus* by human neutrophils. Neth and colleagues reported that opsonophagocytosis of *S. aureus* was increased when exogenous MBL-MASP was added to MBL-deficient serum (138). Additionally, infection with *S. aureus* CP5 in an MBL knockout mouse model resulted in decreased C4b deposition and greater mortality (139). In contrast, Krarup et al. showed that MBL did not bind to encapsulated *S. aureus* (140). Brouwer et al. report a dose dependent MBL binding to *S. aureus and S. pnuemoniae* (132). However, they observed that this binding had no influence on the uptake of these bacterial species by human neutrophils. It is likely that the lectin pathway of complement activation has only a limited contribution in opsonophagocytosis of these bacteria. Clinical studies reported by Moen et al., and Roy et al., demonstrated a small but significant risk of increased invasive pneumococcal disease in patients homozygous for the MBL structural codon

variant allelles -52, -54, -57, and -221(141, 142). In contrast, Kronborg et al., and Brouwer et al., did not demonstrate any role of MBL in the pathogenesis of S. pneumoniae infection in clinical and *in vitro* studies, respectively (132, 143). Similarly, Kazumi Kudo et. al demonstrated that MBL binds to *M. avium* in a calcium-independent and concentration- dependent manner. However, the binding did not enhance bacteria phagocytosis by rat alveolar- and human monocyte-derived macrophages (75). Overall, these findings suggest that MBL substitution therapy may have a protective value for fungal rather than bacterial infections (132).

Interactions and role of MBL in respiratory coronaviruses infection

There is increasing evidence that suggests that MBL may be protective in the initial stages of SARS-CoV-2 infection (144). Serum mannose-binding protein (MBP) levels are highest in childhood and gradually decrease as individuals age. At birth, MBP levels are about 1 µg/mL, attaining a lifetime peak of approximately 2.5 µg/mL within 5 days post birth (145), and are significantly lower in centenarians, octo-and nonagenarians when compared to the general population (146). A bimodal peak pattern of serum MBP levels has also been described, with the initial peak in childhood and the latter peak gradually declining with advancing age (147). In addition, in analyzing MBL2 gene variants, the frequency of high and null activity haplotypes was significantly lower in the elderly compared to the general population. Furthermore, individuals between 80 and 99 years displayed a higher frequency of intermediate activity haplotypes than the general population in the same geographic area (146). In children, sustained low levels of serum MBL and reduced levels at birth are associated with recurrent respiratory infections and otitis media (148).

Polymorphisms in the MBL2 structural gene result in low serum levels, predisposing to coronaviruses infections (144). A genetic polymorphism in codon 54 of MBL exon 1 (A/B variant) results in a low-MBL-producing B allele and an increased risk of severe acute respiratory syndrome coronavirus (SARS-CoV) infection (149). Hongxing et al. observed that MBL gene polymorphisms significantly increase the susceptibility to SARS-CoV infection (150). They show that among infected and control subjects, SARS-CoV infected subjects significantly displayed haplotype pairs that were

associated with medium or low expression of MBL, including the codon 54 variant. In another case-control study, Ip et al., demonstrate MBL's role as a first-line host defense against coronaviruses and that the lectin's deficiency is a susceptibility factor for SARS-CoV infection (50). They report that a higher frequency of haplotypes is associated with low or deficient serum MBL levels in SARS-CoV infection than in control subjects. Serum MBL levels were significantly lower in infected patients compared to the controls. In complementary *in vitro* experiments, they show that deposition of complement C4 on SARS-CoV is enhanced by MBL, and the lectin inhibits infection of fetal rhesus kidney cells (FRhK-4). The lectin's binding to SARS-CoV is dose- and calcium -dependent, and inhibited by mannan, suggesting that it occurs through the carbohydrate recognition domains.

SARS-CoV-2 comprises of glycosylated sites in both the S1 region and the N234 region found next to the ACE2-binding site, that are enriched with mannose sugars (151). Because MBL binds to glycosylated residues, it is likely that the lectin may bind and inhibit the S1-ACE2 interaction in SARS-CoV-2, as previously observed with SARS-CoV (144, 152). MBL interacts with SARS-S glycoprotein and blocks viral binding to the C-type lectin, DC-SIGN and this interaction is postulated to interfere with early pre- or post-receptor-binding events necessary for efficient viral entry (152). Given that polymorphisms in MBL have been linked to susceptibility to coronaviruses infections (50, 149), it is likely that this may be one of the mechanisms through which MBL may interfere with SARS-CoV-2 infection. Whether the heavy glycan shield may actually be a decoy for 'immune evasion' is still being investigated (144, 151). However, what is clear is that there is a role of MBL in the immune response to infection with SARS-CoV-2. Ting et al. established that the N proteins of SARS-CoV, Middle East respiratory syndrome coronavirus (MERS-CoV), and SARS-CoV-2 bind to MASP-2, a key serine protease in the lectin complement pathway of activation, aggravating lung injury (153). Interestingly, blockade of the N protein: MASP-2 interaction significantly alleviated the hyper-activation and reduced lung injury *in vitro* and *in vivo*.

Failure of MBL to maintain adequate control of infection and immunity

Low serum plasma levels of MBL have been associated with susceptibility to invasive infections. The low levels are as a result of genetic influences on MBL expression (154, 155). Nonetheless, scenarios have been described in which MBL results in worsening infection or failure to adequately eliminate pathogens (154). Excessive MBL activation is responsible for imbalances in inflammatory and coagulation responses observed in transplant rejections, inflammatory diseases, and diabetic nephropathy (156, 157). In addition, by upregulating the inflammatory response, MBL appears to worsen pandemic H1N1 (pdmH1N1) and avian H9N2 infections (157, 158). Despite binding to the virus, the interaction with pdmH1N1 is insufficient to allow antiviral activity (158). A single potential glycosylation site is located at the base of the HA globular head of PdmH1N1, however, the virus lacks potential glycosylation sites on the HA globular head region (159). Absence of this glycosylation site in pdmH1N1 and H9N2 results in MBL failure to interfere with viral binding to target cells, despite its binding to virus (158).

Paradoxically, MBL has been reported to predispose to infectious diseases, leprosy and visceral leishmaniasis, infections caused by intracellular parasites (160-162). In fact, patients with these infections had higher MBL levels when compared with controls (162). The high prevalence of variant alleles in control subjects than in patients suggested the benefits of functional MBL efficiency in this group (162). Intracellular parasites rely on phagocytosis to invade host cells, and opsonization by complement further facilitates host cell entry by use of complement receptors. Hence, low MBL levels in the control subjects diminishes the likelihood of complement-mediated phagocytosis (160). These findings however, warrant further study because some other reports have indicated no significant difference in MBL levels of cases and controls, including those with infectious and parasitic pathogens (163, 164).

EXOGENOUS LECTINS AND THEIR ROLES IN MUCOSAL INFECTIONS

GRIFFITHSIN

Griffthsin (GRFT) was discovered during an anti-HIV natural products screen by researchers at the National Cancer Institute (NCI) (165). GRFT, a carbohydrate-binding lectin, is comprised of 121 amino acid residues, and exists as a homodimer complex, Figure 1.1A. Each monomer contains three carbohydrate-binding domains that are attachment ligands for microbes and pathogens that express high-mannose compounds in their structure (165, 166), Figure 1.1B. The GRFT domain-swapped dimer presents as a near perfect three-fold symmetry, with three repeats of an antiparallel four-stranded β-sheet that resembles a β-prism-I motif in the jacalin lectin family (5, 165). GRFT preferentially interacts with terminal sugars when binding with oligosaccharides (7). Structural experiments have demonstrated that all GRFT binding sites are almost identical, and each contains aspartic acid (Asp) residues that interact with mannose (5, 165). Aspartic acid 30, Asp70 and Asp112 interact with mannose O5 and O6 via hydrogen bonding linkages (5). Interestingly, mutations that result in Asp to Alanine (Ala) changes weaken GRFT binding to a mannose column, but do not affect protein folding (167).

Originally extracted from the red algae *Griffithsia sp.* (8), a recombinant form may be expressed and purified from the tobacco plant, *Nicotiana benthamiana* (168), rice endosperm (169), and *Escherichia coli* (170). This has proved essential in making the drug available for testing in clinical studies (165). Expression of GRFT in *Nicotiana benthamiana* using a tobacco mosaic virus -based vector yields gram amounts of the lectin (165, 168, 171). The expressed GRFT is purified using ceramic filtration, two-stage chromatography, and a combination of heat, magnesium chloride and bentonite, followed subsequently by a single chromatographic step (165, 168, 172). Although not as potent as the native dimeric lectin, engineered GRFT monomeric tandemers have also been constructed and investigated for their antiviral activity (9).

A.

B.

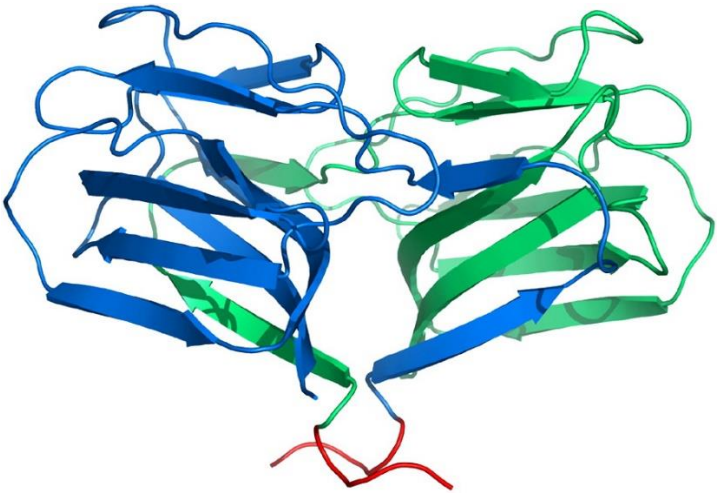

Figure 1.1 Sequence and structure of Griffithsin. (A) Sequence of wild-type GRFT demonstrating amino acids within beta strands (red) and black arrows denoting secondary structure. X is the unknown amino acid in the natural alga-derived extract. The three Asp residues found in the mannose-binding sites are identified in bold. (B) Ribbon trace of a Griffithsin homodimer. Monomer 1 is colored blue while monomer 2 is green. The N-terminal extension that resulted from the cloning procedure is colored red. Amino acid sequence and GRFT image are adapted from Lusvarghi et al. (165), and Ziolkowska et al. (5), respectively.

Broad-spectrum antiviral activity of Griffithsin

GRFT demonstrates antiviral activity against numerous enveloped viruses. This inhibition is attributed to carbohydrate-mediated binding of GRFT to various envelope glycoproteins, despite differences in the predicted glycan quantities in different viral

structures (165). A list of viruses to which GRFT binds, and the respective effective concentrations that inhibit 50% viral replication (EC_{50}) is summarized in Table 1.2 below.

Table 1. 2 GRFT effective concentrations to inhibit 50% virus infection (EC_{50}).

GRFT sample	Virus type	EC_{50} (nM)	Reference
Native GRFT	HIV-1_{RF}	0.043	(8)
Recombinant GRFT	HIV-1_{RoJo}	0.63	(8)
Native GRFT	HIV-1_{ADA}	0.5	(8)
Recombinant GRFT	SARS-$CoV_{200300592}$	280	(5)
Recombinant GRFT	SARS-CoV_{Urbani}	48	(10)
Recombinant GRFT	SARS-CoV_{CuHK}	61	(10)
Recombinant GRFT	HCV_{JFH1}	13.9	(173)
Recombinant GRFT	JEV	20	(174)
Recombinant GRFT	HSV-2	230	(175)

HIV-1: human immunodeficiency virus type 1; SARS-CoV: severe acute respiratory syndrome corona virus; HCV: hepatitis C virus; JEV: Japanese encephalitis virus; HSV-2: herpes simplex virus type 2.

Below, we review GRFT's utility and activity against mucosal infections. An abbreviated list of some of the mucosal pathogens to which GRFT binds, with the respective ligands is presented in Table 1.3.

Table 1. 3 Mucosal pathogen binding ligands for Griffithsin.

Lectin	Pathogen	Binding ligand	Reference
Griffithsin	SARS-CoV-2	Spike (S) protein	(176)
	HIV-1	gp120, gp41, gp160	(8)
	Trichomonas vaginalis	Surface N-glycans	(177)
	Candida albicans	Cell wall α-mannan	(13)

Role of Griffithsin in the modulation of respiratory mucosal infections

Human coronaviruses are enveloped positive-sense single-stranded viruses, that utilize the glycosylated spike (S) protein to interact with host receptors, prior to gaining entry into cells (178). These heavily glycosylated sites (*O*- and *N*-linked) are critical in triggering the host immune response to infection (178, 179). Human coronaviruses HCoV-229E, HCoV-OC43, HCoV-NL63 and HCoV-HKU1 largely cause seasonal and predominantly mild respiratory illnesses (180). HCoV-229E and HCoV-NL63 bind to human aminopeptidase N (APN) and angiotensin-converting enzyme 2 (ACE2), respectively (181, 182). The highly pathogenic and infectious SARS-CoV, MERS-CoV, and SARS-CoV-2 cause life-threatening severe pulmonary injury and pathology (183-185). MERS-CoV binds dipeptidyl peptidase 4 (DPP4) while SARS-CoV and SARS-CoV-2 interact with ACE2 (186-188). GRFT has been shown to bind MERS-CoV spike protein. GRFT inhibits the initial steps in the MERS-CoV infectivity process, and impedes cell entry in a dose-dependent manner (189). In *in vitro* studies, O'Keefe et al. have demonstrated that GRFT inhibits cell infectivity with HCoV-OC43, HCoV-229E and HCoV-NL63 (10). Furthermore, they determined that the lectin inhibits a post-binding step during SARS-CoV cell entry. Intriguingly, in their murine studies, compared to non-treated controls, intranasal GRFT attenuated SARS-CoV -induced respiratory disease severity and pathology, and resulted in lower inflammatory cytokines during infection. These results confirmed the initial experimental findings by Ziolkowska et al., who by using three distinct *in vitro* assays, demonstrated that GRFT inhibited SARS-CoV replication and virus-induced cytopathic effects (5). We have demonstrated that Q-Griffithsin (Q-GRFT), an oxidation-resistant variant of GRFT binds to SARS-CoV-2 spike protein. A Phase 1a clinical trial to determine the pharmacokinetics and tolerability of Q-GRFT, as an intranasal spray application for prophylaxis against COVID-19, is planned. Enrollment of volunteers is anticipated to be completed by the end of 2021.

Hantavirus [Andes virus (ANDV) and Sin Nombre virus (SNV)] infections are rodent-borne (deer mice) infections that may transmit to humans following aerosolization of infected murine urine, feces and saliva (190, 191). These viruses express fusion glycoproteins Gc and Gn in their envelope (192, 193). Hantaviruses infection results in

hantavirus pulmonary syndrome and/ or hemorrhagic fever with renal syndrome (194). In *in vitro* studies, GRFT inhibited ANDV and SNV infectivity in Vero-E6 cells (195). Furthermore, pre-incubation of GRFT with pseudovirions (PsV) revealed that inhibition of infection is likely due to the interaction between hantaviruses and the lectin. Similarly, this study revealed that the trimeric tandemer 3mGRFT inhibited the entry of PsV particles into cells, albeit with a higher potency than GRFT. It remains to be seen if these results will be replicated in *in vivo* models.

Interactions of Griffithsin with the gastrointestinal and rectal mucosal microbiome, pathogens, and immunity

Oral administration of GRFT did not result in any detectable lectin levels in the serum of treated animals, despite the low fecal drug concentrations observed. Regardless, drug levels in the fecal material ably neutralized HIV-Env PsV in *in vitro* assays (196). The gastrointestinal tract secretes various proteases (197) that have the potential to degrade and denature GRFT, given the lectin's peptide nature (165). In *in vitro* studies using commercially available gut proteases, GRFT resisted degradation by the majority of proteases and was only degraded by elastase (198). The lectin resisted proteolytic activity by enzymes pepsin, papain, leucine aminopeptidase, pronase, α-chymotrypsin, proteinase K, endoproteinase, lys-C and trypsin (198). Similarly, we have demonstrated the presence of protease enzymatic activity in human and murine rectal fluids in *in vitro* assays. However, we have determined that Q-GRFT resists proteolytic degradation by proteases in human, mice and macaque rectal fluids (199). It is likely that high stomach acidity may be the most predominant contributor to the denaturation of orally administered GRFT (196). Additionally, the potential for bile salts to degrade GRFT in the gut may warrant investigation.

Condom-less receptive anal intercourse among men who have sex with men is the predominant mode of transmission of new HIV infections in the Western world (200-202). In preliminary studies during the development of GRFT as a microbicide to prevent HIV infection, Girard et al. describe the impact of rectal application of the lectin on Rhesus macaques' mucosa and proteome (203). There were no significant detectable changes in the rectal proteome associated with GRFT gel application. Small and likely

inconsequential changes in the rectal microbiome were detected. These results were indicative of GRFT's tolerability in the rectal environment and further supported the relevancy for its development as a microbicide. In keeping with these findings, using *in vitro* assays, we have demonstrated that Q-GRFT does not inhibit the growth of gut and rectal microbiome components-*Lactobacillus acidophilus*, *Lactobacillus casei*, *Bifidobacterium longum longum*, *Clostridium difficile* and *Bacteroides fragilis* (manuscript in preparation) (199). Furthermore, Gunaydin et al. (204), have established that rectal Q-GRFT gel application is associated with a stable expression of E-cadherin+ cells, responsible for maintaining epithelial integrity. Interestingly, administration of a high GRFT gel concentration was associated with slightly elevated intra-epithelial CD4+ T cells. Repeated dosing resulted in significantly elevated lamina propria CD4+ T cells, targets for HIV infection. The elevated CD4-T cells may not potentiate HIV-1 transmission because a similar study with a hyperosmolar lubricant resulted in elevated rectal mucosal mononuclear cells and cytokines but did not increase the risk of SHIV infection in macaques (205). However, repeat studies using HIV-1 virus infection assays will help in determining the infectivity of these CD4-T cells.

GRFT's binding to HIV-1 glycoproteins gp120, gp41 and gp160 is dependent on glycosylation of these viral coat structures (8). GRFT has demonstrated activity against HIV-1 clades A, B and C (168), is highly potent, blocking CXCR4- and CCR5-tropic viruses and impedes cell-to-cell viral transmission (206). Dimeric GRFT is more potent and efficacious at binding and preventing viral transmission than the monomeric form (207). When combined with tenofovir, maraviroc or enfuvirtide, GRFT exhibited excellent synergistic inhibitory activity against infection of peripheral blood mononuclear cells (PBMCs) and CD4+ MT-4 cells with HIV-1 clade B and C isolates (208). In addition, synergistic and complementary inhibition of viral activity has been demonstrated with broadly neutralizing anti-HIV-1 monoclonal antibodies (mAb) VRC01, PGT121 and PGT126 (209, 210).

Monoclonal antibodies kill HIV-infected cells by targeting relatively conserved epitopes and mediating antibody-dependent cellular cytotoxicity (211). However, viruses often conceal features that would make them susceptible targets of antibody

neutralization (165). Through oligomerization or conformational occlusion, they may hide fundamental structural motifs that are critical for antibody binding. Additionally, viruses may undergo rapid mutation rates leading to high sequence variability in non-essential regions like variable loops, or undergo extensive posttranslational glycosylation, evading antibody detection (165). Because enveloped viruses employ the heavy glycan shield to elude neutralizing antibodies (212), this makes GRFT an ideal strategy that binds to these glycans, ultimately preventing cell infection. Additionally, glycosylation maintains viral fitness following antibody escape mutations (213, 214), further predisposing them to GRFT anti-viral activity.

Against this background and findings, our group is currently recruiting participants in a first-in-humans Phase I clinical trial to determine the pharmacokinetics and tolerability of Q-GRFT for utility as a rectal microbicide against HIV-1 infection and transmission (215).

Impact of Griffithsin on genitourinary mucosal immunity and infections

Like the gastrointestinal and rectal environment, cervicovaginal fluids are comprised of enzymes and are capable of proteolytic degradation of proteins (216). GRFT has demonstrated stability in cervicovaginal secretions and maintains its anti-HIV-1 potency in this environment (206). In human cervical explant assays and in the *in vivo* rabbit vaginal irritation model, GRFT did not induce any significant expression of proinflammatory cytokines and chemokines (168). GRFT binds to *N*-glycans of *Trichomonas vaginalis* (177). Topical murine treatment was associated with lower recovery of the bacterial pathogen in vaginal fluids, suggesting a potential therapeutic role in *Trichomonas* infections (177). Contrastingly, we did not demonstrate any inhibitory activity of GRFT against STI-causative pathogens *C. trachomatis* and *Neisseria gonorrhea* in *in vitro* assays (199). Vulvovaginal candidiasis is one of the leading causes of vaginitis (217) and recurrent *Candida sp.* infections predispose to drug resistance (218). We have demonstrated a novel finding that Q-GRFT binds to α-mannan, a glycosylated component of the *C. albicans* cell wall, in a concentration-dependent manner. Additionally, we have identified that Q-GRFT inhibits the growth of other *Candida* species *C. krusei*, *C. parapsilosis* and *C. glabrata*, including some strains of the

multi-drug resistant *C. auris.* We determined that upon binding, Q-GRFT induces a break down in fungal cell wall integrity, with formation of intracellular reactive oxidative species (13).

GRFT inhibits HIV-1 infection in human vaginal explant models (168). Furthermore, a Griffithsin/ Carrageenan (GRFT/CG) combination formulated as a freeze-dried fast dissolving insert for on-demand use was protective against a vaginal simian immunodeficiency HIV chimeric virus (SHIV) challenge in rhesus macaques (219). Comparably, GRFT/CG was protective against vaginal HPV and HSV-2 PsV challenges in murine models (219). Similarly, sustained GRFT delivery, formulated in nanoparticle-electrospun fiber composites was protective against a lethal vaginal challenge of HSV-2 in murine models (220).

Potential role of Griffithsin in ocular mucosal infections

Numerous respiratory viruses have been identified to have tropism for ocular epithelial tissues, including adenovirus, influenza virus, coronaviruses, rhinovirus and respiratory syncytial virus (221-226). Additionally, increasing evidence for SARS-CoV-2 infection and transmission via ocular tissues in the ongoing COVID-19 pandemic has been documented, although more confirmatory categorical data and studies are needed (227-229). Given GRFT's ability to bind and inhibit infectivity with coronaviruses (as discussed above), there is potential utility of an ocular formulation in preventing transmission. Indeed, Wang et al. in their review, hypothesize that contact lenses able to sustain delivery of GRFT probably via nanoparticles may be protective among health workers and others in close contact with patients (230). However, given the cumbersomeness of daily use of contact lenses, this may not be practical for the majority of users. Given the tendency for GRFT to accumulate and persist in tissues during chronic use (196), further studies are warranted to establish drug levels in ocular epithelial tissues. Befittingly, we have hypothesized that a Q-GRFT ocular eye suspension administered daily may be adequate in preventing coronavirus infection among people at risk of infection. Our initial *in vitro* assays confirm that daily treatment of corneal epithelium results in detectable Q-GRFT levels and does not enhance any expression of proinflammatory cytokines and chemokines (chapter 5).

CONCLUSION

Lectins interact with a diverse array of ligands on microbes and pathogens, mediating a variety of functions. Here, we have summarized the relevant functions of lectins pertinent to mucosal infections and immunity. The rapidly changing scope of discoveries and studies into the function of these molecules, and the need for a wider breadth of antimicrobial agents to counter the rising antimicrobial drug resistance has pushed for the exploration of new molecules and drugs. Indeed, this has resulted in more knowledge about mechanisms and potential roles of lectins in this field. Whether these discoveries and knowledge culminate into new therapeutics and novel diagnostic approaches for utility against current and emerging mucosal infectious diseases and pathogens is yet to be determined.

CHAPTER 2: STABILITY OF Q-GRIFFITHSIN IN THE RECTAL MUCOSAL ENVIRONMENT

INTRODUCTION

In 2019, 1.7 million people were estimated to have acquired new HIV infections worldwide. Sixty two percent (62%) of these infections were among key-at risk populations (including gay men, other men who have sex with men (MSM), transgender people, sex workers, injection drug users and prisoners) (231, 232). In the United States, there were 36,400 new HIV infections in 2018, with the largest percentage of transmission (67%) attributed to male-to-male sexual contact (233). Unprotected receptive anal intercourse (URAI) is associated with a 1.7% HIV transmission risk per coital act, and is higher than that in unprotected vaginal intercourse, 0.08% (234). The vulnerability of the rectal environment to infection is due to the anatomical presence of a single columnar epithelial layer, with predominant expression of activated CD4+ T cells that express CCR5 co-receptor, a binding ligand for HIV-1 (235).

Pre-exposure prophylaxis (PrEP) strategies have been developed and deployed, with a multitude of other approaches still under investigation, to provide on-demand modalities like injectables and topical products, as alternatives to daily PrEP, and improve adherence (236). These include microneedles, electrospun fibers, vaginal films and rings, subdermal implants, microbicide gels, enema and mucoadhesive tablets (237-244). These products deliver potent anti-HIV drugs/ agents to mucosal epithelium involved in sexual contact (245).

Q-GRFT, a virucidal and non- cell entry inhibitor of HIV has also demonstrated potency against other sexually transmitted viruses like HSV-2 and HPV *in vitro* and *in vivo* (175, 219). GRFT binds to glycoproteins in the HIV envelope blocking interaction with CXCR4 and CCR5 receptors, and subsequent cell entry and cell-to-cell transmission

(8, 168). Initially extracted from red sea algae, recombinant forms of the lectin are currently produced in *Nicotiana benthamiana* plants following transduction with GRFT-expressing tobacco mosaic virus vectors (168). GRFT has been demonstrated to be stable in cervical/ vaginal lavage fluids, maintaining its anti-HIV activity and potency in this environment (206).

Our laboratory has developed an oxidation-resistant variant of GRFT, Griffithsin-M78Q (Q-GRFT), for use as a multipurpose topical microbicide to protect people at risk of HIV- and superinfection with STIs like HSV-2 and HPV. Healthy volunteers are currently being enrolled in a first-in-human Phase1 study to determine pharmacokinetics in the rectal environment (246). Because of its protein nature, Q-GRFT may be susceptible to enzymatic degradation and the lectin's activity may be affected by host- and microbiome-derived compounds in the rectum. The activity of Q-GRFT in the rectal environment remains unknown. In this study, we investigated the stability and activity of Q-GRFT in mice, macaque and human rectal fluids and seminal plasma.

MATERIALS AND METHODS

Specimen:

Human rectal fluids and seminal plasma. Human rectal fluids were eluted from rectal swabs that were collected at Magee-Womens Research Institute, University of Pittsburgh, Pittsburgh, Pennsylvania from healthy subjects participating in the PREVENT Phase 1 clinical trial that is developing Griffithsin-M78Q as a rectal microbicide against HIV infection and transmission (246). This study was approved by the University of Pittsburgh Institutional Review Board and was listed as ClinicalTrials.gov Identifier: NCT04032717. At collection, the swabs were placed in the rectum for a few minutes and then stored at -80°C in a LDMS labeled cryogenic vial. To elute the rectal fluids, the frozen rectal swab was thawed at room temperature (20-25°C). One Spin-x microcentrifuge tube (0.45μm cellulose acetate filter) and 1-1.5 mL microcentrifuge tube per sample were used to spin the sponge. The excess handle of the swab/ sponge was removed and discarded using dissection scissors and the swab placed in the upper

chamber of the Spin-X filter unit. Three hundred microliters of Phosphate buffered saline (PBS) were added to the upper chamber. The chamber and collection tube were then centrifuged at 12,000 rpm for 20 minutes at 2-8°C. The filtered solution was aliquoted into 1.5 mL microcentrifuge tubes and stored at -80°C until when assays were performed.

Seminal fluids (sperm cell-free semen) were commercially purchased from Lee BioSolutions, Inc Maryland Heights, MO USA.

Macaque rectal fluids. Rectal fluids were collected from six Rhesus Macaques (*Macaca mulatta*) that were housed at the Centers of Disease Control and Prevention (CDC; Atlanta, GA). Animals were housed in accordance with the Guide for the Care and Use of Laboratory Animals (8^{th} Edition) in an AALAC-accredited facility, according to institutional standard operating procedures. These were adult female Indian-origin macaques with average age of 8.7 years, that were part of a study to evaluate the pharmacokinetics (PK) of Q-GRFT formulated as a 0.3% (w/w), 1.0% and 3.0% Carbopol gel upon intrarectal administration. Rectal fluids used in our study were collected at various times in untreated control animals. All study procedures were performed on anesthetized animals according to methods and procedures approved by CDC's Institutional Animal Care and Use Committee. For the rectal fluids collection, Weck-cel swabs or Merocel sponges, Beaver Visitec Intl Ltd, Fischer Scientific #NC0240644 were used, as described previously (247). Briefly, the swabs or sponges were pre-wet with cold PBS and inserted into the rectum. They were then removed after 5 minutes, and the excess feces scrapped off. The swabs/ sponges were then placed in a Costar Spin-X centrifuge filter (Sigma Cat. #CLS8160) and centrifuged with PBS at 4 °C for 30 minutes at 16000 rpm to elute fluids. The eluates were placed in new Spin-X tubes and stored at -80 °C until when analysis was performed.

Mice rectal fluids. Mice were euthanized and rectal fluids collected following a protocol previously described (248). Briefly, 200 μL of PBS were introduced into the anal canal with a disposable pipette tip. The rinse was gently pipetted in and out of the anal canal a few times and the fluid collected in a microcentrifuge tube. The fluid was stored at -80°C until when analysis was performed.

Physicochemical properties of human and mice rectal fluids. Stored rectal fluids were thawed at room temperature and the aliquots assessed visually for any color intensity and suspended materials. The pH was determined using MColorpHast™ (Merck KGaA, Darmstadt, Germany) universal indicator strips.

Murine and human rectal fluids' protein concentration was determined by the bicinchoninic acid (BCA) assay using the Pierce™ BCA Protein Assay kit. Briefly, the Diluted Albumin (BSA) standards and Working reagents (WR) were prepared following kit instructions. Twenty-five microliters (25µl) of each of the standard and rectal fluid samples were pipetted to a 96-well microplate followed by 200µl of the WR and mixed thoroughly using a plate shaker. The plate was incubated for 30 minutes, and absorbance read at 562nm using a BioTek Synergy plate reader running Gen5 software. A standard curve was plotted (for the BSA standard) and the slope used to determine the protein concentration of the unknown rectal fluid samples.

Protease concentration of murine and human rectal fluids was determined by the casein colorimetric assay using the Pierce Protease Assay kit. Briefly, the assay buffer, Succinylated casein Solution, Trypsin Stock Solution, Trypsin Standard and trinitrobenzenesulfonic acid (TNBSA) Working Solution were prepared as per protocol instructions. One hundred microliters of Succinylated Casein Solution were added to one set of microplate wells and 100µl of assay buffer to a duplicate set of wells, to serve as blanks. Fifty microliters of each unknown rectal fluids or standard sample were added to both Succinylated Casein wells and the corresponding blank wells. The plate was then incubated for 20 minutes at room temperature. Fifty microliters of TNBSA Working solution were added to each well and the plate incubated for 20 minutes. Absorbance in the wells was measured at 450nm, using a BioTek® Synergy HT plate reader running Gen5 software. The change in absorbance was obtained by subtracting the blank from the corresponding well. A standard curve (ΔA_{450} against protease standard concentration) was then plotted and used to assess relative protease activity of the unknown rectal fluids.

The optimized microplate periodic acid-Schiff's reagent (PAS) assay was used to assess for the presence of carbohydrates in murine rectal fluids. Briefly, 25µl of rectal fluids were added to a 96-well microplate, followed by 120µl of freshly prepared 0.06%

periodic acid in 7% acetic acid. The plate was sealed with plastic adhesive tape and incubated at 37°C for 1.5 hours. The mixture was then cooled to room temperature, 100µl of Schiff's reagent added and then mixed thoroughly by pipetting up and down. The plate was then sealed with adhesive plastic tape, shaken for 5 minutes using a plate shaker and color allowed to develop at room temperature for 40 minutes. Absorbance was read at 550nm from a BioTek® Synergy HT plate reader running Gen5 software.

Q-GRFT's binding ability to gp120. Q-GRFT was incubated with rectal fluids and seminal plasma for either 6 hours (macaque rectal fluids) or 24 hours (murine, human rectal fluids and seminal plasma) at 37°C prior to performing a binding ELISA assay. Plates were coated overnight with gp120 diluted in 1X PBS. The plate was then blocked for 2 hours at room temperature using 3% BSA in 1X PBS-T. Incubated sample fluids were added at concentrations starting at 250-300 ng/ml with 2X or 3X dilutions and incubated for 1-2 hours. The primary antibody (rabbit anti-Q-GRFT), followed by secondary antibody (goat anti-rabbit) were then added. To develop the reaction, 3,3',5,5'-Tetramethylbenzidine (TMB) solution was added followed by 1N Sulphuric acid to stop the reaction. Absorbance was read at 450 nm using a BioTek® Synergy HT plate reader running Gen5 software. Nonlinear regression (GraphPad Prism) was used to determine the half maximal effective concentration (EC_{50}) of Q-GRFT binding.

Statistical analysis. Statistical analyses were performed using GraphPad Prism V7. Numerical data are presented as mean $\pm$ standard deviation (SD) or mean $\pm$ standard error of mean (SEM). Experiments and assays were performed in triplicate. Statistical differences between sets of data were evaluated using ANOVA. P-values of ≤ 0.05 were considered significant.

RESULTS

Physical and chemical properties of murine and human rectal fluids

Given the peptide nature of Griffithsin (165) and the variant Q-GRFT, we sought to characterize and identify the physical and chemical properties of rectal fluids that may impact the lectin's stability and activity in this environment. Murine rectal fluids, n=12

(Table 2.1) had an appearance that ranged from clear and colorless (-) to slightly turbid (+), with a pH of 7. Carbohydrates were detected in these fluids, and the protein concentration ranged from 10.60 ± 0.00 µg/mL to 431.93 ± 0.00 µg/mL, with a group mean of 121.88 ± 3.54 µg/mL. Protease activity ranged from 2.76E-05 ± 3.29E-05 µg/ mL trypsin to 3.47 ± 0.00 µg/ mL trypsin, with a group mean of 2.19E-01 ± 3.65E-02 µg/ mL trypsin . Human rectal fluids, n=6 (Table 2.2) ranged from clear and colorless (-) to slightly yellow and mildly turbid (++) in appearance. This is likely related to the levels of fecal-derived substances in the fluids (245). The pH range was 7 to 8, and was consistent with ranges that have been demonstrated from reported human colonic studies (249). Protein concentration was 730.00 µg/mL to 1211.89 µg/mL, with a mean of 917.71 µg/mL, and protease activity 0.198 µg/mL trypsin to 1.069 µg/mL trypsin, with a group mean of 0.38 µg/mL trypsin. Altogether, these results demonstrate that there is a variation in composition, enzymatic activity and physical make up of murine and human rectal fluids. The variation in protease activity is likely in part due to microbiota composition alterations and differences between individuals (250).

Table 2. 1 Physicochemical properties of murine rectal fluids.

Sample ID	Appearance	pH	carbohydrates	Protein Concentration µg/mL	Protease activity µg/mL Trypsin
RL001	-	7	+	20.27 ± 1.65	7.32E-04 ± 5.24E-04
RL002	-	7	+	55.93 ± 7.07	3.23E-05 ± 7.07E-08
RL003	+	7	+	380.60 ± 10.37	258.38 ± 9.23
RL004	-	7	+	76.27 ± 1.18	2.76E-05 ± 3.29E-05
RL005	-	7	+	431.93 ± 0.00	4.92E-02 ± 0.00
RL006	-	7	+	109.93 ± 0.00	3.47 ± 0.00
RL007	-	7	+	86.93 ± 3.06	1.4E-04 ± 6.94E-05
RL008	-	7	+	78.93 ± 9.66	5.18E-01 ± 4.90E-02
RL009	-	7	+	94.93 ± 0.00	5.68E-04 ± 1.40E-03
RL010	-	7	+	10.60 ± 0.00	5.20E-04 + 2.63E-04
RL011	-	7	+	87.60 ± 0.00	4.96E-01 ± 0.11
RL012	-	7	+	28.60 ± 9.43	6.19E-04 ± 3.03E-04

Appearance scored as (-) for clear and colorless, (+) for slightly turbid, (++) for slightly yellow and mildly turbid and (+++) for intense yellow and deeply turbid. PH was determined using MColorpHast™ test strips. Carbohydrates, protein concentration and protease activity were determined by optimized microplate periodic acid-Schiff's reagent assay, bicinchoninic acid assay and casein colorimetric assay respectively.

Table 2.2 Physicochemical properties of human rectal fluids.

Sample ID	Appearance	pH	Protein Concentration µg/mL	Protease activity µg/mL Trypsin
RL1	-	8	802.50	0.237
RL2	-	7	899.38	1.069
RL3	++	7	899.38	0.214
RL4	-	7	963.13	0.198
RL5	-	7	730.00	0.203
RL6	++	7	1211.88	0.338

Appearance scored as (-) for clear and colorless, (+) for slightly turbid, (++) for slightly yellow and mildly turbid and (+++) for intense yellow and deeply turbid. PH was determined using MColorpHast^{TM} test strips. Protein concentration and protease activity were determined by bicinchoninic acid assay and casein colorimetric assay respectively.

Stability of Q-GRFT in mouse, macaque and human rectal fluids, and seminal plasma

To establish any inactivating activity of the lectin in rectal fluids, Q-GRFT was incubated with rectal fluids, starting with an initial concentration of 250 ng/mL, with two-fold dilutions, at 37°C. The lectin's binding activity to gp120 was then determined following incubation. GRFT strongly binds to the HIV envelope glycoprotein 120, inhibiting transitions necessary for cell entry (165). Therefore, we used the ability to bind gp120 in an ELISA assay as a surrogate of GRFT stability following incubation with rectal fluids and seminal plasma. Following incubation for 24 hours with mice rectal fluids (FIG 2.1A), Q-GRFT's binding activity to gp120 was not affected. Upon incubation with macaque rectal fluids (FIG 2.1B) at 37°C for 6 hours, binding activity to gp120 was not affected. Similarly, incubation of Q-GRFT with human rectal fluids (FIG 2.1C) at 37°C for 24 hours did not impact the lectin's binding activity to gp120. Because of the development of Q-GRFT as a potential rectal microbicide for prevention of HIV infection and transmission during condomless anal intercourse, we determined the lectin's binding inhibition in human seminal fluids. In keeping with findings from rectal fluids, incubation in human seminal plasma (FIG 2.1D) for 24 hours at 37°C did not impair gp120 binding.

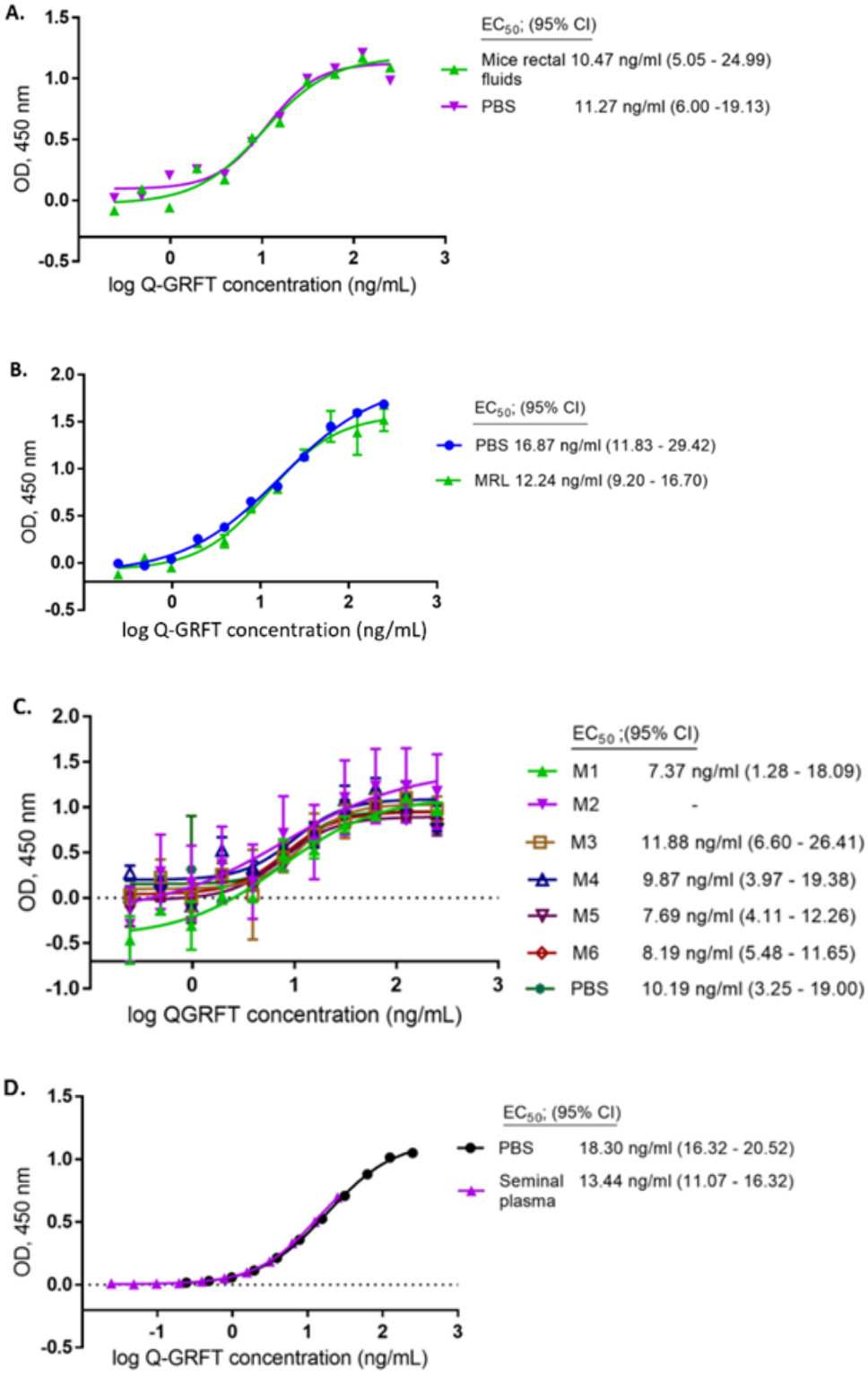

Figure 2. 1 Stability of Q-GRFT in rectal fluids and seminal plasma. Q-GRFT maintains its binding to gp120 following incubation with (**A**) mice rectal fluids, **(B)** macaque rectal

fluids, **(C)** human rectal fluids and **(D)** human seminal plasma. Q-GRFT was incubated at 37°C for 24 hours in mice-, human rectal fluids, and seminal plasma, and for 6 hours in macaque rectal fluids. Representative data from one sample (mice and macaque rectal fluids, and human seminal plasma), and 6 specimens (human seminal plasma) is shown. For all experiments, Q-GRFT was incubated with PBS, as a control. For both fluids and PBS, the initial Q-GRFT concentration of 250 ng/ml was used, with two-fold dilutions performed up to 11 -12 times.

DISCUSSION

The anatomical and physiological properties of the biological environment in which microbicides will work is critical to their applicability (251). In this study, we have demonstrated that rectal fluids consist of varying concentrations of carbohydrates, protein, and proteolytic enzymes, with a fairly stable pH range. Seminal fluids have previously been shown to demonstrate proteolytic enzymatic activity (252, 253). The demonstrated enzymatic activity has the potential to degrade or inactivate any peptide molecules or microbicides administered in the rectal environment. The composition, chemical and physical properties of a microbicide will influence its efficacy and activity on mucosal surfaces (254). In addition, an effective microbicide PrEP modality should withstand any inactivating activity in the rectal environment. Oral administration of GRFT in Sprague Dawley rats was demonstrated to result in detection of active drug in fecal extracts that potently neutralized HIV-Env PsV (196). This supports topical local application given the lectin's ability to withstand degradative properties of the gastrointestinal tract. Local mucosal administration ensures the availability of sufficient and adequate drug product levels in tissues following application. Regardless of the demonstrated proteolytic potential, we have found that Q-GRFT, a protein molecule, maintained the ability to bind to gp120 following incubation with rectal fluids and seminal plasma (Table 2.1, Table 2.2 & Fig 2.1). Interestingly, Fabrice et al., found that the activity of the molecule 5P12-RANTES, a potential HIV microbicide was affected by the diversity of human rectal fluid composition, and that fluids from the same individual collected at different times displayed varying degradative impact on 5P12-RANTES

activity (245). However, they postulate that even at the most aggressive protease activity identified, 5P12-RANTES will likely remain stable, with adequate anti-HIV activity. Rectal microbiota, especially the predominance of *Prevotellaceae* likely predisposes and contributes to HIV acquisition (255). Indeed, studies in non-human primates have demonstrated that microbial differences resulted in differences in SHIV susceptibility with susceptible animals associated with higher inflammatory activity and lower *Firmicutes* and *Bacteroides* and higher *Prevotellaceace* spp. (256). The diverse gut microbiota also contributes to, and shapes the enzymatic response in this environment (257). Human gut microbial differences have been shown to vary at difference sampling times within and between individuals over time (258, 259). Inter-subject differences in microbiome diversity are greater than intra-subject variations (258). Compared to host-derived proteolytic enzymes, the majority of protease activity in the rectal environment is of microbiota-origin (250).

Studies with cervicovaginal fluids have demonstrated that a wide range of factors within this compartment mediate antimicrobial protection and work in concert to protect target cells from infection with HIV. Specifically, beta-defensin 2, macrophage inflammatory protein-3 alpha (MIP 3α), and HIV-specific IgG antibodies in this compartment are associated with protection from virus infection (251, 260). In lieu of this, it is critical that microbicides do not attenuate or diminish local protective properties of the epithelial mucosa in which they act (251). GRFT has previously been shown to exhibit stability in cervicovaginal fluids, which are comprised of an acidic pH, various enzymes, vaginal microflora and macromolecules like mucins (206). Similarly, here, we have demonstrated that in the rectal environment, despite a varying microbiome composition, pH and enzymatic activity (245, 249), Q-GRFT is stable and maintains the ability to bind gp120. Furthermore, the duration of incubation of Q-GRFT with the fluids did not disrupt gp120 binding.

The impact of semen on HIV-1 transmission in the vaginal environment has been extensively studied (261-264), and the effects in the rectum are similar to those observed in this compartment (251). Semen alters the acidic vaginal pH to neutral, fostering an environment prone to yeast infections and vaginosis. Semen in the reproductive tract

induces an influx of activated inflammatory cells and increases the population of leucocytes in the vaginal tract, making them vulnerable to infection with infectious virus in seminal fluids (261-263). Localized irritation and inflammation induced by semen results in further recruitment and activation of more HIV-1 target cells, enhancing virus infection and transmission. The likelihood of survival of cell-free and cell-associated virus is increased by the seminal pH neutralization effect and secretion of semen-derived enhancer of infection (263). Additionally, the electrostatic interaction between spermatozoa and HIV-1 virions promotes virus infection (263). Mucosal movement of HIV virions is increased following vaginal pH neutralization by semen, facilitating rapid viral access to epithelium (265, 266). Contrastingly, studies have also identified antiviral properties of semen. Seminal plasma contains a potent inhibitor that impedes HIV-1 attachment to DC-SIGN (263). Furthermore, in the vaginal environment, HIV is inactivated by radicals generated by oxidation of SP polyamines by diamine oxidase (263). Additionally, cationic polypeptides in seminal plasma contribute to this antiviral effect (263). Interestingly, Buckheit et al., found that diverse semen samples obtained from different donors displayed both inhibitory and enhancement properties of HIV infection (251). In both the vagina and rectum, semen acts as a physical barrier to virus movement towards epithelial target cells (267). However, once trauma or breach of the barrier occurs, inflammatory cytokines promote transmission of infection through the epithelium (251). In our study, incubation of Q-GRFT with seminal fluids did not impede the lectin's binding to gp120. Similarly, Harman et al. (268), demonstrated that L'644, a fusion inhibitor peptide was stable and maintained antiviral activity following incubation in semen and cervicovaginal fluids for 72 hours. It is therefore likely that Q-GRFT will maintain anti-HIV-1 activity in the rectal environment in presence of semen.

One limitation of our study is that we did not confirm detection of Q-GRFT following incubation in rectal fluids and seminal plasma using alternative methods like western blot. However, given the high potency of GRFT in binding gp120, our results are strongly suggestive of stability in this assay.

In summary, results from these experiments suggest that despite the diversity in composition and complexity in the rectal environment, Q-GRFT remains stable and binds

to gp120. It is likely that the lectin will maintain anti-HIV-1 activity in this biological compartment.

CHAPTER 3: IMPACT OF Q-GRFT ON THE GROWTH OF GUT AND RECTAL MICROBIOME, AND MYCOBIOME COMPONENTS

INTRODUCTION

The vaginal and rectal microbiome has been implicated in the modulation and efficacy of microbicide activity (269). Local physiologic responses including the immunologic response, inflammation and epithelial barrier integrity induced by different microbiota (270), may impact the action of different microbicides. Bacterial vaginosis (BV) is a condition in which the acidophilic and aerobic vaginal microbiome, predominantly comprising of *Lactobacillus* is replaced by anaerobic species, predominantly *Gardnerella* (269). BV is associated with an increased risk and susceptibility to HIV infection among women (271). Studies have identified that women without BV and subsequently at a lower risk of HIV infection, had *Lactobacillus* species as the predominant vaginal microbiota, whereas those with BV and at high risk of virus infection display large proportions of *Gardnerella* and *Prevotella,* among other anerobic species (272-274). Vaginal dysbiosis reduced the efficacy of a 1% tenofovor gel in preventing HIV acquisition in women as pre-exposure prophylaxis (269). *Gardenerella vaginalis* in BV likely metabolizes locally applied tenofovir, preventing uptake into mucosal epithelial cells (269). Interestingly, condom use is associated with inflammatory changes and demonstrates functional changes in vaginal bacterial metabolic pathways (275). In men, condomless receptive anal intercourse (CRAI) has been associated with a distinct rectal microbiota, enriched in *Prevotellaceae* family when compared to males who have never practiced receptive anal intercourse (276). When compared to anal intercourse- naïve men, MSM engaging in CRAI displayed elevated Th17 immune cells, higher proliferation of CD8+ T cells, proinflammatory cytokines secretion and signatures associated with epithelial injury and repair (276). In previous HIV clinical trials, the failure of vaginal microbicides to prevent HIV transmission has been suggested to be as a

result of a shift of the local bacterial community with a loss of natural anti-viral protection (277). Indeed, healthy women who were vaginally exposed to either of gel products hydroxyethylcellulose, 6% cellulose sulfate and 4% nonoxynol-9 demonstrated a shift in the microbial community towards that dominant in strict anaerobes, and depleted of *Lactobacillus* species (277). Interestingly, rectal application of Q-GRFT gel in non-human primates did not result in significant changes to local proteome levels during the period of lectin use, but demonstrated an increased abundance of beneficial *Ruminococcaceae* and *Christensenellaceae* taxa (203). Currently, no published data is available detailing the impact of microbicides on vaginal and rectal fungal communities.

Lectins are protein molecules that possess carbohydrate moieties and interact with other cell wall and membrane components via these structures (1). Griffithsin has been widely studied for its activity against the human immunodeficiency virus (HIV) and other viruses (10, 11, 278). Conversely, as a microbicide, Q-GRFT topical use is likely to impact the stability of resident microbiota. Here we report findings about the impact of Q-GRFT on representative gut bacterial and fungal microbiota. We identify and report a novel and the first known antifungal activity of this lectin and postulate a mechanism of action of growth inhibition. Despite no detectable impact on bacterial microbiota, our findings support further exploration and development of this lectin as an antifungal agent given the observed growth inhibitory impact on *Candida* species *in vitro*.

MATERIALS AND METHODS

Griffithsin-M78Q expression and product formulation. The API used in the experiments was recombinantly expressed in the *Nicotiana benthamiana* plant-based system, as described previously (279). Because the original plant-produced recombinant Griffithsin protein is prone to oxidation at methionine-79, a single amino acid substitution replacing met-78 residue with glutamine (Q) in the non-binding domain has been performed, generating a stable variant, Q-GRFT. The M78Q variant is more stable to oxidation than the parent molecule and retains the potency and other characteristics of the parent protein. The API was dissolved in PBS solution, pH 7.4 at 10$\pm$2 mg/mL, and diluted as needed for use in these experiments.

Antiviral activity assays. Anti-HIV activity was assessed *in vitro* using a viral neutralization assay performed with HOS $CD4^+$ $CCR5^+$ (NIH AIDS Reagent Program #3318) cells. HOS cells were cultured in DMEM supplemented with 10% FBS (VWR #97068-085), 1% penicillin/ streptomycin (VWR#97063-708), and 1 μg/mL of puromycin (VWR#97064-280). Using an opaque tissue culture treated white 96-well plate, 50 μL of media was added to each well. This was followed by 50 μL of Q-GRFT diluted 3X from a top concentration of 20 ng/mL in the top wells down the plate. HIV PsV QH069 was diluted 1:4 in medium and 50 μL per well of diluted virus added to every sample and positive control well. The 1:4 dilution had been predetermined to yield enough luminescence (by $TCID_{50}$ assay). The virus and Q-GRFT were incubated for 1 hour at 37°C. HOS cells were harvested from a flask and diluted to 1 x 10^5 cells/mL in culture medium. One hundred microliters of well mixed cells (10,000 cells total per well) were added to every well. The plate was then incubated for 3 days at 37°C. To read the plate, 100 μL of medium were removed from each well and 100 μL of Britelite luciferase assay reagent (Perkin Elmer #6066761) added to every well. Luminescence was measured on a Synergy HT BioTek® plate reader. To establish the percent neutralization for every well, the following formula was used:

$$\text{Percent neutralization} = \frac{\text{RLU sample} - \text{RLU virus control}}{\text{RLU virus control}} * 100.$$

Data was analyzed using non-linear regression and the IC_{50} calculated.

Bacterial growth inhibition assays. Gut and rectal microbiome and mycobiome components were incubated in broth medium in presence of varying concentrations of Q-GRFT for 24 to 72 hours to determine the lectin's growth inhibitory effects. The representative bacterial components tested were purchased from the American Type Culture Collection (ATCC) and are of human origin. Microbiome components: *Escherichia coli* K12 was incubated in Miller's Luria broth (LB broth), while *Lactobacillus acidophilus* and *Lactobacillus casei* were incubated in De Man, Rogosa and Sharpe (MRS) broth. *Bacteroides fragilis* (Nontoxigenic *Bacteroides fragilis* 9343 and Enterotoxigenic *Bacteroides fragilis* 086) was incubated in Brain Heart Infusion media supplemented with clindamycin (BHI-Clindamycin). *Clostridium difficile* ATCC® 51695 and *Bifidobacterium longum longum* ATCC® 15707 were incubated in Brain Heart

Infusion-supplemented (BHIS) media and MRS/ L-cysteine –enriched media, respectively. Bacterial growth measured as OD 600nm, was monitored using a Synergy HT BioTek® plate reader.

MIC and cytotoxicity determination for Q-GRFT against Chlamydia and Neisseria gonorrhea. For determination of the lectin's growth inhibitory *Chlamydia trachomatis* inhibitory effect, 100 µL of McCoy cells (density $5x10^4$ cells/well) were plated in a 96-well plate in Eagle's minimum essential media (EMEM) with 10% Fetal Bovine Serum (FBS) and glutamine for 24 hours. *Chlamydia trachomatis* ATCC VR348B was then added and centrifuged to promote infection. Doxycycline or Q-GRFT was added to the supernatant in triplicate. Cells were then fixed and stained with iodine in absolute methanol and glycerol. The wells were then observed for presence of inclusion bodies. To establish Q-GRFT cytotoxicity to McCoy cells, the McCoy cell density was determined upon Q-GRFT incubation. To establish inhibitory activity against *Neisseria gonorrhoea,* Q-GRFT was added to agar medium inoculated with the pathogen and MIC_{50} determined.

Candida growth inhibition assays. To determine fungal inhibition, 1.0×10^5 cells/mL of *Candida albicans* ATCC® 32032, *Candida glabrata* CDC316, *Candida krusei* CDC397, *Candida parapsilosis* CDC337, *Candida auris* CDC383, *Candida auris* CDC384, *Candida auris* CDC385, *Candida auris* CDC386, *Candida auris* CDC388 and *Candida auris* CDC389 were incubated with varying concentrations of Q-GRFT at 37°C in Sabourand Dextrose culture media. Fungal growth was determined periodically up to 72 hours using either a Bio-Rad TC10™ Automated cell counter, Singapore or an ECHO Rebel hybrid microscope (RBLTEW31), San Diego, USA. All *Candida* isolates tested were of human origin.

Fluorescence microscopy. *Candida albicans* cells were incubated with Fluorescein-labelled 7.8 µM Q-GRFT overnight, followed by DAPI staining. The cells were then fixed in 37% formaldehyde, mounted on glass slides, and visualized using an Axio Scope.A1 microscope, Carl Zeiss MicroImaging GmbH.

Fluorescence binding intensity. *C. albicans* cells were incubated with Fluorescein-labelled 7.8 µM Q-GRFT overnight, washed in PBS, and fluorescence intensity at

excitation/ emission wavelength 480/ 520 nm determined using a BioTek™ Synergy HT plate reader.

Detection of hydrogen peroxide and ROS. The staining procedure using 3,3'-diaminobenzidine (DAB) (280) was employed to detect hydrogen peroxide in *Candida albicans* cells following incubation with Q-GRFT. Briefly, fungal cells (1.0×10^5 cells/mL) were incubated for 2 hours on microslides with either 7.8 µM Q-GRFT, PBS (negative control) or 300 mM hydrogen peroxide (positive control) in the presence of 0.5 mg/mL DAB. Formation of hydrogen peroxide within cells, as a brown pellet, was evaluated microscopically. A count to determine the percentage of brown-stained cells following Q-GRFT treatment in comparison with the controls was performed from at least 3 independent experiments in triplicate.

The direct fluorescence method using H_2DCF-DA (281) was used to assess induction of ROS in *Candida albicans* cells following incubation with Q-GRFT. Briefly, *Candida albicans was grown* overnight from stock solution, to achieve growth in the exponential phase, followed by inoculate into a fresh Peptone Dextrose medium. Cells were then incubated with Q-GRFT (7.8 µM or 0.78 µM) overnight. Cultures were harvested and cell numbers optimized and kept constant for all treatment groups. Harvested cells were then centrifuged at 5000-6000g for 10 minutes followed by washing the pellet twice in PBS. Cells were then incubated for 30 minutes with H_2DCF-DA (10 µM) in PBS in the dark followed by centrifugation. The pellet was washed (2 times) and resuspended in 200µl PBS in a fluorescence/ black 96-well plate. Fluorescence intensity was determined with excitation and emission wavelengths at 504 nm and 524 nm, respectively, using a Synergy HT BioTek® plate reader.

Q-GRFT ability to bind to gp120 and cell wall components. Q-GFT's ability to bind to gp120 and *Candida albicans* cell wall components was determined using an ELISA assay. Briefly, a 96-well MaxiSorp NUNC plate was coated overnight with0.1 mL per well of either gp120, chitin, α-mannan or β-glucan. The plate was then blocked for 2 hours using 3% BSA in 1X PBS-T, 0.3 mL per well. Q-GRFT was then added at a concentration of 250 ng/mL with 2-fold dilutions performed down the plate. The plate was incubated for 1-2 hours at room temperature. A primary antibody, rabbit anti-GRFT,

0.1 mL per well, diluted 1:10,000 in 1X PBS was added and the plate incubated for 1 hour. A secondary antibody, goat anti-rabbit, Southern Biotech 4030-05, diluted at 1:25,000 in 1X PBS, 0.1 mL per well added followed by incubation for 1 hour. TMB solution, 0.1 mL per well was the added for 4 minutes and the reaction stopped with 0.1 mL per well of 1N Sulphuric acid. Absorbance was read at 450 nm using the Synergy HT BioTek® plate reader.

Viability assays. To determine the impact of Q-GRFT on *Candida albicans* viability, the trypan blue exclusion test of cell viability (282), was used. Briefly, *Candida albicans* was incubated with Q-GRFT (7.8 µM) at 37°C overnight followed by staining with 0.4% trypan blue (1 part trypan blue and 1 part cell suspension). The mixture was allowed to incubate at room temperature for ~3 minutes followed by cell evaluation by optical microscopy.

C. albicans viability analysis was also carried out using flow cytometry with BD Horizon™ Fixable Viability Stain 780 (FVS780). Following overnight growth with either Q-GRFT or PBS control, cells were added to complete RPMI medium (supplemented with 1M HEPES, penicillin/ streptomycin, fetal bovine serum and 2-Mercaptoethanol), filtered and centrifuged for 5 minutes at 1600 rpm. One to two million cells were then added to appropriate flow cytometry tubes, followed by washing with FACS buffer (BD Biosciences, San Diego California) for 5 min at 1600 rpm. Cells were then blocked with 2 µL of CD16/32 antibody (BioLegend, San Diego, California) for 10 minutes at 4°C, followed by staining with 1 µL of viability dye, and incubation at 4 °C for 30 minutes. Cells were then fixed, washed, re-suspended in 300 µL of FACS buffer, and analyzed using a BD device (BD LSR Fortessa™, USA), following manufacturer's instructions. Data was analyzed using Flowjo software (Tree Star, Inc, Ashland, Oregon).

***MIC determination*.** The MIC_{50}s and MIC_{90}s were determined by the broth dilution method as described by the European Committee on Antimicrobial Susceptibility Testing (EUCAST) (283).

Scanning electron microscopy. *C. albicans* cells were grown overnight in the presence of either PBS or 7.8 µM Q-GRFT, in Sabourand Dextrose media at 37°C. The media was then rinsed off and cells fixed for 24 hours at 4°C with SEM Fixative (2.5%

glutaraldehyde, 2.5% formaldehyde, 0.1M sodium cacodylate, pH 7.4). Cells were then rinsed and serially dehydrated in ethanol. They were then critically dried using hexamethyldisilazane (HMDS). Cells were then coated with gold/ palladium in a Cressington 108auto/SE sputter coater followed by examination using the Apreo 2 electron microscope.

Candida albicans RNA extraction and Sequencing. A total of 4.0×10^7 yeast cells were used for RNA extraction using the Qiagen RNeasy® Midi Kit, following manufacturer's instructions. DNase treatment was performed using the RNase-Free DNase set purchased from Qiagen®. RNA quantification was carried out spectrophotometrically at 260 nm and 280 nm using a NanoDrop 1000 spectrophotometer (ThermoScientific™, USA). For RNA sequencing, pairwise comparisons were made between treated groups [7.8 µM Q-GRFT (1QG), 0.78 µM (2QG) and 7.8 µM Lec(-)Q-GRFT (3QG)] with vehicle control (4VC). Sequencing was performed as follows:

1. ***Library Preparation***. Libraries were prepared using the Illumina Stranded mRNA Prep, Ligation (Illumina Cat# 20040532), IDT for Illumina RNA UD Indexes Set B, Ligation (Illumina Cat# 20040554). **A**. ***Purify and Fragment mRNA***. mRNAs were purified from 200 ng of total RNA samples with oligo(dT) magnetic RNA Purification Beads and denatured for 5 minutes at 65°C. Then the supernatant was discarded, and the beads were washed with bead wash buffer. Captured polyadenylated RNAs were eluted using Elution buffer at 80°C for 2 min. mRNAs were further purified in a second bead clean-up, then fragmented and primed during elution by adding 19 µl of Fragmentation Mix to the beads and incubating for 8 minutes at 94°C. After fragmentation, 17ul of supernatant was removed from the beads and proceeded immediately to synthesize first strand cDNA. **B.** ***Synthesize First Strand cDNA:*** Following the protocol, 8 µl of First Strand Synthesis Act D Mix and Reverse Transcriptase were added to each sample and heated on a thermocycler using preprogrammed conditions, to produce first strand cDNA from the hexamer-primed RNA fragments. **C.** ***Synthesize Second Strand cDNA:*** Second Strand Marking Mix was added, mixed well, and incubated at 16°C for one hour. Blunt-ended, double-stranded cDNA fragments were then purified using Agencourt AMPure XP Beads at 1.8X. 17.5 µl of elute was collected and stored at -20°C. **D.** ***Adenylate 3'***

Ends**:* Purified samples were mixed with 12.5 µl A-Tailing Mix then incubated on the preprogrammed thermal cycler. An adenine (A) nucleotide was added to the 3′ ends of the blunt fragments. **E. *Ligate Anchors: Ligation Mix and RNA index anchors were added and incubated in a pre-heated thermocycler at 30°C for 10 minutes. Stop Ligation Buffer was immediately added to each sample and mixed well. **F. *Clean Up Fragments:*** The ligated fragments were purified using Agencourt AMPure XP Beads at 0.8X. 20 µl of the elute was collected and used for library amplification. **G. *Amplify Library:*** 12 cycles of PCR reactions were performed to selectively amplify the anchor-ligated DNA fragments and to add indexes and primer sequences for cluster generation. Sample and Barcode Information: Samples were barcoded with IDT for Illumina DNA/RNA UD Indexes as listed in Table 3.1. **H. *Clean Up Library:*** Amplified libraries were purified using Agencourt AMPure XP Beads at 1.0X. 15 µl of eluted libraries were collected and stored at -20°C. **I. *Validate Library:*** The concentration of libraries was measured by Qubit dsDNA HS Assay Kit (Invitrogen Q32851). Libraries were diluted and normalized to the optimal range for Agilent Bioanalyzer analysis using the DNA High Sensitivity Kit (Agilent Technologies, Cat# 5067-4626). **J. *Normalize and Pool Libraries:*** The same amount of libraries were pooled based on the molar concentration from Bioanalyzer.

2. *Library Denaturing and Diluting for MiSeq Nano 300:* Pooled library was run on MiSeq to test quantity and quality, using the MiSeq Reagent Nano Kit V2 300 cycles (Illumina, Cat. No. MS-103-1001). Library and PhiX control (Illumina, Cat. No. FC-110-3001) were denatured and diluted using the standard normalization method following manufacturer's directions, to a final concentration of 12.5 pM. 300 µl of library and 300 ul of PhiX were combined and sequenced on Illumina MiSeq.

3. *Library re-pool:* Based on MiSeq results, equal amounts of libraries were re-pooled for NextSeq run.

4. *Library Denaturing and Diluting for Nextseq 500:* Library and PhiX were denatured and diluted using the standard normalization method following manufacturer's directions.

5. *Sequencing Run:* Sequencing was performed on the University of Louisville Brown Cancer Center Genomics Core Illumina NextSeq 500 using the NextSeq 500/550 75 cycle High Output Kit v2.5 (20024906). The total volume of library was 1.3 ml at 1.8

pM, with 1% PhiX spike in. Two runs were made for the analysis described in this manuscript.

Table 3.1. Sample and Barcode Information

Sample_ID	17_Index_ID	Index 1	15_Index_ID	Index 2
1QG1_Candida	UDP0121	AGAGAACCTA	UDP0121	GGTTATGCTA
1QG2_Candida	UDP0122	GATATTGTGT	UDP0122	ACCACACGGT
1QG3_Candida	UDP0123	CGTACAGGAA	UDP0123	TAGGTTCTCT
2QG1_Candida	UDP0124	CTGCGTTACC	UDP0124	TATGGCTCGA
2QG2_Candida	UDP0125	AGGCCGTGGA	UDP0125	CTCGTGCGTT
2QG3_Candida	UDP0126	AGGAGGTATC	UDP0126	CCAGTTGGCA
3QG1_Candida	UDP0127	GCTGACGTTG	UDP0127	TGTTCGCATT
3QG2_Candida	UDP0128	CTAATAACCG	UDP0128	AACCGCATCG
3QG3_Candida	UDP0129	TCTAGGCGCG	UDP0129	CGAAGGTTAA
4VC1_Candida	UDP0130	ATAGCCAAGA	UDP0130	AGTGCCACTG
4VC2_Candida	UDP0131	TTCGGTGTGA	UDP0131	GAACAAGTAT
4VC3_Candida	UDP0132	ATGTAACGTT	UDP0132	ACGATTGCTG

Bioinformatics data analysis was performed using the pipeline shown in FIG 3.1 below.

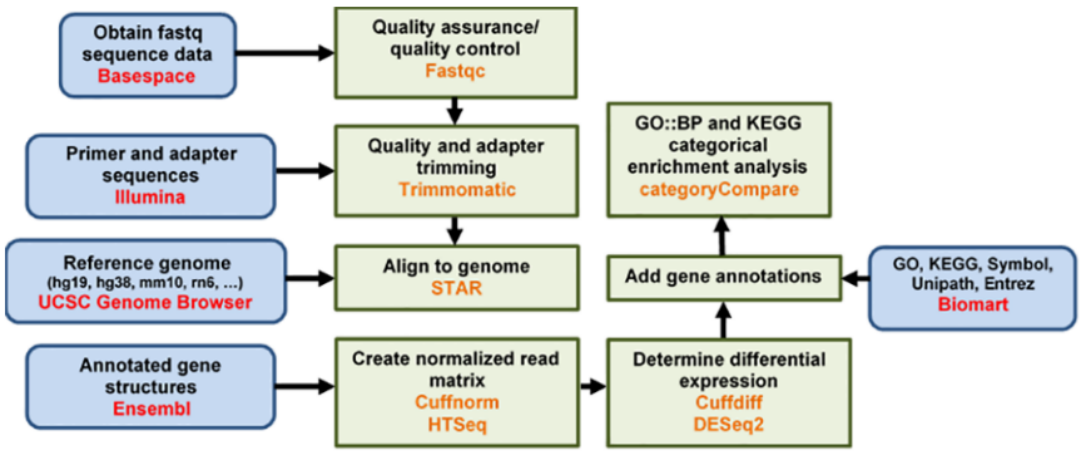

Figure 3. 1 Bioinformatics analysis workflow diagram.

Statistical analysis. Statistical analyses were performed using GraphPad Prism V7. Numerical data are presented as means ± standard deviation (SD) or mean ± standard error of mean (SEM). The number of repetitions and replicates of each assay and experiments are reported individually in the descriptions of each of the findings. Statistical differences between sets of data were evaluated using ANOVA and t-test, where indicated. $P \leq 0.05$ values were considered significant.

RESULTS

Effect of Q-GRFT on HIV replication

Given that GRFT has been shown previously to inhibit HIV replication (206), we determined whether Q-GRFT, a variant of GRFT (unpublished data), retained anti-HIV activity by establishing the lectin's impact on HIV-1 PsV replication. Unlike the mutant lectin-binding site deficient Q-GRFT [Q-GRFT $^{lec\ neg}$], wild type (WT) Q-GRFT inhibited HIV-1 PsV QH069 replication (FIG 3.2**)**. The IC_{50} for lec (-) Q-GRFT was ~27.5 ng/mL while WT Q-GRFT had an IC_{50} of 0.305 ng/mL (95% CI 0.2027 to 0.4380 ng/mL). These results suggest that Q-GRFT prevents HIV-1 PsV replication *in vitro*.

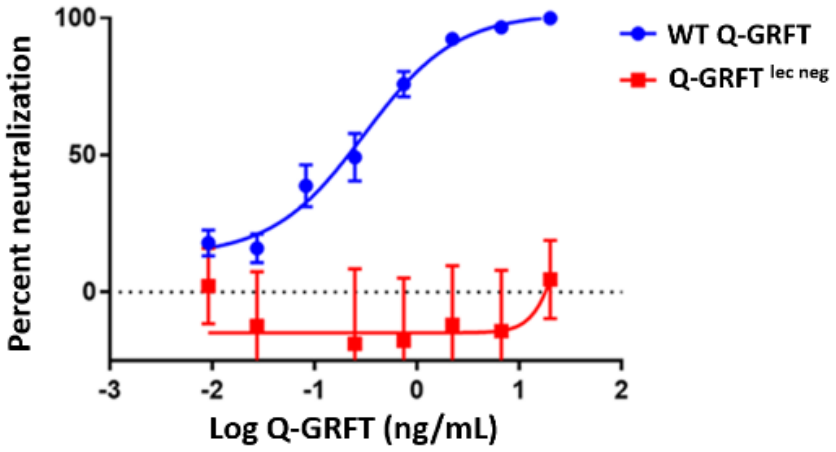

Figure 3. 2 Q-GRFT inhibits HIV PsV QH069 replication. Q-GRFT neutralization activity against HIV PsV was determined using HOS cell assay for anti-HIV PsV activity and luciferase activity. The graph shows percent virus neutralization (mean ± SEM) for Q-GRFT compared Q-GRFT $^{lec\ neg}$ deficient in sugar-binding activity, for HIV PsVQH09

at varying concentrations of the lectin. The calculated IC_{50} of WT Q-GRFT is 0.305 ng/mL. Triplicate assays were performed, and representative data is presented.

Effect of Q-GRFT on the growth of rectal microbiome (bacterial) components

Whilst exploring the impact on proteome and microbiome when GRFT was applied topically as a rectal gel in non-human primates, Girard et. al. found that the lectin induced small, but significant increases in relative abundances of *Ruminococcaceae* NK4A214 and *Christensenellaceae* R-7, but the effect was not sustained at 7 days post application (203). No other significant effects were observed in Rhesus macaque rectal microbiota after application of the gel. Against this background, we investigated the effect of Q-GRFT on the growth of representative bacteria found in the human gut: Aerobes -*Lactobacillus acidophilus* and *Lactobacillus casei;* facultative anaerobe *Escherichia coli* K12; and anaerobes- *Bifidobacterium longum longum* ATCC® 15707, *Clostridium difficile* ATCC® 51695-F2, Enterotoxigenic *Bacteroides fragilis* and Nontoxigenic *Bacteroides fragilis* (FIG 3.3). The selected bacterial components were incubated in presence of varying concentrations of Q-GRFT broth media, and growth established by determining optical density (OD) measurements over time on a plate reader. Q-GRFT had no detectable impact on the growth of any of the bacterial species tested. These data demonstrated that Q-GRFT likely does not inhibit the growth of bacterial microbiome.

We then tested Q-GRFT's growth inhibitory activity against select causative pathogens for sexually transmitted infections, *Chlamydia trachomatis* and *Neisseria gonorrhea*. There was no detectable impact of Q-GRFT on the *in vitro* growth of *Chlamydia trachomatis* and *Neisseria gonorrhea* (Table 3.2).

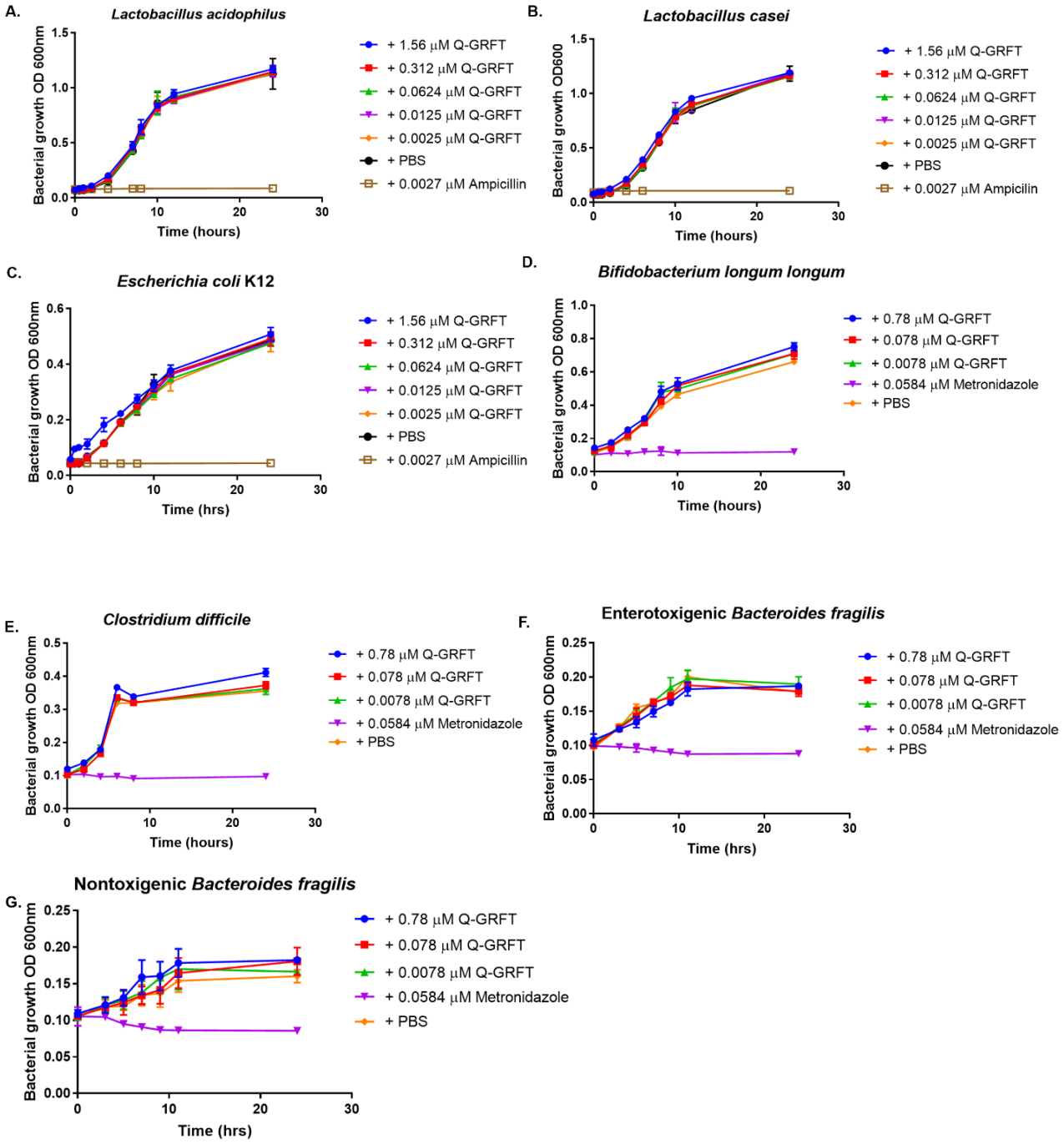

Figure 3. 3 The effect of Q-GRFT on the growth of rectal microbiome (bacterial) components.

(A) *Lactobacillus acidophilus* **(B)** *Lactobacillus casei* **(C)** *Escherichia coli* K12 **(D)** *Bifidobacterium longum longum* ATCC® 15707 **(E)** *Clostridium difficile* ATCC® 51695-F2 **(F)** Enterotoxigenic *Bacteroides fragilis* and **(G)** Nontoxigenic *Bacteroides fragilis.* Microbiome components were incubated with either varying concentrations of Q-GRFT,

PBS vehicle or control antibiotics in broth media and growth monitored periodically up to 24 hours. Data represents results mean ± SD from 3 independent experiments.

Table 3.2. MIC_{50} results for Q-GRFT against *Chlamydia trachomatis* and *Neisseria gonorrhea*.

Compound	*Chlamydia trachomatis*	*Neisseria gonorrhea*
Q-GRFT (µg/ml)	>50	>50
Doxycycline (µg/ml)	0.03	-
Penicillin (µg/ml)	-	0.03

McCoy cells were plated in a 96-well plate and infected with *Chlamydia trachomatis*. Cells were then treated with either Q-GRFT or doxycycline, fixed, stained with iodine, and observed for inclusion bodies to establish MIC_{50}. Q-GRFT was also added to agar medium inoculated with *Neisseria gonorrhea* to determine inhibitory activity against the pathogen.

Effect of Q-GRFT on the growth of Candida albicans

Since yeast and fungi are universally present in gut microbial communities (284), we next investigated the impact of Q-GRFT on the growth of *Candida albicans* ATCC 32032, as a representative of the gut fungal community. Yeast counts were determined using a Bio-Rad TC10^{TM} Automated cell counter, Singapore, or an ECHO Rebel hybrid microscope (RBLTEW31), San Diego, USA. Following incubation with *Candida albicans* for 24, 48 and 72 hours (FIG 3.4A), Q-GRFT significantly inhibited fungal growth; $P<0.0001$ at all concentrations tested (7.80 µM, 0.78 µM and 0.078 µM). We next sought to confirm Q-GRFT's growth inhibitory activity by incubating *C. albicans* with the Q-GRFT variant, Q-GRFT $^{lec\ neg}$, devoid of its glycan binding ability. Incubation of *C. albicans* with various concentrations of Q-GRFT $^{lec\ neg}$ for up to 72 hours did not demonstrate any inhibitory impact on growth (FIG 3.4B), suggesting a role of Q-GRFT's binding on fungal inhibitory activity.

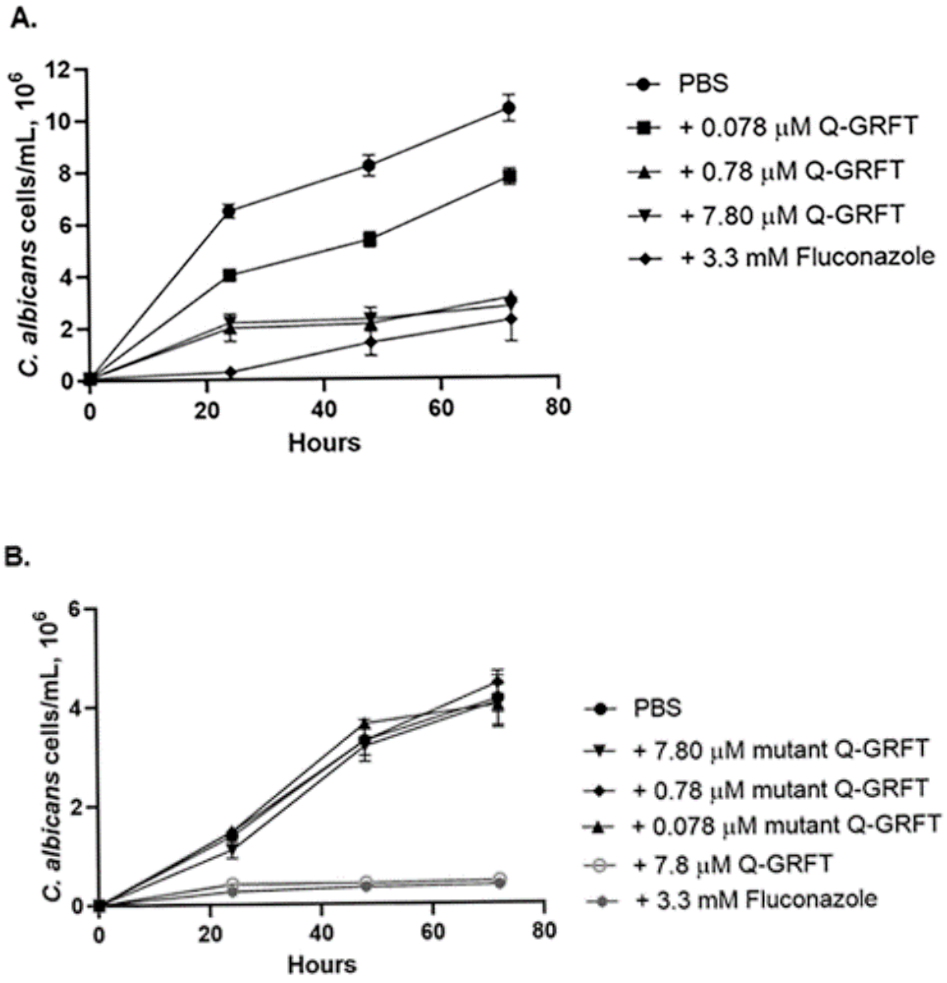

Figure 3. 4 Effect of Q-GRFT on the growth of *Candida albicans*. **(A)** *Candida albicans* ATCC 32032 at a concentration of $1.0x10^5$ cells/mL was incubated with varying concentrations of Q-GRFT and fluconazole control at 37°C in Sabourand Dextrose culture medium and growth monitored at 24, 48, and 72 hours. **(B)** *C. albicans* ($1.0x10^4$ cells/mL) was incubated with varying concentrations of Q-GRFT $^{lec\ neg}$ (7.80 M, 0.78 M), with fluconazole (3.3 mM) and PBS as controls, at 37°C in Sabourand Dextrose culture medium. Growth was monitored at 24, 48, and 72 hours. Fungal counts were performed using either a Bio-Rad TC10^{TM} Automated cell counter, Singapore, or an ECHO Rebel hybrid microscope (RBLTEW31), San Diego, USA. Both experiments were performed in triplicate. Representative data (*Mean* $\pm$ *SD*) from at least 3 independent experiments is shown, with comparisons made using one -way *ANOVA*.

Q-GRFT's growth inhibitory activity is dependent on the lectin's binding to Candida albicans

Since Q-GRFT inhibited the growth of *C. albicans*, we sought to determine if this activity was dependent on Q-GRFT binding. *C. albicans* (1.0×10^5 cells/ mL) was cultured overnight with either Fluorescein-labeled Q-GRFT, unlabeled Q-GRFT or the Fluorescein-labeled Q-GRFT $^{lec\ neg}$. Cells were then centrifuged, washed, and fluorescence intensity of the pellet determined. *C. albicans* incubated with Fluorescein-Q-GRFT displayed the highest fluorescence intensity compared to the non-labeled Q-GRFT ($P<0.0001$) and Fluorescein- Q-GRFT $^{lec\ neg}$ ($P<0.0001$) (FIG 3.5A). To confirm lectin binding, *C. albicans* was cultured overnight with either Fluorescein-Q-GRFT, Q-GRFT or Fluorescein- Q-GRFT $^{lec\ neg}$, and the cells visualized using fluorescence microscopy. Green fluorescence was observed around yeast cells incubated with Fluorescein-Q-GRFT, confirming Q-GRFT's binding to *C. albicans* (FIG 3.5B). No fluorescence was observed following incubation with Fluorescein-Q-GRFT $^{lec\ neg}$ (data not shown).

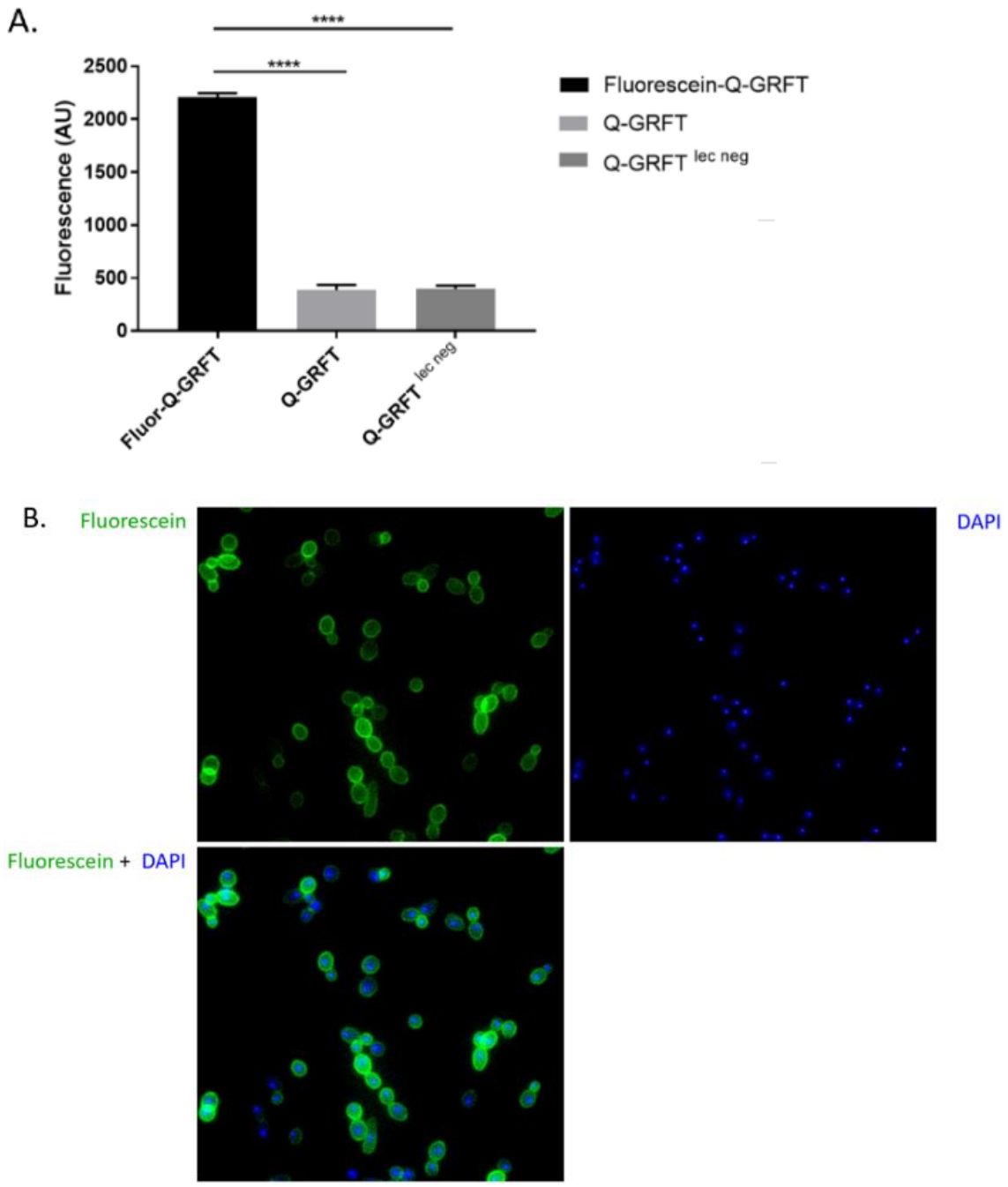

Figure 3. 5 Q-GRFT binds to *Candida albicans*. **(A)** Fluorescence intensity of *Candida albicans* cultured with either Fluorescein-Q-GRFT, Q-GRFT or Q-GRFT $^{lec\ neg}$, at lectin concentrations of 7.8 µM. **(B)** Fluorescence microscopy following culture of *Candida albicans* with Fluorescein-Q-GRFT. Green fluorescence demonstrates localization to *C. albicans* cells. DAPI demonstrates DNA staining. Scale bars are 3 µm. Experiments were

performed in triplicate and repeated at least 3 times. The results shown are *Mean ± SD* **(A)** and representative images of the microscopy studies **(B).**

Q-GRFT binds to Candida albicans cell wall component α-mannan but not chitin or β-glucan

We next investigated the *C. albicans* cell wall components to which Q-GRFT binds. Since the lectin bound to C. *albicans*, we hypothesized that Q-GRFT likely binds to either chitin, glucans or mannans, which are predominant core components of the fungal cell wall (285, 286). In addition, chitin is a polymer of *N*-acetyl-D-glucosamine (287), while mannan is an *N*-glycosylated polysaccharide with oligomannose side chains and branch chain mannose residues (288). Furthermore, β-glucans are composed of linkage glucose units (285). These structures, hence, provide likely binding targets for lectins, including Q-GRFT (6). Using ELISA binding assays (FIG 3.6A), we determined the ability of Q-GRFT to bind to plate-immobilized antigens α-mannan, β-glucan and chitin. Q-GRFT bound to α-mannan with EC_{50} 23.47 ng/mL (95% CI 17.63 to 35.25 ng/mL). Q-GRFT did not bind to chitin or β-glucan. Because Q-GRFT binds to gp120, we next sought to determine if the lectin's binding to the glycoprotein is inhibited in the presence of free and unbound cell wall components α-mannan, chitin or β-glucan in a competition assay. Additionally, as antigens attach to the solid interface in the ELISA assay, they are likely to denature and/ or undergo conformational changes that may affect their interaction with other biomolecules (289). Therefore, Q-GRFT was incubated with either free α-mannan, chitin or β-glucan, prior to determining its binding to gp120. Q-GRFT's binding to gp120 was inhibited in the presence of high concentrations of α-mannan (FIG 3.6B), but not chitin (FIG 3.6C) or β-glucan (FIG 3.6D). Results for EC_{50} and CI values for the free-antigen binding assays are shown in Table 3.3 below. One limitation of the α -mannan binding assay was that we did not demonstrate maximal binding as we did not obtain the plateau readings upon Q-GRFT incubation. However, altogether, results from these binding studies are strongly suggestive that that Q-GRFT binds to α-mannan, but not chitin or β-glucan in the *C. albicans* cell wall.

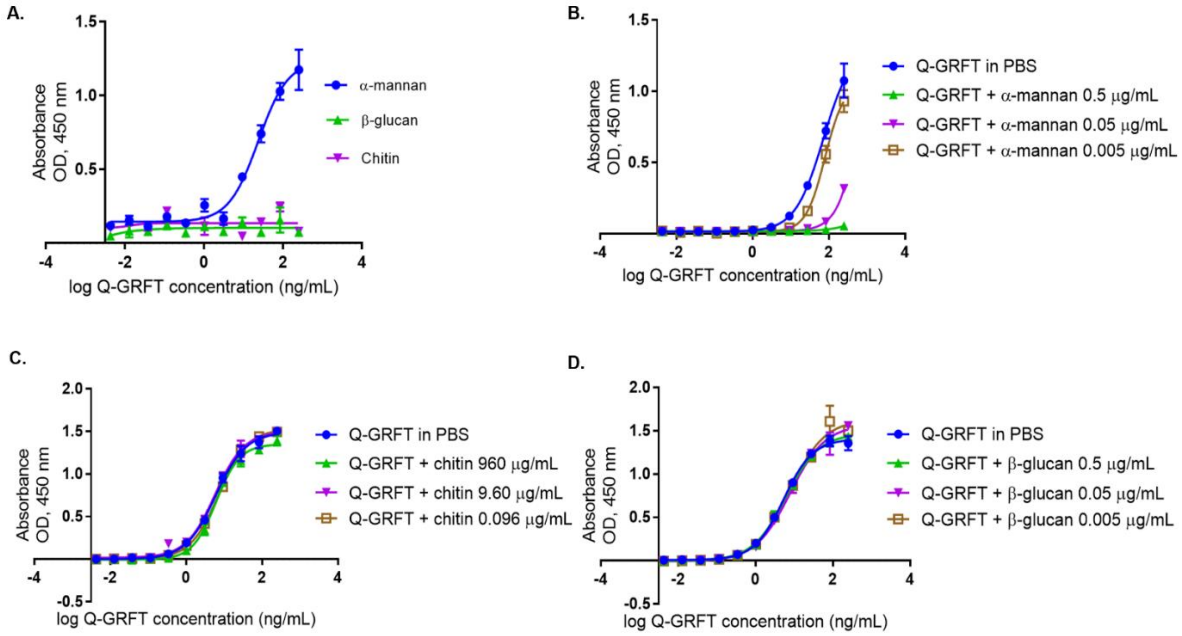

Figure 3. 6 Q-GRFT binds to *C. albicans* cell wall. **(A)** Q-GRFT binds to *C. albicans* cell wall component α-mannan but not chitin or β-glucan. An ELISA binding assay was performed, with the plate coated with 100 µL of either α-mannan (20 µg/mL), chitin (2.0 mg/mL) or β-glucan (40 µg/mL). Q-GRFT's binding to these components was then determined. **(B)** Unlike the low concentration (0.005 µg/mL), higher concentrations of α-mannan (0.5 µg/mL and 0.05 µg/mL) inhibited Q-GRFT's binding to gp120, in a competition ELISA assay. Q-GRFT was incubated with free (unbound) α-mannan and its ability to bind gp120 determined. When incubated with free (unbound) chitin **(C)** and β-glucan **(D)** Q-GRFT's binding to gp120 was not inhibited in a competition ELISA assay. ELISA plates were coated with gp120 for assays in **(B)-(D)** and absorbance determined upon Q-GRFT binding. Experiments were performed in triplicate and repeated at least 3 times. Representative data from the experiments is shown. One-way *ANOVA* was used for all statistical comparisons.

Table 3.3. Competition ELISA assay values (EC_{50} and 95% CI) for Q-GRFT binding to α-mannan, chitin and β-glucan.

Q-GRFT incubation	**EC_{50} (ng/ mL)**	**95% CI (ng/ mL)**
Q-GRFT + α-mannan 0.005 µg/ mL	79.35	69.19 to 97.85
Q-GRFT + α-mannan 0.05 µg/ mL	-	-
Q-GRFT + α-mannan 0. 5 µg/ mL	-	-
Q-GRFT in PBS	72.46	55.17 to 115.10
Q-GRFT + chitin 0.096 µg/ mL	7.30	6.73 to 7.92
Q-GRFT + chitin 9.60 µg/ mL	5.79	4.85 to 6.98
Q-GRFT + chitin 960 µg/ mL	6.18	5.45 to 7.04
Q-GRFT in PBS	6.02	5.23 to 7.00
Q-GRFT + β-glucan 0.005 µg/ mL	7.77	5.90 to 10.58
Q-GRFT + β-glucan 0.05 µg/ mL	7.92	6.51 to 9.90
Q-GRFT + β-glucan 0.5 µg/ mL	6.01	5.37 to 6.77
Q-GRFT in PBS	5.32	4.73 to 6.00

Q-GRFT was incubated with either free α-mannan, chitin, or β-glucan in solution, and the lectin's binding to a 96-well plate-coated gp120 determined. The table summarizes Q-GRFT EC50 and 95% CI values following incubation with the respective α-mannan, chitin, or β-glucan concentrations.

Effect of Q-GRFT on Candida albicans' cell structure, integrity and oxidative status

Treatment of *C. albicans* with helianthus annus (Helja) lectin has been shown to alter membrane permeability and induce intracellular formation of oxidative species (280). Therefore, we hypothesized that Q-GRFT lectin may act similarly, altering fungal cell wall permeability and inducing expression of intracellular reactive oxidative species (ROS), with subsequent cellular injury and/ or damage, leading to leading to cell death. To demonstrate the impact on cell wall integrity, *C. albicans* was incubated with 7.8 µM

Q-GRFT overnight at 37°C, followed by Trypan Blue staining, with the dye uptake demonstrating breached cell wall/ membrane integrity, and penetration into dead/ non-viable cells. Compared to the PBS control, Q-GRFT treatment resulted in significant intracellular blue color staining, indicative of non-viable cells with impaired cell wall integrity, $P<0.0001$ (FIG 3.7A). To further confirm disruption of cell wall and membrane integrity, we next performed live/ dead cell viability staining of 7.8 µM Q-GRFT- and PBS control- treated *C. albicans* cells and measurements determined at flow cytometry (FIG 3.7B and 3.7C). These cells were incubated at 37°C overnight under the respective treatment conditions. FIG 3.7B is a representative image of the gating strategy for both Q-GRFT and PBS-treatments. Fixable Viability Stain 780+ cells were considered as dead cells with disrupted membrane integrity. Q-GRFT treatment resulted in a significantly higher proportion of dead cells, compared to PBS control treatment, $P<0.0001$ (FIG 3.7C).

To investigate the induction of ROS by Q-GRFT, *C. albicans* cells were incubated overnight with 7.8 µM Q-GRFT followed by incubation with 3, 3-diaminobenzidine (DAB) for 2 hours. In the presence of peroxides, DAB is oxidized to an insoluble brown precipitate that is visualized within cells using optical microscopy. Compared to the PBS vehicle treated control, a significantly large proportion of *Candida albicans* cells incubated with Q-GRFT developed a brown intracellular precipitate. Quantification of this effect revealed that the presence of peroxides was significantly higher ($P<0.0017$) following Q-GRFT treatment than with PBS control (FIG 3.7D). To confirm the presence of ROS, we used the H_2DCF-DA assay technique to profile the oxidative status of Q-GRFT- treated and PBS vehicle-treated control cells. This assay is dependent on cellular esterase ability to cleave acetate groups on H_2DCF-DA, releasing an intermediate H_2DCF product which reacts with ROS forming fluorescent 2',7'-dichlorofluorescein (DCF) (281). Compared with PBS vehicle-treated control cells, Q-GRFT treatment was associated with higher fluorescence activity ($P<0.002$, $P<0.006$ for 7.8 µM and 0.78 µM respectively) following H_2DCF assay (FIG 3.7E). Centrifugation of cells during preparation for H_2DCF assay may induce ROS accounting for the low-level induction observed in the negative control (PBS vehicle-treated) cells (281). It is likely

that different Q-GRFT concentrations elicit various levels of cellular stress, accounting for the differences in ROS formation for both 7.8 µM and 0.78 µM Q-GRFT treatments.

To further evaluate any structural changes to *C. albicans* following treatment with Q-GRFT, high resolution scanning electron microscopy (SEM) was performed for both Q-GRFT- treated and -PBS vehicle- treated control cells (FIG 3.8). Yeast cells were treated with either 7.8 µM Q-GRFT or PBS vehicle and incubated overnight at 37°C prior to imaging. The vehicle- treated control cells demonstrated a normal budding pattern, were predominantly spherical to oval in shape (FIG 3.8A), with polar buds and bud scars (FIG 3.8B) and smooth edges and surfaces (FIG 3.8C). Q-GRFT treated cells were spherical to circular (FIG 3.8D, 3.8E), rough in appearance, demonstrated desiccated and wrinkled surfaces with uniform indentations (FIG 3.8E, 3.8F), and with a loss of polar budding (FIG 3.8F).

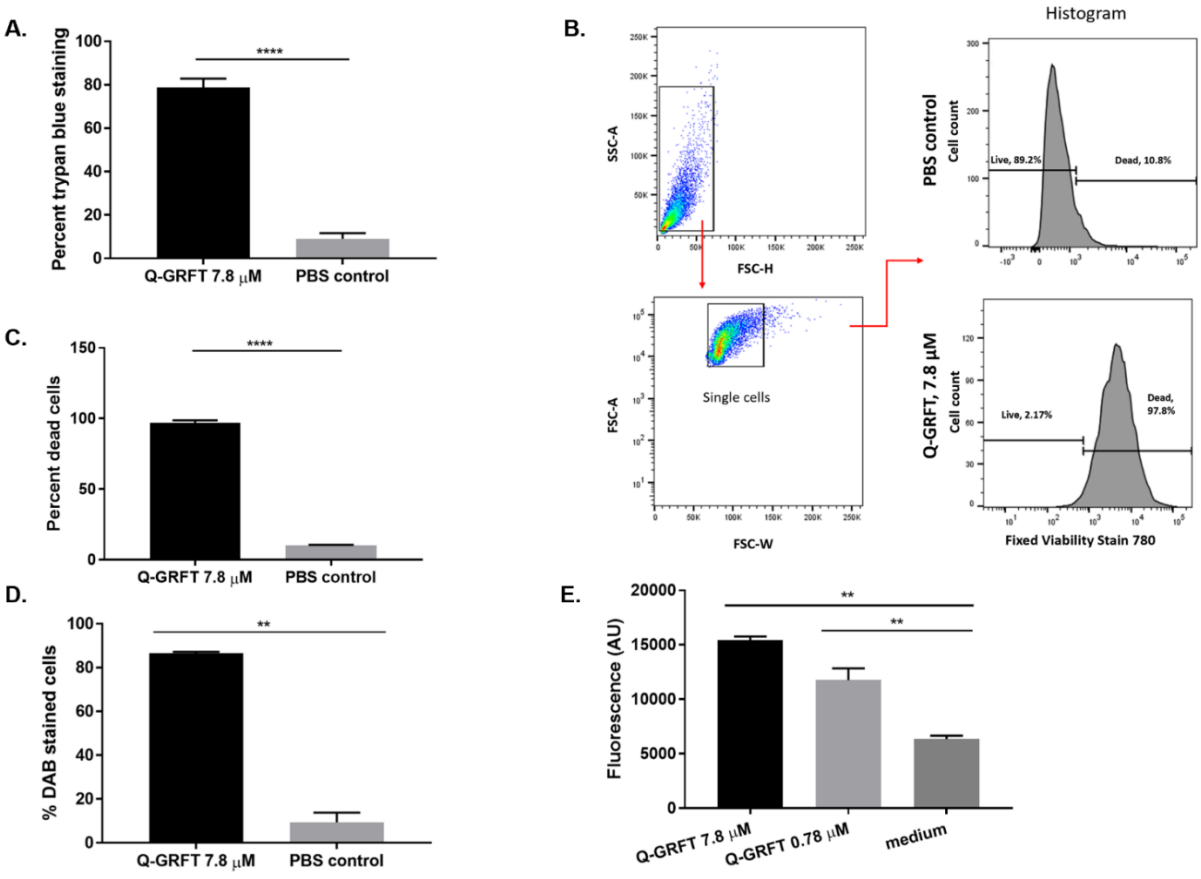

Figure 3. 7 Effect of Q-GRFT on *C. albicans*' cell integrity and oxidative status. **(A)** Yeast cells were incubated in the absence or presence of Q-GRFT (7.8 µM) overnight at

37°C, followed by staining with Trypan Blue to detect non-viable cells. Data is representative of results from at least 3 experiments with 3 biological replicates, *Mean* ± *SD*, $P<.0001$. **(B)** *C. albicans* (1.0×10^5 cells/ mL) was incubated overnight with either Q-GRFT 7.8 µM or PBS control and cell viability determined using flow cytometry. Dead cells were identified following staining with 1 µL Fixable Viability Stain 780 and were those that demonstrated up take of the dye. Representative gating strategy for both Q-GRFT treated, and PBS control-treated cells is presented. **(C)** Quantification of the percentage of dead cells obtained from flow cytometry measurements for Q-GRFT-treated and PBS-treated *C. albicans* in **(B)**. Results show *Mean* ± *SD*, $P<0.0001$. Experiments were performed three times and representative data is shown. **(D)** *Candida albicans* cells were incubated with Q-GRFT (7.8 µM) or PBS overnight followed by incubation in the presence of 0.5 mg/mL DAB for 2 hours to detect hydrogen peroxide. Quantification of the proportion (percentage) of DAB staining cells following either Q-GRFT or PBS treatment for the experiments is shown, *Mean* ± *SD*, $P=.0017$. **(E)** *Candida albicans* was incubated overnight with Q-GRFT (7.8 and 0.78 µM) or medium only at 37°C. Cells were harvested and 3.2×10^6 cells per treatment used for direct fluorescence using the H_2DCF-DA assay to determine Reactive Oxygen Species (ROS) levels in the cells. Experiments were performed in triplicate and representative data is shown, *Mean* ± *SD*, Q-GRFT 7.8 µM $P=0.0015$ and Q-GRFT 0.78 µM $P=0.0068$.

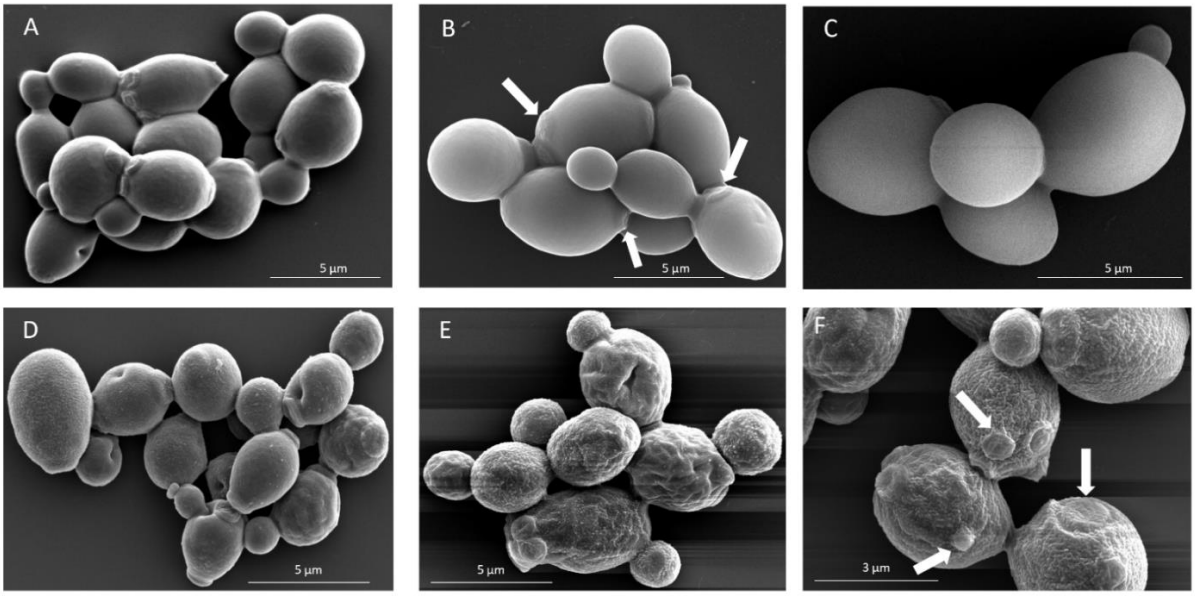

Figure 3. 8 *C. albicans* surface phenotype following treatment with Q-GRFT. *C. albicans* was grown overnight in Sabourand medium in presence of either PBS **(A-C)** or 7.8 µM Q-GRFT **(D-E)** at 37°C. Cells were then observed by SEM. **(A)** Budding morphology of *C. albicans*. Note the spherical to oval appearance of cells. Magnification x7500. **(B)** Cells with smooth surface, polar budding and bud scars (arrows). Magnification x10000. **(C)** Note the smooth cell surface and absence of any 'non-polar' bud scars. Magnification x12500. **(D)** Cells with spherical to circular shape with rough surface. Magnification x7500. **(E)** Note the rough surface, uniform indentations with a desiccated and wrinkled appearance. Magnification x10000. **(F)** Note the loss of polar budding, more circular appearance, and cells with multiple bud scars (arrows). Magnification x17500.

Impact of Q-GRFT on the growth of non-Candida albicans species

Given the recent increase in *Candida* spp. resistance to antifungal drugs (290), we next investigated the impact of Q-GRFT on the growth of human pathogenic non-*Candida albicans* species including the multidrug resistant (MDR) *Candida auris*. Most of the *C. auris* strains isolated from patients and identified in the United States belong to clades originating from South America and South Asia (291). We therefore tested Q-GRFT's growth inhibitory activity on representative isolates from these and other clades

including *C. auris* CDC388 and *C. auris* CDC389 -South Asia clade; *C. auris* CDC385 and *C. auris* CDC386 -South America clade; and *C. auris* CDC383 and *C. auris* CDC384 -Africa clade. The other non-*Candida albicans* species tested included *Candida glabrata* CDC316, *Candida krusei* CDC397 and *Candida parapsilosis* CDC337. Q-GRFT was incubated with *Candida glabrata*, *Candida krusei* and *Candida parapsilosis* at 37°C and growth monitored periodically using an automated cell counter, at 24, 48 and 72 hours. Compared to the medium control, Q-GRFT significantly inhibited the growth of all the species tested, with the greatest effect demonstrated with the 7.80 µM lectin concentration, $P<0.0001$ for all species and concentrations tested (FIG 3.9A, 3.9B, 3.9C). When incubated with *Candida auris*, Q-GRFT significantly inhibited the growth of strains *Candida auris* CDC388 and *Candida auris* CDC389, $P<0.0001$, for the lectin concentrations 0.78 µM and 7.8 µM tested (FIG 3.9D, 3.9E). There was no observable impact on the growth of strains *Candida auris* CDC383 (FIG 3.9F), *Candida auris* CDC384 (FIG 3.9G), *Candida auris* CDC385 (FIG 3.9H) and *Candida auris* CDC386 (FIG 3.9I).

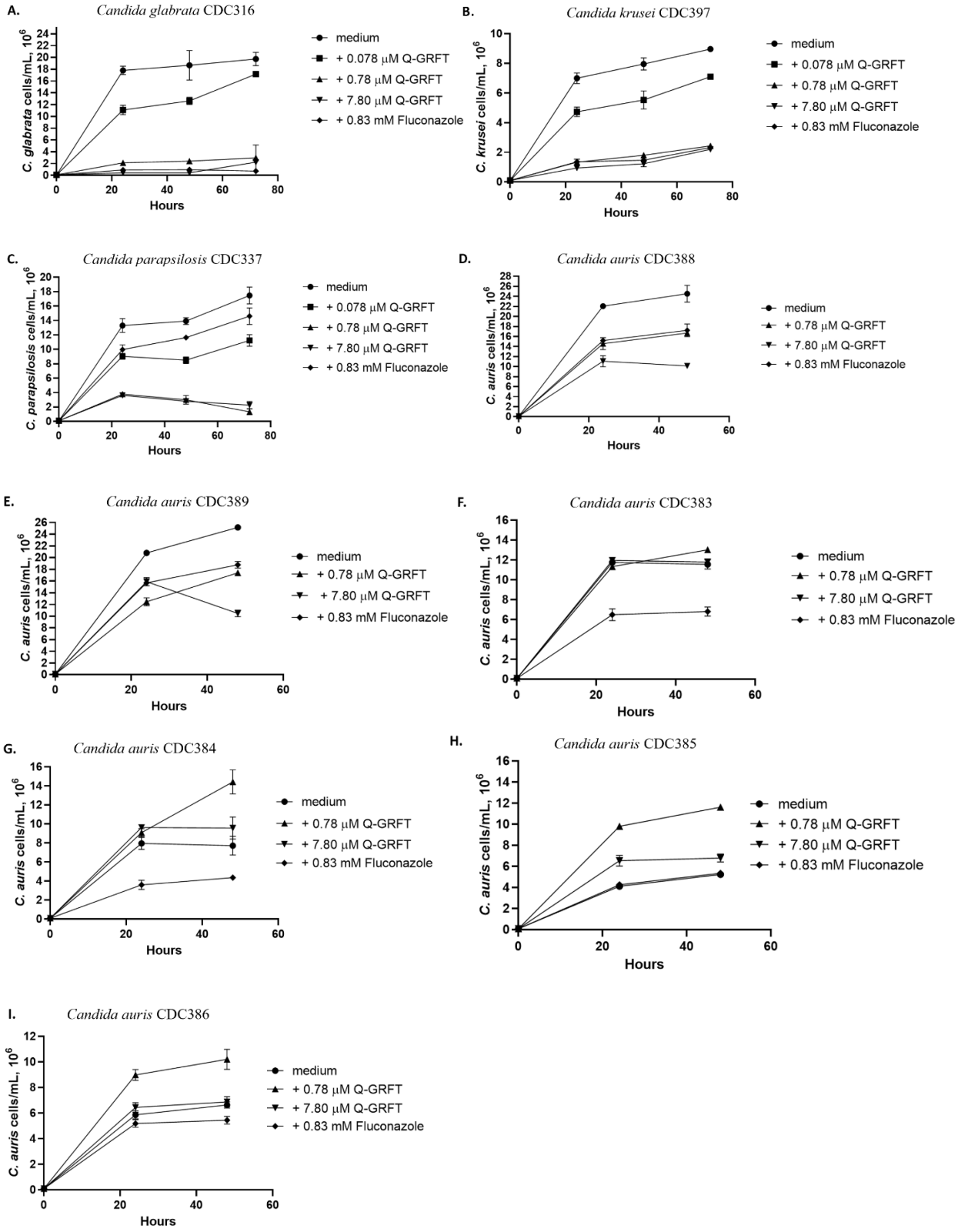

Figure 3. 9 Impact of Q-GRFT on growth of non-*C. albicans* species. **(A)** *Candida glabrata* CDC316 **(B)** *Candida krusei* CDC397 **(C)** *Candida parapsilosis* CDC337 *and*

multi-drug resistant *Candida auris strains* **(D)** *Candida auris* CDC389 **(E)** *Candida auris* CDC389 **(F)** *Candida auris* CDC383 **(G)** *Candida auris* CDC384 **(H)** *Candida auris* CDC385 and **(I)** *Candida auris* CDC386 at a concentration of $1.0x10^5$ cell/mL were incubated with different concentrations of Q-GRFT and fluconazole control at 37°C in Sabourand Dextrose culture media and growth monitored up to 72 hours. Fungal counts were performed using either a Bio-Rad TC10™ Automated cell counter, Singapore, or an ECHO Rebel hybrid microscope (RBLTEW31), San Diego, USA. Data represents mean ± SD from 3 independent experiments and was analyzed using one-way *ANOVA*.

Minimum inhibitory concentrations of Q-GRFT for Candida spp.

Starting with a maximum concentration of 95 µg/mL, MICs were determined for Q-GRFT's activity against different *Candida* isolates and are summarized in Table 3.4. The MIC_{50}s of Q-GRFT for *C. albicans*, *C. glabrata*, *C. parapsilosis*, *C. krusei*, *C. auris* CDC388 and *C. auris* CDC389 were 6, 95, 24, 95, 48 and 95 µg/mL, respectively, while MIC_{90}s for *C. albicans*, *C. parapsilosis* and *C. auris* CDC389 were 95 µg/mL for all isolates, respectively.

Table 3.4. MIC_{50}s and MIC_{90}s of Q-GRFT against different *Candida* species.

***Candida* isolate**	**MIC_{50}** (µg/mL)	**MIC_{90}** (µg/mL)
Candida albicans ATCC32020	6	95
Candida glabrata CDC316	95	-
Candida parapsilosis CDC337	24	95
Candida krusei CDC397	95	-
Candida auris CDC388	48	95
Candida auris CDC389	95	-

RNA expression profile of C. albicans following treatment with Q-GRFT

To better understand the impact of Q-GRFT on *C. albicans* growth and metabolism, we sought to determine the differential RNA expression profile upon lectin treatment. *C. albicans* was treated overnight with either 7.8 µM Q-GRFT (1QG), 0.78 µM Q-GRFT (2QG) or the binding-site deficient lectin 7.8 µM Q-GRFT $^{lec\ neg}$ (3QG), and comparisons made with the untreated control (VC), following RNA isolation and sequencing. The principal component analysis (PCA) results showed that the experimental groups clearly had good separation based on treatment status (FIG 3.10A). Differential expression analysis was performed for the different treatments using DESeq2. When compared to VC, venn diagram analysis identified 1134, 83 and 493 differentially expressed genes (DEGs) that were only unique to 1QG, 2QG and 3QG, respectively (FIG 3.10B). In addition, 587, 55 and 268 genes were uniquely up-regulated DEGs, while 567, 43 and 254 were uniquely down-regulated DEGs for 1QG, 2QG and 3QG, respectively (FIG 3.11A, 3.11B). Cluster analysis of the DEGs for all groups demonstrated significant differences upon treatment (FIG 3.10C, 3.11C). Further analysis of differential expressed genes in the 1QG treatment group demonstrated significant abundant elevations of genes involved in carbohydrate metabolism (GAL10), nitric oxide metabolism (YHB1), filamentous growth (FGR41), and DNA and protein synthesis, among other genes (adjusted p value<0.05). Decreased genes included those involved in RNA synthesis (RNR1), filamentation (RBR1) and phosphate ion transport (PHO84), among others (adjusted p value<0.05) (FIG 3.10D). Kyoto Encyclopedia Analysis of Genes and Genomes (KEGG) pathway analysis indicated that upregulated DEGs following 1QG treatment were highly associated with metabolic pathways, ribosome, metabolites biosynthesis, cell cycle and DNA repair, and genes in response to oxidative stress (like SOD3), among others (Data not shown). The top 20 down-regulated DEGs for 1QG vs VC treatment are shown in Table 3.5. Low dose treatment (2QG) demonstrated elevation of genes required to maintain mitochondrial respiration during stressful periods (AOX1, AOX2, MRF1), glutamate metabolism (GAD1) and cell adhesion and virulence (PGA22), among others. Conversely, genes responsible for meiotic division (MCD1, CCN1), iron metabolism (HMX1) and filamentous growth and hyphae formation during cell stress (SHA3, GIN4), among others were significantly decreased (FIG 3.10D). KEGG pathway analysis indicated that following 2GQ treatment, upregulated DEGs

were highly associated with glycolysis/ gluconeogenesis, carbon metabolism, biosynthesis of secondary metabolites, cell cycle and DNA replication and repair, among others. The top 20 down-regulated DEGs for 2QG vs VC treatment are shown in Table 3.6. Treatment with QGRFT $^{lec\ neg}$ resulted in decreased expression of genes involved in iron metabolism (FRE7, FRE30), copper homeostasis (CTR1), biofilm formation and RNA synthesis (RNR1) (FIG 3.10E). Upon treatment with Q-GRFT $^{lec\ neg}$, KEGG pathway analysis revealed upregulation of metabolic pathways, cell cycle, meiosis and homologous recombination. Interestingly, genes (GPX2, SOD3) produced in response to oxidative stress were among those downregulated with Q-GRFT $^{lec\ neg}$ treatment. The top 20 down-regulated DEGs for 3QG vs VC treatment are shown in Table 3.7. The PANTHER Classification System (292) was used to identify enriched Gene Ontology biological processes for each set of differentially expressed genes. Results revealed that Q-GRFT treatment (1QG) significantly enriched biological processes involved in DNA damage repair, DNA replication, sterol and steroid biosynthesis and disaccharide metabolism (FIG 3.10E). Similarly, 2QG treatment enriched processes involved in DNA and RNA metabolism, carbohydrate metabolism including glucose, galactose and pyruvate and amino acid catabolism (FIG 3.12A). Q-GRFT $^{lec\ neg}$ treatment enriched processes involved in DNA formation and elongation, cell adhesion and biofilm formation (FIG 3.12B).

Given these findings, we next sought to determine if the differences in RNA expression were initiated earlier in *C. albicans* treatment and would be preserved when compared to the overnight treatment. *C. albicans* was cultured overnight, and then incubated with either Q-GRFT, Q-GRFT $^{lec\ neg}$, medium only or with PBS. Samples were incubated at 37°C for 4 hours, followed by RNA sequencing (FIG 13). Compared with medium, PBS and Q-GRFT $^{lec\ neg}$, Q-GRFT upregulated the expression of 113, 2 and 61 genes, respectively. Additionally, 38, 84, and 6 genes were down regulated following Q-GRFT treatment, when compared with medium, PBS and Q-GRFT $^{lec\ neg}$ treatments, respectively (Table 3.8). Genes altered following Q-GRFT treatment were responsible for cell cycle regulation, stress response, cell repair and various other metabolic processes (Table 3.9).

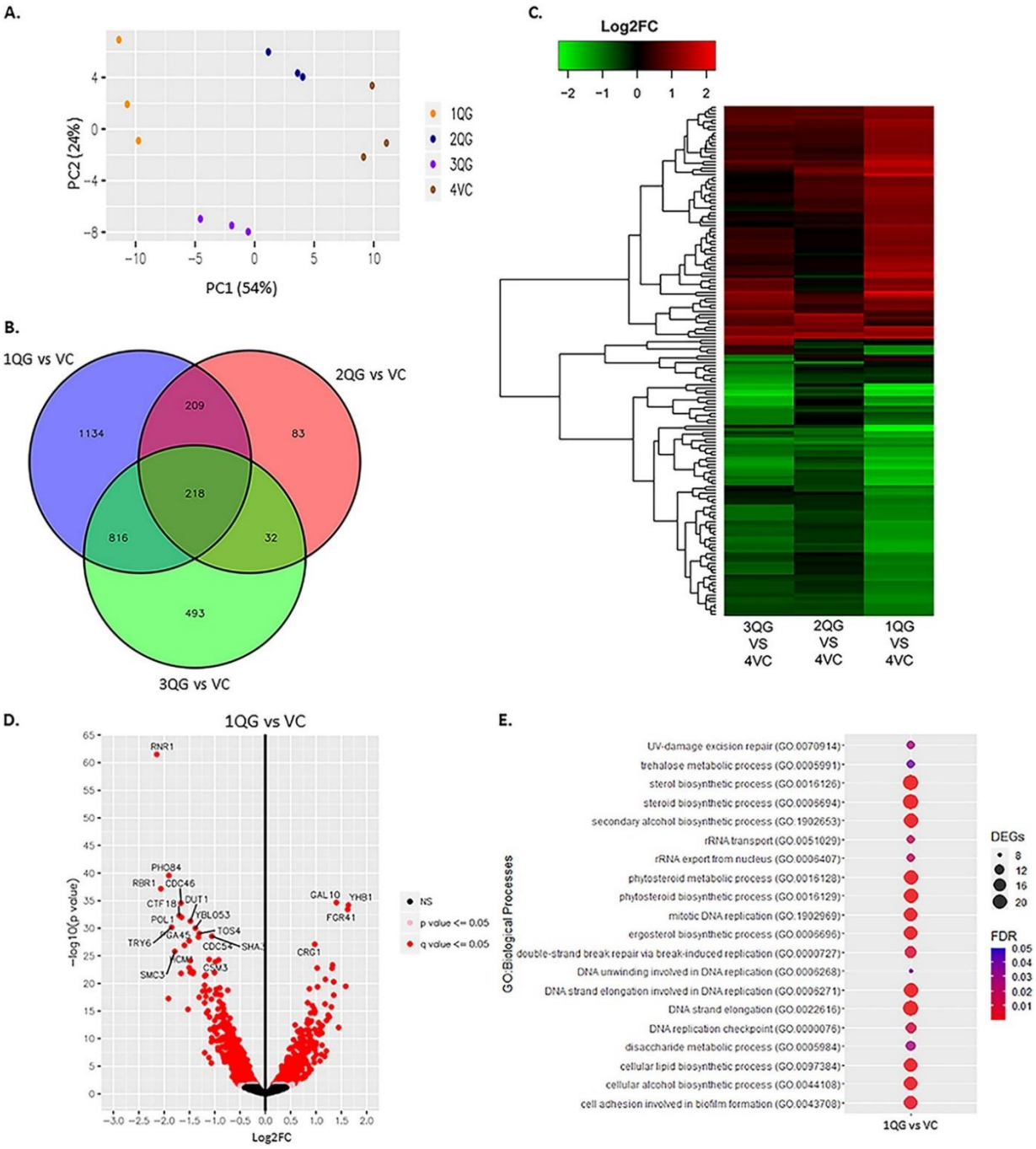

Figure 3. 4 *C. albicans* RNA expression profile following treatment with Q-GRFT. *C. albicans* at a concentration of $1.0x10^5$ cells/mL was incubated overnight at 37°C in SDA medium with either 7.8 µM (1QG), 0.78 µM (2QG), 7.8 µM Q-GRFT $^{lec\ neg}$ (3QG) or control medium (VC). RNA was isolated and sequencing performed to determine expression under the different treatment conditions. Experiments were performed in triplicate. **(A)** Principal Component Analysis (PCA) plot performed on normalized read

counts for all samples. Similar colors represent cells that were subjected to a similar treatment. **(B)** Venn diagram showing shared differentially expressed genes for all DEGs. The intersection of the three circles represents overlapping DEGs among the three treatments. **(C)** Cluster analysis of DEGs for genes showing a differential expression $|Log_2FC| \geq 2$ in the comparison following different treatments. Red color represents upregulation; green color represents downregulation. **(D)** Volcano plot to examine the log2 fold change of DEGs at 1QG treatment, for significance level $p<0.05$ and adjusted p value ($q<0.05$). Log2 fold change on the x-axis is plotted against -log10(p-value) on the y-axis. **(E)** Enriched GO functions of DEGs. Top 20 enriched biological processes with the adjusted p-values (FDR) for the 1QG vs VC treatment group.

Table 3.5. The top 20 down-regulated DEGs for 7.8 µM Q-GRFT treated *C. albicans* (1QG) vs non-treated control (VC) cells.

Gene name/ Description	Log2FC	P-value	Adjusted P-value
RNR1, ribonucleotide-diphosphate reductase subunit	-2.145	3.14E-62	1.95E-58
hypothetical protein CAALFM_C102370CA	-2.255	2.07E-61	6.44E-58
PHO84, phosphate transporter	-1.907	2.76E-40	5.72E-37
RBR1, Repressed by RIM101 protein 1	-2.065	7.04E-38	8.76E-35
CAALFM_C107490CA, DNA-directed DNA polymerase alpha subunit	-1.516	2.01E-35	1.93E-32
CDC46, MCM DNA helicase complex subunit	-1.668	2.85E-35	2.22E-32
CTF18, Ctf18p	-1.7	4.92E-33	2.55E-30
POL1, DNA-directed DNA polymerase alpha catalytic subunit	-1.655	1.02E-32	4.87E-30
DUT1, bifunctional dITP/dUTP diphosphatase	-1.481	5.12E-32	2.27E-29
TRY6, Transcriptional regulator of yeast form adherence 6	-1.852	6.81E-31	2.82E-28
YBL053, Topoisomerase 1-associated factor 1	-1.382	9.75E-31	3.79E-28
TOS4, Tos4p	-1.308	8.96E-30	3.28E-27
hypothetical protein CAALFM_C201420CA	-1.432	9.69E-30	3.35E-27
SHA3, putative serine/threonine protein kinase	-1.055	2.79E-29	9.15E-27
CDC54, MCM DNA helicase complex subunit	-1.321	3.78E-29	1.18E-26
PGA45, Predicted GPI-anchored protein 45	-1.505	1.91E-28	5.41E-26
HCM1, Hcm1p	-1.598	1.22E-27	3.17E-25
SMC3, cohesin subunit	-1.79	1.59E-26	3.96E-24
hypothetical protein CAALFM_C501070CA	-1.306	8.46E-26	2.02E-23
CSM3, Chromosome segregation in meiosis protein 3	-1.108	4.48E-25	9.61E-23

Table 3.6. The top 20 down-regulated DEGs for 0.78 µM Q-GRFT treated *C. albicans* (2QG) vs non-treated control (VC) cells.

Gene name/ Description	Log2FC	P-value	Adjusted P-value
hypothetical protein CAALFM_C201630WA	-0.941	6.53E-15	1.08E-11
MCD1, kleisin alpha	-1.165	6.93E-15	1.08E-11
hypothetical protein CAALFM_C102370CA	-0.907	7.20E-12	7.46E-09
CCN1, Ccn1p	-0.931	8.74E-11	5.44E-08
hypothetical protein CAALFM_C602090CA	-0.759	5.17E-10	2.48E-07
SHA3, putative serine/threonine protein kinase	-0.542	7.51E-09	2.46E-06
HMX1, Hmx1p	-0.984	8.32E-09	2.59E-06
PUT4, Put4p	-0.868	6.19E-08	1.43E-05
hypothetical protein CAALFM_C100090WA	-0.85	8.92E-08	1.91E-05
GIN4, protein kinase	-0.652	1.32E-07	2.64E-05
FRE7, Fre7p	-0.514	1.48E-07	2.88E-05
TNA1, Tna1p	-1.013	3.23E-07	5.43E-05
VID21, Vid21p	-0.804	4.63E-07	7.03E-05
RPP0, ribosomal protein P0	-0.751	5.68E-07	8.16E-05
CAS5, Cas5p	-0.386	5.77E-07	8.16E-05
hypothetical protein CAALFM_C503430WA	-0.698	6.09E-07	8.42E-05
RNR1, ribonucleotide-diphosphate reductase subun	-0.629	9.43E-07	0
MNT2, alpha-1	-0.379	1.38E-06	0
SMC3, cohesin subunit	-0.798	1.44E-06	0
AAT22, Aat22p	-0.608	1.73E-06	0

Table 3.7. The top 20 down-regulated DEGs for 7.8 µM Q-GRFT$^{lec\ neg}$ treated *C. albicans* (3QG) vs non-treated control (VC) cells.

Gene name/ Description	Log2FC	P-value	Adjusted P-value
FRE7, Fre7p	-1.389	4.53E-44	2.82E-40
hypothetical protein CAALFM_C501070CA	-1.562	4.14E-36	1.29E-32
FRE30, Fre30p	-1.312	2.61E-33	5.42E-30
RNR1, ribonucleotide-diphosphate reductase subunit	-1.518	3.65E-32	5.67E-29
PGA45, Predicted GPI-anchored protein 45	-1.595	9.83E-32	1.22E-28
CTR1, high-affinity Cu transporter	-1.034	1.15E-29	1.19E-26
TRY6, Transcriptional regulator of yeast form adherence 6	-1.791	4.31E-29	3.76E-26
PHO84, phosphate transporter	-1.605	4.83E-29	3.76E-26
MET3, sulfate adenylyltransferase	-1.549	1.10E-27	7.59E-25
SOD3, Superoxide dismutase	-1.228	6.88E-23	4.28E-20
DNA-directed DNA polymerase alpha subunit	-1.138	4.81E-21	2.49E-18
CDC46, MCM DNA helicase complex subunit	-1.252	9.57E-21	4.58E-18
GDA1, guanosine diphosphatase	-1.099	1.58E-20	7.02E-18
putative ATPase	-0.908	2.06E-18	8.54E-16
GIT1, Glycerophosphoinositol permease 1	-1.922	4.06E-18	1.58E-15
GPX2, Glutathione peroxidase	-1.028	4.78E-18	1.75E-15
PRI2, DNA primase subunit	-1.385	2.21E-16	7.63E-14
SAM2, methionine adenosyltransferase	-0.887	2.97E-16	9.73E-14
DPB2, DNA polymerase epsilon noncatalytic subunit	-0.818	7.37E-16	2.23E-13
CDC54, MCM DNA helicase complex subunit	-0.946	7.91E-16	2.24E-13

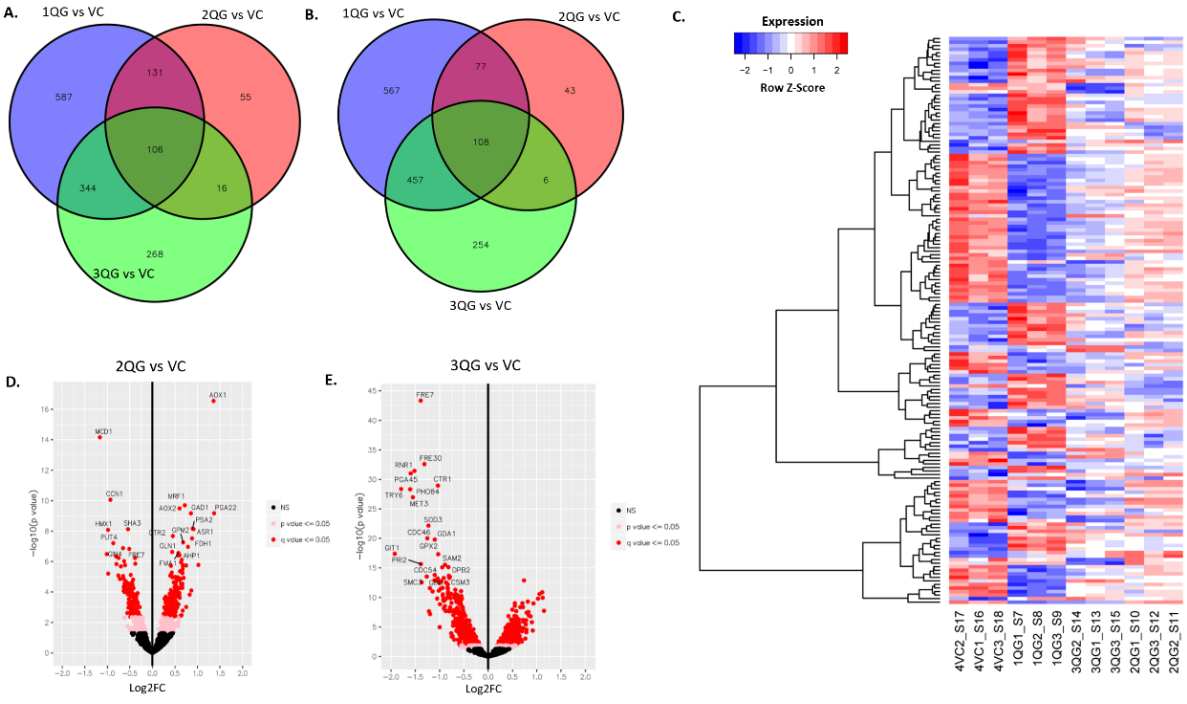

FIG 3.11 *C. albicans* RNA expression profile following treatment with Q-GRFT. *C. albicans* at a concentration of 1.0x10^5 cells/mL was incubated overnight at 37°C in SDA medium with either 7.8 µM (1QG), 0.78 µM (2QG), 7.8 µM Q-GRFT $^{lec\ neg}$ (3QG) or

control medium (VC). RNA was isolated and sequencing performed to determine expression under the different treatment conditions. Experiments were performed in triplicate. Venn diagrams showing shared differentially expressed genes for upregulated DEGs **(A)** and downregulated DEGs **(B)**. The intersections of the three respective circles represent overlapping DEGs among the three treatments. **(C)** Cluster analysis for genes showing a differential expression $|Log_2FC| \geq 2$ in the comparison demonstrating the z-score normalized expression (DESeq2 normalized counts). Volcano plots to examine the log2 fold change of DEGs at 2QG vs VC **(D)** and 3QG vs VC **(E)** treatments, for significance level $p<0.05$ and adjusted p value ($q<0.05$). Log2 fold change on the x-axis is plotted against -log10(p-value) on the y-axis.

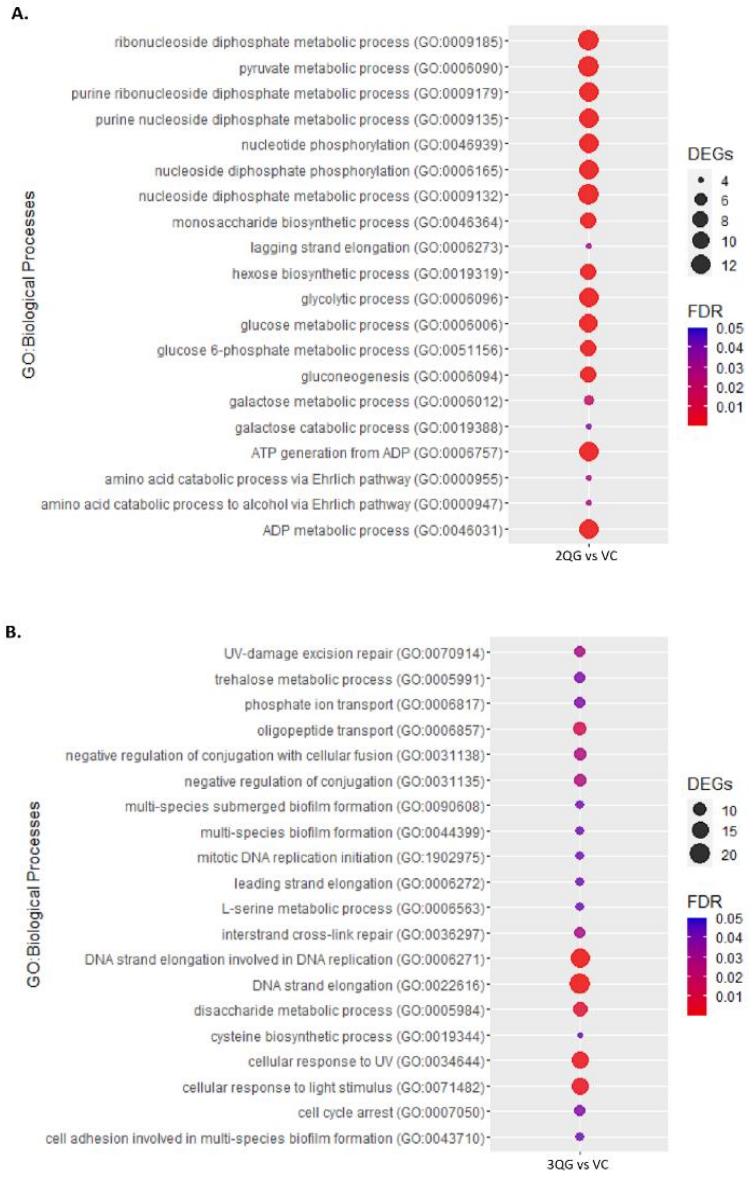

Figure 3. 5 Top 20 enriched GO functions/ biological processes of DEGs with the adjusted *P*-values (FDR): **(A)** 2QG vs VC and **(B)** 3QG vs VC treatment groups.

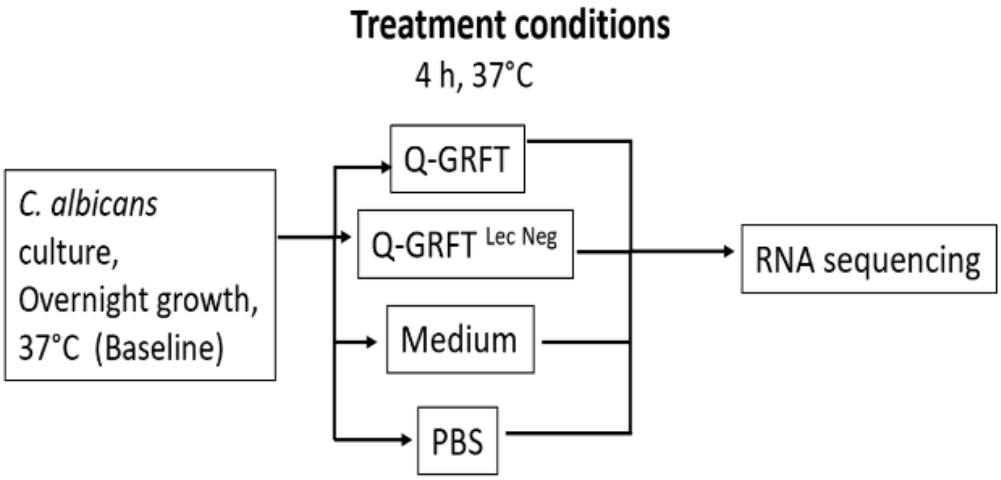

Figure 3.13 Experimental plan to determine early RNA expression following *C. albicans* treatment at different conditions. *C. albicans* was grown overnight, followed by incubation with either Q-GRFT, Q-GRFT $^{\text{Lec Neg}}$, medium only, and PBS for 4 hours at 37C. RNA was then extracted, and sequencing performed**.**

Table 3.8. Comparison of differentially expressed genes following *C. albicans* growth at different conditions.

Contrast	DEGs (ALL)	Up regulated	Down regulated
Q-GRFT v Medium	151	113	38
Q-GRFT v PBS	86	2	84
Q-GRFT v Q-GRFT$^{\text{Lec Neg}}$	67	61	6

Table 3.9. Q-GRFT specific differentially expressed genes following *C. albicans* treatment for 4 hours at 37°C.

Gene	Function
Up regulated	
FAV3	A-1,6-mannase; cell wall biogenesis/ degradation
CYK3	Cytokinesis protein 3
ACE2	Cell wall transcription factor
PEX13	Peroxin-13; fatty acid metabolic activity
HOF1	G1/S specific cyclin
1QGT	Cyclin dependent kinase
Down regulated	
DPS1	Aspartyl-tRNA synthetase, ATP binding, RNA binding
AAT1	Aspartate transaminase, pyridoxal phosphate binding, cellular amino acid metabolism
PHR2	pH-responsive protein 2(apical cell growth and morphogenesis)
AOX2	Alternate oxidase, oxidoreductase, electron transport respiratory chain
SOD4	Cell surface superoxide dismutase
HHT21	Histone h3.1; DNA repair, transcription regulation

Some of the genes up regulated and down regulated, and specific to *C. albicans* treatment with Q-GRFT for 4 hours at 37°C.

DISCUSSION

Our findings reveal that Q-GRFT inhibits HIV-1 PsV replication and the growth of *C. albicans,* with no demonstrable impact on gut bacterial microbiome, and pathogenic *Neisseria gonorrheae* and *Chlamydia trachomatis.* In preventing HIV-1 infection, GRFT inhibits giant cell formation between HIV-infected T cells and non-infected $CD4^+$ target T cells. GRFT also inhibits HIV transmission by blocking $CD4^+$ T cell destruction and viral replication through the DC-SIGN mediated pathway (293). GRFT is highly potent against HIV-1 with activity being demonstrated at sub nanomolar concentrations (293). Our results confirm that Q-GRFT inhibits HIV-1 PsV replication (EC_{50} 0.305 ng/mL), in keeping with what other groups and ours have found with GRFT. Therefore, following modification of the parent lectin, Q-GRFT maintains a potent HIV-1 antiviral effect by inhibiting viral replication.

The gut microbiome plays a role in maintaining health with dysbiosis implicated in promoting inflammation and disease (294, 295). Because Q-GRFT is currently being developed as a topical rectal microbicide (246), the protein nature and structure of the lectin makes interaction with gut and rectal microbiome components inevitable. In a previous study (203), rectal macaque treatment with the lectin did not result in any detrimental changes in the resident bacterial microbiome at post-challenge when compared with the baseline population. Moreover, some gastrointestinal and vaginal microbiota components like *Lactobacillus* species putatively produce lectin proteins that modulate their interactions in the local environment. These lectins may bind pathogens and host cells, disrupting the pathogen-human epithelial binding interaction. *Lactobacilli* lectins may bind to *Staphylococcus aureus* and Group B *Streptococci*, hindering the epithelial attachment (296, 297). Biofilm formation by *Salmonella* Typhimurium and uropathogenic *Escherichia coli* is significantly impaired by the putative lectins, inhibiting infection by these microorganisms (297, 298). In our study, we incubated representative gut bacteria with Q-GRFT for up to 24 -48 hours *in vitro* to establish any impact on the growth of these microbiome components. In keeping with results from Girard et al, (203) we did not detect any growth inhibitory effects for the microbiota components tested. These findings are also similar to reports from the recently approved dapivirine vaginal

ring, that demonstrated no impact of its use on local cervicovaginal immunity and microbiome community (275).

Yeast and fungi are components of the gut mycobiome. Dysbiosis and overgrowth of fungal species results in a shift in the diversity and richness in group members, with subsequent inflammation (299, 300). *Candida spp.* infections pose a major health concern in both immunocompromised patients and immunocompetent individuals (301). Lectins have been investigated for their role as antifungal agents, given the need to develop new antifungal agents and the increasing burden of disease posed by fungi and yeast infections. *Helianthus annuus* lectin derived from sunflower decreased *C. albicans* survival by impairing the cell wall integrity, induced hydrogen peroxide formation and inhibited the yeast to filamentous morphological transition responsible for virulence. The lectin also impairs fungal cell adherence to surfaces and interferes with biofilm development with a resultant reduced coverage area (280). By binding to glucose, mannose and N-acetylglucosamine in the fungal cell wall, other lectins exhibit antifungal activity, with various degrees of growth inhibition. Lectin TEL (from *Talisa esculenta* fruit) inhibited *Saccharomyces cerevisiae, Fusarium moniliforme* and *Colletotrichum lindemuthianum* growth while AML (from soursop *Annona muricata*), which binds glucose and mannose, inhibited *F. solani*, *F. oxysporum* and *Colletotrichum musae* growth. These lectins inhibit fungal spore germination and mycelium growth. They also altered the synthesis of chitin, altering cell wall deposition and formation (302). The lectins DvioL, DRL ConBr are extracts from *Dioclea violacea, D. rostrata* and *Canavalia brasilienis* legumes respectively. These extracts bind glucose and mannose and have demonstrated antifungal activity against yeasts isolated from vaginal secretions, including *C. guilliermondi, C. shehatae, C. membranafaciens* and *K. apiculata* (302-305). Putatively produced lectins from *Lactobacillus* spps have been shown to bind to *C. albicans* and inhibit biofilm formation (297). We determined the impact of Q-GRFT on the growth of *C. albicans*, as a representative of the mycobiome in the gut and colon. We found that Q-GRFT bound to α-mannan in the fungal cell wall and inhibited the growth of *C. albicans.* We also show that the binding and inhibition is via the lectin binding receptor, since the mutant lectin binding site-deficient Q-GRFT variant neither bound to *C. albicans*, nor inhibited fungal growth. Our data suggests that the lectin impaired cell

wall integrity by increasing permeability and likely induced the formation of ROS within the cell.

Q-GRFT exposure to *C. albicans* likely results in an osmotic imbalance, as evidenced by the shriveled appearance and collapsing cells with surface indentations. Lectin-treated cells also demonstrate an increase in budding with multiple bud scars and a loss of the normal polar budding orientation. This is indicative that Q-GRFT-induced changes affect normal cell division. The loss of polar budding and multiple bud scars is an attempt by *C. albicans* to divide multiple times to escape stress-induced conditions (306). Interestingly, *Tos4* gene regulates the G1/S cell cycle phase and promoting cell division (307). Q-GRFT treatment was associated with down-regulation of *Tos4*. Additionally, in response to oxidative stress, *C. albicans* expresses antioxidant genes to neutralize and escape stress, including superoxide dismutase (*SOD*), glutathione peroxidase (*GPX2*), thioredoxin (*TRX*) and thioredoxin reductase (*TRR*) (308). Q-GRFT treatment was associated with up-regulation of *SOD* while cells treated with the non-binding mutant lectin exhibited downregulation of GPX2 and TRR1. Because we have used *in vitro* assays to demonstrate growth inhibition, there is a likelihood for cells incubated with mutant Q-GRFT to undergo stressful growth conditions given volume and space limitations with this assay. When cells grow uninhibited in media, they will reach a critical mass when they start to compete for nutrients within the restricted space. This has the potential to induce metabolic responses within cells to escape these stressful conditions. However, given the clear differential expression of genes following Q-GRFT treatment in comparison to the mutant treated cells, it is evident that the lectin does impact multiple metabolic pathways within *C. albicans* after treatment. In fact, mutant Q-GRFT treated *C. albicans* was associated with increase trehalose metabolism, a hallmark for general stress response (309). Cell cycle arrest, disaccharide metabolism, biofilm formation and DNA strand elongation were among the upregulated pathways following mutant Q-GRFT treatment. Similarly, QG treatment demonstrated upregulated stress response pathways including monosaccharides, glucose, galactose and amino acid metabolism, biofilm formation and DNA replication, among others.

Further experiments that will need to be performed to confirm the mechanism of cell killing are time course determinations that will localize the particular duration at which cell death is initiated or occurs. Additionally, antioxidant experiments upon Q-GRFT treatment will highlight the exact role of the lectin on ROS formation and elucidate its role in cell killing.

Here, we have established that Q-GRFT demonstrates potent inhibitory activity against non-*Candida albicans* species of clinical importance, *Candida glabrata, Candida krusei* and *Candida parapsilosis*. Interestingly, *C. krusei* has been described to harbor innate resistance against fluconazole (310, 311), while azole resistance is increasingly being documented for *C. glabrata* and *C. parapsilosis*. In addition, our study established that Q-GRFT demonstrates growth inhibition of *Candida auris* CDC388 and *Candida auris* CDC389, strains belonging to the South Asia clade, one of those that are dominant in the United States (291). However, growth in strains *Candida auris* CDC383, *Candida auris* CDC384, *Candida auris* CDC385 and *Candida auris* CDC386 was not impacted following incubation with Q-GRFT. *C. auris* exhibits multi drug resistance, and pan-resistant strains have recently been identified (312-316). *N*- and *O*-linked mannans with α-1,2-, α-1,3-, α-1,6- and β-1,2-linked mannose sugar residues make up the structure of mannoproteins in the *Candida* cell wall (317). Because we have identified α-mannan as a binding ligand for Q-GRFT, it is likely that the highly diverse composition of mannan structures and mannosyl residues in different *Candida* species (318) contributes to the differential response to cell treatment and variations in MICs observed in our study. Mannan in *C. albicans* is comprised of branching *N*-linked polysaccharide units and short-chain *O*-linked mannan oligosaccharides. Additionally, the N-linked mannan is made up of a long chain of α-1,6-linked mannose backbone that bridges with oligomannose side chains, predominantly consisting of α-1,2-, α-1,3-, and β-1,2-linked mannose residues with sparse phosphate groups (317-319). The mannan in *C. glabrata* is comprised of small branches with minimal α-mannan content and one or two β-1,2-linked mannose residues (317, 318, 320). The long chain of α-1,2-linked mannose subunits with one or two α-1,6-linked mannose residues, and a few short side chains of α-1,2-linked mannose residues constitute the mannan in *C. krusei* (318, 321, 322). While

C. parapsilosis mannan consists of both of α-1,2-, α-1,3-linked mannose residues that are found in *C. albicans,* it does not comprise of 1-*O*-α-phosphorylated units (323). In addition, contrasting the other pathogenic *Candida* species, *C. auris* mannan is predominant in β-1,2-linked mannose residues (324). These mannan differences in composition and structure are likely to underscore the variations in the growth activity observed when different Candida species were incubated with Q-GRFT. Overall, these findings suggest that Q-GRFT's anti-*Candida* activity may be beneficial as an additional strategy or alternative to the current antifungal treatment, given that growth inhibitory activity was observed in these different strains, despite the structural differences in their cell wall composition, as well as the documented innate resistance to common antifungal agents.

Mucosal transmission of HIV and viral shedding in genital secretions is increased in co-infection with STIs, including *Neisseria gonorrhea* and *Chlamydia trachomatis* (325, 326). Importantly, both these pathogens express mannosylated glycoproteins in their outer membranes (327, 328) that can act as ligands for lectins (329). The *Neisseria gonorrhea* cell wall envelope is rich in β-linked *N*-acetyl-D-glucosamine (D-GlcNAc) and β-D-galactosyl (β-D-Gal) that promote interaction with wheat germ agglutinin and ricin lectins. The other structural polysaccharide components α-N-acetyl-D-galactosamine (α-D-GalNAc) and β-D-Gal linked to GalNAc and/ or GlcNAc promote interaction with soybean agglutinin, peanut agglutinin and *Dolichos biflorus* lectins (330). *Chlamydia trachomatis* possesses terminal mannose structures on the surface and in elementary bodies (EBs). These structures interact with and bind the lectin from *Galanthus nivalis* (GNA), with a resultant GNA-dependent inhibition in the number of intracellular inclusions (EBs). The GNA lectin prevented *Chlamydia trachomatis* infection of McCoy cells (331). In our study, we did not demonstrate any inhibitory effect of Q-GRFT on *Neisseria gonorrhea* and *Chlamydia trachomatis*. However, unlike the GNA lectin (331), Q-GRFT was neither toxic nor inhibitory to the growth of McCoy cells. Our findings do not demonstrate any inhibitory impact of Q-GRFT to the growth of *Neisseria gonorrhea* and *Chlamydia trachomatis*.

In conclusion, we show that Q-GRFT is a potent antiviral against HIV-1 PsV and demonstrate the lectin's first report denoting antifungal activity, with growth inhibition of both *C. albicans* and non-*C. albicans* species, including some strains of the multi drug resistant *C. auris*. The lectin does not impact the growth of resident gut bacterial microbiome components. We identify that Q-GRFT binds to α-mannan via the lectin-binding receptor, with a resultant induction of reactive oxidative species that damage cellular structures, leading to death. These findings underscore the need to further explore the lectin's utility in *in vivo* infections, and future development of Q-GRFT as an antifungal agent.

CHAPTER 4: EFFICACY AND IMMUNOLOGICAL CONSEQUENCE OF Q-GRFT IN VAGINAL CANDIDIASIS

INTRODUCTION

Vulvovaginal candidiasis (VVC) is an ongoing global challenge, and is predominantly caused by the common fungal pathogen, *Candida albicans* (332). Approximately 75% of women will develop at least one episode of vulvovaginal candidiasis during their lifetime (333). About 138 million women globally are affected by recurrent vulvovaginal candidiasis (RVVC) annually, with the numbers expected to increase to 158 million each year, by 2030 (334). *Candida* organisms are commensals in the vagina, with overgrowth resulting in vaginal and vulval inflammation contributing to the pathological hallmarks of infection (335). Factors that predispose women to candidiasis include use of oral contraceptives, hormone replacement therapy, pregnancy and antibiotic use (336, 337). Recurrent vaginal *candida* infections are associated with mental discomfort (218), in addition to the physical symptoms that include pruritus, burning pain, profuse leucorrhea, redness and interrupted and restless sleep as a result of vulval and vaginal mucosal irritation (338, 339).

The major drugs currently used for the treatment of vaginal candidiasis include azoles, echinocandins, and polyenes. Unfortunately, there are increasing reports of resistance by fungal pathogens to these antifungals (340-342). The resistance is attributed to the static function of many antifungals, in addition to microbial recalcitrance upon repeated drug exposure (343, 344). In addition, long-term drug use, prophylactic administration, and exposure to antifungals through agriculture and contaminated food consumption contribute to the growing trend of drug resistance (345-347). In addition, intrinsic natural resistance to antifungal therapy has been demonstrated in some pathogenic fungal species including azole-resistant *Aspergillus* species (348), fluconazole-resistant *C. krusei* (349) and *C. glabrata* (350), and echinocandin- resistant

Cryptococcus neoformans. This demonstrates the urgent need to develop more antifungal agents and strategies relevant to the eradication of these infections. The vaginal mucosa is the first line of defense against *Candida* through maintaining an acidic mucosal pH that is not optimal for *Candida* and providing anatomical and physiological barriers to infection (351, 352). *Candida* overgrowth triggers an epithelial cell-mediated cytokine response, with a resultant recruitment of immune cells like neutrophils, dendritic cells, and T cells (351, 353, 354). Symptomatic infection demonstrates elevated cellular infiltration with PMNs and variable fungal presence, whereas protection from VVC has been associated with limited or absent inflammatory responses in the vagina (355). A balance between Th2/ Th1 cytokines has been suggested as the determinant in susceptibility to and pathogenesis of vulvovaginal candidiasis and RVVC (356, 357). Th2 cytokines are associated with susceptibility to pathogenic infection, with Th1 cytokines conferring protection. In dermal and oral candidiasis, Th17- induced IL-17 and IL-22 have been identified as key mediators, conferring immunity against *C. albicans* infection (358, 359). Acting in concert, these cytokines recruit neutrophils into epithelial tissues, induce the production of antimicrobial peptides in mucosa, and up-regulate pro-inflammatory cytokines (360-362), promoting antifungal immunity. Notwithstanding, IL-17's role in mediating immune responses in vaginal candidiasis is still controversial (363, 364). Interestingly, recently, Il-17 has also been associated with a rapid protection of vaginal epithelial cells in early candidiasis infection (353).

Numerous endogenous and plant-derived lectins have previously demonstrated *in vitro* antifungal activity (302, 365). Griffithsin (GRFT) is a lectin originally derived from red alga *Griffithsia* sp. GRFT has demonstrated broad-spectrum antiviral properties and activity (10, 11, 278). Native GRFT is prone to oxidation (366), and the Palmer group developed an engineered form, Griffithsin-M78Q (Q-GRFT), with improved stability, and similar antiviral activity to GRFT. Using *in vitro* studies, we have demonstrated a novel antifungal activity of Q-GRFT, with potent growth inhibition of *Candida* species including *C. albicans, C. parapsilosis, C. krusei, C. glabrata* and against strains of the pan-resistant *C. auris* (13). To our knowledge, no study has reported efficacy of Q-GRFT in vaginal candidiasis *in vivo* models. Here, we investigated the efficacy of Q-GRFT in vaginal candidiasis using prophylactic and therapeutic murine models. We describe the

impact of topical Q-GRFT administration on vaginal fungal burden and the immunological consequence of *C. albicans* infection in the context of topical Q-GRFT therapy.

MATERIALS AND METHODS

Mice

Female CBA/J mice (Jackson Laboratories) were maintained under specific pathogen-free conditions in the Center for Translational Research vivarium, at the University of Louisville, Louisville, Kentucky.

Candida albicans and vaginal inoculation

The *C. albicans* ATCC 32020 strain was grown on Sabourand dextrose agar plates overnight at 30 ℃ prior to use, and cell preparation done with slight modifications to the animal model development protocol by Conti et al. (367). Briefly, 10 milliliters of Sabourand dextrose media were inoculated with 1 colony of *C. albicans* from the agar plate and incubated at 30 ℃ with shaking for 18 hours. Cells were then sub-cultured 1:100 dilution overnight, followed by preparation of 1.0×10^8 cells/mL blastospores from the stationary phase, that were suspended in sterile PBS. Cells were kept on ice until when vaginal inoculation was performed in mice. Twenty microliters of the *C. albicans* preparation were dispensed into each mouse's vagina using a P50 positive displacement pipettor.

Estradiol Treatment, Lavage, and Fungal Burden

Estradiol at a concentration of 0.5 mg/mL was dissolved in sesame oil. Mice were then injected subcutaneously with 100 µL of the hormonal preparation in the lower abdomen 3 days prior to *C. albicans* challenge, and then once weekly for the duration of the experiment. To perform the lavage, 100 µL of sterile PBS were dispensed into the mouse vagina and aspirated back and forth several times, and then transferred to labelled Eppendorf tubes on ice. The lavage was then diluted 1:100, and 50 µL of the diluted fluid

plated on Sabourand agar. Colli rollers were used to spread the lavage. The plates were incubated at 30 °C for 24-48 hours, and colonies counted to establish the fungal burden.

Vaginal treatment

Forty microliters (40 µL) of a 1% Q-GRFT gel formulated in Carbopol (400 ng), 40 µL of Carbopol placebo gel, 100 µL of nystatin solution at a concentration of 20 mg/mL (Mayne Pharma, Greenville, NC, USA) and 100 µL of sterile 1X PBS were instilled per vaginum in mice from the different animal groups, using appropriate pipettors.

Hematoxylin and Eosin, Periodic acid Schiff staining

For Hematoxylin and Eosin (H & E) staining, sections were deparaffinized and placed in xylene. Sections were then hydrated in alcohol and water baths and stained in hematoxylin for 3 minutes. They were then washed in running water for 5 minutes, differentiated in 1% acid alcohol for 5 minutes, washing in running tap water, dipped in alkaline solution (ammonia water) and washed again. They were subsequently stained in 1% Eosin Y for 10 minutes, washed in tap water for 3 minutes, dehydrated in increasing concentrations of alcohols and then cleared in xylene. Sections were then mounted and observed under a microscope.

For periodic acid Schiff (PAS) staining, sections were dewaxed followed by incubated in 0.5% periodic acid for 5 minutes, washed in running tap water for 3 minutes and then immersed in Schiff's reagent for 15 minutes. Sections were then washed in tap water for 5 minutes, counterstained with hematoxylin for 2 minutes, washed in running tap water for 3 minutes, dehydrated in ethanol and cleared in xylene for 5 minutes. Sections were then mounted with Entellan® and a cover slip applied. The sections were then viewed under a microscope.

Flow Cytometry and Luminex analysis

Cellular phenotypic analysis was carried out using flow cytometry with the following antibodies: CD45 and CD11b (BD Biosciences, San Diego California), and F480 (BioLegend, San Diego, California), Ly6G and viability dye (BD Horizon). Vaginal

lavage specimens were added to complete RPMI medium (supplemented with 1M HEPES, penicillin/ streptomycin, fetal bovine serum and 2-Mercaptoethanol), filtered and centrifuged for 5 minutes at 1600 rpm. One million cells were then added to appropriate flow cytometry tubes, followed by washing with FACS buffer (BD Biosciences, San Diego California) for 5 min at 1600 rpm. Cells were then blocked with 2 µL of CD16/32 antibody (BioLegend, San Diego, California) for 10 minutes. An antibody mix was prepared for the surface staining primary antibodies, added to the mixture followed by incubation at 4 °C for 30 minutes. Cells were washed, re-suspended in 300 µL of FACS buffer, and analyzed using a BD device (BD LSR Fortessa^{TM}, USA), following manufacturer's instructions. Data was analyzed using Flowjo software (Tree Star, Inc, Ashland, Oregon).

Vaginal lavage supernatants were analyzed for cytokines by a mouse Cytokine/ Chemokine Th17 Magnetic Bead Panel (EMD Millipore, St. Charles, MO). The panel was subsequently analyzed with a Milliplex MAP Kit on a MagPix with Luminex xMAP technology, following the manufacturer's directions.

Statistical Analysis

Where appropriate, tests used to determine significance between experiments are outlined in the figure legends of each figure. Data are representative of 2-4 independent experiments for each time points. One way ANOVA was performed using GraphPad Prism7.05 (GraphPad Software, Inc, La Jolla, California) to determine statistical difference. A P value ≤ 0.05 was considered significant.

Ethics Statement

This study was approved by and carried out in accordance with recommendations of the University of Louisville Institutional Animal Care and Use Committee (IACUC), under IACUC ID 19453.

RESULTS

Q-GRFT reduced the fungal burden in a Preventative model of murine vaginal candidiasis

To evaluate the efficacy of Q-GRFT in a preventative/ prophylactic murine model, we established an experimental model for vaginal infection (FIG 4.1A), based on that described by Conti et. al (367). Female CBA/J mice were injected subcutaneously with estradiol, followed by twice daily vaginal instillation of a Carbopol gel formulation similar to a product that we previously demonstrated had HSV-2 inhibitory activity (368). The Carbopol gel formulation delivered 400µg Q-GRFT per dose twice daily for 5 days. We challenged the animals with *C. albicans* on day 3. Vaginal lavage was performed on 24 hours following administration of the final Q-GRFT treatment. We determined the efficacy of Q-GRFT in the prevention of vaginal candidiasis by establishing the fungal burden in vaginal lavage fluids after vaginal pre-treatment, fungal inoculation, and follow-up treatment with Q-GRFT. Fungal burden was evaluated by plating lavage fluids on Sabourand agar plates that were incubated for 48 hours at 30°C, followed by counting of colonies. Our results demonstrated that Q-GRFT treatment resulted in a significantly lower fungal burden when compared with the infected untreated controls (P=0.0417) (FIG 4.1B). Similarly, treatment with the positive control nystatin, a polyene antifungal agent, resulted in a significantly lower fungal burden (P=0.0016), while there was no inhibition demonstrated with PBS (P=0.4849) and placebo (P=0.5963) when compared with the infected controls. Additionally, uninfected animals did not demonstrate any fungal growth (P=0.0016).

Upon infection and epithelial penetration, tissue resident-macrophages are among the initial immune cells that encounter *Candida*, and phagocytose the fungal cells to achieve clearance (369). Furthermore, pro-inflammatory cytokines released by macrophages and epithelial cells recruit neutrophils and inflammatory monocytes to eradicate *Candida* infection (369, 370). Therefore, using flow cytometry, we sought to determine if pre-treatment with Q-GRFT influenced the expression of vaginal innate immune cells [neutrophils ($CD45^+$,$Ly6G^+$,$CD11b^+$) (FIG 4.1C top) and mononuclear phagocytes ($CD45^+$,$CD11^+$,$F4/80^+$) (FIG 4.1C bottom) in a vaginal infection murine

model. Compared to infected controls, there was no difference in the population of neutrophils following pre-treatment with either Q-GRFT ($P>0.9999$), placebo ($P>0.9999$), or PBS ($P>0.6510$) (FIG 4.1D). In addition, treatment with nystatin resulted in significantly higher populations of neutrophils ($P=0.0011$), while uninfected animals had lower neutrophils ($P=0.0483$), in comparison with infected controls. Similarly, there was no difference in mononuclear phagocyte populations following treatment with Q-GRFT ($P=0.9461$), placebo ($P=0.9155$), and PBS ($P=0.6263$), in comparison with the infected controls. Nystatin resulted in higher monocyte populations ($P=0.0380$), while uninfected animals demonstrated significantly lower monocytes ($P=0.0368$) than infected animals. These results demonstrate that while Q-GRFT significantly inhibits *Candida* growth in a preventative murine model, unlike nystatin treatment, the protective effect does not occur in the context of inflammatory immune responses.

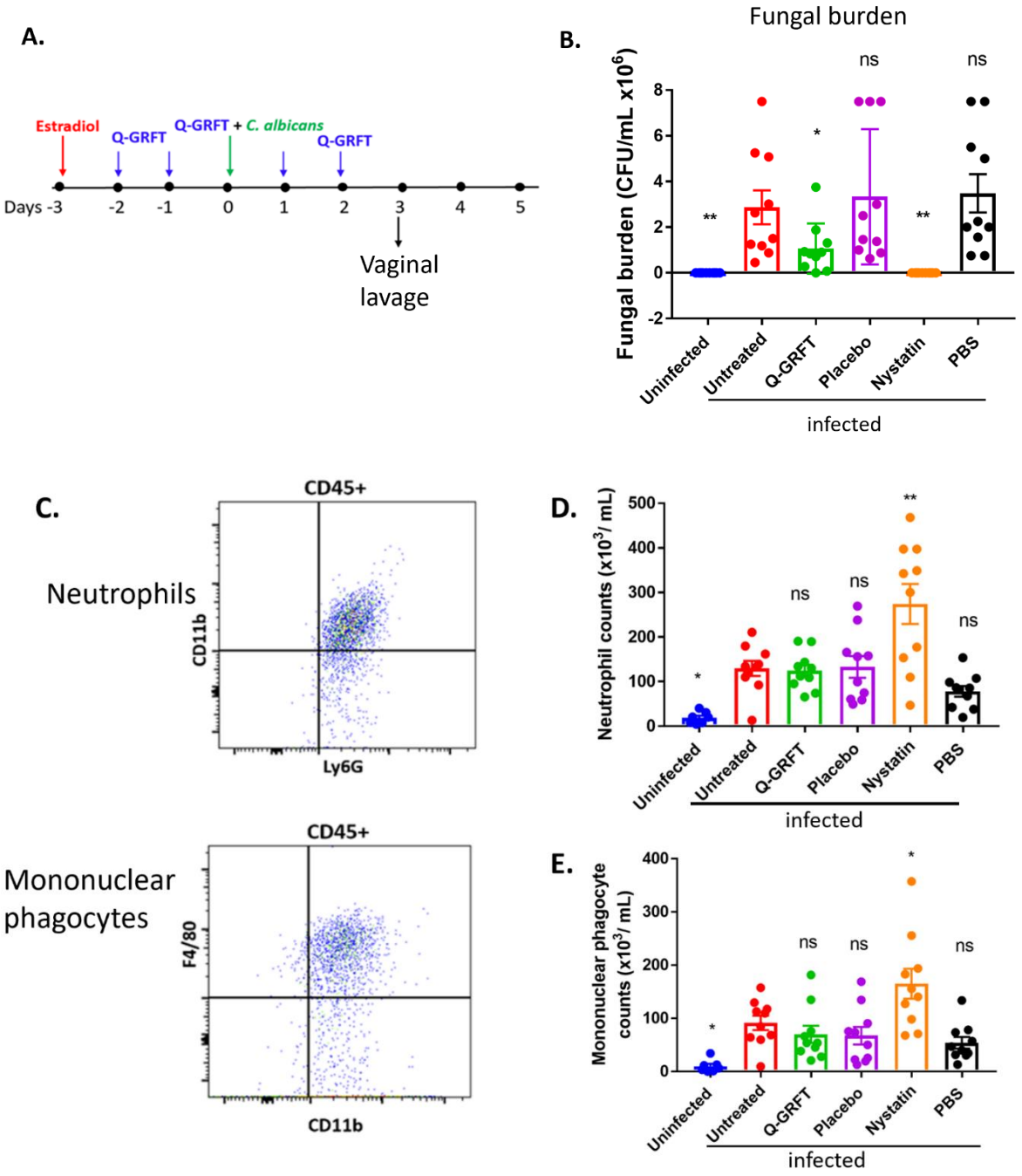

Figure 4. 2 Q-GRFT significantly inhibits vaginal fungal infection in a prophylaxis model of murine candidiasis. **(A)** Experimental scheme. CBA/J mice (N= 10 per group) were estradiol-treated at Day -3, followed by twice daily instillation of either Q-GRFT gel, nystatin solution, PBS, or Carbopol placebo gel per vaginum for the next 5 days. At Day 0, mice were inoculated with 20 µL of *C. albicans* blastospores at a cell concentration of 1.0 X 10^8 CFU/mL, per vaginum. A vaginal lavage was performed 24

hours after the final dose administration. **(B)** Vaginal fungal burden (CFU/mL) following treatment, for mice in **(A).** Each dot represents one mouse, N=10 mice per group. Experiments were performed and repeated at least 2 times, and representative data of *Mean ± SEM* is shown. **(C)** Flow cytometry gating strategy for neutrophils, and mononuclear phagocytes in the vaginal lavage. Neutrophils were identified as $CD45^{+}Ly6G^{+}CD11b^{+}$, while monocytes were $CD45^{+}CD11^{+}F4/80^{+}$ cells. **(D)** Neutrophil and **(E)** mononuclear phagocyte cell populations in the vaginal lavage following the respective treatments. N=10 animals per group, and each dot represents a population of cells from a single mouse. Measurements are representative of cell populations from experiments performed at least 2 times. *Mean ± SEM* data is presented. For all experiments, *one-way ANOVA* was used for statistical analyses, and $P \leq 0.05$ was considered significant.

Q-GRFT Enhanced Clearance of Vaginal Candidiasis In a Therapeutic Murine Model

To study the role of Q-GRFT in the treatment of candidiasis, a murine therapeutic experimental model was developed, (FIG 4.2A), based on that described by Conti et. al (367). Mice were injected subcutaneously with estradiol, followed by inoculation with *C. albicans* vaginally 3 days later. Vaginal lavage was performed on day 4 following fungal challenge, to determine baseline fungal burden. Twice daily vaginal instillation of 400µg Q-GRFT was started on day 5 and continued for a total of 7 days. A vaginal lavage was performed 24 hours after the final dose to determine fungal burden by colony counts on Sabourand agar plates, and immune response to treatment using flow cytometry and Luminex ELISA assay. Pre-treatment fungal burden (FIG 4.2B) confirmed that all mice had established vaginal infection prior to initiating treatment, with no significant differences in fungal burden in any of the infected groups prior to initiation of treatment. Compared to placebo, treatment with topical vaginal Q-GRFT gel resulted in a significant inhibition of *C. albicans* burden ($P=0.0379$), similar to that seen with the control nystatin ($P=0.0003$), at the end of the dosing period (FIG 4.2C). FIG 4.2D depicts the representative fungal growth on Sabourand agar plates following incubation for 48 hours, at 30°C for the infected controls (left) and Q-GRFT treated animals (right). These results

indicated that Q-GRFT was an effective treatment for vaginal candidiasis in a murine model.

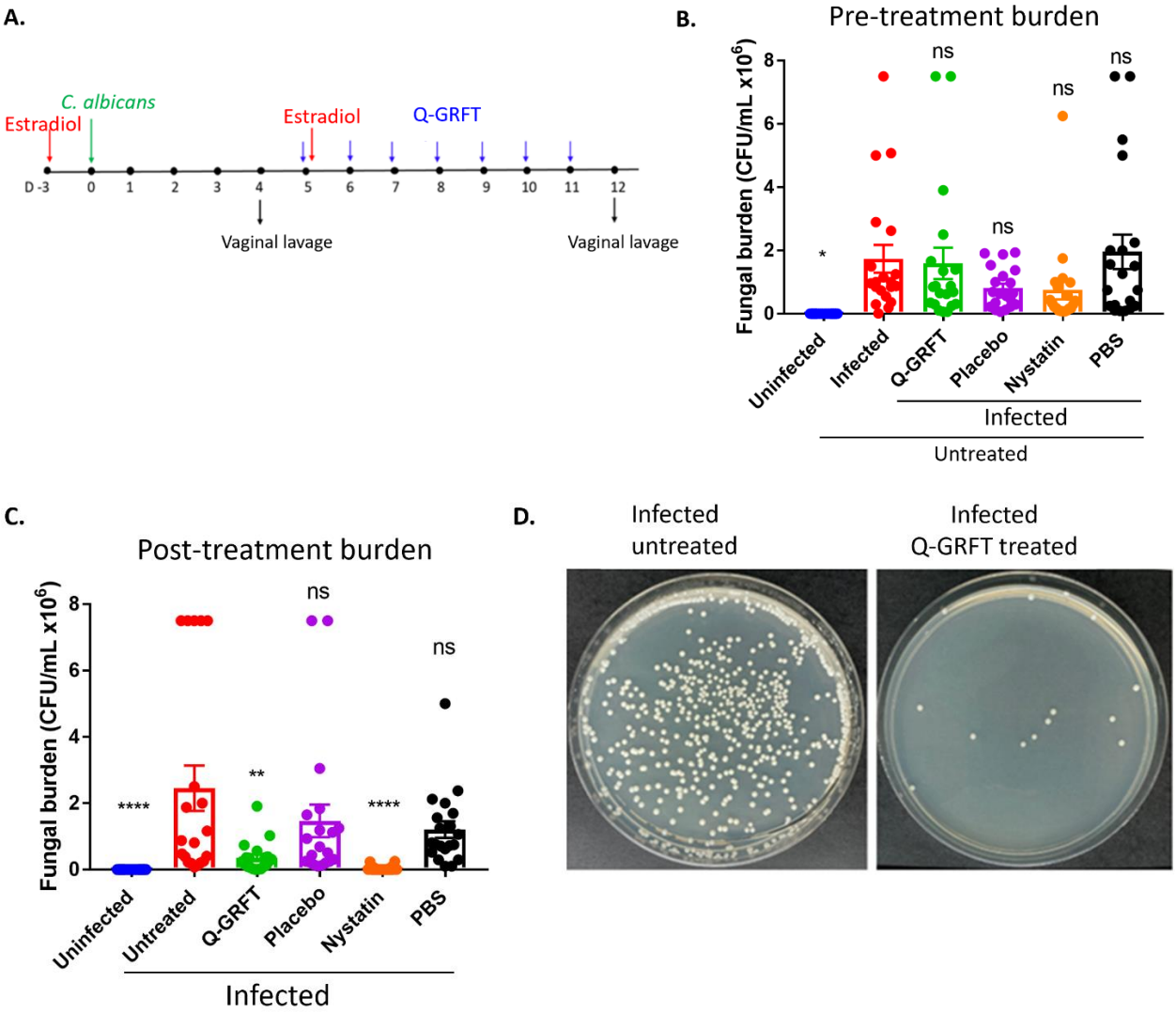

Figure 4. 3 Efficacy of Q-GRFT in a murine model of vaginal candidiasis. **(A)** Experimental scheme. CBA/J mice were estradiol-treated, followed by vaginal inoculation with 20 µL of *C. albicans* blastospores at a cell concentration of 1.0 X 10^8 CFU/mL 3 days later. Treatment with either Q-GRFT, nystatin, placebo, or PBS by vaginal instillation was started on Day 5 following inoculation and continued twice daily for a total of 7 days, respectively. Vaginal lavage was performed at Day 4 and Day 12 to establish pre-treatment and post-treatment fungal burden, respectively. **(B)** Day 4 (pre-

treatment) Vaginal fungal burden (CFU/mL), and **(C)** Day 12 (post-treatment) burden. Each dot represents one mouse, N=20 mice per group. Experiments were performed at least 2-3 times and representative data from 2 experiments, *Mean ± SEM* is shown. *One-way ANOVA* was used for statistical analyses and $P \leq 0.05$ was considered significant. **(D)** Representative photographs of *C. albicans* culture colonies for vaginal lavage fluids collected from untreated infected controls (Left) and Q-GRFT treated mice (Right).

Treatment With Q-GRFT Does Not Induce Overt Changes in Innate Immune Cell Phenotypes in Vaginal Candidiasis

Upon epithelial penetration, tissue resident-macrophages are among the initial immune cells that encounter *Candida* and will phagocytose the fungal cells to achieve clearance (369). Additionally, pro-inflammatory cytokines released by macrophages and epithelial cells, will recruit neutrophils and inflammatory monocytes to eradicate *Candida* infection (369, 370). Therefore, we next sought to determine if treatment with Q-GRFT influenced the expression of vaginal innate immune cells, neutrophils ($CD45^+$,$Ly6G^+$,$CD11b^+$), (FIG 4.3A), and mononuclear phagocytes ($CD45^+$,$CD11b^+$,$F4/80^+$), (FIG 4.3B), in candidiasis using flow cytometry. Compared to infected controls, Q-GRFT did not induce any significant changes in populations of both neutrophils, $P=0.7279$, and mononuclear phagocytes, $P=0.1960$. Similarly, neutrophils populations were not significantly different between infected controls and nystatin treated mice, $P=0.1771$, while monocytes were elevated following treatment, $P=0.0055$. Compared with the infected untreated controls, uninfected mice demonstrated significantly lower neutrophils ($P=0.0039$), but not mononuclear phagocytes, $P=0.0873$. Both placebo and PBS did not result in any changes in neutrophil ($P=0.3626$, $P=0.111$), and monocyte ($P=0.2464$, $P=0.9939$) populations, respectively. These results demonstrate that Q-GRFT does not induce overt changes in neutrophil and mononuclear phagocytic populations following vaginal infection with *C. albicans*.

Q-GRFT is Associated With Expression of Lower Amounts of Cytokines IFNɣ and IL-10, but not IL-22 and IL-23

The Th1/ Th17 immune interplay contributes to fungal immunity and tolerance in the vaginal mucosa (355-357), with elevated levels of related cytokines associated with pathogen clearance. IL-22 contributes to polymorphonuclear neutrophilic response and alarmin production, and low levels of the cytokine have been associated with chronic and recurrent mucosal fungal infection (355). Interestingly, some clinical observations have not demonstrated deficiencies of Th17 cytokines in blood or vaginal fluids of patients with RVVC (371, 372). Working in concert with transforming growth factor (TGF-β), IL-6 promotes the differentiation of naïve CD4+ T cells to Th17 phenotype (373). Murine tolerance to VVC has been associated with IL-10 (355, 374), while clearance is increased with secretion of Th1 associated cytokine, interferon gamma (IFNɣ) (353, 375, 376). In addition, local IL-23 is protective in VVC, with low levels likely to correlate with increased susceptibility to *C. albicans* infection (377). We therefore sought to establish the expression profile of vaginal cytokines in lavage fluids following Q-GRFT treatment in VVC. Cytokines were assayed using the Luminex xMAP, a multiplex ELISA assay method. Compared to the infected untreated controls, Q-GRFT was associated with lower expression of IFNɣ ($P<0.0001$) (FIG 4.3C), and IL-10 ($P=0.0365$) (FIG 4.3F). Additionally, there was no significant difference in the expression of cytokines IL-22 ($P>0.9999$) (FIG 4.3D) and IL-23 ($P=0.1955$) (FIG 4.3E), following Q-GRFT treatment. These findings were in keeping with what was observed following nystatin treatment that demonstrated lower IFNɣ ($P<0.0001$), and IL-10 ($P=0.0457$), but not IL-22 ($P>0.999$) and IL-23 ($P=0.4924$). However, unlike in both untreated infected animals and PBS controls, Il-22 and IL-23 following Q-GRFT and nystatin treatments demonstrated a trend towards lower cytokine levels. In comparison with the infected untreated controls, both placebo and PBS treatments did not demonstrate any differences in expression of either IFNɣ (P=0.6012, P=0.1303), IL-22 (P=0.2470, P>0.9999), IL-23 (P=0.0895, P=0.2656), or IL-10 (P=0.1336, P=0.9508), respectively. Uninfected controls demonstrated lower IFNɣ (P<0.0001), IL-22 (P=0.0261), IL-23 (P=0.0103), and IL-10 (P=0.0032). These results suggest that the lower IFNɣ and IL-10 cytokines expressed following Q-GRFT treatment are likely related to a lower fungal burden, compared to the

infected untreated controls. It is also likely that IL-22 and IL-23 decline over a longer period following vaginal fungal clearance, given the trend towards lower cytokine levels observed in this study.

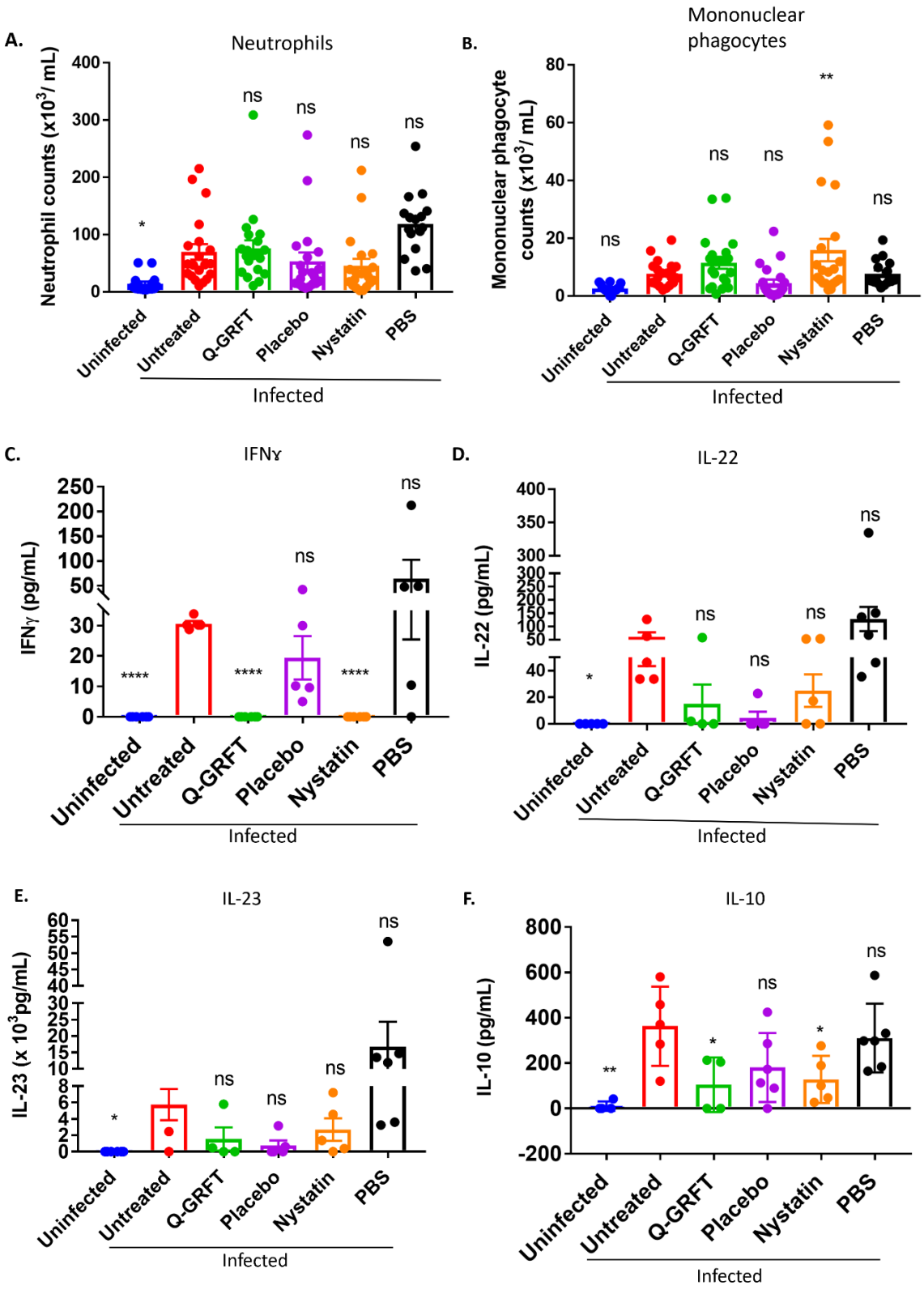

Figure 4. 4 Q-GRFT treatment is associated with lower levels of vaginal inflammation in candidiasis.

(A) Neutrophil and **(B)** mononuclear phagocyte cell populations in the vaginal lavage following infection and respective treatments. N=20 animals per group, and each dot represents a population of cells from a single mouse. Measurements are representative of cell populations from experiments performed at least 2 times. *Mean* $\pm$ *SEM* data is presented. **(C)**, **(D)**, **(E)**, and **(F)** are cytokine levels in vaginal washes of CBA/J mice collected after 7 days of twice daily topical treatment with either Q-GRFT, nystatin, PBS, or placebo. Mice were inoculated with 20 µL (1.0×10^8 cfu/mL) of *C. albicans* blastophores, and cytokines measured using the Luminex xMAP multiplex ELISA assay. **(C)** IFNɣ. **(D)** IL-22. **(E)** IL-23 and **(F)** IL-10. Each dot represents cytokine measurements from a single animal, and analyses were performed in duplicate. Measurements are representative of results from at least 2 independent experiments. *Mean* $\pm$ *SEM* data is presented. ANOVA was used for statistical analysis, with $P \leq 0.05$ considered significant.

Histology of Vaginal Tissue Following Treatment With Q-GRFT Demonstrates Paucity of Infection

To further investigate the effect of Q-GRFT on vaginal candidiasis, we evaluated the impact of topical administration on the histology of infected tissues at the end of the drug treatment period. Microscopic analysis revealed that infected untreated animals displayed significant vaginal luminal congestion with high fungal growth/ burden (FIG 4.4A, 4.4B and 4.4C), unlike Q-GRFT-treated animals that displayed lower congestion (FIG 4.4D, 4.4E and 4.4F). Consistent with our microbiological observations, H&E and PAS staining demonstrated that Q-GRFT was an effective treatment against treated vaginal candidiasis.

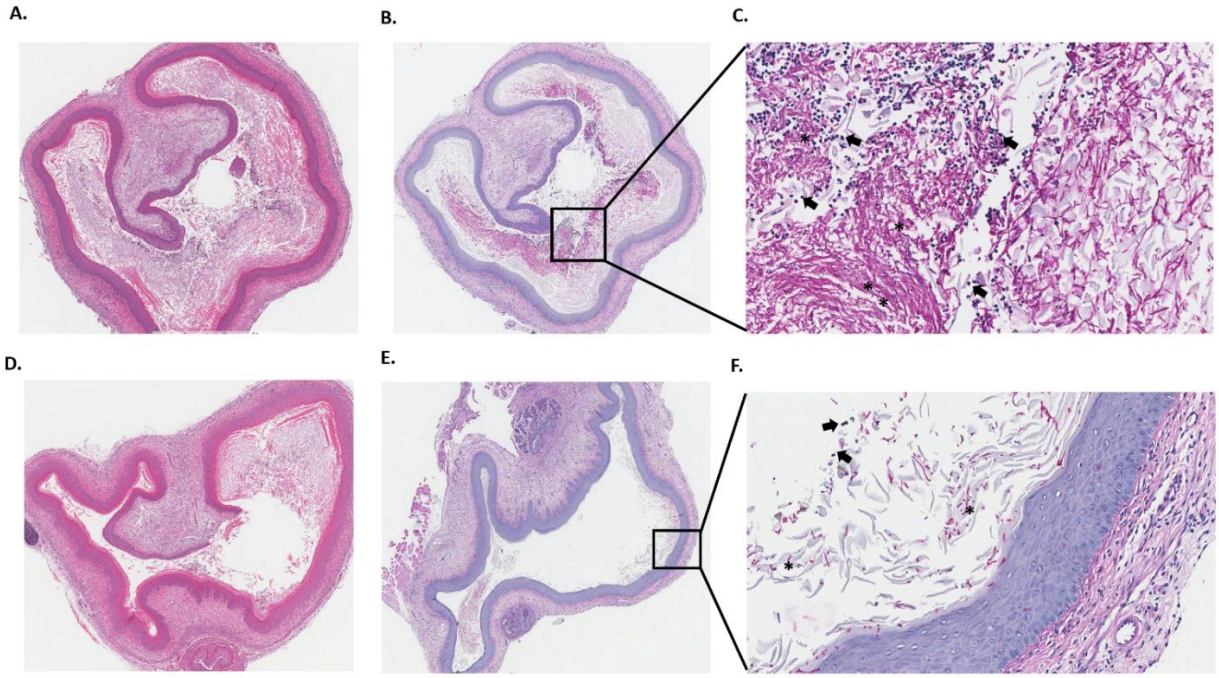

Figure 4. 5 Histological evaluation of vaginal candidiasis following treatment with Q-GRFT.

CBA/J mice were infected with *C. albicans* vaginally. 5 days later, topical treatment was initiated with Q-GRFT gel (vaginally) twice daily for 7 days. Post-treatment (Day 12) tissue histology is presented. **(A)** Representative H&E staining of mice vaginal tissue in the infected, untreated group. **(B)** and **(C)** PAS staining of infected, untreated mice. Note the high vaginal luminal congestion with fungal growth/ burden. **(D)** Representative H&E staining of vagina tissues from Q-GRFT treated mice. **(E)** and **(F)**, PAS staining of vaginal tissue from Q-GRFT-treated mice. Note: (*) represents fungal hyphae and black arrows depict neutrophils in the vagina.

DISCUSSION

Our study demonstrated that Q-GRFT significantly inhibited vaginal infection in a prophylactic model and enhanced fungal clearance in a therapeutic murine model of candidiasis. Cytokines expressed in the vagina following *C. albicans* infection induce large populations of neutrophils in the epithelium, underscoring their mucosal immune cell activation and recruitment function (353). Elevated levels of cytokines are likely

required to initiate and maintain mucosal protection and homeostasis following *C. albicans* vaginal infection (353, 378). Additionally, Zhang et al. showed that epithelial treatment with nystatin, further enhanced the initial immune process generated early in infection, resulting in fungal clearance (353). In our preventive model, we have demonstrated that pre-treatment with Q-GRFT prevented infection establishment, but did not affect neutrophil and monocyte populations, in comparison with infected control animals. In the therapeutic model, unlike the infected controls, treatment with Q-GRFT was effective in fungal clearance and was associated with expression of lower quantities of cytokines IFNɣ and IL-10, but not IL-22 and IL-23, with a predominance of non-viable *C. albicans* cells. These results are similar to observations in the nystatin treatment animals.

Human live vaginal challenge studies have demonstrated that protection from candidiasis is associated with asymptomatic colonization with *Candida*, and the absence of any inflammatory response. Additionally, a heavy inflammatory response with cellular predominance of PMNs is observed in symptomatic disease (364). Furthermore, a positive correlation has been observed between PMN infiltration and vaginal fungal burden in a subset of individuals (335). Comparably, in murine studies, a heavy vaginal infiltration with PMNs has been observed in subsets of inoculated animals, despite no impact on the fungal burden (379, 380). Given the failure in characterizing disease severity in murine models based on clinical signs and symptoms of vaginitis, the rigid criteria based on high and low PMN responses ably predicts symptomatic and asymptomatic conditions in mice with VVC (379, 381). In fact, *in vitro* PMN migration assays have demonstrated that vaginal lavage fluids from high PMN (symptomatic) mice have higher chemotactic activity, when compared to those from low PMN (asymptomatic) animals (379).

Cytokines and chemokines secretion by epithelial cells is only minimally changed upon treatment with Griffithsin (382). Additionally, we have demonstrated that daily topical epithelial treatment with Q-GRFT results in drug accumulation in tissues (chapter 5). Furthermore, multiple topical Q-GRFT application in macaques was associated with a small, and likely insignificant increase in frequencies of rectal mucosal $CD4^+$ cells (204).

Therefore, in the preventive model, daily treatment with Q-GRFT likely resulted in drug accumulation in vaginal mucosal tissues, with a resultant direct inhibitory effect against *C. albicans* infection establishment. Griffithsin's inability to trigger an overt inflammatory response likely accounts for the lack of difference in the populations of neutrophils and monocytes triggered upon infection, in comparison with control animals.

Infection with *C. albicans* likely triggered cytokines early in infection in the therapeutic model, leading to attraction and activation of innate immune cells among all mice inoculated with fungal blastospores. Treatment with Q-GRFT and the control nystatin resulted in fungal clearance, albeit with detectable low fungal burden upon completion of the dosing period. This low fungal burden may subsequently contribute to the ensuing recruitment of immune cells into the vagina, likely maintaining the antigenic trigger for cytokine production. Given that there was no difference in the levels of IL-22 and IL-23 in both Q-GRFT and nystatin treated animals, it is plausible that the rate of cytokines decline lags the rate of fungal clearance. Moreover, Oesterreicher et al. have demonstrated that cytokine dysregulation may often persist, even after fungal pathogen clearance when different antimycotics are used (383).

Pro-inflammatory cytokines are highly expressed in vaginal infection to enhance the clearance of *Candida* infection. In humans, *Candida*-specific T_H cells secrete IL-17 and IFNɤ, with the T_H1-induced interferons aiding in the activation of fungicidal activities of macrophages and neutrophils (384-386). In addition, working cooperatively, Th17- produced IL-17 and IL-22 cytokines facilitate mucosal protection against *Candida* infection by inducing neutrophil recruitment and activation, epithelial cell activation and release of β-defensins (370, 387, 388). Additionally, IL-23 demonstrates a protective role during the early phase of candidiasis by expanding Th17 effector cells and regulating IL-22 production (389, 390). Interestingly, in humans, protection from vaginal candidiasis appears to be independent of T_H17 cell responses, despite their role in other mucosal tissues antifungal immunity (370, 371, 391). In murine models, neutrophil recruitment in response to chemotactic S100 alarmins produced by vaginal epithelial cells has been demonstrated to be independent of IL-17 (392). T_H2 signaling has demonstrated mixed results with regards to immunity to fungal infection (370). Wild type mice deficient of

IL-4 or IL-10 have been reported to demonstrate increased resistance to candidiasis (393). Contrastingly, studies have demonstrated IL-4's critical function in the development of protective responses to *Candida* infection (394). Moreover, Mencacci et al. have reported that in IL-12 deficient mice, IL-10 is required for the development of potent T_H1 immunity to candidiasis (395). In these mice, exogenous IL-10 attenuated IL-4 production and enhanced resistance to infection through inhibition of the CTLA-4/B7-2 costimulatory pathway. They further postulate that a positive regulatory loop exists between IL-12 and IL-10, which hinders innate antifungal immunity, but is essential for optimal co-stimulation of IL-12-dependent CD4+Th1 cells. IL-10, an anti-inflammatory cytokine, inhibits T_H1 cells, NK cells and macrophages activity, hindering pathogen elimination and contributing to tissue damage in presence of infection (396). Cytokines and chemokines are constitutively produced by vaginal epithelial cells in variable amounts (397). However, there is an increase in their production during infection with *C. albicans*, with a predominance of proinflammatory cytokines (397). In response to infection, production of T_H1 cytokines IL-12 and IFNɣ, and T_H2 cytokines TGFβ and IL-10, was increased (397). In our study, Q-GRFT treatment was associated with lower vaginal cytokines IFNɣ and IL-10, when compared to the infected control animals. Additionally, there was no demonstrable difference in cytokines IL-22 and IL-23 for all infected mice, regardless of treatment status. Cytokines IL-22 and IL-23, secreted in response to the initial vaginal infection, are still elevated upon completion of the 7 days treatment, despite the resultant low fungal burden. It is likely that the observed trend towards lower levels of these cytokines is related to the delayed period of decline following treatment. Indeed, De Luca et al. observed that IL-22 was still detectably elevated 7 days after infection in gut mucosal tissue (390). Given that IL-23 stimulates IL-22 production (390), this may likely also explain the persistently elevated levels of both cytokines in all infected mice experimental groups at the end of the treatment period.

So far, there is no demonstrated toxicity, T-cell activation, or immunological stimulation of GRFT or Q-GRFT in *in vitro* and *in vivo* studies (203, 382, 398). We have previously suggested in *in vitro* studies that Q-GRFT binds to α-mannan *in C. albicans'* cell wall, impairs membrane barrier integrity and likely induces reactive oxygen species

formation, with resultant damage to intracellular organelles (13). Here, we have demonstrated that Q-GRFT significantly inhibited infection in a preventive model, and enhanced candidiasis clearance in murine therapeutic studies, with associated lower pro-inflammatory and anti-inflammatory cytokines. Altogether, these data demonstrate that delivery of Q-GRFT to the vagina significantly inhibited *C. albicans* infection, leading to a lower fungal burden, that in turn triggered a lower expression of inflammatory cytokines. Q-GRFT has shown promise in preventing viral sexually transmitted infections, including HSV-2 and HIV-1 (219, 220, 368, 399). Our data demonstrate additional potential for utility of Q-GRFT vaginal dosage forms in both preventing and treating candidiasis, and further support incorporation of Q-GRFT in multipurpose STI prevention modalities.

CHAPTER 5: DEVELOPMENT OF Q-GRFT AS AN INTRANASAL SPRAY FOR BROAD-SPECTRUM CORONAVIRUSES PROPHYLAXIS

INTRODUCTION

Over the past 2 decades, three coronaviruses of the Betacoronavirus genus have emerged as serious human pathogens. The ongoing COVID-19 pandemic has caused over 200 million infections globally and over 614,000 deaths to-date in the United States.

The virus that causes COVID-19, SARS-CoV-2, replicates efficiently in the upper respiratory tract – the nasopharynx and oropharynx – as well as in lungs and gastrointestinal tissue (400). High viral replication in the nasopharynx in the early stages of infection, prior to symptom onset, accounts for the high transmissibility of SARS-CoV-2. While ocular transmission has been reported (228, 229, 401, 402), respiratory aerosols and droplets are the most frequent sources of human transmission events (403, 404). Consequently, the development of an intranasal spray that inhibits replication of virus in the upper respiratory tract is an effective strategy to curb virus spread and will provide synergy to vaccine approaches and biomedical interventions, such as personal protective equipment (PPE) and measures like social-distancing and frequent hand washing, in eliminating the pandemic.

The PREVENT-CoV (PRe-Exposure prevention of Viral ENTry of CoronaViruses) study seeks to demonstrate feasibility for application of an intranasal drug delivery approach as a technology to prevent the establishment of upper respiratory infection. This study will be the first-in-human application of Q-GRFT as an intranasal product. Q-GRFT is an oxidation-resistant variant of Griffithsin (GRFT), a lectin initially extracted from red sea algae (279). GRFT and the variant Q-GRFT, are expressed and

produced by recombinant methods in *Nicotiana benthamiana* plants (279). The GRFT homodimer remains remarkably stable in the environment due to its thermal melting temperature over 78°C, and resists digestion by human and bacterial proteases (405, 406), and has negligible *in vitro* and *in vivo* host toxicity (407). The broad-spectrum antiviral lectin GRFT binds oligomannose glycans that represent a significant fraction of the *N*-linked glycan molecules present on the heavily glycosylated coronavirus S protein (408). GRFT strongly inhibits viral entry by binding to a broad array of coronaviruses, including SARS-CoV (409); MERS-CoV (410, 411); and SARS-CoV-2 (176, 412). GRFT also targets high-mannose glycan structures present on many pathogenic enveloped viruses including human immunodeficiency viruses (HIV) types 1 and 2, herpes simplex virus type 2 (HSV-2), hepatitis C virus (HCV), Japanese encephalitis virus (JEV), porcine epidemic diarrhea virus (PEDV), while exhibiting a remarkable safety profile (10, 189, 405, 413-418).

Our overarching goal is to develop Q-GRFT, the active pharmaceutical ingredient (API), as a non-vaccine broad-spectrum COVID-19 pre- and post-exposure prophylactic in the form of a daily administered nasal spray product. The long-term durability of antibody response to vaccines is not yet well established, and booster doses will be required to maintain effective immunity to SARS-CoV-2 (419, 420). Vaccine hesitancy continues to hinder public vaccination rates (421). Additional tools for prevention are needed to effectively impact the current pandemic. Moreover, certain vulnerable groups, such as organ transplant recipients, may not develop adequate immune responses after vaccination. To this end, an intranasal spray product like Q-GRFT would provide a much-needed strategy for infection prevention, especially in light of the constant evolution of SARS-CoV-2, which will inevitably prolong the pandemic. While other studies have proposed developing intranasal products for utility against SARS-CoV-2 (422-424), our program is the first to evaluate intranasal administration of the Q-GRFT lectin and will establish nasal pharmacokinetic (PK) characteristics for this drug candidate when administered via this route. Inflammatory responses including cytokine storms are associated with poor outcomes in COVID-19 (425). Q-GRFT's inability to trigger significant mucosal and systemic inflammation makes it an ideal candidate as an alternative strategy against coronaviruses (382). Additionally, as coronaviruses mutate to

avoid immune detection, it is unlikely that they will lose the glycan shield and sugars to which Q-GRFT binds. This is because loss of envelope glycans results in attenuated cell infectivity, which is detrimental to virus survival (213, 214). Furthermore, while other strategies like neutralizing antibodies target specific epitopes in the virus structure, Q-GRFT interacts with a wider array of ligands in the virus envelope, facilitating its broad-spectrum antiviral activity (176, 214). Interestingly, GRFT has demonstrated a significantly higher potency (about 11-fold higher) than remdesivir in inhibiting live SARS-COV-2 infection (IC_{50} 63 nmol/L vs EC_{50} 0.77 μmol/L) (176, 426).

The rationale for the development of a Q-GRFT intranasal spray is based upon several criteria. Prophylactic intranasal spray products are designed to deliver medications locally in nasal cavities or systemically. Local drug delivery, the primary focus of our product, likely prevents or at least significantly reduces the acquisition of respiratory infections with a high concentration of product in the respiratory cavity. Local drug delivery is also a logical choice of product delivery for viral respiratory infections including SARS-CoV-2, whose initial point of entry/ infection in the body occurs predominantly via the nasal cavity. This delivery site avoids hepatic first-pass metabolism of the product (427). Even though Q-GRFT may be subjected to local enzymatic activity in the nasal environment, studies elsewhere have demonstrated the lectin's ability to withstand and avoid degradation in the presence of protease activity (206). Additionally, it is a convenient, easy-to-use approach, and is widely accepted as a method of drug administration for a variety of disease processes (428, 429), even as chronic therapy.

The role of lectins in nasal preparations is increasingly being explored due to their unique properties. Upon binding to cell surface receptors, lectins may remain on the surface or may be internalized by receptor-mediated endocytosis. The dual properties enable lectins to act as a direct drug delivery mechanism or play a role in active cell-mediated drug uptake (430). The major drawback of this delivery approach is the possibility of premature drug inactivation or early shedding by mucous drainage (431). Other impediments to overcome with intranasal drug delivery include the continuous outward ciliary movement on the epithelial apical surface that clears trapped substances,

as well as nasal proteases and pH considerations that may impact drug stability (431). Several studies have shown that lectins trigger low ciliary clearance and scant mucosal irritation (168, 432). The lectin wheat germ agglutinin (WGA) has been used as part of a lectin-modified nanoparticles intranasal delivery approach: WGA binds to N-acetyl-D-glucosamine and sialic acid moieties that are abundant in the nasal cavity and olfactory mucosa. Due to its potent mucosal binding, WGA conjugation with mucoadhesive polymers resulted in increased drug delivery to the target site (433).

The intranasal delivery approach has previously been explored for efficacy against respiratory infections with mixed results, necessitating the need for the continued development of preventative modalities in this area. Preclinical evaluation of a nasal spray containing carrageenan showed that the sulfated polysaccharide derived from red seaweeds (Rhodophyceae) maintained antiviral effectiveness against human rhinoviruses and human coronavirus OC43 in *in vitro* assays (434). Intranasal sprays with interferons were also shown to protect human volunteers from infection with coronavirus, influenza, and rhinoviruses (435). In a randomized, double-blind, placebo-controlled exploratory study evaluating the antiviral efficacy and safety of an Iota-carrageenan containing nasal spray, patients infected with any respiratory virus and intranasally treated with the polysaccharide recovered 1.9 days faster from common cold symptoms compared to placebo-treated individuals, (P=0.046). In addition, when Iota-carrageenan was administered within 48 hours of development of the common cold symptoms, the polysaccharide was associated with lower viral replication (P=0.009), and expression of pro-inflammatory markers (436). Given that immunocompromised individuals may not mount a sufficient immune response to completely eliminate infections (437, 438), this may hinder the utility of a carrageenan product in disease prevention. However, the study was not designed to investigate carrageenan's preventative effects in healthy individuals. Intranasal antibody prophylaxis also showed great promise against viral respiratory tract infections in animals along with clinical efficacy in human studies (439-441).

Altogether, these background data and studies strongly support the development of a Q-GRFT intranasal spray to prevent the establishment of SARS-CoV-2 infection.

This strategy will synergize with prevention approaches that include the use of vaccines and physical interventions like PPE.

Here, we present preclinical results from engineered human epithelia, *ex-vivo* and cadaver studies. The studies provide evidence of Q-GRFT detection in epithelial tissues and confirmed the ability to quantify Q-GRFT in nasal, nasopharyngeal, and oropharyngeal fluids. We also outline the clinical protocol for the planned PREVENT-CoV Phase 1a clinical study that will evaluate the safety, tolerability, and pharmacokinetics of intranasal administration of Q-GRFT in healthy male and female volunteers. Secondary endpoints for the study will include user perceptions, acceptability, and the impact of product use on participants' olfactory sensation, and quality of life. The data generated from this study will support further development of Q-GRFT in future clinical studies, as a nasally administered drug candidate against coronavirus infection.

MATERIALS AND METHODS

Approval to conduct this Phase 1a study has been granted by the University of Louisville Institutional Review Board, under IRB# 21.0704, and the trial will be carried out in compliance with Good Clinical Practices conduct. The study has also received authorization for the intranasal use of Q-GRFT under Investigational New Drug Application (IND) #151381.

MatTek epithelial tissue treatment and Q-GRFT concentration determination

Apical corneal and airway epithelial tissues in MatTek™ (MatTek Corporation, Ashland, MA, U.S.A.) tissue were treated with either 67 µg/mL, 6.7 µg/mL, or 0.67 µg/mL Q-GRFT, and drug concentrations determined in tissue wash fluids, per the manufacturer's instructions. Upon arrival, the 6-well plates were prepared by the addition of tissue-specific maintenance media. The tissue cap containing epithelial tissue was placed in the prepared well plate and incubated overnight at 37°C, 5% CO_2. Excess accumulated mucus was then carefully removed by aspiration, followed by gentle rinsing of the apical surface twice with 400 µL assay media. Basolateral media was then removed and replaced with 1mL fresh assay media, as appropriate for each tissue type. One hundred fifty microliters of various concentrations of Q-GRFT were added to the

apical tissue surface followed by incubation for 1 hour at 37°C, 5% CO_2. Apical contents were aspirated, tissue washed once with 400 µL assay buffer, and plates incubated for 24 hours at 37°C, 5% CO_2. Samples were collected from the apical surface by washing with 400 µL assay buffer and stored at -80°C, until concentration determination. The same preparation procedure was followed every twenty-four hours to obtain samples at 48 hours, 72 hours, 96 hours, and 120 hours. After collecting the last sample, tissues were lysed with 1 mL of Trizol and stored at -80°C. Q-GRFT concentrations in the collected specimens were determined by ELISA.

Human fresh tissue Q-GRFT concentration determination

To evaluate whether intranasally administered Q-GRFT would be detected in the nasal cavity, a fresh-tissue study was performed using a recently donated human cadaver. Two squirts (100 µL per squirt) of fluorescein-labeled Q-GRFT nasal spray solution were instilled into each nasal cavity using a multidose nasal spray actuator. Nasal, nasopharyngeal, and oropharyngeal cavities were swabbed every 15 minutes under endoscopic guidance. Swab contents were eluted with PBS, and Q-GRFT concentrations determined by either ELISA or fluorescence determination. For both ELISA and fluorescence determinations, standard Q-GRFT concentrations were prepared and serially diluted, prior to generation of a standard curve using optical density (OD) and fluorescence measurements. A BioTek Synergy HT plate reader (Vermont, U.S.A.) running Gen5 software was used. Specimen concentrations were determined by making comparisons with the standard curves generated, respectively.

Luminex cytokines

Cytokine concentrations were determined following collection of tissue wash fluids from the MatTek tissues mentioned above. Prior to analysis, protein concentrations were determined using a bicinchoninic acid (BCA) protein assay (Pierce™ BCA Protein Assay Kit, Thermo Scientific, Rockford, IL, USA), according to manufacturer's protocol. Concentrations were normalized for all samples prior to loading on a Human Cytokine/ Chemokine Magnetic Bead Panel (EMD Millipore Corporation, Billerica, MA, U.S.A.). The panel was analyzed with a Milliplex MAP Kit on a MagPix with Luminex xMAP technology (Luminex, Northbrook, IL, USA).

Statistical analysis

Where appropriate, tests used to determine significance between experiments are outlined in the figure legends of each figure. Data are representative of 2-3 independent experiments for each time points. One way ANOVA was performed using GraphPad Prism7.05 (GraphPad Software, Inc, La Jolla, California) to determine statistical difference. A *P* value $\leq$0.05 was considered significant

PRE-CLINICAL EXPERIMENTAL STUDY RESULTS

Q-GRFT Accumulates and is Detected in ex vivo Epithelial Tissues Upon Treatment

We evaluated the ability to detect and quantify Q-GRFT in the airway and corneal epithelia following topical application in MatTek™ EpiAirway and EpiCornea tissues. Epithelial tissues were treated with either 67 µg/mL, 6.7 µg/mL, or 0.67 µg/mL Q-GRFT for one hour daily, followed by washing, and a 24-hour incubation period. The tissues were then washed and Q-GRFT in the epithelial wash fluids was quantified by ELISA. This was repeated daily for 5 days (120 hours). In EpiAirway epithelia, there was a significant dose-cumulative effect that was observed with 67 µg/mL Q-GRFT, with the drug levels initially accumulating up to 96 hours following treatment, then subsequently declining at the 120-hour period (FIG 5.1). Table 5.1 shows the *P*-values for the different Q-GRFT concentrations when drug levels in treated EpiAirway tissues were compared with cells only controls. Similarly, epithelial drug accumulation was observed with 67 µg/mL Q-GRFT in EpiCornea tissue up to 96 hours, with a decline in concentration at 120 hours, when treated tissues were compared with untreated controls (FIG 5.1). Table 5.2 shows P-values for comparisons made between Q-GRFT treated EpiCornea tissues and cells only controls. Loss of epithelial cell viability after 96 hours likely accounted for the reduction in Q-GRFT concentrations observed at 120 hours.

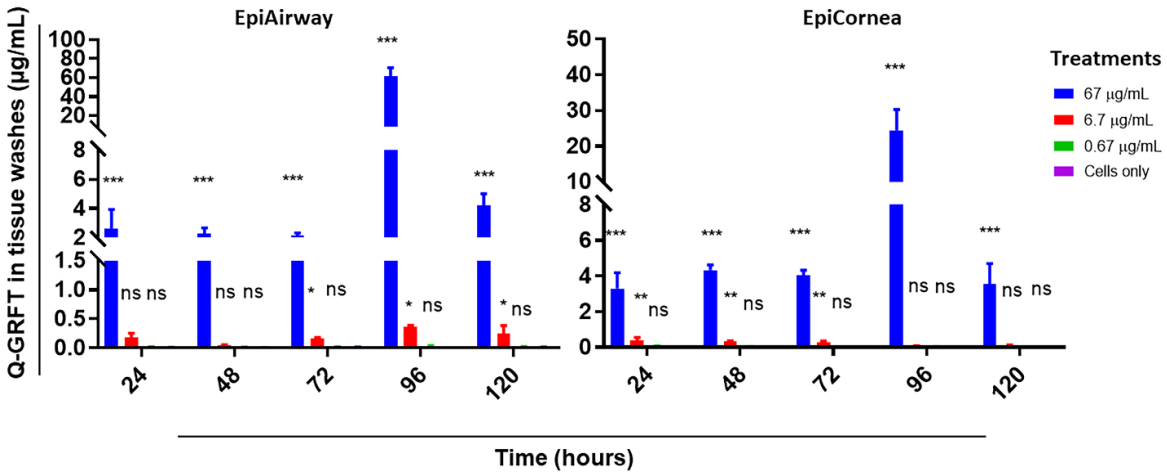

Figure 5. 1 Q-GRFT accumulation by dose in epithelial tissues following treatment. MatTek™ EpiAirway (left) and EpiCornea (right) epithelial tissues were treated with either 67 µg/mL, 6.7 µg/mL, or 0.67 µg/mL Q-GRFT, incubated for 1 hour at 37°C, 5% CO_2, washed, then incubated for 24 hours, washed and Q-GRFT levels determined in the tissue wash fluids by ELISA. Treatment and Q-GRFT determination was repeated once daily for up to 120 hours. Experiments were performed at least two times, in triplicate. *Mean* ± *SEM* values are presented. Statistical analysis was performed by one way ANOVA. $P \leq 0.05$ was determined as significant.

Table 5.1 *P*-values for EpiAirway tissues treatment with Q-GRFT.

	***P*- value**				
	24 hours	**48 hours**	**72 hours**	**96 hours**	**120 hours**
Q-GRFT treatments					
67 µg/mL	0.0231	<0.0001	<0.0001	<0.0001	<0.0001
6.7 µg/mL	0.8969	0.9190	0.2381	0.9594	0.7022
0.67 µg/mL	0.9946	0.9889	0.9885	0.9994	0.9935

Table 5.2 *P*-values for EpiAirway tissues treatment with Q-GRFT.

	***P*- value**				
	24 hours	**48 hours**	**72 hours**	**96 hours**	**120 hours**
Q-GRFT treatments					
67 µg/mL	0.0002	<0.0001	<0.0001	<0.0001	0.0006
6.7 µg/mL	0.9298	0.0579	0.6413	>0.9999	0.9988
0.67 µg/mL	0.9990	0.9997	0.9998	>0.9999	>0.9999

Q-GRFT Does Not Affect the Basal expression of Inflammatory cytokines in Epithelial Tissues Following Treatment

We next sought to establish if treatment of epithelia with Q-GRFT induced secretion of any inflammatory cytokines. Using the apical wash fluids collected from the tissues at the end of the dosing period, we determined the inflammatory cytokines expression profile. Cytokines were assayed using the Luminex xMAP multiplex ELISA assay method. When compared with untreated cells-only controls, there was no detectable difference in the expression of either pro-inflammatory or anti-inflammatory cytokines by both EpiAirway (FIG 5.2) and EpiCornea tissues (FIG 5.3). These results demonstrated that *in vitro*, Q-GRFT does not significantly affect basal expression of epithelial cytokines.

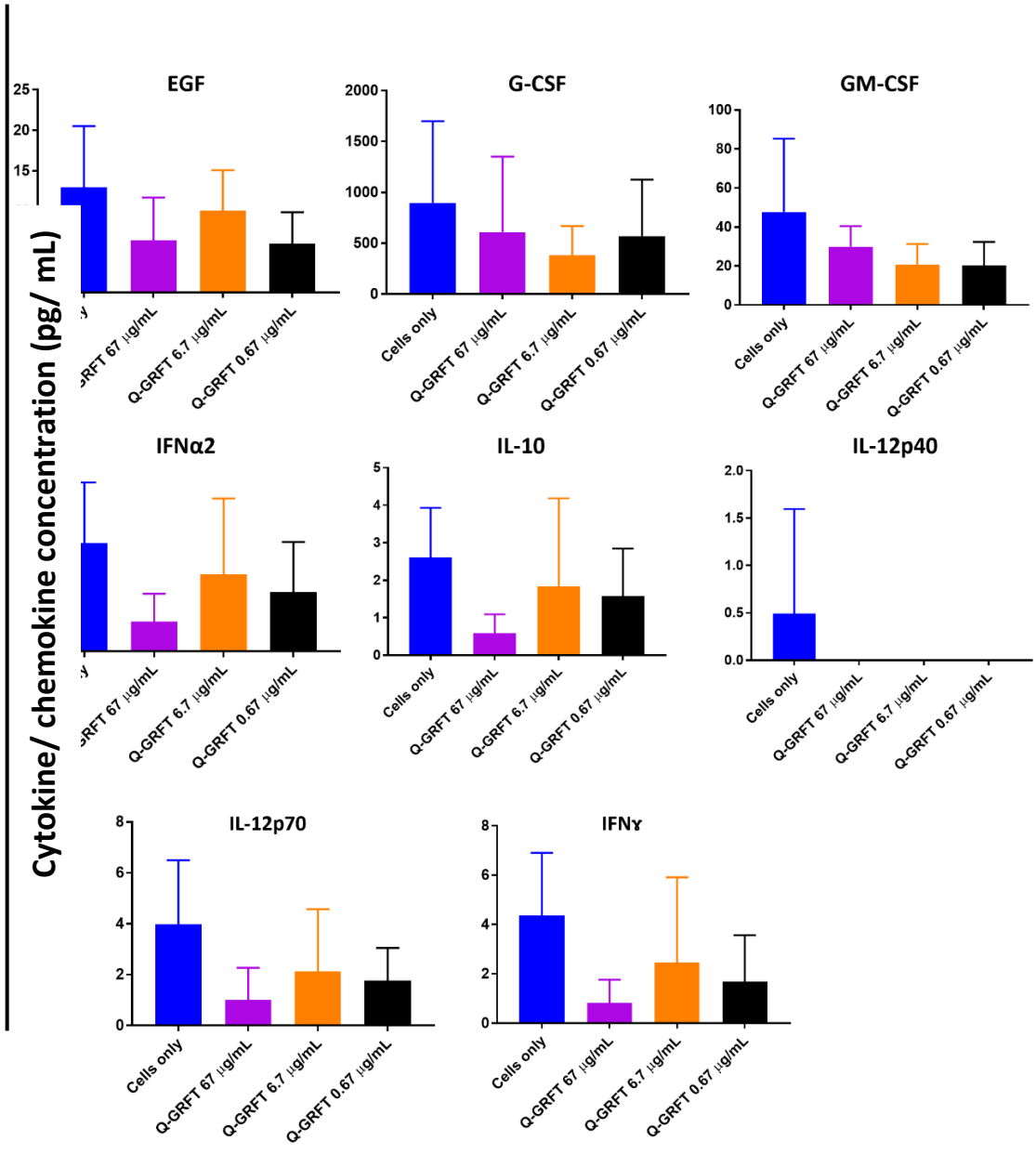

Figure 5. 2 Q-GRFT does affect basal expression of inflammatory cytokines in airway epithelium. MatTek™ EpiAirway tissues were treated with either 67 µg/mL, 6.7 µg/mL, or 0.67 µg/mL Q-GRFT, incubated for 1 hour at 37°C, 5% CO_2, washed, then incubated for 24 hours, washed, and incubated for 24 hours. This treatment was repeated once daily for up to 120 hours. Wash fluids at 120 hours were used to measure cytokines, using Luminex xMAP multiplex ELISA assay. Experiments were performed in triplicate, *N*=6

samples per treatment group, and *Mean* ± *SD* values are presented. Statistical analysis was performed by one way ANOVA. $P \leq 0.05$ was determined as significant.

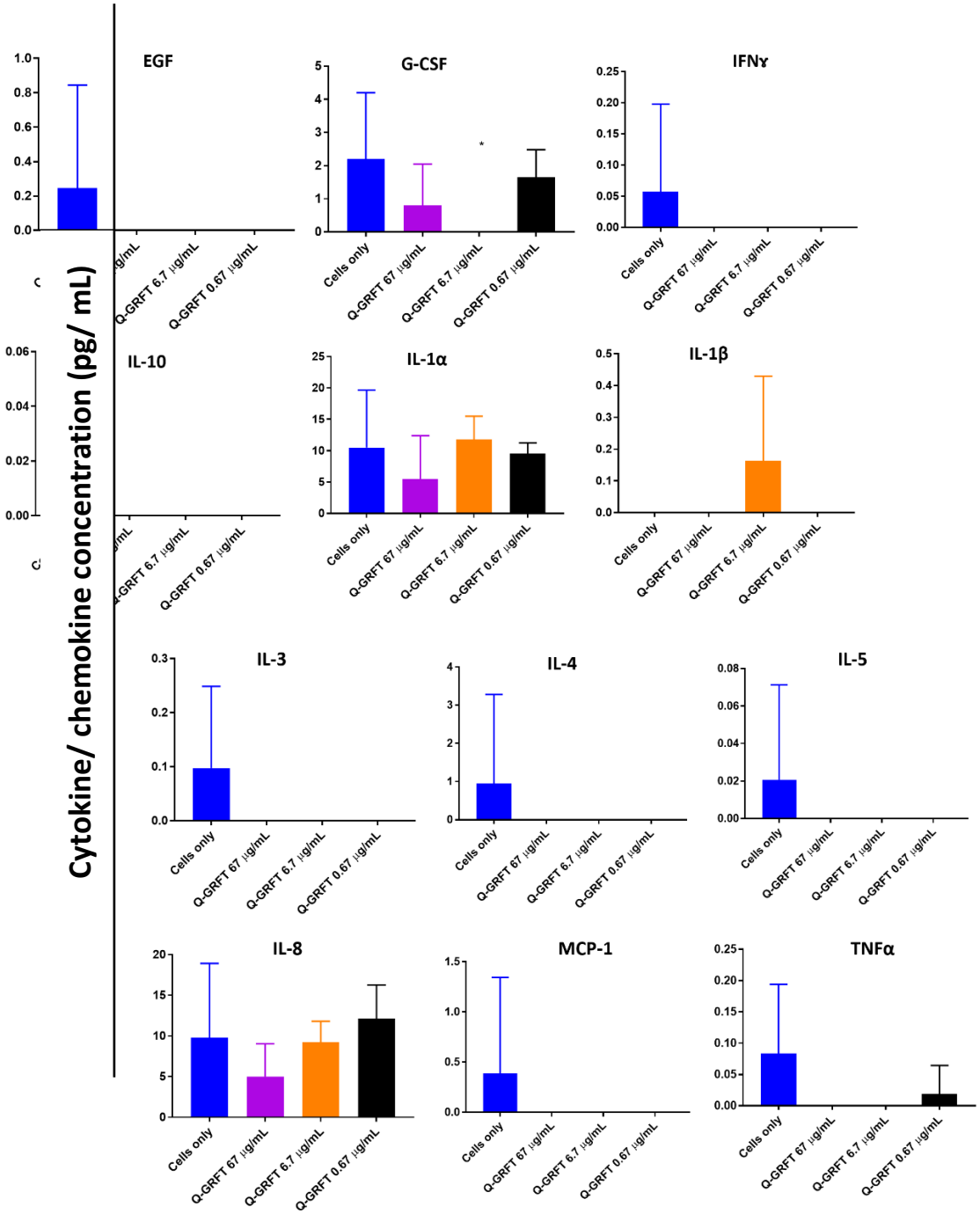

Figure 5. 3 Q-GRFT does not affect basal expression of inflammatory cytokines in cornea epithelium. MatTek™ EpiCornea tissues were treated with either 67 µg/mL, 6.7 µg/mL, or 0.67 µg/mL Q-GRFT, incubated for 1 hour at 37°C, 5% CO_2, washed, then

incubated for 24 hours, washed again, and incubated for 24 hours. This treatment was repeated once daily for up to 120 hours. Wash fluids at 120 hours were used to measure cytokines, using Luminex xMAP multiplex ELISA assay. Experiments were performed in triplicate, N=6 samples per treatment group, and $Mean \pm SD$ values are presented. Statistical analysis was performed by ANOVA. $P \leq 0.05$ was determined as significant.

Q-GRFT is Detected and Quantifiable in The Human Nasal Cavity, Nasopharynx, and Oropharynx

To develop and validate assays for the detection of Q-GRFT in the planned clinical trial, we performed a fresh tissue study with topical application of Q-GRFT spray in the nasal cavity. Here, two sprays (100 µL per spray) of fluorescein-labelled Q-GRFT were instilled in the nasal cavity of a human cadaver (body donated within 24 hours of death), followed by observation for drug dispersion and specimen collection under endoscopic guidance by the study rhinologist (FIG 5.4). Specimens were collected from the right nasal cavity (NCR), left nasal cavity (NCL), right nasopharynx (NPR), left nasopharynx (NPL), right oropharynx (ROP), and left oropharynx (LOP) every 15 minutes, with efforts made to sample different sites at each collection time. Care was taken to avoid the swab coming into contact with the cavity walls during sampling. Nasal samples were taken from the middle nasal turbinate. The nasal cavity epithelium was pink with normal anatomical findings (FIG 5.4A). Q-GRFT was uniformly distributed along all nasal cavity walls and the oropharynx (FIG 5.4B and FIG 5.4C).

The specimens collected were eluted in PBS prior to quantification by ELISA and fluorescein determination (FIG 5.5). Swabs collected from the different sites demonstrated variations in weight (FIG 5.5A). Quantification of Q-GRFT concentrations by both fluorescence activity and ELISA demonstrated variations in drug levels sampled from different anatomical sites. However, there was observable similarity in the drug concentrations measured by both methods from specimens obtained from the same site (FIG 5.5B and FIG 5.5C). Hence, these findings demonstrate that ELISA and fluorescence assay are reliable methods for quantifying Q-GRFT concentrations. We will

utilize the ELISA assay to quantify drug concentrations for specimens collected in the planned clinical study.

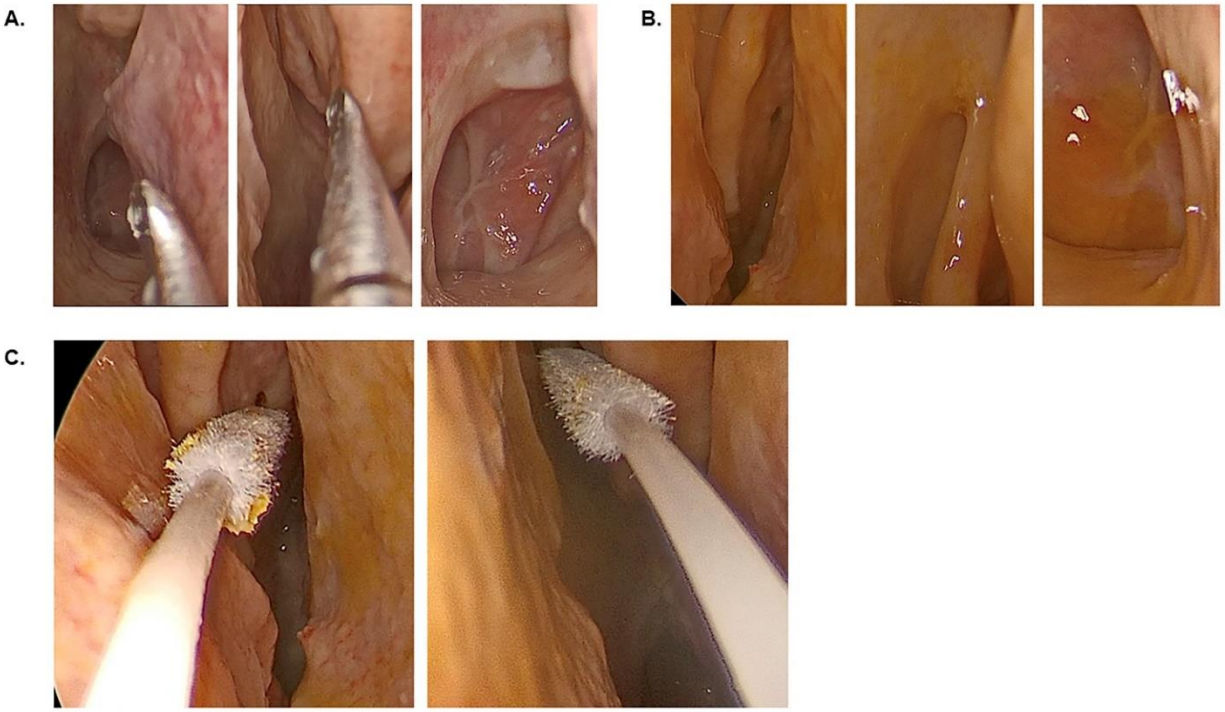

Figure 5. 4 Q-GRFT is detectable in the human nasal cavity, nasopharynx, and oropharynx.

A fresh tissue study was performed with a donor human cadaver (body donated within 24 hours of death) to assess the dispersion properties, establish, and validate assays to determine Q-GRFT concentrations in nasal, nasopharyngeal, and oropharyngeal fluids. Fluorescein-labelled Q-GRFT was instilled in the nasal cavity as an intranasal spray, 2 squirts per nostril, visualization and sampling was done under endoscopic guidance by a rhinologist. **(A)** Left nasal cavity (left), left middle turbinate (middle), and oropharynx prior to Q-GRFT treatment. Note the pink color of the epithelium. **(B)** Left nasal cavity (left), left middle turbinate (middle), and oropharynx (right) following intranasal Q-GRFT administration. The yellow-brown color of the Fluorescein-Q-GRFT depicts drug dispersion after administration. **(C)** Swab in the left nasal cavity (left) and right nasal cavity (right) during sampling of the respective middle turbinates.

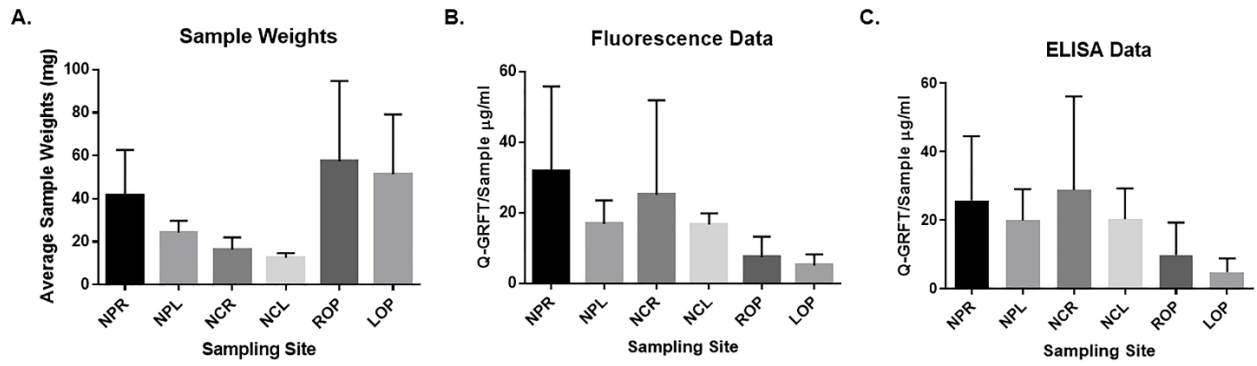

Figure 5. 5 Q-GRFT is quantifiable in the human nasal cavity, nasopharynx, and oropharynx. A fresh tissue study was performed with a donor human cadaver (recently died within 24 hours) to assess the drug levels and validate ELISA and fluorescence assays for collected nasal, nasopharyngeal, and oropharyngeal fluids. Fluorescein-labelled Q-GRFT was instilled in the nasal cavity as an intranasal spray, 2 squirts (100 µL per squirt) per nostril, visualization, and sampling was done under endoscopic guidance. **(A)** Weight of samples collected from different anatomical sites. **(B)** Q-GRFT concentrations from fluids collected from the respective anatomic sites, as determined by fluorescence intensity method. **(C)** Q-GRFT concentrations from fluids collected from the respective anatomic sites, as determined by the ELISA assay method. Measurements were done in triplicate and repeated at least 2-3 times. Representative data, *Mean ± SD* is shown. Data was analyzed using one-way ANOVA. (NPR-right nasopharynx; NPL-left nasopharynx; NCR-right nasal cavity; NCL-left nasal cavity; ROP-right oropharynx and LOP-left oropharynx).

PHASE 1A CLINICAL STUDY PROTOCOL DESIGN

Study Objectives

The primary objective of this first-in-human intranasal exposure study is to evaluate the safety, tolerability, and pharmacokinetics (PK) of Q-GRFT intranasal spray administered as a single dose in a Phase 1a trial. Secondary objectives include the assessment of user perceptions and acceptability, and the impact of product use on participants' olfactory sensation, and quality of life.

Clinical Study Design

This will be a randomized, double-blind, single-site trial. In this Phase 1a study (FIG 5.6), 18 participants will be randomly assigned 2:1 to either Study Arm 1 or 2 to receive either a single dose of study product or placebo under direct observation (Table 5.3). Due to the 2:1 randomization, stratification will be balanced to safeguard for extreme allocation distribution (such as all females being assigned to the placebo arm). Although a 'healthy population' will be enrolled, biological sex (male, female) and race (white and other) will be considered as stratification factors. In the placebo arm, 3 males and 3 females will be enrolled; this will comprise 4 whites (split between male and female) and 2 others (split between male and female); enrollment for the treatment arm will be double the distribution in the placebo arm. Replacements will be planned to substitute for dropouts due to reasons unrelated to the treatment. Three age and sex-matched participants will be held in reserve for participants that drop out after drug exposure prior to completing a full follow-up for safety. Participants in Arm 1 will receive a single dose of Q-GRFT study product delivered intranasally as two sprays (200 µL per nostril), for a total dose of 3.0 mg. Participants in Arm 2 will receive a single dose of placebo product, delivered intranasally as two sprays per nostril. This intranasal product will contain the same ingredients as the study product minus the active Q-GRFT component. Following administration of the intranasal product in both arms, PK sampling will be performed at different time points (1 hour, 6 hours, 24 hours, and 3 days post-dose administration), followed by a safety review after 24 hours, 3 days, and 2-3 weeks later with a phone call. If this clinical dose is determined safe and acceptable, the study will advance to Phase 1b to assess future dose loading questions or de-escalation adjustments.

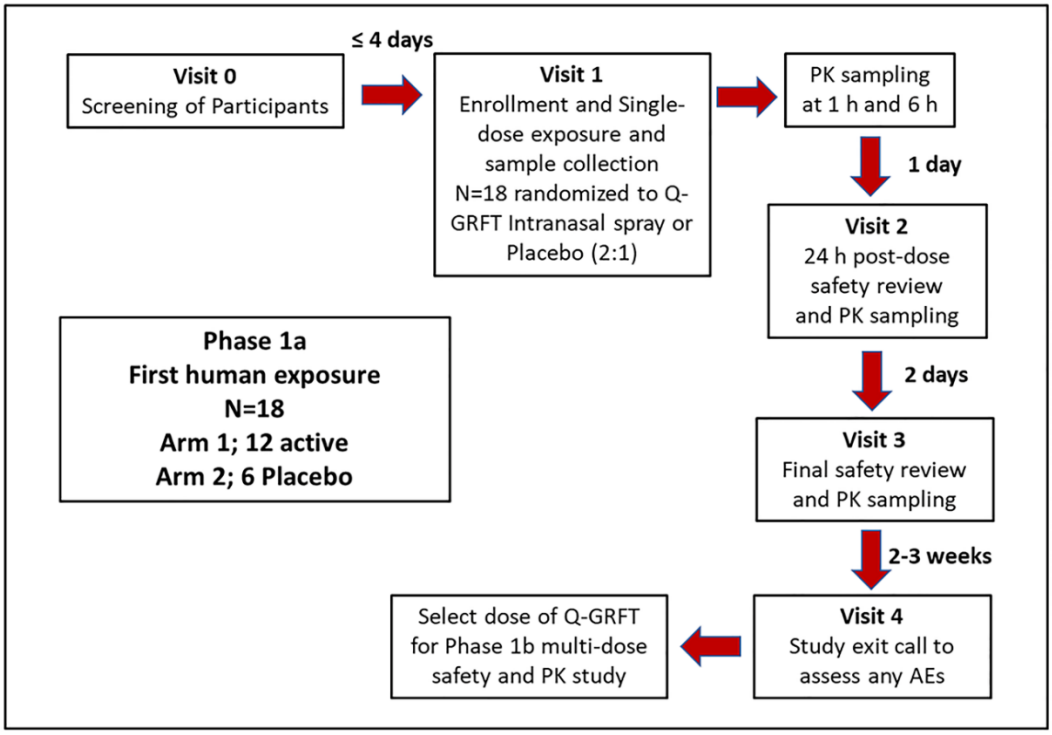

Figure 5. 6 Phase 1a study design.

Table 5.3. Phase 1a Study Arms

Arm	**N**	**Method of Assignment**	**Study Product**	**Dosing**
1	12	Randomized, Double-blind	Q-GRFT Intranasal spray (7.5 mg/ mL)	Single-dose, one time
2	6	Randomized, Double-blind	Placebo Intranasal spray	Single administration

Study Participants/ Population

The study population will consist of healthy male or female individuals who will satisfy the following inclusion criteria.

Inclusion Criteria

Participants will be aged 18-60 years at screening; have a negative SARS-CoV-2 test using the rapid antigen test at screening; be able and willing to provide written informed consent; be able to provide adequate information for locator purposes; be available to return for all study visits, barring unforeseen circumstances; and agree not to participate in other research studies involving drugs and/or medical devices during the study period. In addition, female participants should not be pregnant at the baseline or enrollment visit or breastfeeding during the study and must be: either post-menopausal or using (or willing to use) an acceptable form of contraception (e.g., abstinence, barrier method, IUD, hormonal contraception, surgical sterilization, or vasectomization of male partner); male participants in heterosexual relationships should be willing to use barrier methods during intercourse, and/ or have their partners using any of the acceptable forms of contraception listed above. Participants should have no plans to receive any vaccines while on the study or be able to safely defer vaccinations until completion of study participation. Furthermore, they must agree to not use intranasally-applied medication for the duration of the study.

Exclusion Criteria

Participants will be excluded if they meet these criteria or have any of the conditions: ongoing moderate to severe allergic rhinitis or asthma, history of chronic obstructive pulmonary disease (COPD), or chronic rhinitis with ongoing sinusitis. Additionally, participants will not be enrolled if they report any of the following at the screening visit: ongoing common cold or flu-like symptoms for 48 hours prior to the screening, including sore throat, blocked nose, runny nose, cough, or sneezing; participants known to experience moderate or severe or higher seasonal allergies, such as hay fever, (symptoms in excess of mild, intermittent nasal rhinorrhea, sneezing, or

itchy/watery eyes); participants who report non-therapeutic injection drug use in the 6 months prior to screening, including those who report recreational snorted drug use; participants who report prescription medication/ concomitant therapy use other than for contraception and antibiotics. Prohibited medications include systemic steroids, intranasal medicines, among others. Participants who actively smoke at the time of screening; those with a known allergy to methylparaben, propylparaben, or any ingredients of the formulated drug product; individuals who take systemic immunomodulatory medications (Thalidomide, Lenalidomide, Pomalidomide, Imiquimod, etc.), anticoagulants, or other drugs assessed by the site Investigator as invalidating within the 4 weeks prior to the enrollment; those with a history of alcohol/ substance abuse within 6 months of study enrollment; subjects with a history of any vaccination within the 2 weeks prior to enrollment; participants enrolled in another research study involving drugs or medical devices within the 4 weeks prior to PREVENT-CoV enrollment; and those who have plans to relocate away from the study site area during the period of study participation.

Furthermore, participants with any of the following laboratory abnormalities at Screening will not be enrolled: white blood cell count < 2,000 cells/mm^3 or > 15,000 cells/mm^3; hemoglobin <12 g/dL for men and <11 g/dL for women; calculated creatinine clearance >1.1 x upper limit of normal (ULN); alanine transaminase (ALT) and/or aspartate aminotransferase (AST) > 1.1 × the site laboratory ULN; total bilirubin > 1.1 x ULN; and ≥ +1 glucose or +2 protein on urinalysis (UA). Additionally, participants may not be enrolled if they report any other condition or prior therapy that, in the opinion of the investigator, would preclude informed consent, make study participation unsafe, make the individual unsuitable for the study, or unable to comply with the study requirements. Such conditions may include but are not limited to, a current or recent history (within last 6 months) of severe, progressive, or uncontrolled substance abuse, renal, hepatic, hematological, gastrointestinal, endocrine, pulmonary, neurological, cerebral disease, or severe nasal septum deviation, or other conditions that may cause nasal obstruction like nasal polyps or prior nasal/ sinus surgery.

Study Product

The intranasal spray product used in the cadaver study, and which will be utilized in the Phase 1a study contains Q-GRFT (7.5 mg/mL) as the active pharmaceutical ingredient (10 mg/mL Q-GRFT stock solution in phosphate-buffered saline, pH 7.4), water-soluble preservatives (parabens), a viscosity modifying agent (lambda carrageenan polymer), stabilizing agent, acidifying agent, and solvents (PBS and purified water). The placebo intranasal spray will be identical to the active product formulation minus the API.

Study Procedures

Participants Recruitment, Screening, and Retention

Male and female participants will be recruited from a variety of sources, using key strategies that will include: clinician-patient referrals; use of existing "study registries" that contain the names and phone numbers of individuals who have given informed consent to be reached for future studies for which they may be eligible; participant referrals (participants may refer their friends or partners who meet eligibility criteria); and passive self-referral by interested individuals who see a study poster or brochure. Both male and female participants will be recruited, and strategies will be undertaken to ensure equitable opportunity to enroll from members of both biological sex to the extent possible. Additionally, minorities that are representatives of the diversity of Jefferson County, Louisville, KY will be sought. Enrollment will be performed at the University of Louisville, Louisville, KY.

Volunteers will be prescreened to determine eligibility. Approximately 40 volunteers will be screened to enroll 18 participants meeting the eligibility criteria. Study staff will meet as needed to discuss the ongoing recruitment status, targets, and strategies. Staff will follow up with all persons who express an interest in the study to ensure that screening appointments are scheduled in a timely manner.

Once enrolled, the study site will make every effort to retain participants for the duration of follow-up in order to minimize loss-to-follow-up bias. This will be done through exhaustive explanation of the study visit schedule and procedural requirements during the informed consent process both in-person and using a pre-recorded information video, and re-emphasis at each study visit; thorough explanation of the importance of all dosing and sampling phases to the overall success of the study; use of appropriate and timely visit reminder mechanisms (via email and/or telephone); and immediate and multifaceted follow-up on missed visits.

Informed Consent, Clinic Visits, and Assessment

All participants will provide written informed consent prior to participation in the study. Participants will have a right to withdraw from the study at any time for any reason.

Participants will be prescreened using online questionnaires and telephone interviews, and selected volunteers will be invited for the screening visit at the next available appointment. At Visit 0, written informed consent will be obtained, along with locator information, demographics, and medical history. A brief physical examination including a visual inspection of the nose and throat and an assessment of olfaction will be conducted. A baseline quality-of-life questionnaire (Short Form-12 item; SF-12) will also be administered. Eligible participants will have blood, urine, nasal, and throat specimens collected, and a rapid COVID-19 test performed. Baseline specimens (plasma samples, nasal, nasopharyngeal, and oropharyngeal fluids) will also be collected using a swab for baseline PD and cytokines evaluation.

Visit 1 (enrollment and single-dose exposure) will occur 3-4 days following screening at Visit 0. Here, eligibility will be confirmed, and a complete clinical assessment performed. Plasma samples will be obtained for storage for future research, and repeat blood tests performed if indicated, for follow up of any prior abnormal blood tests. Participants will then receive either the single-dose Q-GRFT DP intranasal spray or placebo, two sprays into each nostril, as per the randomization assignment. PK sample collection will then occur at 1 hour and 6 hours post-dosing.

Visit 2 will occur 24 hours post-dosing and will include clinical evaluation and PK sampling. Nasal, nasopharyngeal, and oropharyngeal fluids will be collected. Blood will be collected for cytokine evaluation and plasma storage for future research. Olfaction will be assessed using the Brief Smell Identification Test (BSIT) and an acceptability questionnaire will be completed.

Visit 3 will be the final safety evaluation and PK sampling visit and will occur 2 days after visit 2. Here, participants will complete a product acceptability questionnaire, the SF-12, and undergo a symptom-directed physical exam, including a nose and throat inspection. Olfaction will also be assessed. Blood will be collected for full hemogram and storage. In addition, nasal, nasopharyngeal, and oropharyngeal fluids will be collected, and the product acceptability questionnaire administered.

A final Phase 1a study exit phone call (visit 4) will be made to the participants within 2-3 weeks after visit 3 to inquire about any adverse events that the participant may have experienced as a result of product administration. The product acceptability questionnaire will again be administered in an online format. If this initial dose exposure is found to be safe and tolerated, the study will proceed to Phase 1b.

Intervention Groups

Eighteen enrolled participants will be randomly assigned 2:1 to receive either study product or placebo arms. Based on prior studies with similar eligibility requirements, the site is expected to enroll 6 participants per week. Accrual is anticipated to take approximately 2-4 weeks.

Drug and Dose selection

Our extensive studies with rectal toxicology in rats and rabbits did not reach a maximum tolerated dose, even though animals were dosed with a 30 mg/mL gel formulation that delivered a tissue concentration measured in PK assays at more than 1,000 fold the EC_{90} of HIV-1 (196). Both mice and Syrian Golden hamsters have been treated with GRFT intranasally in efficacy studies against SARS-CoV (442) and NiV (443), respectively. Rhesus macaques have been exposed to nebulized GRFT. No toxicity has been reported in these studies, and the anticipation extends to the studies described in

this proposal. Evidence of Q-GRFT distribution to the brain is perhaps the most significant toxicity risk that we may encounter, which will result in the need for extensive neurotoxicity assessments in the toxicology studies planned to support Phase 2 clinical studies.

Based on efficacy observed in the SARS-CoV, NiV, and MERS-CoV models, 7.5 mg/ mL of Q-GRFT (total dose of 3.0 mg) will be administered to participants in Phase 1a. This dose is 1000- fold higher than the effective dose (EC_{50}) that was protective in tissue exposure experiments (unpublished).

Outcome Measures

The endpoints selected for this study are appropriate measures of prophylactic preventative effect. A single dose exposure will be used to determine the safety, acceptability, and PK of a Q-GRFT intranasal spray product in preventing SARS-CoV-2 infection.

Safety and Tolerability

Routine Clinical Laboratory Tests

Routine hematology, blood chemistry, and urinalysis will be performed for participants, as described in Table 5.4. A complete blood count with differential, blood chemistry, urinalysis, and pregnancy test (βhCG) for female volunteers will be performed at the screening visit. Repeat hematology and a comprehensive metabolic panel will be performed at Visits 3.

Physical Examination and Nasal Endoscopy

A complete physical examination will be performed per Table 5.4. An abbreviated physical examination, including a nose and throat exam, and routine examination of the lungs, heart, abdomen, skin, and central nervous system will be performed. Subsequent nasal endoscopy will be performed by the study rhinologist during PK sample collection to ensure accuracy and consistency at all time points. The direct visualization afforded by endoscopy will allow for swabbing the same anatomic

location at each sampling time point, reducing sampling variability. Additionally, this will mitigate participant discomfort during the sampling procedure.

Vital Signs

Vital signs (heart rate, blood pressure, temperature, and respiratory rate) will be measured as specified in Table 5.4 after the subject sits quietly for 5 minutes on all visits and as clinically indicated.

Body weight and Height

Bodyweight and height will be recorded at the initial health assessment, with weight measured again at subsequent study clinical visits.

Olfactory Assessment

Evaluation of olfactory function will be performed at the time points specified in Table 5.4. Sense of smell will be determined using the University of Pennsylvania BSIT, a validated assessment of olfactory function (444). The BSIT assesses an individual's ability to detect odors at a suprathreshold level. The test consists of 12 items provided in a 12-page booklet. On each page, there is a "scratch and sniff" strip embedded with a microencapsulated odorant along with 4 choice options. The participant smells the strip and chooses the odor from the four choices listed (445). Scores range from 0-12. The BSIT has demonstrated good reliability (r=.71) and takes less than 5 minutes to complete.

Any clinically significant change from baseline on follow-up assessments will be recorded as an adverse event (AE). If the changes are persistent, a full neurological evaluation will be performed.

Quality of Life

Quality of Life will be determined by the Short Form (SF)-12, a truncated, reliable version of the SF-36. The SF-12 uses 12 questions to evaluate eight domains that provide a general assessment of health-related quality of life from the participant’s perspective (446). The SF-12 includes subscales to assess mental and physical

functioning. Subscales are scored according to publisher specifications and standardized to allow comparison to the general US adult population.

Any clinically significant change from baseline on follow-up assessments will be recorded as an adverse event (AE). If the changes are persistent, a full neurological evaluation will be performed.

Product Acceptability Assessment

Product acceptability, feasibility, and tolerability will be evaluated by a questionnaire as specified in Table 5.4. Questionnaire items are derived from existing, validated questionnaires with adaptation for the current study (447). Participant experience and opinion of efficacy, sensory perceptions, spray characteristics, administration process, applicator design, and use regimen will be assessed. Responses will help determine product characteristics disliked or considered likely to challenge future sustained use by participants. Items are rated on 5-point Likert scales. The proportion of participants reporting product characteristics considered a barrier to use will be calculated. A Likert scale rating of lower than 3/5 on a given item will be considered a 'dislike' or potential barrier to future product use.

Pharmacokinetics Assessment and Ex Vivo Efficacy

As per Table 5.4, nasal, nasopharyngeal, and oropharyngeal swabs will be collected at visits 0, 1, 2 and 3, to determine the drug concentration. Inhibition of SARS-CoV-2 infectivity will be assessed by plaque reduction neutralization assay (PRNT) and correlations with Q-GRFT drug levels established.

Tolerability Assessment and Management- Adverse events

Throughout the study, each participant's condition will be closely monitored. Signs and symptoms of possible adverse events (AEs) may be reported by the study participants or observed by staff. They will be elicited from the participants by using direct or indirect questions like *'How have you felt since your last visit to the clinic?'* and '*Have you experienced any changes in your wellbeing since receiving the study product?*'

All AEs, whether reported by the subject, elicited by staff, or observed by the investigator, will be recorded. The start and end dates, AE-specific severity, relationship to study drug, and any actions taken to address the AE will also be documented. Outcomes such as whether AE resulted in death, required or necessitated hospitalization, any persistent or significant disability/ incapacity, any intervention to prevent these outcomes, and whether the events and actions taken were reported to the Data and Medical Monitor, Institutional Review Board (IRB) and study sponsor will be recorded.

Serious adverse events (SAEs) occurring in a study participant or any worsening of SAEs at any time during the study will be reported within 24 hours to the investigator, who will then immediately inform the Medical Monitor and IRB. For female participants, if any pregnancy occurs during the study, the investigator will immediately notify the Medical Monitor and IRB upon learning of the occurrence.

Tolerability of Q-GRFT in study volunteers will be derived from the frequency of AEs and study withdrawal due to any reported discomfort during the dosing period. As per Table 5.4, blood samples will be collected as previously described. If toxicity is identified following drug administration, the subject will be re-evaluated with a full physical examination and repeat blood tests performed to confirm toxicity. If the repeat tests are normal, this will be documented. Additionally, if still abnormal, appropriate action will be taken, and subsequent blood draws performed serially until resolution is documented.

Sample and Data Storage

Samples and data collected will be stored at the University of Louisville Clinical Trials Unit (CTU) and CPM laboratory, Louisville, KY. IRB approval will be sought for all the study procedures. Consent for samples and data storage will be provided by all participants. All biospecimens collected during the study will be de-identified, processed, and analyzed blindly until study completion. Similarly, electronic data will be de-identified, stored on secured servers with encryption, and accessed only by authorized users. A REDCap online database system hosted at the University of Louisville will be utilized to store, secure, organize, and analyze data (448). Responses on paper questionnaires will be entered to REDCap by study personnel. Upon conclusion of the

study, the de-identified stored specimens and data will be made available for use by other researchers and investigators upon request to the Principal Investigator.

Table 5.4. Schedule of Phase 1a Study Visits and Evaluations.

Assessment	**Visit 0** **Screening**	**Visit 1** **Enrollment, single dose exposure**	**Visit 2** **Safety assessment**	**Visit 3** **Final safety review, PK sampling**	**Visit 4** **(Phone call)**
Informed Consent	X				
Inclusion/Exclusion	X	X			
Medical History	X	X			
Pregnancy (urine βhCG)	X				
Concomitant Medications	X	X	X	X	X
Demographics	X				
Locator Information	X	X	X	X	X
Randomization		X			
Study Dosing		Dose 1			
Vital signs	X	X	X	X	
Physical Exam	X	X	X	X	
Nose and Throat Exam	X	X	X	X	
Nasal, Nasopharyngeal, & Oropharyngeal Swab collection	X	X	X	X	
COVID-19 Rapid Antigen test	X				
Hematology: Complete blood count (CBC)	X			X	
Comprehensive Metabolic Panel (CMP)	X			X	
Urinalysis	X				
Plasma sample for Q-GRFT Detection		X	X	X	
Plasma sample for SARS-CoV 2 antibodies detection	X				
Cytokines evaluation	X		X		
AEs		X	X	X	X
Quality of life assessment	X			X	
Olfactory function assessment	X		X	X	
Product acceptability questionnaire			X	X	X

Planned Analyses

Data Analyses

All participants who receive the study product will be included in the safety and efficacy analyses. All intra-and inter-participant outcome measures collected during the study period will be analyzed by an experienced biostatistician.

Data will be summarized following recommended standard guidelines. Data from sets of patients that complete each study visit and any reasons for early study termination will be noted and compared across study arms. Descriptive statistics (median, mean, standard error, standard deviation, minimum and maximum) will be used to summarize data for doses received and study visits completed. Similarly, demographic and baseline characteristics for participants in all groups will be summarized using descriptive statistics. Biomarker changes between pre- and post-dosing will be analyzed using paired tests. Descriptive summary statistics will be reported according to observed data, and missing data will not be imputed. Bayesian and likelihood estimates will be used for limited analyses where formal inferential statistics will be required for participants with missing follow-up assessments. A P value $\leq .05$ will be considered statistically significant.

Safety Analyses

Concomitant/ ongoing Medications. Any concomitant medications including those not related to the study product will be coded according to the World Health Organization (WHO) Drug dictionary and tabulated by the dosing group.

Adverse Events. Incidence of all treatment-related AEs and treatment-emergent AEs (TEAEs) will be summarized. A TEAE is an event that first occurs or worsens in intensity following the administration of a study drug. The Medical Dictionary for Regulatory Activities (MedDRA) will be used to classify AEs by system organ class and preferred term. For incidence reporting, when participants report more than one AE that will have been coded to the same system organ class or preferred term, the participant will be counted only once for that system organ class or preferred term. Events that occur between the signing of informed consent and the first study drug administration will be

recorded. A list of possible AEs including the participant incidence of TEAEs, treatment-related AEs, SAEs, deaths, and AEs resulting in study termination, will be constructed. For the stratification of AEs by severity, the worst severity for each participant during the study will be presented. Appropriate generalized linear models will be used for comparisons of significant differences between groups.

In addition, for the safety analysis, the number and frequency of ≥ Grade 2 AEs and ≥ Grade 1 nasal cavity-related AEs will be tabulated for the intranasal administration method. To determine whether AEs are occurring excessively, the proportion of subjects that experience an AE will be calculated for a method of administration. A single summary outcome of this type (yes/no) can be reasonably assumed to follow a Bernoulli distribution. Table 5.5 and Table 5.6 show, for selected true underlying rates between .01 and .45, the probability of zero, one or more, and two or more subjects experiencing AEs in a sample group of participants.

Table 5.5. Analysis of Safety Event Frequency for Arms of Size 12 (Q-GRFT nasal spray).

Event Rate (%)	**P(0 events |=12)**	**P(>=1 events |=12)**	**P(>=2 events |=12)**	**P(>=3 events |=12)**
1	0.886	0.114	0.006	0.000
5	0.540	0.460	0.118	0.020
10	0.282	0.718	0.341	0.111
15	0.142	0.858	0.557	0.264
25	0.032	0.968	0.842	0.609
35	0.006	0.994	0.958	0.849
45	0.001	0.999	0.992	0.958

Table 5.6. Analysis of Safety Event Frequency for Arms of Size 6 (placebo spray).

Event Rate (%)	P(0 events |=6)	P(>=1 events |=6)	P(>=2 events |=6)	P(>=3 events |=6)
1	0.941	0.059	0.001	0.000
5	0.735	0.265	0.033	0.002
10	0.531	0.469	0.114	0.016
15	0.377	0.623	0.224	0.047
25	0.178	0.822	0.466	0.169
35	0.075	0.925	0.681	0.353
45	0.028	0.972	0.836	0.558

The study will be paused for clinical data safety review in the event that four or more study participants in the treatment arm or two or more participants in the placebo arm experience an AE ≥ Grade 3. With 18 total subjects, the probability that 3 or more AE ≥ Grade 3 events occur given a true Grade 3 or more AE rate is shown in Table 5.7. Hence, it is highly unlikely that the study will be paused unless the true AE ≥ Grade 3 event rate is 10% or more.

Serious Adverse Events. In a similar manner to AEs above, SAEs will be listed and summarized. The sponsor will be notified of any SAEs within 24 hours of their discovery.

Clinical Laboratory Results. Blood samples will be measured in a qualified clinical laboratory. Descriptive statistics will be used for actual values and any changes from baseline will be tabulated by study visit. Clinical laboratory values outside of the normal reference ranges post-baseline will be recorded and analyzed using appropriate binary measures. Any changes from the baseline to worsening severity in the laboratory values will be recorded and analyzed with appropriate test statistics.

Vital signs. Data observed at baseline and any change from baseline will be determined for all measurements at the clinic visits. These data will be summarized with descriptive statistics and analyzed using an appropriate generalized linear mixed model.

Study Objectives. As mentioned above, patients will be closely monitored for any adverse events and toxicity, with repeat blood draws until AE resolution. To account for the inherent correlation, repeated measures statistics will be included in a repeated measures factor analysis with random effects. For the exploratory objectives, correlations will be determined between Q-GRFT drug levels obtained at PK sampling with SARS-CoV-2 infectivity *in vitro* and *ex vivo*. For olfactory sensation and quality of life, Spearman's statistics and Student's *t*-tests will be used for correlation analysis and comparisons between groups, respectively.

Table 5.7. Analysis of Safety Event Frequency for both Arms of Size 18.

Event Rate (%)	**P(0 events |=18)**	**P(>=1 events |=18)**	**P(>=2 events |=18)**	**P(>=3 events |=18)**
1	0.835	0.165	0.014	0.001
5	0.397	0.603	0.226	0.058
10	0.150	0.850	0.550	0.266
15	0.054	0.946	0.776	0.520
25	0.006	0.994	0.961	0.865
35	0.000	1.000	0.995	0.976
45	0.000	1.000	1.000	0.997

DISCUSSION

The initial SARS-CoV pandemic was reported in 2002-2003 (409), while MERS-CoV outbreaks have continued to-date since the first human case was identified in 2012 (411, 449). Coronaviruses have also been responsible for seasonal noncomplicated upper and lower respiratory tract infections (450, 451). The ongoing COVID-19 pandemic, caused by SARS-CoV-2 has resulted in unprecedented worldwide pandemonium. Unlike

the response to the multiple epidemics and pandemics due to coronaviruses in the past, only the current COVID-19 pandemic has resulted in rapid and fast-paced development of effective vaccines to curb infection (452).

Treatments that have received either Emergency Use Authorization or full approval by the FDA for utility in treatment and/ or prevention include Remdesivir (453); monoclonal antibodies like sotrovimab, and casirivimab plus imdevimab; and vaccines, including products marketed by Pfizer-BioNTech, Moderna, and Janssen to date (454); The search for more effective approaches and treatments is on-going (455, 456). A non-vaccine broad-spectrum prophylactic nasal spray provides an ideal adjunctive strategy to prevent virus infection and transmission. This is warranted since long-term data about the durability of antibodies in the elderly and immunocompromised individuals following vaccination is still under investigation (457). Furthermore, numerous reports have emerged of vaccinated individuals being re-infected with SARS-CoV-2 (458). The current spread and transmission of new viral variants complicate the current approved therapeutic and prevention modalities (459).

Studies have shown that intranasal sprays can decrease the risk of acquisition and establishment of viral respiratory infections. In rodent models, intranasal spray with low pH gel and antibody prophylaxis prevented infection with influenza virus (460, 461). Pilot studies in humans with hypertonic nasal saline irrigation (462) and Rupintrivir nasal spray (463) have demonstrated efficacy against viral upper respiratory infections including Rhinovirus colds. Our network of collaborators and other researchers have shown that GRFT inhibits viral entry of all coronaviruses tested, including SARS-CoV, MERS-CoV, and SARS-CoV-2 (10, 176, 189). Moreover, delivery of GRFT to the upper respiratory tract provides significant protection from SARS-CoV (464), MERS-CoV (unpublished), and paramyxovirus Nipah virus (11) in animal models. This observation is also supported by our preliminary data showing that pre-exposure treatment with Q-GRFT protected 3-dimensional human airway tissues from SARS-CoV-2 infection and reduced viral replication (unpublished). In addition, our *in vitro* epithelial tissue treatment studies have demonstrated that topical application of Q-GRFT results in detectable drug levels in tissue washes, which accumulate with repeat administration.

Given the urgent need for therapeutic interventions to prevent the spread of the COVID-19 pandemic, we strongly believe that Q-GRFT API in an intranasal spray will protect against SARS-CoV-2 infection and transmission. Our hypothesis is further supported by our preliminary findings in the fresh tissue study, where Q-GRFT application demonstrated the ability of Q-GRFT to disperse and will likely protect against SARS-CoV-2 cell entry.

In light of this background and preliminary findings, our PREVENT-CoV Phase 1a study will assess the safety, acceptability, and pharmacokinetics of Q-GRFT intranasal spray as broad-spectrum prophylactic for coronavirus infections. This study will be the first proof of concept trial to determine if a Q-GRFT intranasal spray formulation is safe and acceptable for human use. Clinically relevant endpoints have been carefully selected, including olfactory function and determination of PK parameters. Q-GRFT intranasal spray is a topically administered product with a low likelihood of systemic side effects. Although the expectation is the demonstration of a low risk of toxicity, careful assessments of safety, including systemic symptomatology, will be undertaken in this trial with special consideration for issues related to central nervous system toxicity. This is due to the potential for Q-GRFT exposure via the olfactory epithelium when administered through the nasal route. The design of this study will allow for the exploration of these questions while protecting the safety of participants.

For the drug to prevent coronavirus infection, it is critical that the product must be present in the appropriate anatomical site and at the ideal concentration, throughout the period of exposure to infection. Consequently, the multicompartmental PK included in this study will generate important data that, in combination with the SARS-CoV-2 neutralization findings, will help determine if the test product has the appropriate profile to support further development in Phase 1b and subsequent clinical trials.

CHAPTER 6: CONCLUSION AND FUTURE DIRECTIONS

SUMMARY OF Q-GRFT INTERACTIONS AND UTILITY IN MUCOSAL INFECTIONS AND IMPLICATIONS FOR FUTURE RESEARCH

Throughout this work, we have analyzed Q-GRFT interactions in the mucosal environment and determined the lectin's impact on related infections using both murine models and *in vitro* assays. Our overarching hypothesis was that Q-GRFT was stable in mucosal epithelia and would likely be an ideal alternative strategy for the prevention and treatment of infections in this environment. A number of hypotheses were explored. First, we hypothesized that Q-GRFT was stable in rectal mucosa. To test this hypothesis, we incubated Q-GRFT with murine, macaque and human rectal fluids, and determined the lectin's ability to bind gp120. Additionally, Q-GRFT was incubated with human seminal fluids prior to determining its binding to gp120. Next, we hypothesized that Q-GRFT could inhibit the growth of gut and rectal microbiome components. To test this, Q-GRFT was incubated with bacterial and fungal representative components of gut and rectal microbiota, and their growth monitored periodically. Based on results demonstrating *in vitro* inhibition of *C. albicans* growth, we next hypothesized that Q-GRFT in a murine model would be efficacious and eliminate fungal infection in a vaginal candidiasis model. Finally, given results from previous studies, we hypothesized that an intranasal formulation of Q-GRFT would be effective as prophylaxis against coronaviruses infection in the human population. To test this hypothesis, using airway and corneal epithelia, we determined whether Q-GRFT is detectable following topical tissue treatment. Next, in a fresh-tissue cadaver study, we administered Q-GRFT as an intranasal spray to determine the pattern of dispersion, and to establish whether the drug will be detected upon sampling. Lastly, we designed a protocol for a Phase 1a study, to establish safety, tolerability, and pharmacokinetics of Q-GRFT intranasal spray following a single dose administration.

From the findings of this work, a number of conclusions can be made about potential implications, and taken altogether, support future development of Q-GRFT as a potential strategy for the treatment of select mucosal infections.

Q-GRFT was stable and maintained its ability to bind to gp120 following incubation with murine, macaque and human rectal fluids, and seminal plasma.

Glycoprotein 120 binding studies with Q-GRFT following incubation of the lectin with murine, macaque, and human rectal fluids, including human seminal fluids demonstrated that the lectin remains stable, in the rectal environment. Additional studies that evaluated the composition of rectal fluids demonstrated the presence of protease enzymes, proteins and carbohydrates in rectal fluids, with a pH range of 7-8. Despite the degradative enzymes in these fluids, Q-GRFT maintained the ability to bind gp120 following incubation. Interestingly, incubation for both brief and extended durations (6 hours versus 24 hours) demonstrated no significant impact on gp120 binding. One limitation in our experiments is that we did not confirm the stability of Q-GRFT following incubation with an alternative method like western blot. Additionally, when antigens are coated on plates in ELISA assays, there is a likelihood of conformational changes altering their interaction with other molecules (289). Conformational changes in gp120 may have impacted Q-GRFT binding in these assays. Nonetheless, the data suggested that Q-GRFT may remain stable in the rectal environment and supports further evaluation of its potential as an antimicrobial agent in animal and human studies. Furthermore, our stability results in rectal fluids are in keeping with earlier studies of Griffithsin's stability in cervicovaginal fluids (206).

Q-GRFT inhibits the growth of fungal microbiome component C. albicans, but not bacterial components.

In broth media, the growth of bacterial microbiome components *Lactobacillus acidophillus*, *Lactobacillus casei*, *Escherichia coli*, *Bifidobactrium longum longum*, *Clostridium dificile*, Enterotoxigenic *Bacteroides fragilis* and Nontoxigenic *Bacteroides fragilis* was not impacted by incubation with Q-GRFT. Contrastingly, we made a novel finding, that the growth of fungal component *C. albicans* was inhibited following incubation with Q-GRFT. We have established that Q-GRFT likely binds to cell wall α-

mannan, but not chitin or β-glucan in *C. albicans*. We further demonstrated that Q-GRFT binding is associated with a breach in cell wall and membrane integrity, and appears to induce formation of reactive oxidative species, with subsequent cell death. Additionally, binding induces the expression of genes responsible for the cell's reaction to stressful stimuli, including those involved in neutralizing ROS formation and escaping stress. Furthermore, we have established that Q-GRFT binds to other *Candida* strains, including *C. glabrata, C. krusei, C. parapsilosis*, and the multi-and pan-resistant *C. auris*. Given the differences in MIC_{50}s and MIC_{90}s demonstrated, we postulated that variations in the cell wall composition of α-mannosyl sugars likely contribute to the differential response observed following incubation of Q-GRFT with different *Candida* strains. Interestingly, we also demonstrated significant growth inhibition of isolates in the C. *auris* South Asia clade, that is predominant in the United States. These results signify the potential of Q-GRFT as an alternative strategy against fungal infections.

Q-GRFT is efficacious against vaginal candidiasis in prophylaxis and therapeutic murine models.

In prophylactic and therapeutic murine models of vaginal candidiasis, we have demonstrated that Q-GRFT significantly inhibited infection and enhanced *C. albicans* clearance, respectively. Additionally, lower quantities of pro-inflammatory cytokines and innate immune cells were observed following vaginal Q-GRFT treatment, when comparisons were made with infected, untreated animals. These findings suggest Q-GRFT is associated with higher fungal clearance, with subsequently lower antigenic stimulation of cytokines, predisposing to the lower pro-inflammatory response observed in the lectin treated animals. Moreover, it is likely that the initial vaginal infection triggers recruitment of the immune cells, that persist even beyond the period of drug administration. Because we assessed the immune cells response and population 12 days post-infection, it is possible that changes may occur at even later timepoints. From our data, Q-GRFT appears not to directly impact changes in the immune response to vaginal candidiasis. The lack of immune stimulation is in keeping with earlier studies that have not demonstrated any direct induction of immunity and inflammatory response when Q-

GRFT was applied either topically or systemically (204, 382). Key to note however, is that the investigations in these studies were not done in the context of on-going infection.

Q-GRFT is detectable in epithelial tissues upon topical treatment and was quantifiable in human nasal and pharyngeal mucosal membranes in a fresh-tissue cadaver study, in preparation for a Phase 1a clinical trial to establish safety, acceptability, and PK of an intranasal spray.

Given its broad-spectrum antiviral activity, Griffithsin has been demonstrated binding to coronaviruses. In response to the on-going COVID-19 pandemic, we are developing an intranasal spray as a pre-exposure prophylaxis against coronaviruses. In *in vitro* studies with air way and corneal epithelia, we have demonstrated that Q-GRFT is detectable and quantifiable following tissue treatment. Additionally, in a fresh human tissue cadaver study, we determined that upon instillation, Q-GRFT disperses widely in the nasal cavity, and is detected in nasopharyngeal and oropharyngeal compartments. The mucosa in these anatomic cavities contains receptors for coronaviruses. Using ELISA and fluorescence experiments, we have established assays that precisely determine drug levels in nasal, nasopharyngeal, and oropharyngeal cavities following administration. Furthermore, the planned Phase 1a study will enable assessment of the safety, tolerability, and pharmacokinetics of Q-GRFT intranasal spray in a first-in-human nasal exposure of the drug product, in preparation for future efficacy studies, as prophylaxis against coronaviruses.

In summary Q-GRFT is stable in the rectal mucosal environment, and maintains its ability to bind gp120, despite the presence of degradative enzymes in these cavities. Although no impact has been demonstrated on bacterial microbiome, Q-GRFT inhibits the growth of fungal microbial component *C. albicans* as well as other *Candida* species of clinical importance. Furthermore, Q-GRFT is efficacious in the treatment of vaginal candidiasis in a murine model. The lectin's broad-spectrum antiviral activity extends to include coronaviruses, and Q-GRFT is detectable in nasal, nasopharyngeal, oropharyngeal, and ocular epithelial mucosa, tissues that possess receptors with binding targets for coronaviruses. Intranasal application of a Q-GRFT spray formulation resulted in detectable and quantifiable drug levels, which were comparably evaluable using both

ELISA and fluorescence assays. A planned phase 1a clinical study will establish baseline safety, tolerability and pharmacokinetic characteristics that will be critical in future development of Q-GRFT as an intranasal prophylaxis against coronaviruses.

DISCUSSION

For rectally administered drugs to achieve maximal efficacy, the product should be able to withstand any degradative activity in this environment. Interestingly, the rectal environment is adjudged to be remarkably constant and stable and demonstrates low enzymatic activity when compared to other regions of the gastrointestinal tract (465). In addition, in spite of the relatively small surface area of the mucosa in this region, delivery of drugs via this route results in significant local and systemic levels (466). In fact, following systemic absorption, drugs delivered rectally partially bypass the liver, avoiding significant hepatic first-pass effect (466, 467). Our study has suggested that the lectin Q-GRFT is stable when incubated with rectal fluids. Studies have revealed that numerous lectins are stable and can withstand aggressive environments like acidic pH, heat and enzymatic activity, retaining their ability to interact with cell membrane glycans (468). This has subsequently resulted in studies that have evaluated the utility of lectins in gastrointestinal and colorectal cancers and other pathologies (469). Dietary wheat germ agglutinin (WGA) has been investigated as a modality to deliver protein drugs to gastrointestinal mucosa when orally administered, and the lectin has demonstrated only minimal degradation by brush border proteases (468). Other lectins that have demonstrated stability and binding to glycans in mucin despite the degradative gastrointestinal environment are *Viscum album* from mistletoe, *Urtica dioica* agglutinin from stinging nettle, *Tricum vulgaris* from wheat germ, *Galanthus nivalis* from snowdrop, *Canavalia ensiformis* from jack bean, *Phaseolus vulgaris* from kidney bean, *Ulex europaeus* from gorse and *Lotus tetragonolobus* from the asparagus pea (470). The stability demonstrated by other lectins supports our studies to develop Q-GRFT as a drug product for utility in the rectal environment. However, since we have demonstrated this stability *in vitro*, there is a need to evaluate Q-GRFT's resistance to degradation in an *in vivo* setting. Ideal experiments would include performing an SDS/ PAGE or Western blot

analysis of Q-GRFT that has been administered rectally in murine, macaque or human fluids. The findings would confirm existence or absence of any degradative impact on Q-GRFT in rectal mucosa.

Additionally, we demonstrate no impact on the growth of bacterial components of the microbiome. *In vivo* studies in macaques have identified that GRFT does not demonstrate any significant impact on the bacterial proteome (203). Contrastingly, some other lectins have demonstrated antibacterial activity, including against some of the isolates we tested in our study. A lectin extracted from the mushroom *Sparassis latifolia* demonstrated antibacterial activity against *Escherichia coli*, *Staphylococcus aureus* and *Pseudomonas aerug*inosa (471). The chitin-binding potato lectin, *Solanum tuberosum* has inhibitory activity against *Escherichia coli*, *Listeria monocytogenes* and *Salmonella entiritidis (472)*. The MCL lectin from mollusks *Mytilus californianus* is specific for D-galactose and *N*-acetyl-D-galactosamine. MCL inhibited the growth of *Escherichia coli* and *Lactobacillus planatarum* (473). It is possible that differences in the binding glycan targets for Q-GRFT and other lectins account for the diverging impact on bacterial microbiota and pathogens.

GRFT is the most potent lectin demonstrating anti-HIV-1 activity that has been studied so far (165). The gp120 spike on the HIV envelope has about 11 high-mannose oligosaccharides with which GRFT interacts (166). The lectin displays high affinity and potency interactions at low picomolar concentrations that are essential in its antiviral inhibitory activity (6). Amino acid aspartate residues in the binding site (Asp 30, Asp 70, and Asp 112) are crucial for high mannose interactions (6). Indeed, point mutations in each amino acid partially inhibited gp120 binding, while GRFT variants with mutations of all aspartate residues were deprived of HIV-1 binding ability (167).

GRFT demonstrates synergistic antiviral activity with tenofovir (reverse transcriptase inhibitor), enfuvirtide (gp41 fusion peptide inhibitor), and maraviroc (CCR5 antagonist) (208). In CCR5-tropic cell fusion assays, covalent linkages between GRFT and C37, a gp41-binding peptide resulted in a several-fold increase in the lectin's potency, compared to when GRFT was used alone (474). Combinations of GRFT with various antiretroviral drugs (entry inhibitors, integrase inhibitors, protease inhibitors and

reverse transcriptase inhibitors) demonstrated synergistic and additive effects, reducing cell to cell fusion, and high potency against CD4+ T cell destruction (293). GRFT/ antiretroviral drugs combinations also inhibited viral replication in T cells via inhibition of DC-SIGN-mediated transmission (293). GRFT's activity has also been explored in combination with other carbohydrate binding agents. GRFT has demonstrated synergistic activity against HIV-1, HIV-2, and other lectin-resistant HIV-1 strains when combined with *Hippearstrum* hybrid agglutinin, *Galanthum nivalis* agglutinin, a mannose-specific mAb 2G12, microvirin, and banana lectin (475). Glycans on HIV-1 gp120 shield neutralization-sensitive epitopes from antibody recognition (476). The glycan at position 386 of gp120 shields the CD4 binding domain (476). Disruption of mannose molecules on gp120 by GRFT likely increases antibody-dependent neutralization of HIV-1 virions (166). GRFT enhanced the interaction between gp120 and 48d mAb, which recognizes a CD4 binding domain (477). Furthermore, GRFT enhanced the binding of HIV-1 to plates coated with mAbs b12 and b6 (476). These findings suggest that GRFT triggers the exposure of CD4-binding sites on gp120, and promote binding enhancements and neutralization synergy between the lectin and some mAbs (476).

The intact dimeric GRFT is required for effective anti-HIV-1 activity (9). Monomeric GRFT (mGRFT) created by inserting either 2 or 4 amino acids at the dimerization interface did not demonstrate adequate anti-HIV-1 activity, despite viral binding at the carbohydrate-binding sites (9, 166). The HIV-1 envelope displays few gp120 spikes (7 to 14) per virion (478, 479). It is postulated that this is a viral adaptation to evade humoral immunity by limiting multivalent interacts with B cell receptors, given the wide distance between spikes, attenuating the B cell response (480-482), and preventing binding by antibodies that would enhance neutralization (482). As with many other antivirals, HIV-1 may evade the inhibitory activity conferred by GRFT. Viral resistance to GRFT is largely via the loss of envelope glycosylation sites on gp120 (166). The loss of glycosylation sites at positions 234 and 295 led to resistance to natural GRFT (477). Furthermore, de-glycosylation at positions 295, 448, N295, and N448 were associated with attenuated sensitivity to GRFT (483, 484). Loss of glycosylation at position 230, 234, 241, 289 in the C2 region, and 339, 392, and 448 in the C3-C4 region

reduced GRFT inhibitory activity (485). Glycan rearrangement in V4 has also been shown to induce reduced HIV-1 sensitivity to GRFT (485).

Preliminary data and preclinical studies suggest that Q-GRFT will probably be an effective antiviral from the prevention of HIV-1 infection and transmission in the rectal epithelium. Q-GRFT has demonstrated efficacy and utility as a single agent for use against infection and transmission. However, given the rapidly mutating character of HIV-1, there is need to further explore Q-GRFT utility as part of a combination regimen for HIV-1 infection prevention in the rectal environment.

We have shown that Q-GRFT binds to *C. albicans* and suggested that the lectin induces ROS formation, with a breach in cell wall integrity. Antifungal activity of currently used drugs has been established. Polyenes penetrate the fungal cell wall and bind to ergosterol, causing membrane damage (486). Azoles inhibit C14α demethylation of lanosterol, interfering with ergosterol synthesis, a component of the cell wall (487). Despite divergent modes of activity, these antifungal drugs alter cellular metabolism and respiration, and ultimately result in ROS formation (488). Interestingly, ROS is critical in cell proliferation, hypoxia adaptation and cell fate determination, however, excessive ROS causes irreversible damage leading to cell death (489). Metabolic changes and damage that is initiated upon antifungal interaction with cells results in activation of stress-like responses, that trigger signaling through the RAS/ PKA pathway (488). Deletions in RAS pathway genes *RAS1* or *RAS2* enhanced resistance to antifungal treatment, while deletion of effector kinases *TPK1*, *TPK2* and *TPK3* delayed cell killing (488). It is also suggested that other pathways may be recruited, with the cell subsequently activating mitochondrial activity and switching from fermentation to respiration Abrupt induction of mitochondrial activity leads to overproduction of toxic ROS, in a manner likely dependent on the tricarboxylic acid (TCA) cycle and electron transport chain pathways (488). Furthermore, antifungal treatment was associated with cellular accumulation of monosaccharides and disaccharides like glucose, fructose, mannose, and disaccharide trehalose. Because production of these sugars is expensive to the cell requiring a lot to energy to achieve, these metabolic changes likely alter respiration with subsequent ROS overproduction by the dysfunctional mitochondria

(488). Ultimately, cell death occurs. It is suggested that antifungal stress may closely mimic and mirror that due to effects like heat, osmotic stress, and alcoholic stress, which all result in induction of stress-related pathways (488). This is evidenced by the similarities in over-activated cellular pathways that are triggered, collapse of cellular ATP levels, and ROS production in both scenarios (488, 490-492). Antifungal treatment elevates the AMP/ATP ratio through the rapid consumption of ATP in heightened cellular metabolism (488). In both bacteria and yeast, ROS damages DNA by introducing double-strand breaks, and other forms of cellular damage like proteins, and membranes that lead to cell death (488, 493, 494).

Similarly, several lectins have been found to demonstrate antifungal activity with the induction of ROS formation. The *Machaerium acutifolium* (*Ma*L) lectin which inhibits the growth of *C. albicans* and *C. parapsilosis*, alters membrane structure and induces ROS production in *Candida parapsilosis* (495). *Ma*L, an N-acetyl-D-glucosamine-binding lectin altered plasma membrane proton-pump ATPase activity, induced the production of ROS following oxidative stress, with resultant DNA damage. The mannose-binding lectin, Helja, derived from sunflower plant, inhibited the growth of C. tropicalis and C. albicans. In addition, Helja induced numerous morphological changes including inhibiting pseudohyphae formation, altered membrane permeability and resulted in the production of ROS (496). In our study, Q-GRFT treatment resulted in enhanced cellular metabolism including pathways responsible for glucose metabolism, disaccharide synthesis, galactose metabolism, as well as trehalose metabolic processes. This is indicative of cellular response to stress conditions induced following Q-GRFT treatment. In addition, antioxidant genes like SOD were upregulated, suggestive of fungal response to oxidative stress and ROS formation. Q-GRFT further upregulated processes involved in DNA damage repair, double strand breaks, ATP formation, pathways that suggested DNA injury following lectin treatment. Altogether, these data suggest induction of stressful conditions upon Q-GRFT treatment, with induction of intracellular processes that may subsequently trigger cell death via a ROS-dependent pathway. Experiments specifically evaluating mitochondrial ROS production, including oxidative phosphorylation following Q-GRFT treatment will aid in identifying the specific role of this pathway in fungal response to the lectin.

In murine studies, we have shown that Q-GRFT significantly prevented infection and enhanced fungal clearance in a therapeutic model. We also demonstrated that Q-GRFT's antifungal activity was not associated with an inflammatory response, when compared to the nystatin-treated control group. The fact that Q-GRFT did not require an inflammatory response to inhibit infection is likely a positive property for this lectin, especially among immunocompromised individuals who may not mount adequate responses. Indeed, in a rat model, nystatin demonstrated protection against *C. albicans*, but up-regulated INFɤ-related cellular responses, IL-17 signaling and enhanced vaginal epithelial cell (VEC) - IgG mediated immunity (353). Contrastingly, clotrimazole treatment blocks *C. albicans*-induced epithelial cell lysis and prevents fungal activation of the epithelial 'danger response' without inducing inflammation (497). Clotrimazole attenuates local inflammation and significantly reduces the vaginal neutrophilic infiltration associated with candidiasis (497). Indeed, in the absence of fungal infection, clotrimazole inhibited epithelial TNF-α-induced IL-8 production and NF-κB activity (498). High resolution scanning electron microscopy experiments will be helpful in assessing fungal phenotypic changes in murine vaginal candidiasis. In addition, RNA sequencing studies will aid in identifying if the *in vitro* gene expression profiles we demonstrated herein are preserved in *in vivo* infections.

Our studies propose developing Q-GRFT for the prevention and treatment of mucosal infections, including HIV-1, vaginal candidiasis, and SARS-CoV-2. It is anticipated that Q-GRFT use in these infections will likely involve daily dosing for either short periods or a couple of days for vaginal candidiasis and coronaviruses infection. As a rectal microbicide, it is likely to be used 'as needed' or an 'on demand' product. Subsequently, serial exposures or chronic use may be associated with the risk of eliciting immunogenicity in the form of anti-drug antibodies (ADAs) (499). These ADAs are either neutralizing antibodies that dampen the benefit of the biotherapeutic agent administered, or non-neutralizing antibodies that may also attenuate efficacy by impacting pharmacokinetics, pharmacodynamics, and drug clearance (500). Interestingly, studies have reported the existence of antibodies against non-human sugars and proteins in healthy individuals (501, 502). Therefore, being algal-derived, it is plausible that Q-GRFT may be recognized as foreign, triggering an immune response from the body. In

the murine candidiasis studies described here, we did not assess for ADAs. Immunogenicity in animal models does not predict that in humans. However, these data are useful evaluations since immunogenicity in the preclinical models may reveal potential antibody related toxicities that warrant monitoring in human studies (503). In the planned Phase 1a study, volunteers will receive a single dose intranasal Q-GRFT spray. Subsequent exposures will include a multi-dosing regimen. Patient plasma samples will be collected to evaluate both baseline and subsequent ADAs, with quantification of specific antibody titers and isotypes/ subclasses. This is important because the initial exposure primes, while multiple repeat administrations boost the host immune response, and produce high affinity, high-titer, class switched antibodies (500). If Q-GRFT induces antibody responses upon administration, epitope de-immunization strategies that reduce immunogenicity of sequence-modified proteins may be utilized to dampen the effect. These include rational amino acid substitutions in the peptide sequence without affecting functionality, and attachment of epitope-masking moieties to decrease immunogenicity (500, 504).

RECOMMENDATIONS FOR FURTHER STUDY

While our studies have established the efficacy and potential utility of Q-GRFT in mucosal infections, a number of questions and areas that necessitate further exploration have been uncovered. It is therefore recommended that further research and experiments be designed to obtain answers to these questions.

Does Q-GRFT impact the growth of other mucosal fungal infections?

Fungal pathogens *A. fumigatus*, *Cryptococccus* and *Mucorales* are known to cause mucosal infections that involve oral cavity epithelia, ocular tissues, pulmonary infections, gastrointestinal tract, and oral lining (505-508), and these often lead to invasive infections among immunocompromised individuals. The *A. fumigatus* cell wall consists of galactomannan in its structure (509), while that of *C. neoformans* includes mannoproteins in the outer surface layer (510). Additionally, *Mucorales* also harbor mannan and mannoproteins in their cell wall (511). In our *in vitro* experiments, we have identified α-

mannan as a likely ligand for Q-GRFT interaction in the *Candida* cell wall structure. Thus, it would seem possible that Q-GRFT may bind to other fungal pathogens, especially those that display mannose, and mannan-like structures in their cell wall. Therefore, *in vitro* experiments need to be done to determine any inhibitory activity of Q-GRFT to the growth of other fungal pathogens. Additionally, where effective, animal studies will be crucial in determining if this activity is preserved in an *in vivo* setting.

Will Q-GRFT be effective in systemic fungal infections?

Mucosal fungal infections often result in systemic infections. We have demonstrated that Q-GRFT is efficacious in treating vaginal candidiasis in a murine model. Additionally, previous studies observed that intravenous administration of a single dose resulted in detection of GRFT in serum up to 96 hours post-treatment (196). Designing studies to assess the impact of Q-GRFT on systemic fungal infections, including candidiasis and other invasive mycoses due to susceptible pathogens will provide valuable insights into the lectin's efficacy in related maladies.

What is the impact of Q-GRFT on resident fungal mycobiome in nasal cavity, vagina, gut and rectum?

In our study, we have demonstrated that Q-GRFT induces death of *Candida*. Fungi are often members of the communities that make up commensals in the nasal cavity, gut, rectum, and vagina environment. Usually, an imbalance in the microbial community, as seen following antibiotics use (512, 513), leads to overgrowth and proliferation of *Candida* (514), with resultant pathogenesis. As mentioned above, Q-GRFT is currently being developed as a rectal microbicide for the prevention of HIV infection. We plan to administer Q-GRFT intranasally for COVID-19 prophylaxis in human subjects. The over-riding question, following the studies performed above, is what the impact of chronic or recurrent drug use will be on the fungal communities in these environments? Will this result in death of fungal components with the resultant overgrowth of bacterial members, which may lead to pathogenesis? Interestingly, chronic rectal treatment in macaques did not demonstrate any major detrimental changes in the bacterial microbiome, except the proliferation of *Ruminococcaceae* and *Christensenellaceae* (203). However, this study was not designed to assess the impact of

GRFT on fungal composition and how this ultimately affected bacterial components. Studies to assess this scenario may need to be done to answer this question.

Will Q-GRFT's antifungal effect be maintained in human subjects?

Many drugs show efficacy in animal studies but fail to replicate the similar effects in human clinical trials. Animal studies are needed to establish if the efficacy of Q-GRFT in vaginal candidiasis will be maintained in human studies. These studies may be designed to assess and compare Q-GRFT efficacy with the standard of care for women with vaginal candidiasis or RVVC. In addition, determining the efficacy in drug-resistant *Candida* infections as a single drug, or in combination with other therapeutic antifungals will enable the determination of its ideal role in vaginal candidiasis.

How does Q-GRFT work in a setting of immune suppression?

From our experiments, it is likely that Q-GRFT binds to *C. albicans* and results in the direct killing of the fungal pathogen. Additionally, our animal studies demonstrated that the inflammatory response was lower following Q-GRFT treatment than in untreated animals. The innate immune response to *Candida* infection is responsible for mediating and mounting a response to clear infection. It is likely that while Q-GRFT reduces the fungal burden and vaginal colonization, the immune response may eliminate additional *Candida* pathogens that may persist. Although our studies were not designed to directly assess the additional contribution of innate and adaptive immunity during Q-GRFT use, this is a likely scenario, given that immunocompromised individuals require longer antifungal treatment durations than immunocompetent individuals (515). Therefore, it is important to study the efficacy of Q-GRFT in candidiasis, in a setting of immunosuppression.

Will Q-GRFT be an effective intranasal prophylactic application against SARS-CoV-2 infection? Will the efficacy be maintained for SARS-CoV-2 variants?

We have demonstrated that topical application of corneal and airway epithelium results in detectable Q-GRFT in these tissues. Whether these results translate into infection blockade will need to be established in Phase 2 and 3 clinical trials. Furthermore, Q-GRFT's efficacy in the setting of multiple emerging SARS-CoV-2

variants will need to be studied in order to ascertain its potential utility in mucosal infections.

Can ocular Q-GRFT prevent SARS-CoV-2 infection?

Multiple viruses establish infection through both nasal and ocular tissues (516, 517). Animal and human studies are needed to determine the efficacy of infection prevention of a Q-GRFT ocular formulation or suspension. This is also an area worth studying, given the numerous reports suggestive of the ocular route as a portal of SARS-CoV-2 infection in humans (228, 229, 518).

REFERENCES

1. Berg JM, Tymoczko JL, Stryer L. 2002. Lectins are specific carbohydrate-binding proteins. Biochemistry:333-335.
2. Wright JR. 2005. Immunoregulatory functions of surfactant proteins. Nature Reviews Immunology 5:58-68.
3. Jensenius H, Klein DC, van Hecke M, Oosterkamp TH, Schmidt T, Jensenius JC. 2009. Mannan-binding lectin: structure, oligomerization, and flexibility studied by atomic force microscopy. Journal of molecular biology 391:246-259.
4. Johannes L, Jacob R, Leffler H. 2018. Galectins at a glance. Journal of cell science 131.
5. Ziółkowska NE, O'Keefe BR, Mori T, Zhu C, Giomarelli B, Vojdani F, Palmer KE, McMahon JB, Wlodawer A. 2006. Domain-swapped structure of the potent antiviral protein griffithsin and its mode of carbohydrate binding. Structure 14:1127-1135.
6. Ziółkowska NE, Shenoy SR, O'Keefe BR, McMahon JB, Palmer KE, Dwek RA, Wormald MR, Wlodawer A. 2007. Crystallographic, thermodynamic, and molecular modeling studies of the mode of binding of oligosaccharides to the potent antiviral protein griffithsin. PROTEINS: Structure, Function, and Bioinformatics 67:661-670.
7. Ziółkowska NE, Shenoy SR, O'Keefe BR, Wlodawer A. 2007. Crystallographic studies of the complexes of antiviral protein griffithsin with glucose and N-acetylglucosamine. Protein science 16:1485-1489.
8. Mori T, O'Keefe BR, Sowder II RC, Bringans S, Gardella R, Berg S, Cochran P, Turpin JA, Buckheit Jr RW, McMahon JB. 2005. Isolation and characterization of griffithsin, a novel HIV-inactivating protein, from the red alga Griffithsia sp. Journal of Biological Chemistry 280:9345-9353.
9. Moulaei T, Shenoy SR, Giomarelli B, Thomas C, McMahon JB, Dauter Z, O'Keefe BR, Wlodawer A. 2010. Monomerization of viral entry inhibitor griffithsin elucidates the relationship between multivalent binding to carbohydrates and anti-HIV activity. Structure 18:1104-1115.
10. O'Keefe BR, Giomarelli B, Barnard DL, Shenoy SR, Chan PK, McMahon JB, Palmer KE, Barnett BW, Meyerholz DK, Wohlford-Lenane CL. 2010. Broad-spectrum in vitro activity and in vivo efficacy of the antiviral protein griffithsin against emerging viruses of the family Coronaviridae. Journal of virology 84:2511-2521.
11. Lo MK, Spengler JR, Krumpe LR, Welch SR, Chattopadhyay A, Harmon JR, Coleman-McCray JD, Scholte FE, Hotard AL, Fuqua JL. 2020. Griffithsin Inhibits Nipah Virus Entry and Fusion and Can Protect Syrian Golden Hamsters From Lethal Nipah Virus Challenge. The Journal of infectious diseases 221:S480-S492.
12. CDC. 2013. Antibiotic Resistance Threats in the United States, 2013.

13. Nabeta HW, Kouokam JC, Lasnik AB, Fuqua JL, Palmer KE. 2021. Novel Antifungal Activity of Q-Griffithsin, a Broad-Spectrum Antiviral Lectin. Microbiol Spectr doi:10.1128/Spectrum.00957-21:e0095721.
14. Ordonez SR, Veldhuizen EJ, van Eijk M, Haagsman HP. 2017. Role of soluble innate effector molecules in pulmonary defense against fungal pathogens. Frontiers in microbiology 8:2098.
15. Kim JK, Kim S-S, Rha KW, Kim C-H, Cho JH, Lee C-H, Lee J-G, Yoon J-H. 2007. Expression and localization of surfactant proteins in human nasal epithelium. American Journal of Physiology-Lung Cellular and Molecular Physiology 292:L879-L884.
16. Watson A, Madsen J, Clark H. 2020. SP-A and SP-D: dual functioning immune molecules with antiviral and 1 immunomodulatory properties. Frontiers in Immunology.
17. Douda DN, Jackson R, Grasemann H, Palaniyar N. 2011. Innate immune collectin surfactant protein D simultaneously binds both neutrophil extracellular traps and carbohydrate ligands and promotes bacterial trapping. The Journal of Immunology 187:1856-1865.
18. Casals C, Campanero-Rhodes MA, García-Fojeda B, Solís D. 2018. The role of collectins and galectins in lung innate immune defense. Frontiers in immunology 9:1998.
19. Sorensen GL. 2018. Surfactant protein D in respiratory and non-respiratory diseases. Frontiers in medicine 5:18.
20. Nayak A, Dodagatta-Marri E, Tsolaki AG, Kishore U. 2012. An insight into the diverse roles of surfactant proteins, SP-A and SP-D in innate and adaptive immunity. Frontiers in immunology 3:131.
21. Beharka AA, Crowther JE, McCormack FX, Denning GM, Lees J, Tibesar E, Schlesinger LS. 2005. Pulmonary surfactant protein A activates a phosphatidylinositol 3-kinase/calcium signal transduction pathway in human macrophages: participation in the up-regulation of mannose receptor activity. The Journal of Immunology 175:2227-2236.
22. Kuronuma K, Sano H, Kato K, Kudo K, Hyakushima N, Yokota S-i, Takahashi H, Fujii N, Suzuki H, Kodama T. 2004. Pulmonary surfactant protein A augments the phagocytosis of Streptococcus pneumoniae by alveolar macrophages through a casein kinase 2-dependent increase of cell surface localization of scavenger receptor A. Journal of Biological Chemistry 279:21421-21430.
23. Tenner AJ, Robinson SL, Borchelt J, Wright J. 1989. Human pulmonary surfactant protein (SP-A), a protein structurally homologous to C1q, can enhance FcR-and CR1-mediated phagocytosis. Journal of Biological Chemistry 264:13923-13928.
24. Gil M, McCormack FX, LeVine AM. 2009. Surfactant protein A modulates cell surface expression of CR3 on alveolar macrophages and enhances CR3-mediated phagocytosis. Journal of Biological Chemistry 284:7495-7504.
25. Thawer S, Auret J, Schnoeller C, Chetty A, Smith K, Darby M, Roberts L, Mackay R-M, Whitwell HJ, Timms JF. 2016. Surfactant protein-D is essential for immunity to helminth infection. PLoS pathogens 12:e1005461.

26. Funk CJ, Wang J, Ito Y, Travanty EA, Voelker DR, Holmes KV, Mason RJ. 2012. Infection of human alveolar macrophages by human coronavirus strain 229E. The Journal of general virology 93:494.
27. van de Wetering JK, van Remoortere A, Vaandrager AB, Batenburg JJ, van Golde LM, Hokke CH, van Hellemond JJ. 2004. Surfactant Protein D Binding to Terminal α1-3–Linked Fucose Residues and to Schistosoma mansoni. American journal of respiratory cell and molecular biology 31:565-572.
28. McCormack FX, Festa AL, Andrews RP, Linke M, Walzer PD. 1997. The carbohydrate recognition domain of surfactant protein A mediates binding to the major surface glycoprotein of Pneumocystis carinii. Biochemistry 36:8092-8099.
29. Stefano JAD, Myers JD, Pont DD, Foy JM, Theus SA, Walzer PD. 1998. Cell wall antigens of Pneumocystis carinii trophozoites and cysts: purification and carbohydrate analysis of these glycoproteins. Journal of Eukaryotic Microbiology 45:334-343.
30. Vuk-Pavlovic Z, Standing JE, Crouch EC, Limper AH. 2001. Carbohydrate recognition domain of surfactant protein D mediates interactions with Pneumocystis carinii glycoprotein A. American journal of respiratory cell and molecular biology 24:475-484.
31. O'Riordan DM, Standing JE, Kwon KY, Chang D, Crouch EC, Limper AH. 1995. Surfactant protein D interacts with Pneumocystis carinii and mediates organism adherence to alveolar macrophages. The Journal of clinical investigation 95:2699-2710.
32. HARTSHORN KL, WHITE MR, VOELKER DR, COBURN J, ZANER K, CROUCH EC. 2000. Mechanism of binding of surfactant protein D to influenza A viruses: importance of binding to haemagglutinin to antiviral activity. Biochemical Journal 351:449-458.
33. Madan T, Kishore U, Shah A, Eggleton P, Strong P, Wang J, Aggrawal S, Sarma P, Reid K. 1997. Lung surfactant proteins A and D can inhibit specific IgE binding to the allergens of Aspergillus fumigatus and block allergen-induced histamine release from human basophils. Clinical & Experimental Immunology 110:241-249.
34. Qadi M, Lopez-Causapé C, Izquierdo-Rabassa S, Mateu Borrás M, Goldberg JB, Oliver A, Albertí S. 2016. Surfactant protein A recognizes outer membrane protein OprH on Pseudomonas aeruginosa isolates from individuals with chronic infection. The Journal of infectious diseases 214:1449-1455.
35. McNeely TB, Coonrod JD. 1994. Aggregation and opsonization of type A but not type B Hemophilus influenzae by surfactant protein A. American journal of respiratory cell and molecular biology 11:114-122.
36. Gaiha GD, Dong T, Palaniyar N, Mitchell DA, Reid KB, Clark HW. 2008. Surfactant protein A binds to HIV and inhibits direct infection of CD4+ cells, but enhances dendritic cell-mediated viral transfer. The Journal of Immunology 181:601-609.
37. Leth-Larsen R, Zhong F, Chow VT, Holmskov U, Lu J. 2007. The SARS coronavirus spike glycoprotein is selectively recognized by lung surfactant protein D and activates macrophages. Immunobiology 212:201-211.

38. Van de Wetering J, Coenjaerts F, Vaandrager A, Van Golde L, Batenburg J. 2004. Aggregation of Cryptococcus neoformans by surfactant protein D is inhibited by its capsular component glucuronoxylomannan. Infection and immunity 72:145-153.
39. Ferguson JS, Voelker DR, McCormack FX, Schlesinger LS. 1999. Surfactant protein D binds to Mycobacterium tuberculosis Bacilli and Lipoarabinomannan via carbohydrate-lectin interactions resulting in reduced phagocytosis of the bacteria by macrophages1. The Journal of immunology 163:312-321.
40. Curciarello R, Steele A, Cooper D, MacDonald TT, Kruidenier L, Kudo T. 2014. The role of Galectin-1 and Galectin-3 in the mucosal immune response to Citrobacter rodentium infection. PloS one 9:e107933.
41. Okumura CY, Baum LG, Johnson PJ. 2008. Galectin-1 on cervical epithelial cells is a receptor for the sexually transmitted human parasite Trichomonas vaginalis. Cellular microbiology 10:2078-2090.
42. Fichorova RN, Yamamoto HS, Fashemi T, Foley E, Ryan S, Beatty N, Dawood H, Hayes GR, St-Pierre G, Sato S. 2016. Trichomonas vaginalis lipophosphoglycan exploits binding to galectin-1 and-3 to modulate epithelial immunity. Journal of Biological Chemistry 291:998-1013.
43. Estevam RB, da Silva NMJW, da Silva W, Fonseca FM, de Oliveira AG, de Lima Pereira SA, Pereira TL, Adad SJ, Rodrigues VJ, Rodrigues DBR. 2017. Modulation of Galectin-3 and Galectin 9 in gastric mucosa of patients with chronic gastritis and positive Helicobacter pylori infection. Pathology-Research and Practice 213:1276-1281.
44. Lujan AL, Croci DO, Tudela JAG, Losinno AD, Cagnoni AJ, Mariño KV, Damiani MT, Rabinovich GA. 2018. Glycosylation-dependent galectin–receptor interactions promote Chlamydia trachomatis infection. Proceedings of the National Academy of Sciences 115:E6000-E6009.
45. Cerliani JP, Blidner AG, Toscano MA, Croci DO, Rabinovich GA. 2017. Translating the 'sugar code'into immune and vascular signaling programs. Trends in biochemical sciences 42:255-273.
46. Mercier S, St-Pierre C, Pelletier I, Ouellet M, Tremblay MJ, Sato S. 2008. Galectin-1 promotes HIV-1 infectivity in macrophages through stabilization of viral adsorption. Virology 371:121-129.
47. Almeida F, Wolf JM, Da Silva TA, DeLeon-Rodriguez CM, Rezende CP, Pessoni AM, Fernandes FF, Silva-Rocha R, Martinez R, Rodrigues ML. 2017. Galectin-3 impacts Cryptococcus neoformans infection through direct antifungal effects. Nature communications 8:1-13.
48. Hatanaka O, Rezende CP, Moreno P, Fernandes FF, Brito PKMO, Martinez R, Coelho C, Roque-Barreira MC, Casadevall A, Almeida F. 2019. Galectin-3 inhibits Paracoccidioides brasiliensis growth and impacts paracoccidioidomycosis through multiple mechanisms. Msphere 4.
49. Steichen AL, Simonson TJ, Salmon SL, Metzger DW, Mishra BB, Sharma J. 2015. Alarmin function of galectin-9 in murine respiratory tularemia. PloS one 10:e0123573.

50. Ip WE, Chan KH, Law HK, Tso GH, Kong EK, Wong WH, To YF, Yung RW, Chow EY, Au KL. 2005. Mannose-binding lectin in severe acute respiratory syndrome coronavirus infection. Journal of Infectious Diseases 191:1697-1704.
51. Haczku A, Atochina EN, Tomer Y, Chen H, Scanlon ST, Russo S, Xu J, Panettieri Jr RA, Beers MF. 2001. Aspergillus fumigatus-induced allergic airway inflammation alters surfactant homeostasis and lung function in BALB/c mice. American journal of respiratory cell and molecular biology 25:45-50.
52. Krane M, Griese M. 2003. Surfactant protein D in serum from patients with allergic bronchopulmonary aspergillosis. European Respiratory Journal 22:592-595.
53. Wu Y, Liu Z, Wei R, Pan S, Mao N, Chen B, Han J, Zhang F, Holmskov U, Xia Z. 2009. Elevated plasma surfactant protein d (SP-D) levels and a direct correlation with anti-severe acute respiratory syndrome coronavirus-specific IgG antibody in SARS patients. Scandinavian journal of immunology 69:508-515.
54. Kerget B, Kerget F, Koçak AO, Kızıltunç A, Araz Ö, Uçar EY, Akgün M. 2020. Are serum interleukin 6 and surfactant protein D levels associated with the clinical course of COVID-19? Lung 198:777-784.
55. Saito A, KURONUMA K, Moniwa K, Kodama K, Takahashi S, Takahashi H, Chiba H. 2020. Serum surfactant protein A and D may be novel biomarkers of COVID-19 pneumonia severity.
56. Walls AC, Park Y-J, Tortorici MA, Wall A, McGuire AT, Veesler D. 2020. Structure, function, and antigenicity of the SARS-CoV-2 spike glycoprotein. Cell 181:281-292. e6.
57. Hsieh M-H, Beirag N, Murugaiah V, Chou Y-C, Kuo W-S, Kao H-F, Madan T, Kishore U, Wang J-Y. 2020. Human Surfactant Protein D Binds S1 and Receptor Binding Domain of Spike protein and acts as an entry inhibitor of SARS-CoV-2 Pseudotyped viral particles in vitro. bioRxiv.
58. Madan T, Biswas B, Varghese P, Subedi R, Pandit H, Idicula-Thomas S, Kundu I, Rooge SB, Aggarwal R, Tripathi D. 2020. A recombinant fragment of Human surfactant protein D binds Spike protein and inhibits infectivity and replication of SARS-CoV-2 in clinical samples. bioRxiv.
59. Benne C, Kraaijeveld C, Van Strijp J, Brouwer E, Harmsen M, Verhoef J, Van Golde L, Van Iwaarden J. 1995. Interactions of surfactant protein A with influenza A viruses: binding and neutralization. Journal of Infectious Diseases 171:335-341.
60. LeVine AM, Whitsett JA, Hartshorn KL, Crouch EC, Korfhagen TR. 2001. Surfactant protein D enhances clearance of influenza A virus from the lung in vivo. The Journal of Immunology 167:5868-5873.
61. LeVine AM, Gwozdz J, Stark J, Bruno M, Whitsett J, Korfhagen T. 1999. Surfactant protein-A enhances respiratory syncytial virus clearance in vivo. The Journal of clinical investigation 103:1015-1021.
62. LeVine AM, Hartshorn K, Elliott J, Whitsett J, Korfhagen T. 2002. Absence of SP-A modulates innate and adaptive defense responses to pulmonary influenza infection. American Journal of Physiology-Lung Cellular and Molecular Physiology 282:L563-L572.

63. Al-Qahtani AA, Murugaiah V, Bashir HA, Pathan AA, Abozaid SM, Makarov E, Nal-Rogier B, Kishore U, Al-Ahdal MN. 2019. Full-length human surfactant protein A inhibits influenza A virus infection of A549 lung epithelial cells: a recombinant form containing neck and lectin domains promotes infectivity. Immunobiology 224:408-418.
64. Al-Ahdal MN, Murugaiah V, Varghese PM, Abozaid SM, Saba I, Al-Qahtani AA, Pathan AA, Kouser L, Nal B, Kishore U. 2018. Entry inhibition and modulation of pro-inflammatory immune response against influenza A virus by a recombinant truncated surfactant protein D. Frontiers in immunology 9:1586.
65. Madan T, Eggleton P, Kishore U, Strong P, Aggrawal SS, Sarma PU, Reid K. 1997. Binding of pulmonary surfactant proteins A and D to Aspergillus fumigatus conidia enhances phagocytosis and killing by human neutrophils and alveolar macrophages. Infection and immunity 65:3171-3179.
66. Madan T, Kishore U, Singh M, Strong P, Clark H, Hussain EM, Reid KB, Sarma PU. 2001. Surfactant proteins A and D protect mice against pulmonary hypersensitivity induced by Aspergillus fumigatus antigens and allergens. The Journal of clinical investigation 107:467-475.
67. Madan T, Reid KB, Clark H, Singh M, Nayak A, Sarma PU, Hawgood S, Kishore U. 2010. Susceptibility of mice genetically deficient in SP-A or SP-D gene to invasive pulmonary aspergillosis. Molecular immunology 47:1923-1930.
68. Madan T, Kishore U, Singh M, Strong P, Hussain EM, Reid KB, Sarma PU. 2001. Protective role of lung surfactant protein D in a murine model of invasive pulmonary aspergillosis. Infection and immunity 69:2728-2731.
69. Singh M, Madan T, Waters P, Sonar S, Singh SK, Kamran MF, Bernal AL, Sarma PU, Singh VK, Crouch EC. 2009. Therapeutic effects of recombinant forms of full-length and truncated human surfactant protein D in a murine model of invasive pulmonary aspergillosis. Molecular immunology 46:2363-2369.
70. Walenkamp A, Verheul A, Scharringa J, Hoepelman I. 1999. Pulmonary surfactant protein A binds to Cryptococcus neoformans of without promoting phagocytosis. European journal of clinical investigation 29:83-92.
71. Giles SS, Zaas AK, Reidy MF, Perfect JR, Wright JR. 2007. Cryptococcus neoformans is resistant to surfactant protein A mediated host defense mechanisms. PLoS One 2:e1370.
72. Geunes-Boyer S, Beers MF, Perfect JR, Heitman J, Wright JR. 2012. Surfactant protein D facilitates Cryptococcus neoformans infection. Infection and immunity 80:2444-2453.
73. Atochina EN, Beck JM, Preston AM, Haczku A, Tomer Y, Scanlon ST, Fusaro T, Casey J, Hawgood S, Gow AJ. 2004. Enhanced lung injury and delayed clearance of Pneumocystis carinii in surfactant protein A-deficient mice: attenuation of cytokine responses and reactive oxygen-nitrogen species. Infection and immunity 72:6002-6011.
74. Yong S-J, Vuk-Pavlovic Z, Standing JE, Crouch EC, Limper AH. 2003. Surfactant protein D-mediated aggregation of Pneumocystis carinii impairs phagocytosis by alveolar macrophages. Infection and immunity 71:1662-1671.
75. Kudo K, Sano H, Takahashi H, Kuronuma K, Yokota S-i, Fujii N, Shimada K-i, Yano I, Kumazawa Y, Voelker DR. 2004. Pulmonary collectins enhance

phagocytosis of Mycobacterium avium through increased activity of mannose receptor. The Journal of Immunology 172:7592-7602.
76. Ragas A, Roussel L, Puzo G, Rivière M. 2007. The Mycobacterium tuberculosis cell-surface glycoprotein apa as a potential adhesin to colonize target cells via the innate immune system pulmonary C-type lectin surfactant protein A. Journal of biological chemistry 282:5133-5142.
77. Lim B-L, Wang J-Y, Holmskov U, Hoppe H-J, Reid KB. 1994. Expression of the carbohydrate recognition domain of lung surfactant protein D and demonstration of its binding to lipopolysaccharides of gram-negative bacteria. Biochemical and biophysical research communications 202:1674-1680.
78. LeVine AM, Whitsett JA, Gwozdz JA, Richardson TR, Fisher JH, Burhans MS, Korfhagen TR. 2000. Distinct effects of surfactant protein A or D deficiency during bacterial infection on the lung. The Journal of Immunology 165:3934-3940.
79. Minutti CM, Jackson-Jones LH, García-Fojeda B, Knipper JA, Sutherland TE, Logan N, Rinqvist E, Guillamat-Prats R, Ferenbach DA, Artigas A. Local amplifiers of IL-4Ra–mediated macrophage activation promote repair in lung and liver.
80. Madsen J, Tornøe I, Nielsen O, Koch C, Steinhilber W, Holmskov U. 2003. Expression and localization of lung surfactant protein A in human tissues. American journal of respiratory cell and molecular biology 29:591-597.
81. Madsen J, Kliem A, Tornøe I, Skjødt K, Koch C, Holmskov U. 2000. Localization of lung surfactant protein D on mucosal surfaces in human tissues. The Journal of Immunology 164:5866-5870.
82. MacNeill C, Umstead TM, Phelps DS, Lin Z, Floros J, Shearer DA, Weisz J. 2004. Surfactant protein A, an innate immune factor, is expressed in the vaginal mucosa and is present in vaginal lavage fluid. Immunology 111:91-99.
83. Ujma S, Carse S, Chetty A, Horsnell W, Clark H, Madsen J, Mackay R-M, Watson A, Griffiths M, Katz AA. 2019. Surfactant protein a impairs genital HPV16 pseudovirus infection by innate immune cell activation in a murine model. Pathogens 8:288.
84. Van Iwaarden J, Van Strijp J, Visser H, Haagsman H, Verhoef J, Van Golde L. 1992. Binding of surfactant protein A (SP-A) to herpes simplex virus type 1-infected cells is mediated by the carbohydrate moiety of SP-A. Journal of Biological Chemistry 267:25039-25043.
85. Van Iwaarden J, Van Strijp J, Ebskamp M, Welmers A, Verhoef J, Van Golde L. 1991. Surfactant protein A is opsonin in phagocytosis of herpes simplex virus type 1 by rat alveolar macrophages. American Journal of Physiology-Lung Cellular and Molecular Physiology 261:L204-L209.
86. Madsen J, Gaiha GD, Palaniyar N, Dong T, Mitchell DA, Clark HW. 2013. Surfactant Protein D modulates HIV infection of both T-cells and dendritic cells. PLoS One 8:e59047.
87. Dodagatta-Marri E, Mitchell DA, Pandit H, Sonawani A, Murugaiah V, Idicula-Thomas S, Nal B, Al-Mozaini MM, Kaur A, Madan T. 2017. Protein–Protein interaction between surfactant Protein D and Dc-sign via c-Type lectin Domain can suppress hiV-1 Transfer. Frontiers in immunology 8:834.

88. Liu FT, Rabinovich GA. 2010. Galectins: regulators of acute and chronic inflammation. Annals of the New York Academy of Sciences 1183:158-182.
89. Liu F-T, Patterson RJ, Wang JL. 2002. Intracellular functions of galectins. Biochimica et Biophysica Acta (BBA)-General Subjects 1572:263-273.
90. Popa SJ, Stewart SE, Moreau K. Unconventional secretion of annexins and galectins, p 42-50. *In* (ed), Elsevier,
91. Dings RP, Miller MC, Griffin RJ, Mayo KH. 2018. Galectins as molecular targets for therapeutic intervention. International journal of molecular sciences 19:905.
92. Yang M-L, Chen Y-H, Wang S-W, Huang Y-J, Leu C-H, Yeh N-C, Chu C-Y, Lin C-C, Shieh G-S, Chen Y-L. 2011. Galectin-1 binds to influenza virus and ameliorates influenza virus pathogenesis. Journal of virology 85:10010-10020.
93. Velagapudi R, Hsueh Y-P, Geunes-Boyer S, Wright JR, Heitman J. 2009. Spores as infectious propagules of Cryptococcus neoformans. Infection and immunity 77:4345-4355.
94. Bocca AL, Amaral AC, Teixeira MM, Sato PK, Shikanai-Yasuda MA, Soares Felipe MS. 2013. Paracoccidioidomycosis: eco-epidemiology, taxonomy and clinical and therapeutic issues. Future microbiology 8:1177-1191.
95. Queiroz-Telles F, Escuissato DL. Pulmonary paracoccidioidomycosis, p 764-774. *In* (ed), © Thieme Medical Publishers,
96. Lippert E, Falk W, Bataille F, Kähne T, Naumann M, Goeke M, Herfarth H, Schoelmerich J, Rogler G. 2007. Soluble galectin-3 is a strong, colonic epithelial-cell-derived, lamina propria fibroblast-stimulating factor. Gut 56:43-51.
97. Santucci L, Fiorucci S, Rubinstein N, Mencarelli A, Palazzetti B, Federici B, Rabinovich GA, Morelli A. 2003. Galectin-1 suppresses experimental colitis in mice. Gastroenterology 124:1381-1394.
98. Norling LV, Sampaio AL, Cooper D, Perretti M. 2008. Inhibitory control of endothelial galectin-1 on in vitro and in vivo lymphocyte trafficking. The FASEB Journal 22:682-690.
99. Ilarregui JM, Croci DO, Bianco GA, Toscano MA, Salatino M, Vermeulen ME, Geffner JR, Rabinovich GA. 2009. Tolerogenic signals delivered by dendritic cells to T cells through a galectin-1-driven immunoregulatory circuit involving interleukin 27 and interleukin 10. Nature immunology 10:981.
100. Pabst O. 2012. New concepts in the generation and functions of IgA. Nature Reviews Immunology 12:821-832.
101. Liang C-C, Li C-S, Weng I-C, Chen H-Y, Lu H-H, Huang C-C, Liu F-T. 2018. Galectin-9 Is Critical for Mucosal Adaptive Immunity through the T Helper 17–IgA Axis. The American journal of pathology 188:1225-1235.
102. Gunn B, Schneider J, Shansab M, Bastian AR, Fahrbach K, Smith A, Mahan A, Karim M, Licht A, Zvonar I. 2016. Enhanced binding of antibodies generated during chronic HIV infection to mucus component MUC16. Mucosal immunology 9:1549-1558.
103. Rabinovich G, Castagna L, Landa C, Riera CM, Sotomayor C. 1996. Regulated expression of a 16-kd galectin-like protein in activated rat macrophages. Journal of leukocyte biology 59:363-370.

104. Zuñiga E, Rabinovich GA, Iglesias MM, Gruppi A. 2001. Regulated expression of galectin-1 during B-cell activation and implications for T-cell apoptosis. Journal of leukocyte biology 70:73-79.
105. Sato S, Ouellet M, St-Pierre C, Tremblay MJ. 2012. Glycans, galectins, and HIV-1 infection. Annals of the New York Academy of Sciences 1253:133-148.
106. St-Pierre C, Manya H, Ouellet M, Clark GF, Endo T, Tremblay MJ, Sato S. 2011. Host-soluble galectin-1 promotes HIV-1 replication through a direct interaction with glycans of viral gp120 and host CD4. Journal of virology 85:11742-11751.
107. Kaltner H, Seyrek K, Heck A, Sinowatz F, Gabius H-J. 2002. Galectin-1 and galectin-3 in fetal development of bovine respiratory and digestive tracts. Cell and tissue research 307:35-46.
108. Chen H-Y, Wang S-F, Hsu DKH, Chen Y-MA, Liu F-T. 2014. Galectin-3 translocates to virological synapse and promotes HIV-1 transfer (VIR1P. 1000). Am Assoc Immnol.
109. Wang S-F, Tsao C-H, Lin Y-T, Hsu DK, Chiang M-L, Lo C-H, Chien F-C, Chen P, Arthur Chen Y-M, Chen H-Y. 2014. Galectin-3 promotes HIV-1 budding via association with Alix and Gag p6. Glycobiology 24:1022-1035.
110. Fujii K, Munshi UM, Ablan SD, Demirov DG, Soheilian F, Nagashima K, Stephen AG, Fisher RJ, Freed EO. 2009. Functional role of Alix in HIV-1 replication. Virology 391:284-292.
111. Rabinovich GA, Baum LG, Tinari N, Paganelli R, Natoli C, Liu F-T, Iacobelli S. 2002. Galectins and their ligands: amplifiers, silencers or tuners of the inflammatory response? Trends in immunology 23:313-320.
112. Uehara F, Ohba N, Ozawa M. 2001. Isolation and characterization of galectins in the mammalian retina. Investigative ophthalmology & visual science 42:2164-2172.
113. Ishida K, Panjwani N, Cao Z, Streilein JW. 2003. Participation of pigment epithelium in ocular immune privilege. 3. Epithelia cultured from iris, ciliary body, and retina suppress T-cell activation by partially non-overlapping mechanisms. Ocular immunology and inflammation 11:91-105.
114. Rubinstein N, Alvarez M, Zwirner NW, Toscano MA, Ilarregui JM, Bravo A, Mordoh J, Fainboim L, Podhajcer OL, Rabinovich GA. 2004. Targeted inhibition of galectin-1 gene expression in tumor cells results in heightened T cell-mediated rejection: a potential mechanism of tumor-immune privilege. Cancer cell 5:241-251.
115. Mauris J, Mantelli F, Woodward AM, Cao Z, Bertozzi CR, Panjwani N, Godula K, Argüeso P. 2013. Modulation of ocular surface glycocalyx barrier function by a galectin-3 N-terminal deletion mutant and membrane-anchored synthetic glycopolymers. PloS one 8:e72304.
116. Chung CD, Patel VP, Moran M, Lewis LA, Miceli MC. 2000. Galectin-1 induces partial TCR ζ-chain phosphorylation and antagonizes processive TCR signal transduction. The Journal of Immunology 165:3722-3729.
117. Muiño JC, Juárez CP, Luna JD, Castro CC, Wolff EG, Ferrero M, Romero-Piffiguer MD. 1999. The importance of specific IgG and IgE autoantibodies to retinal S antigen, total serum IgE, and sCD23 levels in autoimmune and infectious uveitis. Journal of clinical immunology 19:215-222.

118. Baum LG, Blackall DP, Arias-Magallano S, Nanigian D, Uh SY, Browne JM, Hoffmann D, Emmanouilides CE, Territo MC, Baldwin GC. 2003. Amelioration of graft versus host disease by galectin-1. Clinical Immunology 109:295-307.
119. Romero MD, Muino JC, Bianco GA, Ferrero M, Juarez CP, Luna JD, Rabinovich GA. 2006. Circulating anti-galectin-1 antibodies are associated with the severity of ocular disease in autoimmune and infectious uveitis. Investigative ophthalmology & visual science 47:1550-1556.
120. Dick AD, Siepmann K, Dees C, Duncan L, Broderick C, Liversidge J, Forrester JV. 1999. Fas–Fas Ligand–Mediated Apoptosis within Aqueous during Idiopathic Acute Anterior Uveitis. Investigative ophthalmology & visual science 40:2258-2267.
121. Sumiyoshi M, Ricciuto J, Tisdale A, Gipson IK, Mantelli F, Argüeso P. 2008. Antiadhesive character of mucin O-glycans at the apical surface of corneal epithelial cells. Investigative ophthalmology & visual science 49:197-203.
122. Ricciuto J, Heimer SR, Gilmore MS, Argüeso P. 2008. Cell surface O-glycans limit Staphylococcus aureus adherence to corneal epithelial cells. Infection and immunity 76:5215-5220.
123. Yu L-G, Andrews N, Zhao Q, McKean D, Williams JF, Connor LJ, Gerasimenko OV, Hilkens J, Hirabayashi J, Kasai K. 2007. Galectin-3 interaction with Thomsen-Friedenreich disaccharide on cancer-associated MUC1 causes increased cancer cell endothelial adhesion. Journal of Biological Chemistry 282:773-781.
124. Argüeso P, Guzman-Aranguez A, Mantelli F, Cao Z, Ricciuto J, Panjwani N. 2009. Association of cell surface mucins with galectin-3 contributes to the ocular surface epithelial barrier. Journal of Biological Chemistry 284:23037-23045.
125. Woodward A, Mauris J, Argüeso P. 2013. Binding of transmembrane mucins to galectin-3 limits herpesvirus 1 infection of human corneal keratinocytes. Journal of virology 87:5841-5847.
126. Rajasagi NK, Suryawanshi A, Sehrawat S, Reddy PB, Mulik S, Hirashima M, Rouse BT. 2012. Galectin-1 reduces the severity of herpes simplex virus-induced ocular immunopathological lesions. The Journal of Immunology 188:4631-4643.
127. Choteau L, Parny M, Francois N, Bertin B, Fumery M, Dubuquoy L, Takahashi K, Colombel J-F, Jouault T, Poulain D. 2016. Role of mannose-binding lectin in intestinal homeostasis and fungal elimination. Mucosal Immunology 9:767-776.
128. Wang W, Song X, Wang L, Song L. 2018. Pathogen-derived carbohydrate recognition in molluscs immune defense. International journal of molecular sciences 19:721.
129. Lionakis MS, Netea MG. 2013. Candida and host determinants of susceptibility to invasive candidiasis. PLoS Pathog 9:e1003079.
130. Gow NA, Van De Veerdonk FL, Brown AJ, Netea MG. 2012. Candida albicans morphogenesis and host defence: discriminating invasion from colonization. Nature reviews microbiology 10:112-122.
131. Damiens S, Poissy J, François N, Salleron J, Jawhara S, Jouault T, Poulain D, Sendid B. 2012. Mannose-binding lectin levels and variation during invasive candidiasis. Journal of clinical immunology 32:1317-1323.

132. Brouwer N, Dolman KM, van Houdt M, Sta M, Roos D, Kuijpers TW. 2008. Mannose-binding lectin (MBL) facilitates opsonophagocytosis of yeasts but not of bacteria despite MBL binding. The Journal of Immunology 180:4124-4132.
133. Ghiran I, Barbashov SF, Klickstein LB, Tas SW, Jensenius JC, Nicholson-Weller A. 2000. Complement receptor 1/CD35 is a receptor for mannan-binding lectin. The Journal of experimental medicine 192:1797-1808.
134. Whibley N, Gaffen SL. 2014. Brothers in arms: Th17 and Treg responses in Candida albicans immunity. PLoS Pathog 10:e1004456.
135. Garred P, Larsen F, Seyfarth J, Fujita R, Madsen HO. 2006. Mannose-binding lectin and its genetic variants. Genes & Immunity 7:85-94.
136. Eisen DP. 2010. Mannose-binding lectin deficiency and respiratory tract infection. Journal of innate immunity 2:114-122.
137. Mandal RK, Khan MA, Hussain A, Dar SA, Aloufi S, Jawed A, Wahid M, Panda AK, Lohani M, Akhter N. 2019. Association of MBL2 gene polymorphisms with pulmonary tuberculosis susceptibility: trial sequence meta-analysis as evidence. Infection and drug resistance 12:185.
138. Neth O, Jack DL, Johnson M, Klein NJ, Turner MW. 2002. Enhancement of complement activation and opsonophagocytosis by complexes of mannose-binding lectin with mannose-binding lectin-associated serine protease after binding to Staphylococcus aureus. The Journal of Immunology 169:4430-4436.
139. Shi L, Takahashi K, Dundee J, Shahroor-Karni S, Thiel S, Jensenius JC, Gad F, Hamblin MR, Sastry KN, Ezekowitz RAB. 2004. Mannose-binding lectin-deficient mice are susceptible to infection with Staphylococcus aureus. The Journal of experimental medicine 199:1379-1390.
140. Krarup A, Sørensen UBS, Matsushita M, Jensenius JC, Thiel S. 2005. Effect of capsulation of opportunistic pathogenic bacteria on binding of the pattern recognition molecules mannan-binding lectin, L-ficolin, and H-ficolin. Infection and immunity 73:1052-1060.
141. Moens L, Van Hoeyveld E, Peetermans WE, De Boeck C, Verhaegen J, Bossuyt X. 2006. Mannose-binding lectin genotype and invasive pneumococcal infection. Human immunology 67:605-611.
142. Roy S, Knox K, Segal S, Griffiths D, Moore CE, Welsh KI, Smarason A, Day NP, McPheat WL, Crook DW. 2002. MBL genotype and risk of invasive pneumococcal disease: a case-control study. The Lancet 359:1569-1573.
143. Kronborg G, Weis N, Madsen HO, Pedersen SS, Wejse C, Nielsen H, Skinhøj P, Garred P. 2002. Variant mannose-binding lectin alleles are not associated with susceptibility to or outcome of invasive pneumococcal infection in randomly included patients. Journal of Infectious Diseases 185:1517-1520.
144. Matricardi PM, Dal Negro RW, Nisini R. 2020. The first, holistic immunological model of COVID-19: implications for prevention, diagnosis, and public health measures. Pediatric Allergy and Immunology.
145. Terai I, Kobayashi K. 1993. Perinatal changes in serum mannose-binding protein (MBP) levels. Immunology letters 38:185-187.
146. Tomaiuolo R, Ruocco A, Salapete C, Carru C, Baggio G, Franceschi C, Zinellu A, Vaupel J, Bellia C, Sasso BL. 2012. Activity of mannose-binding lectin in centenarians. Aging cell 11:394-400.

147. Terai I, KOBAYAsHi K, Fujita T, Hagiwara K. 1993. Human serum mannose binding protein (MBP): development of an enzyme-linked immunosorbent assay (ELISA) and determination of levels in serum from 1085 normal Japanese and in some body fluids. Biochemical medicine and metabolic biology 50:111-119.
148. Thorarinsdottir H, Ludviksson B, Vikingsdottir T, Leopoldsdottir M, Ardal B, Jonsson T, Valdimarsson H, Arason G. 2005. Childhood levels of immunoglobulins and mannan-binding lectin in relation to infections and allergy. Scandinavian journal of immunology 61:466-474.
149. Tu X, Chong WP, Zhai Y, Zhang H, Zhang F, Wang S, Liu W, Wei M, Siu NHO, Yang H. 2015. Functional polymorphisms of the CCL2 and MBL genes cumulatively increase susceptibility to severe acute respiratory syndrome coronavirus infection. Journal of Infection 71:101-109.
150. Zhang H, Zhou G, Zhi L, Yang H, Zhai Y, Dong X, Zhang X, Gao X, Zhu Y, He F. 2005. Association between mannose-binding lectin gene polymorphisms and susceptibility to severe acute respiratory syndrome coronavirus infection. The Journal of infectious diseases 192:1355-1361.
151. Watanabe Y, Allen JD, Wrapp D, McLellan JS, Crispin M. 2020. Site-specific analysis of the SARS-CoV-2 glycan shield. BioRxiv.
152. Zhou Y, Lu K, Pfefferle S, Bertram S, Glowacka I, Drosten C, Pöhlmann S, Simmons G. 2010. A single asparagine-linked glycosylation site of the severe acute respiratory syndrome coronavirus spike glycoprotein facilitates inhibition by mannose-binding lectin through multiple mechanisms. Journal of virology 84:8753-8764.
153. Gao T, Hu M, Zhang X, Li H, Zhu L, Liu H, Dong Q, Zhang Z, Wang Z, Hu Y. 2020. Highly pathogenic coronavirus N protein aggravates lung injury by MASP-2-mediated complement over-activation. MedRxiv.
154. Eisen DP, Minchinton RM. 2003. Impact of mannose-binding lectin on susceptibility to infectious diseases. Clinical Infectious Diseases 37:1496-1505.
155. Neth O, Jack DL, Dodds AW, Holzel H, Klein NJ, Turner MW. 2000. Mannose-binding lectin binds to a range of clinically relevant microorganisms and promotes complement deposition. Infection and immunity 68:688-693.
156. Bouwman LH, Roep BO, Roos A. 2006. Mannose-binding lectin: clinical implications for infection, transplantation, and autoimmunity. Human immunology 67:247-256.
157. De Pascale G, Cutuli SL, Pennisi MA, Antonelli M. 2013. The role of mannose-binding lectin in severe sepsis and septic shock. Mediators of inflammation 2013.
158. Ling MT, Tu W, Han Y, Mao H, Chong WP, Guan J, Liu M, Lam KT, Law HK, Peiris JM. 2012. Mannose-binding lectin contributes to deleterious inflammatory response in pandemic H1N1 and avian H9N2 infection. Journal of Infectious Diseases 205:44-53.
159. Job ER, Deng Y-M, Tate MD, Bottazzi B, Crouch EC, Dean MM, Mantovani A, Brooks AG, Reading PC. 2010. Pandemic H1N1 influenza A viruses are resistant to the antiviral activities of innate immune proteins of the collectin and pentraxin superfamilies. The Journal of Immunology 185:4284-4291.

160. Garred P, Harboe M, Oettinger T, Koch C, Svejgaard A. 1994. Dual role of mannan-binding protein in infections: another case of heterosis? International Journal of Immunogenetics 21:125-131.
161. de Miranda Santos IK, Costa CH, Krieger H, Feitosa MF, Zurakowski D, Fardin B, Gomes RB, Weiner DL, Harn DA, Ezekowitz RAB. 2001. Mannan-binding lectin enhances susceptibility to visceral leishmaniasis. Infection and immunity 69:5212-5215.
162. Kalia N, Singh J, Kaur M. 2021. The ambiguous role of mannose-binding lectin (MBL) in human immunity. Open Medicine 16:299-310.
163. Dahl M, Tybjærg-Hansen A, Schnohr P, Nordestgaard BG. 2004. A population-based study of morbidity and mortality in mannose-binding lectin deficiency. The Journal of experimental medicine 199:1391-1399.
164. Tacx A, Groeneveld A, Hart M, Aarden L, Hack C. 2003. Mannan binding lectin in febrile adults: no correlation with microbial infection and complement activation. Journal of clinical pathology 56:956-959.
165. Lusvarghi S, Bewley CA. 2016. Griffithsin: an antiviral lectin with outstanding therapeutic potential. Viruses 8:296.
166. Lee C. 2019. Griffithsin, a highly potent broad-spectrum antiviral lectin from red algae: from discovery to clinical application. Marine drugs 17:567.
167. Xue J, Gao Y, Hoorelbeke B, Kagiampakis I, Zhao B, Demeler B, Balzarini J, LiWang PJ. 2012. The role of individual carbohydrate-binding sites in the function of the potent anti-HIV lectin griffithsin. Molecular pharmaceutics 9:2613-2625.
168. O'Keefe BR, Vojdani F, Buffa V, Shattock RJ, Montefiori DC, Bakke J, Mirsalis J, d'Andrea A-L, Hume SD, Bratcher B. 2009. Scaleable manufacture of HIV-1 entry inhibitor griffithsin and validation of its safety and efficacy as a topical microbicide component. Proceedings of the National Academy of Sciences 106:6099-6104.
169. Vamvaka E, Arcalis E, Ramessar K, Evans A, O'Keefe BR, Shattock RJ, Medina V, Stöger E, Christou P, Capell T. 2016. Rice endosperm is cost-effective for the production of recombinant griffithsin with potent activity against HIV. Plant biotechnology journal 14:1427-1437.
170. Giomarelli B, Schumacher KM, Taylor TE, Sowder II RC, Hartley JL, McMahon JB, Mori T. 2006. Recombinant production of anti-HIV protein, griffithsin, by auto-induction in a fermentor culture. Protein expression and purification 47:194-202.
171. Hahn S, Giritch A, Bartels D, Bortesi L, Gleba Y. 2015. A novel and fully scalable A grobacterium spray-based process for manufacturing cellulases and other cost-sensitive proteins in plants. Plant biotechnology journal 13:708-716.
172. Fuqua JL, Wanga V, Palmer KE. 2015. Improving the large scale purification of the HIV microbicide, griffithsin. BMC biotechnology 15:1-10.
173. Meuleman P, Albecka A, Belouzard S, Vercauteren K, Verhoye L, Wychowski C, Leroux-Roels G, Palmer KE, Dubuisson J. 2011. Griffithsin has antiviral activity against hepatitis C virus. Antimicrobial agents and chemotherapy 55:5159-5167.

174. Ishag HZ, Li C, Huang L, Sun M-x, Wang F, Ni B, Malik T, Chen P-y, Mao X. 2013. Griffithsin inhibits Japanese encephalitis virus infection in vitro and in vivo. Archives of virology 158:349-358.
175. Levendosky K, Mizenina O, Kleinbeck K, Kizima L, Rodriguez A, Jean-Pierre N, Robbiani M, O'Keefe BR, Zydowsky T, Fernández-Romero JA. 2014. Antiviral Activity and Mode of Action of Griffithsin against HSV-2 and HPV: Preliminary Studies of a Potential non-ARV Combination Microbicide. AIDS Research and Human Retroviruses 30:A203-A204.
176. Cai Y, Xu W, Gu C, Cai X, Qu D, Lu L, Xie Y, Jiang S. 2020. Griffithsin with a broad-spectrum antiviral activity by binding glycans in viral glycoprotein exhibits strong synergistic effect in combination with a pan-coronavirus fusion inhibitor targeting sars-cov-2 spike s2 subunit. Virologica Sinica 35:857-860.
177. Chatterjee A, Ratner DM, Ryan CM, Johnson PJ, O'Keefe BR, Secor WE, Anderson DJ, Robbins PW, Samuelson J. 2015. Anti-retroviral lectins have modest effects on adherence of Trichomonas vaginalis to epithelial cells in vitro and on recovery of Tritrichomonas foetus in a mouse vaginal model. PloS one 10:e0135340.
178. Shajahan A, Supekar NT, Gleinich AS, Azadi P. 2020. Deducing the N-and O-glycosylation profile of the spike protein of novel coronavirus SARS-CoV-2. Glycobiology 30:981-988.
179. Andersen KG, Rambaut A, Lipkin WI, Holmes EC, Garry RF. 2020. The proximal origin of SARS-CoV-2. Nature medicine 26:450-452.
180. Corman VM, Muth D, Niemeyer D, Drosten C. 2018. Hosts and sources of endemic human coronaviruses. Advances in virus research 100:163-188.
181. Yeager CL, Ashmun RA, Williams RK, Cardellichio CB, Shapiro LH, Look AT, Holmes KV. 1992. Human aminopeptidase N is a receptor for human coronavirus 229E. Nature 357:420-422.
182. Hofmann H, Pyrc K, Van Der Hoek L, Geier M, Berkhout B, Pöhlmann S. 2005. Human coronavirus NL63 employs the severe acute respiratory syndrome coronavirus receptor for cellular entry. Proceedings of the National Academy of Sciences 102:7988-7993.
183. Weiss SR, Navas-Martin S. 2005. Coronavirus pathogenesis and the emerging pathogen severe acute respiratory syndrome coronavirus. Microbiology and molecular biology reviews 69:635-664.
184. Zheng J. 2020. SARS-CoV-2: an emerging coronavirus that causes a global threat. International journal of biological sciences 16:1678.
185. Coleman CM, Frieman MB. 2014. Coronaviruses: important emerging human pathogens. Journal of virology 88:5209-5212.
186. Raj VS, Mou H, Smits SL, Dekkers DH, Müller MA, Dijkman R, Muth D, Demmers JA, Zaki A, Fouchier RA. 2013. Dipeptidyl peptidase 4 is a functional receptor for the emerging human coronavirus-EMC. Nature 495:251-254.
187. Li W, Moore MJ, Vasilieva N, Sui J, Wong SK, Berne MA, Somasundaran M, Sullivan JL, Luzuriaga K, Greenough TC. 2003. Angiotensin-converting enzyme 2 is a functional receptor for the SARS coronavirus. Nature 426:450-454.

188. Shang J, Ye G, Shi K, Wan Y, Luo C, Aihara H, Geng Q, Auerbach A, Li F. 2020. Structural basis of receptor recognition by SARS-CoV-2. Nature 581:221-224.
189. Millet JK, Séron K, Labitt RN, Danneels A, Palmer KE, Whittaker GR, Dubuisson J, Belouzard S. 2016. Middle East respiratory syndrome coronavirus infection is inhibited by griffithsin. Antiviral research 133:1-8.
190. Schmaljohn C, Hjelle B. 1997. Hantaviruses: a global disease problem. Emerging infectious diseases 3:95.
191. Botten J, Mirowsky K, Ye C, Gottlieb K, Saavedra M, Ponce L, Hjelle B. 2002. Shedding and intracage transmission of Sin Nombre hantavirus in the deer mouse (Peromyscus maniculatus) model. Journal of Virology 76:7587-7594.
192. Guardado-Calvo P, Bignon EA, Stettner E, Jeffers SA, Pérez-Vargas J, Pehau-Arnaudet G, Tortorici MA, Jestin J-L, England P, Tischler ND. 2016. Mechanistic insight into bunyavirus-induced membrane fusion from structure-function analyses of the hantavirus envelope glycoprotein Gc. PLoS pathogens 12:e1005813.
193. Mittler E, Dieterle ME, Kleinfelter LM, Slough MM, Chandran K, Jangra RK. 2019. Hantavirus entry: Perspectives and recent advances. Advances in virus research 104:185-224.
194. Hooper J, Larsen T, Custer D, Schmaljohn C. 2001. A lethal disease model for hantavirus pulmonary syndrome. Virology 289:6-14.
195. Shrivastava-Ranjan P, Lo MK, Chatterjee P, Flint M, Nichol ST, Montgomery JM, O'Keefe BR, Spiropoulou CF. 2020. Hantavirus Infection Is Inhibited by Griffithsin in Cell Culture. Frontiers in cellular and infection microbiology 10:619.
196. Barton C, Kouokam JC, Hurst H, Palmer KE. 2016. Pharmacokinetics of the antiviral lectin griffithsin administered by different routes indicates multiple potential uses. Viruses 8:331.
197. Motta J-P, Martin L, Vergnolle N. 2011. Proteases/antiproteases in inflammatory bowel diseases, p 173-215, Proteases and Their Receptors in Inflammation. Springer.
198. Moncla BJ, Pryke K, Rohan LC, Graebing PW. 2011. Degradation of naturally occurring and engineered antimicrobial peptides by proteases. Advances in bioscience and biotechnology (Print) 2:404.
199. Nabeta H, Steyn S, Lasnik A, McGowan I, Fuqua J, Kouokam JC, Palmer KE. Activity of Griffithsin-M78Q, an HIV Entry Inhibitor, in the Rectal Environment, p 4-7. *In* (ed),
200. Patel P, Borkowf CB, Brooks JT, Lasry A, Lansky A, Mermin J. 2014. Estimating per-act HIV transmission risk: a systematic review. AIDS (London, England) 28:1509.
201. Beyrer C, Sullivan P, Sanchez J, Baral SD, Collins C, Wirtz AL, Altman D, Trapence G, Mayer K. 2013. The increase in global HIV epidemics in MSM. Aids 27:2665-2678.
202. (UNAIDS) UJPoHA. 2016. Global AIDS update 2016.:1-13.
203. Girard L, Birse K, Holm JB, Gajer P, Humphrys MS, Garber D, Guenthner P, Noël-Romas L, Abou M, McCorrister S. 2018. Impact of the griffithsin anti-HIV

microbicide and placebo gels on the rectal mucosal proteome and microbiome in non-human primates. Scientific reports 8:1-13.
204. Günaydın G, Edfeldt G, Garber DA, Asghar M, Noël-Romas L, Burgener A, Wählby C, Wang L, Rohan LC, Guenthner P. 2019. Impact of Q-Griffithsin anti-HIV microbicide gel in non-human primates: In situ analyses of epithelial and immune cell markers in rectal mucosa. Scientific reports 9:1-12.
205. Vishwanathan SA, Morris MR, Wolitski RJ, Luo W, Rose CE, Blau DM, Tsegaye T, Zaki SR, Garber DA, Jenkins LT. 2015. Rectal application of a highly osmolar personal lubricant in a macaque model induces acute cytotoxicity but does not increase risk of SHIV infection. PLoS One 10:e0120021.
206. Emau P, Tian B, O'keefe B, Mori T, McMahon J, Palmer K, Jiang Y, Bekele G, Tsai C. 2007. Griffithsin, a potent HIV entry inhibitor, is an excellent candidate for anti-HIV microbicide. Journal of medical primatology 36:244-253.
207. Xue J, Hoorelbeke B, Kagiampakis I, Demeler B, Balzarini J, LiWang PJ. 2013. The griffithsin dimer is required for high-potency inhibition of HIV-1: evidence for manipulation of the structure of gp120 as part of the griffithsin dimer mechanism. Antimicrobial agents and chemotherapy 57:3976-3989.
208. Férir G, Palmer KE, Schols D. 2011. Synergistic activity profile of griffithsin in combination with tenofovir, maraviroc and enfuvirtide against HIV-1 clade C. Virology 417:253-258.
209. Hamorsky KT, Grooms-Williams TW, Husk AS, Bennett LJ, Palmer KE, Matoba N. 2013. Efficient single tobamoviral vector-based bioproduction of broadly neutralizing anti-HIV-1 monoclonal antibody VRC01 in Nicotiana benthamiana plants and utility of VRC01 in combination microbicides. Antimicrobial agents and chemotherapy 57:2076-2086.
210. Fischer K, Nguyen K, LiWang PJ. 2019. Griffithsin retains anti-HIV-1 potency with changes in gp120 glycosylation and complements broadly neutralizing antibodies PGT121 and PGT126. Antimicrobial agents and chemotherapy 64.
211. Williams KL, Stumpf M, Naiman NE, Ding S, Garrett M, Gobillot T, Vézina D, Dusenbury K, Ramadoss NS, Basom R. 2019. Identification of HIV gp41-specific antibodies that mediate killing of infected cells. PLoS pathogens 15:e1007572.
212. Li Y, Liu D, Wang Y, Su W, Liu G, Dong W. 2021. The Importance of Glycans of Viral and Host Proteins in Enveloped Virus Infection. Frontiers in Immunology 12:1544.
213. Kosik I, Ince WL, Gentles LE, Oler AJ, Kosikova M, Angel M, Magadán JG, Xie H, Brooke CB, Yewdell JW. 2018. Influenza A virus hemagglutinin glycosylation compensates for antibody escape fitness costs. PLoS pathogens 14:e1006796.
214. Lynch RM, Wong P, Tran L, O'Dell S, Nason MC, Li Y, Wu X, Mascola JR. 2015. HIV-1 fitness cost associated with escape from the VRC01 class of CD4 binding site neutralizing antibodies. Journal of virology 89:4201-4213.
215. Palmer K. 2019. Griffithsin-based Rectal Microbicides for PREvention of Viral ENTry (PREVENT). University of Louisville, KY: National Institute of Allergy and Infectious Disease.
216. Shaw JL, Smith CR, Diamandis EP. 2007. Proteomic analysis of human cervico-vaginal fluid. Journal of proteome research 6:2859-2865.
217. Lopez JEM. 2015. Candidiasis (vulvovaginal). BMJ Clinical Evidence 2015.

218. Sobel JD. 2016. Recurrent vulvovaginal candidiasis. American journal of obstetrics and gynecology 214:15-21.
219. Derby N, Lal M, Aravantinou M, Kizima L, Barnable P, Rodriguez A, Lai M, Wesenberg A, Ugaonkar S, Levendosky K. 2018. Griffithsin carrageenan fast dissolving inserts prevent SHIV HSV-2 and HPV infections in vivo. Nature communications 9:1-9.
220. Tyo KM, Lasnik AB, Zhang L, Mahmoud M, Jenson AB, Fuqua JL, Palmer KE, Steinbach-Rankins JM. 2020. Sustained-release Griffithsin nanoparticle-fiber composites against HIV-1 and HSV-2 infections. Journal of Controlled Release 321:84-99.
221. Olofsson S, Kumlin U, Dimock K, Arnberg N. 2005. Avian influenza and sialic acid receptors: more than meets the eye? The Lancet infectious diseases 5:184-188.
222. Schaap GJ, de Jong JC, van Bijsterveld OP, Beekhuis WH. 1979. A new intermediate adenovirus type causing conjunctivitis. Archives of Ophthalmology 97:2336-2338.
223. Koopmans M, Wilbrink B, Conyn M, Natrop G, van der Nat H, Vennema H, Meijer A, van Steenbergen J, Fouchier R, Osterhaus A. 2004. Transmission of H7N7 avian influenza A virus to human beings during a large outbreak in commercial poultry farms in the Netherlands. The Lancet 363:587-593.
224. Hall CB, Douglas R, Schnabel KC, Geiman JM. 1981. Infectivity of respiratory syncytial virus by various routes of inoculation. Infection and immunity 33:779-783.
225. Van Der Hoek L, Pyrc K, Jebbink MF, Vermeulen-Oost W, Berkhout RJ, Wolthers KC, Wertheim-van Dillen PM, Kaandorp J, Spaargaren J, Berkhout B. 2004. Identification of a new human coronavirus. Nature medicine 10:368-373.
226. Dreizin R, Vikhnovich E, Borovkova N, Ponomareva T. 1971. The use of indirect fluorescent antibody technique in studies on the reproduction of rhinoviruses and for the detection of rhinoviral antigen in materials from patients with acute respiratory diseases and conjunctivitides. Acta virologica 15:520.
227. Bacherini D, Biagini I, Lenzetti C, Virgili G, Rizzo S, Giansanti F. 2020. The COVID-19 pandemic from an ophthalmologist's perspective. Trends in molecular medicine 26:529-531.
228. Zhou Y, Zeng Y, Tong Y, Chen C. 2020. Ophthalmologic evidence against the interpersonal transmission of 2019 novel coronavirus through conjunctiva. MedRxiv.
229. Lu C-w, Liu X-f, Jia Z-f. 2020. 2019-nCoV transmission through the ocular surface must not be ignored. Lancet (London, England) 395:e39.
230. Wang L, Deng Y. 2020. The need for ocular protection for health care workers during SARS-CoV-2 outbreak and a hypothesis for a potential personal protective equipment. Frontiers in public health 8.
231. UNAIDS, UNAIDS. 2020. Global AIDS Update. https://www.unaids.org/sites/default/files/media_asset/2020_global-aids-report_en.pdf. Accessed March 14 2021.

232. HIV.gov. 2021. Global Statistics: The Global HIV/ AIDS Epidemic. https://www.hiv.gov/hiv-basics/overview/data-and-trends/global-statistics. Accessed March 14 2021.
233. HIV.gov. 2021. U.S. Statistics. https://www.hiv.gov/hiv-basics/overview/data-and-trends/statistics#:~:text=HIV%20incidence%20remained%20stable%20in,among%20all%20other%20age%20groups. Accessed March 14 2021.
234. Boily M-C, Baggaley RF, Wang L, Masse B, White RG, Hayes RJ, Alary M. 2009. Heterosexual risk of HIV-1 infection per sexual act: systematic review and meta-analysis of observational studies. The Lancet infectious diseases 9:118-129.
235. Anton PA, Elliott J, Poles MA, McGowan IM, Matud J, Hultin LE, Grovit-Ferbas K, Mackay CR, Chen IS, Giorgi JV. 2000. Enhanced levels of functional HIV-1 co-receptors on human mucosal T cells demonstrated using intestinal biopsy tissue. Aids 14:1761-1765.
236. Beymer MR, Holloway IW, Pulsipher C, Landovitz RJ. 2019. Current and future PrEP medications and modalities: On-demand, injectables, and topicals. Current hiv/aids Reports 16:349-358.
237. Parikh UM, Dobard C, Sharma S, Cong M-e, Jia H, Martin A, Pau C-P, Hanson DL, Guenthner P, Smith J. 2009. Complete protection from repeated vaginal simian-human immunodeficiency virus exposures in macaques by a topical gel containing tenofovir alone or with emtricitabine. Journal of virology 83:10358-10365.
238. Nel A, Haazen W, Nuttall J, Romano J, Rosenberg Z, van Niekerk N. 2014. A safety and pharmacokinetic trial assessing delivery of dapivirine from a vaginal ring in healthy women. Aids 28:1479-1487.
239. Robinson JA, Marzinke MA, Bakshi RP, Fuchs EJ, Radebaugh CL, Aung W, Spiegel HM, Coleman JS, Rohan LC, Hendrix CW. 2017. Comparison of dapivirine vaginal gel and film formulation pharmacokinetics and pharmacodynamics (FAME 02B). AIDS research and human retroviruses 33:339-346.
240. McCrudden M, Larrañeta E, Jarrahian C, Zehrung D, Rein-Weston A, Donnelly R. 2016. Two-step casting of dissolving MN arrays for use in the sustained release of rilpivirine for HIV pre-exposure prophylaxis. Proc 43rd Annu Meet Controlled Release Soc 174.
241. Gunawardana M, Remedios-Chan M, Miller CS, Fanter R, Yang F, Marzinke MA, Hendrix CW, Beliveau M, Moss JA, Smith TJ. 2015. Pharmacokinetics of long-acting tenofovir alafenamide (GS-7340) subdermal implant for HIV prophylaxis. Antimicrobial agents and chemotherapy 59:3913-3919.
242. Tyo KM, Vuong HR, Malik DA, Sims LB, Alatassi H, Duan J, Watson WH, Steinbach-Rankins JM. 2017. Multipurpose tenofovir disoproxil fumarate electrospun fibers for the prevention of HIV-1 and HSV-2 infections in vitro. International journal of pharmaceutics 531:118-133.
243. Hoang T, Date AA, Ortiz JO, Young T-W, Bensouda S, Xiao P, Marzinke M, Rohan L, Fuchs EJ, Hendrix C. 2019. Development of rectal enema as microbicide (DREAM): Preclinical progressive selection of a tenofovir prodrug enema. European Journal of Pharmaceutics and Biopharmaceutics 138:23-29.

244. Khan AB, Thakur RS. 2018. Design and evaluation of mucoadhesive vaginal tablets of tenofovir disoproxil fumarate for pre-exposure prophylaxis of HIV. Drug development and industrial pharmacy 44:472-483.
245. Cerini F, Offord R, McGowan I, Hartley O. 2017. Stability of 5P12-RANTES, a candidate rectal microbicide, in human rectal lavage. AIDS research and human retroviruses 33:768-777.
246. Brand R. https://clinicaltrials.gov/ct2/show/record/NCT04032717. Accessed 12/08/2020.
247. Girard L, Birse K, Holm JB, Gajer P, Humphrys MS, Garber D, Guenthner P, Noël-Romas L, Abou M, McCorrister S. 2018. Impact of the griffithsin anti-HIV microbicide and placebo gels on the rectal mucosal proteome and microbiome in non-human primates. Scientific reports 8:8059.
248. Hu J, Budgeon LR, Cladel NM, Balogh K, Myers R, Cooper TK, Christensen ND. 2015. Tracking vaginal, anal and oral infection in a mouse papillomavirus infection model. Journal of General Virology 96:3554-3565.
249. Evans D, Pye G, Bramley R, Clark A, Dyson T, Hardcastle J. 1988. Measurement of gastrointestinal pH profiles in normal ambulant human subjects. Gut 29:1035-1041.
250. Carroll IM, Ringel-Kulka T, Ferrier L, Wu MC, Siddle JP, Bueno L, Ringel Y. 2013. Fecal protease activity is associated with compositional alterations in the intestinal microbiota. PLoS One 8:e78017.
251. Buckheit KW, Buckheit RW. 2012. Factors important to the prioritization and development of successful topical microbicides for HIV-1. Molecular biology international 2012.
252. Lukač J, Koren E. 1979. Mechanism of liquefaction of the human ejaculate II. Role of collagenase-like peptidase and seminal proteinase. Reproduction 56:501-506.
253. Holsberger D, Rice C, Thurston R. 2002. Localization of a proteolytic enzyme within the efferent and deferent duct epithelial cells of the turkey (Meleagris gallopavo) using immunohistochemistry. Biology of reproduction 67:276-281.
254. Torjesen K, Marrazzo JM, Hillier SL, Cates Jr W. 2013. Topical Microbicides for Human Immunodeficiency Virus and Sexually Transmitted Disease Prevention, p 213-227, Sexually Transmitted Diseases. Elsevier.
255. Abdool Karim SS, Baxter C, Passmore JAS, McKinnon LR, Williams BL. 2019. The genital tract and rectal microbiomes: their role in HIV susceptibility and prevention in women. Journal of the International AIDS Society 22:e25300.
256. Sui Y, Dzutsev A, Venzon D, Frey B, Thovarai V, Trinchieri G, Berzofsky JA. 2018. Influence of gut microbiome on mucosal immune activation and SHIV viral transmission in naive macaques. Mucosal immunology 11:1219-1229.
257. Rowland I, Gibson G, Heinken A, Scott K, Swann J, Thiele I, Tuohy K. 2018. Gut microbiota functions: metabolism of nutrients and other food components. European journal of nutrition 57:1-24.
258. Eckburg PB, Bik EM, Bernstein CN, Purdom E, Dethlefsen L, Sargent M, Gill SR, Nelson KE, Relman DA. 2005. Diversity of the human intestinal microbial flora. science 308:1635-1638.

259. David LA, Maurice CF, Carmody RN, Gootenberg DB, Button JE, Wolfe BE, Ling AV, Devlin AS, Varma Y, Fischbach MA. 2014. Diet rapidly and reproducibly alters the human gut microbiome. Nature 505:559-563.
260. Ghosh M, Fahey JV, Shen Z, Lahey T, Cu-Uvin S, Wu Z, Mayer K, Wright PF, Kappes JC, Ochsenbauer C. 2010. Anti-HIV activity in cervical-vaginal secretions from HIV-positive and-negative women correlate with innate antimicrobial levels and IgG antibodies. PloS one 5:e11366.
261. Pandya IJ, Cohen J. 1985. The leukocytic reaction of the human uterine cervix to spermatozoa. Fertility and sterility 43:417-421.
262. Thompson L, Barratt C, Bolton A, Cooke I. 1992. The leukocytic reaction of the human uterine cervix. American journal of reproductive immunology 28:85-89.
263. Doncel GF, Joseph T, Thurman AR. 2011. Role of Semen in HIV-1 Transmission: Inhibitor or facilitator? American journal of reproductive immunology 65:292-301.
264. Ludman BG. 1999. Human seminal plasma protein allergy: a diagnosis rarely considered. Journal of Obstetric, Gynecologic & Neonatal Nursing 28:359-363.
265. Lai SK, Hida K, Shukair S, Wang Y-Y, Figueiredo A, Cone R, Hope TJ, Hanes J. 2009. Human immunodeficiency virus type 1 is trapped by acidic but not by neutralized human cervicovaginal mucus. Journal of virology 83:11196-11200.
266. Lai SK, Wang Y-Y, Hida K, Cone R, Hanes J. 2010. Nanoparticles reveal that human cervicovaginal mucus is riddled with pores larger than viruses. Proceedings of the National Academy of Sciences 107:598-603.
267. Lai BE, Geonnotti AR, DeSoto MG, Montefiori DC, Katz DF. 2010. Semi-solid gels function as physical barriers to human immunodeficiency virus transport in vitro. Antiviral research 88:143-151.
268. Harman S, Herrera C, Armanasco N, Nuttall J, Shattock RJ. 2012. Preclinical evaluation of the HIV-1 fusion inhibitor L'644 as a potential candidate microbicide. Antimicrobial agents and chemotherapy 56:2347-2356.
269. Velloza J, Heffron R. 2017. The vaginal microbiome and its potential to impact efficacy of HIV pre-exposure prophylaxis for women. Current Hiv/aids Reports 14:153-160.
270. Kelley CF, Kraft CS, De Man TJ, Duphare C, Lee H-W, Yang J, Easley KA, Tharp GK, Mulligan MJ, Sullivan PS. 2017. The rectal mucosa and condomless receptive anal intercourse in HIV-negative MSM: implications for HIV transmission and prevention. Mucosal immunology 10:996.
271. Spear GT, St John E, Zariffard M. 2007. Bacterial vaginosis and human immunodeficiency virus infection. AIDS Research and Therapy 4:1-5.
272. Price JT, Vwalika B, Hobbs M, Nelson JA, Stringer EM, Zou F, Rittenhouse KJ, Azcarate-Peril A, Kasaro MP, Stringer JS. 2019. Highly diverse anaerobe-predominant vaginal microbiota among HIV-infected pregnant women in Zambia. PloS one 14:e0223128.
273. Anahtar MN, Byrne EH, Doherty KE, Bowman BA, Yamamoto HS, Soumillon M, Padavattan N, Ismail N, Moodley A, Sabatini ME. 2015. Cervicovaginal bacteria are a major modulator of host inflammatory responses in the female genital tract. Immunity 42:965-976.

274. Li D, Chi X-Z, Zhang L, Chen R, Cao J-r, Sun X-y, Yang H-q, Liao Q-p. 2020. Vaginal microbiome analysis of healthy women during different periods of gestation. Bioscience Reports 40.
275. Noel-Romas L, Hoger S, Mccorriser S, Westmacott G, Marrazzo J, Hillier S, Dezzutti C, Squires K, Bunge K, Burgener A. 2020. Influence of dapivirine vaginal ring use on cervicovaginal immunity and functional microbiome in adolescent girls. AIDS (London, England).
276. Kelley CF, Kraft CS, De Man TJ, Duphare C, Lee H-W, Yang J, Easley KA, Tharp GK, Mulligan MJ, Sullivan PS. 2017. The rectal mucosa and condomless receptive anal intercourse in HIV-negative MSM: implications for HIV transmission and prevention. Mucosal immunology 10:996-1007.
277. Ravel J, Gajer P, Fu L, Mauck CK, Koenig SS, Sakamoto J, Motsinger-Reif AA, Doncel GF, Zeichner SL. 2012. Twice-daily application of HIV microbicides alters the vaginal microbiota. MBio 3.
278. Mori T, O'Keefe BR, Sowder RC, Bringans S, Gardella R, Berg S, Cochran P, Turpin JA, Buckheit RW, McMahon JB. 2005. Isolation and characterization of griffithsin, a novel HIV-inactivating protein, from the red alga Griffithsia sp. Journal of Biological Chemistry 280:9345-9353.
279. Fuqua JL, Hamorsky K, Khalsa G, Matoba N, Palmer KE. 2015. Bulk production of the antiviral lectin griffithsin. Plant biotechnology journal 13:1160-1168.
280. Del Rio M, de la Canal L, Pinedo M, Mora-Montes HM, Regente M. 2019. Effects of the binding of a Helianthus annuus lectin to Candida albicans cell wall on biofilm development and adhesion to host cells. Phytomedicine 58:152875.
281. James J, Fiji N, Roy D, MG DA, Shihabudeen MS, Chattopadhyay D, Thirumurugan K. 2015. A rapid method to assess reactive oxygen species in yeast using H 2 DCF-DA. Analytical Methods 7:8572-8575.
282. Strober W. 2015. Trypan blue exclusion test of cell viability. Current protocols in immunology 111:A3. B. 1-A3. B. 3.
283. Rodriguez-Tudela J, Arendrup M, Barchiesi F, Bille J, Chryssanthou E, Cuenca-Estrella M, Dannaoui E, Denning D, Donnelly J, Dromer F. 2008. EUCAST Definitive Document EDef 7.1: method for the determination of broth dilution MICs of antifungal agents for fermentative yeasts: Subcommittee on Antifungal Susceptibility Testing (AFST) of the ESCMID European Committee for Antimicrobial Susceptibility Testing (EUCAST)∗. Clinical microbiology and infection 14:398-405.
284. Sam QH, Chang MW, Chai LYA. 2017. The fungal mycobiome and its interaction with gut bacteria in the host. International journal of molecular sciences 18:330.
285. Garcia-Rubio R, de Oliveira HC, Rivera J, Trevijano-Contador N. 2020. The fungal cell wall: Candida, Cryptococcus, and Aspergillus species. Frontiers in microbiology 10:2993.
286. Free SJ. 2013. Fungal cell wall organization and biosynthesis. Advances in genetics 81:33-82.
287. Chen J-K, Shen C-R, Yeh C-H, Fang B-S, Huang T-L, Liu C-L. 2011. N-acetyl glucosamine obtained from chitin by chitin degrading factors in Chitinbacter tainanesis. International journal of molecular sciences 12:1187-1195.

288. Shibata N, Suzuki A, Kobayashi H, Okawa Y. 2007. Chemical structure of the cell-wall mannan of Candida albicans serotype A and its difference in yeast and hyphal forms. Biochemical Journal 404:365-372.
289. Gibbs J, Kennebunk M. 2001. Immobilization Principles–Selecting the Surface. ELISA technical bulletin 1:1-8.
290. Whaley SG, Berkow EL, Rybak JM, Nishimoto AT, Barker KS, Rogers PD. 2017. Azole antifungal resistance in Candida albicans and emerging non-albicans Candida species. Frontiers in microbiology 7:2173.
291. Tsay S, Welsh RM, Adams EH, Chow NA, Gade L, Berkow EL, Poirot E, Lutterloh E, Quinn M, Chaturvedi S. 2017. Notes from the field: ongoing transmission of Candida auris in health care facilities—United States, June 2016–May 2017. MMWR Morbidity and mortality weekly report 66:514.
292. Mi H, Ebert D, Muruganujan A, Mills C, Albou L-P, Mushayamaha T, Thomas PD. 2021. PANTHER version 16: a revised family classification, tree-based classification tool, enhancer regions and extensive API. Nucleic Acids Research 49:D394-D403.
293. Férir G, Palmer KE, Schols D. 2012. Griffithsin, alone and combined with all classes of antiretroviral drugs, potently inhibits HIV cell-cell transmission and destruction of CD4+ T cells. Journal of Antivirals and Antiretrovirals 4:103-112.
294. Shreiner AB, Kao JY, Young VB. 2015. The gut microbiome in health and in disease. Current opinion in gastroenterology 31:69.
295. Kinross JM, Darzi AW, Nicholson JK. 2011. Gut microbiome-host interactions in health and disease. Genome medicine 3:14.
296. Zarate G, Nader-Macias M. 2006. Influence of probiotic vaginal lactobacilli on in vitro adhesion of urogenital pathogens to vaginal epithelial cells. Letters in Applied Microbiology 43:174-180.
297. Imholz N. 2015. Molecular and functional analyses of lectins in gastrointestinal and vaginal Lactobacillus species.
298. Atassi F, Brassart D, Grob P, Graf F, Servin AL. 2006. Vaginal Lactobacillus isolates inhibit uropathogenic Escherichia coli. FEMS microbiology letters 257:132-138.
299. Iliev ID, Leonardi I. 2017. Fungal dysbiosis: immunity and interactions at mucosal barriers. Nature Reviews Immunology 17:635.
300. Li Q, Wang C, Tang C, He Q, Li N, Li J. 2014. Dysbiosis of gut fungal microbiota is associated with mucosal inflammation in Crohn's disease. Journal of clinical gastroenterology 48:513.
301. Low C-Y, Rotstein C. 2011. Emerging fungal infections in immunocompromised patients. F1000 medicine reports 3.
302. Gomes BS, Siqueira ABS, Maia RdCC, Giampaoli V, Teixeira EH, Arruda FVS, Nascimento KSd, Lima ANd, Souza-Motta CM, Cavada BS. 2012. Antifungal activity of lectins against yeast of vaginal secretion. Brazilian Journal of Microbiology 43:770-778.
303. Cavada BS. 1996. Isolation and partial characterization of a lectin from Dioclea rostrata Benth seeds. R Bras Fisiol Veg 8:31-36.
304. Cavada B, Moreira R, Oliveira Jd, Grangeiro T. 1993. Primary structures and functions of plant lectins. Revista Brasileira de Fisiologia Vegetal 5:193-201.

305. Barbosa T, Arruda S, Cavada B, Grangeiro TB, Freitas LARd, Barral-Netto M. 2001. In vivo lymphocyte activation and apoptosis by lectins of the Diocleinae subtribe. Memórias do Instituto Oswaldo Cruz 96:673-678.
306. De N, Nollin D. 1975. Scanning Electron Microscopy Of Candida Albicans After In Vitro Treatment With Miconazole.
307. Kim SM, Tripathi VP, Shen K-F, Forsburg SL. 2020. Checkpoint regulation of nuclear Tos4 defines S phase arrest in fission yeast. G3: Genes, Genomes, Genetics 10:255-266.
308. Enjalbert B, Nantel A, Whiteway M. 2003. Stress-induced gene expression in Candida albicans: absence of a general stress response. Molecular biology of the cell 14:1460-1467.
309. Van Dijck P, De Rop L, Szlufcik K, Van Ael E, Thevelein JM. 2002. Disruption of the Candida albicans TPS2 gene encoding trehalose-6-phosphate phosphatase decreases infectivity without affecting hypha formation. Infection and Immunity 70:1772-1782.
310. Marichal P, Gorrens J, Coene MC, Jeune LL, Bossche HV. 1995. Origin of differences in susceptibility of Candida krusei to azole antifungal agents: Die Ursache der Empfindlichkeitsunterschiede bei Candida krusei für Azol-Antimykotika. Mycoses 38:111-117.
311. Pfaller Mt, Diekema Dt, Gibbs Dt, Newell V, Nagy E, Dobiasova S, Rinaldi M, Barton R, Veselov A, Group GAS. 2008. Candida krusei, a multidrug-resistant opportunistic fungal pathogen: geographic and temporal trends from the ARTEMIS DISK Antifungal Surveillance Program, 2001 to 2005. Journal of clinical microbiology 46:515-521.
312. Alfouzan W, Dhar R, Albarrag A, Al-Abdely H. 2019. The emerging pathogen Candida auris: A focus on the Middle-Eastern countries. Journal of infection and public health 12:451-459.
313. Lockhart SR, Etienne KA, Vallabhaneni S, Farooqi J, Chowdhary A, Govender NP, Colombo AL, Calvo B, Cuomo CA, Desjardins CA. 2017. Simultaneous emergence of multidrug-resistant Candida auris on 3 continents confirmed by whole-genome sequencing and epidemiological analyses. Clinical Infectious Diseases 64:134-140.
314. Chowdhary A, Kumar VA, Sharma C, Prakash A, Agarwal K, Babu R, Dinesh K, Karim S, Singh S, Hagen F. 2014. Multidrug-resistant endemic clonal strain of Candida auris in India. European journal of clinical microbiology & infectious diseases 33:919-926.
315. Ostrowsky B, Greenko J, Adams E, Quinn M, O'Brien B, Chaturvedi V, Berkow E, Vallabhaneni S, Forsberg K, Chaturvedi S. 2020. Candida auris isolates resistant to three classes of antifungal medications—New York, 2019. Morbidity and Mortality Weekly Report 69:6.
316. Ademe M, Girma F. 2020. Candida auris: From multidrug resistance to pan-resistant strains. Infection and Drug Resistance 13:1287.
317. Shibata N, Kobayashi H, Suzuki S. 2012. Immunochemistry of pathogenic yeast, Candida species, focusing on mannan. Proceedings of the Japan Academy, Series B 88:250-265.

318. Nguyen TNY, Padungros P, Wongsrisupphakul P, Sa-Ard-Iam N, Mahanonda R, Matangkasombut O, Choo M-K, Ritprajak P. 2018. Cell wall mannan of Candida krusei mediates dendritic cell apoptosis and orchestrates Th17 polarization via TLR-2/MyD88-dependent pathway. Scientific reports 8:1-16.
319. Fradin C, Poulain D, Jouault T. 2000. β-1, 2-linked oligomannosides from Candida albicans bind to a 32-kilodalton macrophage membrane protein homologous to the mammalian lectin galectin-3. Infection and immunity 68:4391-4398.
320. Takahashi S, Kudoh A, Okawa Y, Shibata N. 2012. Significant differences in the cell-wall mannans from three Candida glabrata strains correlate with antifungal drug sensitivity. The FEBS journal 279:1844-1856.
321. Kogan G, Pavliak V, Šandula J, Masler L. 1988. Novel structure of the cellular mannan of the pathogenic yeast Candida krusei. Carbohydrate research 184:171-182.
322. Akemi N, Takako S, Yoshimura F. 1982. Immunochemical determinant and serological specificity of Candida krusei. Molecular immunology 19:367-373.
323. Shibata N, Ikuta K, Imai T, Satoh Y, Satoh R, Suzuki A, Kojima C, Kobayashi H, Hisamichi K, Suzuki S. 1995. Existence of Branched Side Chains in the Cell Wall Mannan of Pathogenic Yeast, Candida albicans: Structure-Antigenicity Relationship Between The Cell Wall Mannans Of Candida Albicans And Candida Parapsilosis (∗). Journal of Biological Chemistry 270:1113-1122.
324. Yan L, Xia K, Yu Y, Miliakos A, Chaturvedi S, Zhang F, Chen S, Chaturvedi V, Linhardt RJ. 2020. Unique cell surface mannan of yeast pathogen Candida auris with selective binding to IgG. ACS infectious diseases 6:1018-1031.
325. A Jarvis G, L Chang T. 2012. Modulation of HIV transmission by Neisseria gonorrhoeae: molecular and immunological aspects. Current HIV research 10:211-217.
326. Kilmarx PH, Mock PA, Levine WC. 2001. Effect of Chlamydia trachomatis coinfection on HIV shedding in genital tract secretions. Sexually Transmitted Diseases 28:347-348.
327. Mubaiwa TD, Hartley-Tassell LE, Semchenko EA, Jen FE-C, Srikhanta YN, Day CJ, Jennings MP, Seib KL. 2017. The glycointeractome of serogroup B Neisseria meningitidis strain MC58. Scientific reports 7:1-9.
328. Swanson AF, Ezekowitz RAB, Lee A, Kuo C-c. 1998. Human mannose-binding protein inhibits infection of HeLa cells by Chlamydia trachomatis. Infection and immunity 66:1607-1612.
329. Mazalovska M, Kouokam JC. 2018. Lectins as promising therapeutics for the prevention and treatment of HIV and other potential coinfections. BioMed research international 2018.
330. Allen PZ, Connelly MC, Apicella MA. 1980. Interaction of lectins with Neisseria gonorrhoeae. Canadian journal of microbiology 26:468-474.
331. Amin K, Beillevaire D, Mahmoud E, Hammar L, MARDH PA, FRÖMAN G. 1995. Binding of Galanthus nivalis lectin to Chlamvdia trachomatis and inhibition of in vitro infection. APMIS 103:714-720.
332. Sobel JD. 1985. Epidemiology and pathogenesis of recurrent vulvovaginal candidiasis. American journal of obstetrics and gynecology 152:924-935.

333. Sobel JD. 2007. Vulvovaginal candidosis. The Lancet 369:1961-1971.
334. Denning DW, Kneale M, Sobel JD, Rautemaa-Richardson R. 2018. Global burden of recurrent vulvovaginal candidiasis: a systematic review. The Lancet Infectious Diseases 18:e339-e347.
335. Fidel Jr PL, Barousse M, Espinosa T, Ficarra M, Sturtevant J, Martin DH, Quayle AJ, Dunlap K. 2004. An intravaginal live Candida challenge in humans leads to new hypotheses for the immunopathogenesis of vulvovaginal candidiasis. Infection and immunity 72:2939-2946.
336. Rivers CA, Adaramola OO, Schwebke JR. 2011. Prevalence of bacterial vaginosis and vulvovaginal candidiasis mixed infection in a southeastern american STD clinic. Sexually transmitted diseases 38:672-674.
337. Fischer G, Bradford J. 2011. Vulvovaginal candidiasis in postmenopausal women: the role of hormone replacement therapy. Journal of lower genital tract disease 15:263-267.
338. Qu S, Chen L, Tian H, Wang Z, Wang F, Wang L, Li J, Ji H, Xi L, Feng Z. 2019. Effect of perillaldehyde on prophylaxis and treatment of vaginal candidiasis in a murine model. Frontiers in microbiology 10:1466.
339. Peters BM, Yano J, Noverr MC, Fidel Jr PL. 2014. Candida vaginitis: when opportunism knocks, the host responds. PLoS Pathog 10:e1003965.
340. Toda M, Williams SR, Berkow EL, Farley MM, Harrison LH, Bonner L, Marceaux KM, Hollick R, Zhang AY, Schaffner W. 2019. Population-based active surveillance for culture-confirmed candidemia—four sites, United States, 2012–2016. MMWR Surveillance Summaries 68:1.
341. Alexander BD, Johnson MD, Pfeiffer CD, Jiménez-Ortigosa C, Catania J, Booker R, Castanheira M, Messer SA, Perlin DS, Pfaller MA. 2013. Increasing echinocandin resistance in Candida glabrata: clinical failure correlates with presence of FKS mutations and elevated minimum inhibitory concentrations. Clinical infectious diseases 56:1724-1732.
342. Baddley JW, Patel M, Bhavnani SM, Moser SA, Andes DR. 2008. Association of fluconazole pharmacodynamics with mortality in patients with candidemia. Antimicrobial agents and chemotherapy 52:3022-3028.
343. Sobel J, Zervos M, Reed B, Hooton T, Soper D, Nyirjesy P, Heine M, Willems J, Panzer H. 2003. Fluconazole susceptibility of vaginal isolates obtained from women with complicated Candida vaginitis: clinical implications. Antimicrobial agents and chemotherapy 47:34-38.
344. Pappas PG, Kauffman CA, Andes DR, Clancy CJ, Marr KA, Ostrosky-Zeichner L, Reboli AC, Schuster MG, Vazquez JA, Walsh TJ. 2016. Clinical practice guideline for the management of candidiasis: 2016 update by the Infectious Diseases Society of America. Clinical Infectious Diseases 62:e1-e50.
345. Verweij PE, Chowdhary A, Melchers WJ, Meis JF. 2016. Azole resistance in Aspergillus fumigatus: can we retain the clinical use of mold-active antifungal azoles? Clinical Infectious Diseases 62:362-368.
346. Silva MFdO, Costa LMd. 2012. A indústria de defensivos agrícolas. BNDES Setorial, n 35, mar 2012, p 233–276.

347. Brauer VS, Rezende CP, Pessoni AM, De Paula RG, Rangappa KS, Nayaka SC, Gupta VK, Almeida F. 2019. Antifungal agents in agriculture: Friends and foes of public health. Biomolecules 9:521.
348. Leonardelli F, Macedo D, Dudiuk C, Cabeza MS, Gamarra S, Garcia-Effron G. 2016. Aspergillus fumigatus intrinsic fluconazole resistance is due to the naturally occurring T301I substitution in Cyp51Ap. Antimicrobial agents and chemotherapy 60:5420-5426.
349. Sanguinetti M, Posteraro B, Lass-Flörl C. 2015. Antifungal drug resistance among Candida species: mechanisms and clinical impact. Mycoses 58:2-13.
350. Morio F, Jensen RH, Le Pape P, Arendrup MC. 2017. Molecular basis of antifungal drug resistance in yeasts. International journal of antimicrobial agents 50:599-606.
351. Moyes DL, Naglik JR. 2011. Mucosal immunity and Candida albicans infection. Clinical and Developmental Immunology 2011.
352. Diamond G, Beckloff N, Ryan L. 2008. Host defense peptides in the oral cavity and the lung: similarities and differences. Journal of dental research 87:915-927.
353. Zhang X, Li T, Chen X, Wang S, Liu Z. 2018. Nystatin enhances the immune response against Candida albicans and protects the ultrastructure of the vaginal epithelium in a rat model of vulvovaginal candidiasis. BMC microbiology 18:1-11.
354. Weindl G, Naglik JR, Kaesler S, Biedermann T, Hube B, Korting HC, Schaller M. 2007. Human epithelial cells establish direct antifungal defense through TLR4-mediated signaling. The Journal of clinical investigation 117:3664-3672.
355. De Luca A, Carvalho A, Cunha C, Iannitti RG, Pitzurra L, Giovannini G, Mencacci A, Bartolommei L, Moretti S, Massi-Benedetti C. 2013. IL-22 and IDO1 affect immunity and tolerance to murine and human vaginal candidiasis. PLoS pathogens 9:e1003486.
356. Barousse Mt, Van Der Pol Bt, Fortenberry D, Orr D, Fidel P. 2004. Vaginal yeast colonisation, prevalence of vaginitis, and associated local immunity in adolescents. Sexually transmitted infections 80:48-53.
357. Ouyang W, Chen S, Liu Z, Wu Y, Li J. 2008. Local Th1/Th2 cytokine expression in experimental murine vaginal candidiasis. Journal of Huazhong University of Science and Technology [Medical Sciences] 28:352-355.
358. Conti HR, Gaffen SL. 2015. IL-17–Mediated immunity to the opportunistic fungal pathogen Candida albicans. The Journal of Immunology 195:780-788.
359. Onishi RM, Gaffen SL. 2010. Interleukin-17 and its target genes: mechanisms of interleukin-17 function in disease. Immunology 129:311-321.
360. Sparber F, LeibundGut-Landmann S. 2015. Interleukin 17-mediated host defense against Candida albicans. Pathogens 4:606-619.
361. Goupil M, Cousineau-Côté V, Aumont F, Sénéchal S, Gaboury L, Hanna Z, Jolicoeur P, de Repentigny L. 2014. Defective IL-17-and IL-22-dependent mucosal host response to Candida albicans determines susceptibility to oral candidiasis in mice expressing the HIV-1 transgene. BMC immunology 15:1-13.
362. Hernández-Santos N, Gaffen SL. 2012. Th17 cells in immunity to Candida albicans. Cell host & microbe 11:425-435.

363. Pietrella D, Rachini A, Pines M, Pandey N, Mosci P, Bistoni F, d'Enfert C, Vecchiarelli A. 2011. Th17 cells and IL-17 in protective immunity to vaginal candidiasis. PloS one 6:e22770.
364. Yano J, Kolls JK, Happel KI, Wormley F, Wozniak KL, Fidel Jr PL. 2012. The acute neutrophil response mediated by S100 alarmins during vaginal Candida infections is independent of the Th17-pathway. PloS one 7:e46311.
365. Wang M, Wang F, Yang J, Zhao D, Wang H, Shao F, Wang W, Sun R, Ling M, Zhai J. 2013. Mannan-binding lectin inhibits Candida albicans-induced cellular responses in PMA-activated THP-1 cells through Toll-like receptor 2 and Toll-like receptor 4. PLoS One 8:e83517.
366. Kramzer LF, Hamorsky KT, Graebing PW, Wang L, Fuqua JL, Matoba N, Lasnik AB, Moncla BJ, Zhang J, Palmer KE. 2021. Preformulation characterization of griffithsin, a biopharmaceutical candidate for HIV prevention. AAPS PharmSciTech 22:1-13.
367. Conti HR, Huppler AR, Whibley N, Gaffen SL. 2014. Animal models for candidiasis. Current protocols in immunology 105:19.6. 1-19.6. 17.
368. Nixon B, Stefanidou M, Mesquita PM, Fakioglu E, Segarra T, Rohan L, Halford W, Palmer KE, Herold BC. 2013. Griffithsin protects mice from genital herpes by preventing cell-to-cell spread. Journal of virology 87:6257-6269.
369. Netea MG, Brown GD, Kullberg BJ, Gow NA. 2008. An integrated model of the recognition of Candida albicans by the innate immune system. Nature Reviews Microbiology 6:67-78.
370. Netea MG, Joosten LA, Van Der Meer JW, Kullberg B-J, Van De Veerdonk FL. 2015. Immune defence against Candida fungal infections. Nature Reviews Immunology 15:630-642.
371. Ferwerda B, Ferwerda G, Plantinga TS, Willment JA, van Spriel AB, Venselaar H, Elbers CC, Johnson MD, Cambi A, Huysamen C. 2009. Human dectin-1 deficiency and mucocutaneous fungal infections. New England Journal of Medicine 361:1760-1767.
372. Lev-Sagie A, Nyirjesy P, Tarangelo N, Bongiovanni AM, Bayer C, Linhares IM, Giraldo PC, Ledger WJ, Witkin SS. 2009. Hyaluronan in vaginal secretions: association with recurrent vulvovaginal candidiasis. American journal of obstetrics and gynecology 201:206. e1-206. e5.
373. Korn T, Bettelli E, Oukka M, Kuchroo VK. 2009. IL-17 and Th17 Cells. Annual review of immunology 27:485-517.
374. Chen S, Li S, Wu Y, Liu Z, Li J. 2008. Local expression of vaginal Th1 and Th2 cytokines in murine vaginal candidiasis under different immunity conditions. Journal of Huazhong University of Science and Technology [Medical Sciences] 28:476-479.
375. Carvalho LP, Bacellar O, Neves N, de Jesus AR, Carvalho EM. 2002. Downregulation of IFN-γ production in patients with recurrent vaginal candidiasis. Journal of allergy and clinical immunology 109:102-105.
376. Gozalbo D, Maneu V, Gil ML. 2014. Role of IFN-gamma in immune responses to Candida albicans infections.
377. Yan W, Zhijian T, Zhixiang L, Dechao X, Jiawen L. 2006. Local IL-23 expression in murine vaginal candidiasis and its relationship with infection and

immune status. Journal of Huazhong University of Science and Technology [Medical Sciences] 26:245-247.
378. Naglik JR, Moyes DL, Wächtler B, Hube B. 2011. Candida albicans interactions with epithelial cells and mucosal immunity. Microbes and Infection 13:963-976.
379. Yano J, Lilly E, Barousse M, Fidel Jr PL. 2010. Epithelial cell-derived S100 calcium-binding proteins as key mediators in the hallmark acute neutrophil response during Candida vaginitis. Infection and immunity 78:5126-5137.
380. Fidel Jr PL, Cutright JL, Tait L, Sobel JD. 1996. A murine model of Candida glabrata vaginitis. Journal of Infectious Diseases 173:425-431.
381. Yano J, Noverr MC, Fidel Jr PL. 2012. Cytokines in the host response to Candida vaginitis: Identifying a role for non-classical immune mediators, S100 alarmins. Cytokine 58:118-128.
382. Kouokam JC, Huskens D, Schols D, Johannemann A, Riedell SK, Walter W, Walker JM, Matoba N, O'Keefe BR, Palmer KE. 2011. Investigation of griffithsin's interactions with human cells confirms its outstanding safety and efficacy profile as a microbicide candidate. Plos one 6:e22635.
383. Oesterreicher Z, Eberl S, Zeitlinger M. 2020. Impact of different antimycotics on cytokine levels in an in vitro aspergillosis model in human whole blood. Infection 48:65-73.
384. Zielinski CE, Mele F, Aschenbrenner D, Jarrossay D, Ronchi F, Gattorno M, Monticelli S, Lanzavecchia A, Sallusto F. 2012. Pathogen-induced human TH 17 cells produce IFN-γ or IL-10 and are regulated by IL-1β. Nature 484:514-518.
385. Shalaby M, Aggarwal BB, Rinderknecht E, Svedersky L, Finkle B, Palladino M. 1985. Activation of human polymorphonuclear neutrophil functions by interferon-gamma and tumor necrosis factors. The Journal of Immunology 135:2069-2073.
386. Nathan CF, Murray HW, Wiebe ME, Rubin BY. 1983. Identification of interferon-gamma as the lymphokine that activates human macrophage oxidative metabolism and antimicrobial activity. The Journal of experimental medicine 158:670-689.
387. Eyerich S, Wagener J, Wenzel V, Scarponi C, Pennino D, Albanesi C, Schaller M, Behrendt H, Ring J, Schmidt-Weber CB. 2011. IL-22 and TNF-α represent a key cytokine combination for epidermal integrity during infection with Candida albicans. European journal of immunology 41:1894-1901.
388. Liang SC, Tan X-Y, Luxenberg DP, Karim R, Dunussi-Joannopoulos K, Collins M, Fouser LA. 2006. Interleukin (IL)-22 and IL-17 are coexpressed by Th17 cells and cooperatively enhance expression of antimicrobial peptides. Journal of Experimental Medicine 203:2271-2279.
389. Zelante T, De Luca A, D'Angelo C, Moretti S, Romani L. 2009. IL-17/Th17 in anti-fungal immunity: What's new? European journal of immunology 39:645-648.
390. De Luca A, Zelante T, D'angelo C, Zagarella S, Fallarino F, Spreca A, Iannitti R, Bonifazi P, Renauld J-C, Bistoni F. 2010. IL-22 defines a novel immune pathway of antifungal resistance. Mucosal immunology 3:361-373.
391. Milner JD, Brenchley JM, Laurence A, Freeman AF, Hill BJ, Elias KM, Kanno Y, Spalding C, Elloumi HZ, Paulson ML. 2008. Impaired Th 17 cell differentiation in subjects with autosomal dominant hyper-IgE syndrome. Nature 452:773-776.

392. Yano J, Kolls JK, Happel KI, Wormley F, Wozniak KL, Fidel Jr PL. 2012. The acute neutrophil response mediated by S100 alarmins during vaginal Candida infections is independent of the Th17-pathway.
393. Mencacci A, Perruccio K, Bacci A, Cenci E, Benedetti R, Martelli MF, Bistoni F, Coffman R, Velardi A, Romani L. 2001. Defective antifungal T-helper 1 (TH1) immunity in a murine model of allogeneic T-cell–depleted bone marrow transplantation and its restoration by treatment with TH2 cytokine antagonists. Blood, The Journal of the American Society of Hematology 97:1483-1490.
394. Mencacci A, Del Sero G, Cenci E, d'Ostiani CF, Bacci A, Montagnoli C, Kopf M, Romani L. 1998. Endogenous interleukin 4 is required for development of protective CD4+ T helper type 1 cell responses to Candida albicans. The Journal of experimental medicine 187:307-317.
395. Mencacci A, Cenci E, Del Sero G, d'Ostiani CF, Mosci P, Trinchieri G, Adorini L, Romani L. 1998. IL-10 is required for development of protective Th1 responses in IL-12-deficient mice upon Candida albicans infection. The Journal of Immunology 161:6228-6237.
396. Couper KN, Blount DG, Riley EM. 2008. IL-10: the master regulator of immunity to infection. The Journal of Immunology 180:5771-5777.
397. Steele C, Fidel Jr PL. 2002. Cytokine and chemokine production by human oral and vaginal epithelial cells in response to Candida albicans. Infection and immunity 70:577-583.
398. Kouokam JC, Lasnik AB, Palmer KE. 2016. Studies in a murine model confirm the safety of griffithsin and advocate its further development as a microbicide targeting HIV-1 and other enveloped viruses. Viruses 8:311.
399. Tyo KM, Lasnik AB, Zhang L, Jenson AB, Fuqua JL, Palmer KE, Steinbach-Rankins JM. 2020. Rapid-release griffithsin fibers for dual prevention of HSV-2 and HIV-1 infections. Antimicrobial agents and chemotherapy 64:e02139-19.
400. Wolfel R, Corman VM, Guggemos W, Seilmaier M, Zange S, Muller MA, Niemeyer D, Jones TC, Vollmar P, Rothe C, Hoelscher M, Bleicker T, Brunink S, Schneider J, Ehmann R, Zwirglmaier K, Drosten C, Wendtner C. 2020. Virological assessment of hospitalized patients with COVID-2019. Nature doi:10.1038/s41586-020-2196-x.
401. Chen X, Yu H, Mei T, Chen B, Chen L, Li S, Zhang X, Sun X. 2020. SARS-CoV-2 on the ocular surface: is it truly a novel transmission route? British Journal of Ophthalmology.
402. Bacherini D, Biagini I, Lenzetti C, Virgili G, Rizzo S, Giansanti F. 2020. The COVID-19 pandemic from an ophthalmologist's perspective. Trends in Molecular Medicine.
403. Bahl P, Doolan C, de Silva C, Chughtai AA, Bourouiba L, MacIntyre CR. 2020. Airborne or droplet precautions for health workers treating COVID-19? J Infect Dis doi:10.1093/infdis/jiaa189.
404. van Doremalen N, Bushmaker T, Morris DH, Holbrook MG, Gamble A, Williamson BN, Tamin A, Harcourt JL, Thornburg NJ, Gerber SI, Lloyd-Smith JO, de Wit E, Munster VJ. 2020. Aerosol and Surface Stability of SARS-CoV-2 as Compared with SARS-CoV-1. N Engl J Med 382:1564-1567.

405. O'Keefe BR, Vojdani F, Buffa V, Shattock RJ, Montefiori DC, Bakke J, Mirsalis J, d'Andrea AL, Hume SD, Bratcher B, Saucedo CJ, McMahon JB, Pogue GP, Palmer KE. 2009. Scaleable manufacture of HIV-1 entry inhibitor griffithsin and validation of its safety and efficacy as a topical microbicide component. Proc Natl Acad Sci U S A 106:6099-104.
406. Ziółkowska NE, O'Keefe BR, Mori T, Zhu C, Giomarelli B, Vojdani F, Palmer KE, McMahon JB, Wlodawer A. 2006. Domain-swapped structure of the potent antiviral protein griffithsin and its mode of carbohydrate binding. Structure 14:1127-35.
407. Lusvarghi S, Bewley CA. 2016. Griffithsin: An Antiviral Lectin with Outstanding Therapeutic Potential. Viruses 8.
408. Watanabe Y, Allen JD, Wrapp D, McLellan JS, Crispin M. 2020. Site-specific glycan analysis of the SARS-CoV-2 spike. Science doi:10.1126/science.abb9983.
409. Kawashima K, Matsumoto T, Akashi H. 2016. Disease outbreaks: Critical biological factors and control strategies, p 173-204, Urban Resilience. Springer.
410. Al-Osail AM, Al-Wazzah MJ. 2017. The history and epidemiology of Middle East respiratory syndrome corona virus. Multidisciplinary respiratory medicine 12:1-6.
411. Ramshaw RE, Letourneau ID, Hong AY, Hon J, Morgan JD, Osborne JC, Shirude S, Van Kerkhove MD, Hay SI, Pigott DM. 2019. A database of geopositioned Middle East respiratory syndrome coronavirus occurrences. Scientific data 6:1-13.
412. Alsaidi S, Cornejal N, Mahoney O, Melo C, Verma N, Bonnaire T, Chang T, O'Keefe BR, Sailer J, Zydowsky TM. 2021. Griffithsin and Carrageenan Combination Results in Antiviral Synergy against SARS-CoV-1 and 2 in a Pseudoviral Model. Marine Drugs 19:418.
413. Meuleman P, Albecka A, Belouzard S, Vercauteren K, Verhoye L, Wychowski C, Leroux-Roels G, Palmer KE, Dubuisson J. 2011. Griffithsin has antiviral activity against hepatitis C virus. Antimicrob Agents Chemother 55:5159-67.
414. Mori T, O'Keefe BR, Sowder RC, 2nd, Bringans S, Gardella R, Berg S, Cochran P, Turpin JA, Buckheit RW, Jr., McMahon JB, Boyd MR. 2005. Isolation and characterization of griffithsin, a novel HIV-inactivating protein, from the red alga Griffithsia sp. J Biol Chem 280:9345-53.
415. Nixon B, Stefanidou M, Mesquita PM, Fakioglu E, Segarra T, Rohan L, Halford W, Palmer KE, Herold BC. 2013. Griffithsin protects mice from genital herpes by preventing cell-to-cell spread. J Virol 87:6257-69.
416. Ishag HZ, Li C, Wang F, Mao X. 2016. Griffithsin binds to the glycosylated proteins (E and prM) of Japanese encephalitis virus and inhibit its infection. Virus Res 215:50-4.
417. Ishag HZ, Li C, Huang L, Sun MX, Wang F, Ni B, Malik T, Chen PY, Mao X. 2013. Griffithsin inhibits Japanese encephalitis virus infection in vitro and in vivo. Arch Virol 158:349-58.
418. Li L, Yu X, Zhang H, Cheng H, Hou L, Zheng Q, Hou J. 2019. In vitro antiviral activity of Griffithsin against porcine epidemic diarrhea virus. Virus Genes 55:174-181.
419. Silva-Cayetano A, Foster WS, Innocentin S, Belij-Rammerstorfer S, Spencer AJ, Burton OT, Fra-Bidó S, Le Lee J, Thakur N, Conceicao C. 2021. A booster dose

enhances immunogenicity of the COVID-19 vaccine candidate ChAdOx1 nCoV-19 in aged mice. Med 2:243-262. e8.
420. Mahase E. 2021. Covid-19: Booster dose will be needed in autumn to avoid winter surge, says government adviser. British Medical Journal Publishing Group.
421. Beleche T, Ruhter J, Kolbe A, Marus J, Bush L, Sommers B. 2021. COVID-19 Vaccine Hesitancy: Demographic Factors, Geographic Patterns, and Changes Over Time. Published online 27.
422. Frank S, Brown SM, Capriotti JA, Westover JB, Pelletier JS, Tessema B. 2020. In Vitro Efficacy of a Povidone-Iodine Nasal Antiseptic for Rapid Inactivation of SARS-CoV-2. JAMA Otolaryngology–Head & Neck Surgery 146:1054-1058.
423. Kwon D. 2021. Antibody-laden nasal spray could provide COVID protection—and treatment. Nature Publishing Group.
424. Hoseini-Tavassol Z, Ejtahed H-S, Soroush A-R, Sajjadpour Z, Hasani-Ranjbar S, Larijani B. 2021. Natural Derived Nasal Spray; a Proposed Approach for COVID-19 Disease Control. Infectious Disorders Drug Targets.
425. Tang Y, Liu J, Zhang D, Xu Z, Ji J, Wen C. 2020. Cytokine storm in COVID-19: the current evidence and treatment strategies. Frontiers in immunology 11:1708.
426. Wang M, Cao R, Zhang L, Yang X, Liu J, Xu M, Shi Z, Hu Z, Zhong W, Xiao G. 2020. Remdesivir and chloroquine effectively inhibit the recently emerged novel coronavirus (2019-nCoV) in vitro. Cell research 30:269-271.
427. Upadhyay S, Parikh A, Joshi P, Upadhyay U, Chotai N. 2011. Intranasal drug delivery system-A glimpse to become maestro. Journal of applied pharmaceutical science 1:34-44.
428. Chhajed S, Sangale S, Barhate S. 2011. Advantageous nasal drug delivery system: a review. International Journal of Pharmaceutical Sciences and Research 2:1322.
429. Misra A, Kher G. 2012. Drug delivery systems from nose to brain. Current pharmaceutical biotechnology 13:2355-2379.
430. Illum L. 2003. Nasal drug delivery—possibilities, problems and solutions. Journal of controlled release 87:187-198.
431. Pires A, Fortuna A, Alves G, Falcão A. 2009. Intranasal drug delivery: how, why and what for? Journal of pharmacy & pharmaceutical sciences 12:288-311.
432. Chen J, Zhang C, Liu Q, Shao X, Feng C, Shen Y, Zhang Q, Jiang X. 2012. Solanum tuberosum lectin-conjugated PLGA nanoparticles for nose-to-brain delivery: in vivo and in vitro evaluations. Journal of drug targeting 20:174-184.
433. Gao X. 2007. Lectin-conjugated nanoparticles for drugs delivery into brain following intranasal administrationShanghai: Univ Fudan.
434. Graf C, Bernkop-Schnürch A, Egyed A, Koller C, Prieschl-Grassauer E, Morokutti-Kurz M. 2018. Development of a nasal spray containing xylometazoline hydrochloride and iota-carrageenan for the symptomatic relief of nasal congestion caused by rhinitis and sinusitis. International journal of general medicine 11:275.
435. Tyrrell D. 1986. The efficacy and tolerance of intranasal interferons: studies at the Common Cold Unit. Journal of Antimicrobial Chemotherapy 18:153-156.
436. Eccles R, Meier C, Jawad M, Weinmüllner R, Grassauer A, Prieschl-Grassauer E. 2010. Efficacy and safety of an antiviral Iota-Carrageenan nasal spray: a

randomized, double-blind, placebo-controlled exploratory study in volunteers with early symptoms of the common cold. Respiratory research 11:108.
437. Channappanavar R, Zhao J, Perlman S. 2014. T cell-mediated immune response to respiratory coronaviruses. Immunologic research 59:118-128.
438. Dandekar AA, Perlman S. 2005. Immunopathogenesis of coronavirus infections: implications for SARS. Nature reviews immunology 5:917-927.
439. Touch SM, Spitzer AR. 1999. Palivizumab, a humanized respiratory syncytial virus monoclonal antibody, reduces hospitalization from respiratory syncytial virus infection in high-risk infants. Clinical Pediatrics 38:556.
440. Ramisse F, Deramoudt F-X, Szatanik M, Bianchi A, Binder P, Hannoun C, Alonso J-M. 1998. Effective prophylaxis of influenza A virus pneumonia in mice by topical passive immunotherapy with polyvalent human immunoglobulins or F (ab′) 2 fragments. Clinical and experimental immunology 111:583.
441. Bansal G, Hatfield J, Young J, Top F, Prince G, Horswood R, Hemming V, Hensen S. 1991. Efficacy of passively administered monoclonal antibodies against respiratory syncytial virus infection in cotton rats. Vaccines 91:283-288.
442. O'Keefe BR, Giomarelli B, Barnard DL, Shenoy SR, Chan PK, McMahon JB, Palmer KE, Barnett BW, Meyerholz DK, Wohlford-Lenane CL, McCray PB, Jr. 2010. Broad-spectrum in vitro activity and in vivo efficacy of the antiviral protein griffithsin against emerging viruses of the family Coronaviridae. J Virol 84:2511-21.
443. Lo MK, Spengler JR, Krumpe LRH, Welch SR, Chattopadhyay A, Harmon JR, Coleman-McCray JD, Scholte FEM, Hotard AL, Fuqua JL, Rose JK, Nichol ST, Palmer KE, O'Keefe BR, Spiropoulou CF. 2020. Griffithsin Inhibits Nipah Virus Entry and Fusion and Can Protect Syrian Golden Hamsters From Lethal Nipah Virus Challenge. J Infect Dis doi:10.1093/infdis/jiz630.
444. Doty RL, Marcus A, William Lee W. 1996. Development of the 12-item cross-cultural smell identification test (CC-SIT). The Laryngoscope 106:353-356.
445. Doty RL. 2007. Office procedures for quantitative assessment of olfactory function. Am J Rhinol 21:460-73.
446. Ware Jr JE, Kosinski M, Keller SD. 1996. A 12-Item Short-Form Health Survey: construction of scales and preliminary tests of reliability and validity. Medical care:220-233.
447. Crawford B, Stanford RH, Wong AY, Dalal AA, Bayliss MS. 2011. Psychometric validation of the experience with allergic rhinitis nasal spray questionnaire. Patient related outcome measures 2:127.
448. Harris PA, Taylor R, Thielke R, Payne J, Gonzalez N, Conde JG. 2009. A metadata-driven methodology and workflow process for providing translational research informatics support. J Biomed Inform 42:377-81.
449. Al-Osail AM, Al-Wazzah MJ. 2017. The history and epidemiology of Middle East respiratory syndrome corona virus. Multidisciplinary respiratory medicine 12:20.
450. Geller C, Varbanov M, Duval RE. 2012. Human coronaviruses: insights into environmental resistance and its influence on the development of new antiseptic strategies. Viruses 4:3044-3068.

451. Docea AO, Tsatsakis A, Albulescu D, Cristea O, Zlatian O, Vinceti M, Moschos SA, Tsoukalas D, Goumenou M, Drakoulis N. 2020. A new threat from an old enemy: Re-emergence of coronavirus. International journal of molecular medicine 45:1631-1643.
452. Lurie N, Saville M, Hatchett R, Halton J. 2020. Developing Covid-19 vaccines at pandemic speed. New England Journal of Medicine.
453. Beigel JH, Tomashek KM, Dodd LE, Mehta AK, Zingman BS, Kalil AC, Hohmann E, Chu HY, Luetkemeyer A, Kline S. 2020. Remdesivir for the treatment of Covid-19. New England Journal of Medicine.
454. FDA. 2021. COVID-19 Vaccines. https://www.fda.gov/emergency-preparedness-and-response/coronavirus-disease-2019-covid-19/covid-19-vaccines. Accessed
455. Huang E, Jordan SC. 2020. Tocilizumab for Covid-19—The Ongoing Search for Effective Therapies. Mass Medical Soc.
456. Lundgren JD, Grund B, Barkauskas CE, Holland TL, Gottlieb RL, Sandkovsky U, Brown SM, Knowlton KU, Self WH, Files DC. 2020. A Neutralizing Monoclonal Antibody for Hospitalized Patients with Covid-19. The New England journal of medicine.
457. Castrucci MR. 2018. Factors affecting immune responses to the influenza vaccine. Hum Vaccin Immunother 14:637-646.
458. Bergwerk M, Gonen T, Lustig Y, Amit S, Lipsitch M, Cohen C, Mandelboim M, Gal Levin E, Rubin C, Indenbaum V. 2021. Covid-19 Breakthrough Infections in Vaccinated Health Care Workers. New England Journal of Medicine.
459. Moore JP, Offit PA. 2021. SARS-CoV-2 vaccines and the growing threat of viral variants. Jama 325:821-822.
460. Rennie P, Bowtell P, Hull D, Charbonneau D, Lambkin-Williams R, Oxford J. 2007. Low pH gel intranasal sprays inactivate influenza viruses in vitro and protect ferrets against influenza infection.
461. Weltzin R, Monath TP. 1999. Intranasal antibody prophylaxis for protection against viral disease. Clinical microbiology reviews 12:383-393.
462. Ramalingam S, Graham C, Dove J, Morrice L, Sheikh A. 2019. A pilot, open labelled, randomised controlled trial of hypertonic saline nasal irrigation and gargling for the common cold. Scientific reports 9:1-11.
463. Hayden FG, Turner RB, Gwaltney JM, Chi-Burris K, Gersten M, Hsyu P, Patick AK, Smith GJ, Zalman LS. 2003. Phase II, randomized, double-blind, placebo-controlled studies of ruprintrivir nasal spray 2-percent suspension for prevention and treatment of experimentally induced rhinovirus colds in healthy volunteers. Antimicrobial agents and chemotherapy 47:3907-3916.
464. Wohlford-Lenane C, Giomarelli B, McMahon J, O'Keefe B, Meyerholz D, McCray P. 2009. Protective Role of Griffithsin in Severe Acute Respiratory Syndrome Pulmonary Infection, p A5954, D46 Treatment Of Respiratory Infections. American Thoracic Society.
465. Jannin V, Lemagnen G, Gueroult P, Larrouture D, Tuleu C. 2014. Rectal route in the 21st Century to treat children. Advanced drug delivery reviews 73:34-49.
466. Hua S. 2019. Physiological and pharmaceutical considerations for rectal drug formulations. Frontiers in pharmacology 10:1196.

467. De Boer A, De Leede L, Breimer D. 1984. Drug absorption by sublingual and rectal routes. British journal of anaesthesia 56:69-82.
468. Gabor F, Schwarzbauer A, Wirth M. 2002. Lectin-mediated drug delivery: binding and uptake of BSA-WGA conjugates using the Caco-2 model. International journal of pharmaceutics 237:227-239.
469. Estrada-Martínez LE, Moreno-Celis U, Cervantes-Jimenez R, Ferriz-Martínez RA, Blanco-Labra A, Garcia-Gasca T. 2017. Plant lectins as medical tools against digestive system cancers. International journal of molecular sciences 18:1403.
470. Bies C, Lehr C-M, Woodley JF. 2004. Lectin-mediated drug targeting: history and applications. Advanced drug delivery reviews 56:425-435.
471. Chandrasekaran G, Lee Y-C, Park H, Wu Y, Shin H-J. 2016. Antibacterial and antifungal activities of lectin extracted from fruiting bodies of the Korean cauliflower medicinal mushroom, Sparassis latifolia (Agaricomycetes). International journal of medicinal mushrooms 18.
472. Hasan I, Ozeki Y, Kabir SR. 2014. Purification of a novel chitin-binding lectin with antimicrobial and antibiofilm activities from a Bangladeshi cultivar of potato (Solanum tuberosum).
473. Breitenbach Barroso Coelho L, Marcelino dos Santos Silva P, Felix de Oliveira W, De Moura M, Viana Pontual E, Soares Gomes F, Guedes Paiva P, Napoleão T, dos Santos Correia M. 2018. Lectins as antimicrobial agents. Journal of applied microbiology 125:1238-1252.
474. Kagiampakis I, Gharibi A, Mankowski MK, Snyder BA, Ptak RG, Alatas K, LiWang PJ. 2011. Potent strategy to inhibit HIV-1 by binding both gp120 and gp41. Antimicrobial agents and chemotherapy 55:264-275.
475. Férir G, Huskens D, Palmer KE, Boudreaux DM, Swanson MD, Markovitz DM, Balzarini J, Schols D. 2012. Combinations of griffithsin with other carbohydrate-binding agents demonstrate superior activity against HIV type 1, HIV type 2, and selected carbohydrate-binding agent-resistant HIV type 1 strains. AIDS research and human retroviruses 28:1513-1523.
476. Alexandre KB, Gray ES, Pantophlet R, Moore PL, McMahon JB, Chakauya E, O'Keefe BR, Chikwamba R, Morris L. 2011. Binding of the mannose-specific lectin, griffithsin, to HIV-1 gp120 exposes the CD4-binding site. Journal of virology 85:9039-9050.
477. Alexandre KB, Gray ES, Lambson BE, Moore PL, Choge IA, Mlisana K, Karim SSA, McMahon J, O'Keefe B, Chikwamba R. 2010. Mannose-rich glycosylation patterns on HIV-1 subtype C gp120 and sensitivity to the lectins, Griffithsin, Cyanovirin-N and Scytovirin. Virology 402:187-196.
478. Chertova E, Bess Jr JW, Crise BJ, Sowder RC, Schaden TM, Hilburn JM, Hoxie JA, Benveniste RE, Lifson JD, Henderson LE. 2002. Envelope glycoprotein incorporation, not shedding of surface envelope glycoprotein (gp120/SU), is the primary determinant of SU content of purified human immunodeficiency virus type 1 and simian immunodeficiency virus. Journal of virology 76:5315-5325.
479. Zhu P, Chertova E, Bess J, Lifson JD, Arthur LO, Liu J, Taylor KA, Roux KH. 2003. Electron tomography analysis of envelope glycoprotein trimers on HIV and simian immunodeficiency virus virions. Proceedings of the National Academy of Sciences 100:15812-15817.

480. Ota T, Doyle-Cooper C, Cooper AB, Huber M, Falkowska E, Doores KJ, Hangartner L, Le K, Sok D, Jardine J. 2012. Anti-HIV B Cell lines as candidate vaccine biosensors. The Journal of Immunology 189:4816-4824.
481. Schiller J, Chackerian B. 2014. Why HIV virions have low numbers of envelope spikes: implications for vaccine development. PLoS pathogens 10:e1004254.
482. Klein JS, Bjorkman PJ. 2010. Few and far between: how HIV may be evading antibody avidity. PLoS pathogens 6:e1000908.
483. Hu B, Du T, Li C, Luo S, Liu Y, Huang X, Hu Q. 2015. Sensitivity of transmitted and founder human immunodeficiency virus type 1 envelopes to carbohydrate-binding agents griffithsin, cyanovirin-N and Galanthus nivalis agglutinin. Journal of General Virology 96:3660-3666.
484. Huang X, Jin W, Griffin GE, Shattock RJ, Hu Q. 2011. Removal of two high-mannose N-linked glycans on gp120 renders human immunodeficiency virus 1 largely resistant to the carbohydrate-binding agent griffithsin. Journal of general virology 92:2367-2373.
485. Alexandre KB, Moore PL, Nonyane M, Gray ES, Ranchobe N, Chakauya E, McMahon JB, O'Keefe BR, Chikwamba R, Morris L. 2013. Mechanisms of HIV-1 subtype C resistance to GRFT, CV-N and SVN. Virology 446:66-76.
486. Ostrosky-Zeichner L, Casadevall A, Galgiani JN, Odds FC, Rex JH. 2010. An insight into the antifungal pipeline: selected new molecules and beyond. Nature reviews Drug discovery 9:719-727.
487. Xiao L, Madison V, Chau AS, Loebenberg D, Palermo RE, McNicholas PM. 2004. Three-dimensional models of wild-type and mutated forms of cytochrome P450 14α-sterol demethylases from Aspergillus fumigatus and Candida albicans provide insights into posaconazole binding. Antimicrobial agents and chemotherapy 48:568-574.
488. Belenky P, Camacho D, Collins JJ. 2013. Fungicidal drugs induce a common oxidative-damage cellular death pathway. Cell reports 3:350-358.
489. Zhao RZ, Jiang S, Zhang L, Yu ZB. 2019. Mitochondrial electron transport chain, ROS generation and uncoupling. International journal of molecular medicine 44:3-15.
490. Gasch AP, Spellman PT, Kao CM, Carmel-Harel O, Eisen MB, Storz G, Botstein D, Brown PO. 2000. Genomic expression programs in the response of yeast cells to environmental changes. Molecular biology of the cell 11:4241-4257.
491. Soufi B, Kelstrup CD, Stoehr G, Fröhlich F, Walther TC, Olsen JV. 2009. Global analysis of the yeast osmotic stress response by quantitative proteomics. Molecular bioSystems 5:1337-1346.
492. Osório H, Moradas-Ferreira P, Sillero MAG, Sillero A. 2004. In Saccharomyces cerevisiae, the effect of H 2 O 2 on ATP, but not on glyceraldehyde-3-phosphate dehydrogenase, depends on the glucose concentration. Archives of microbiology 181:231-236.
493. Dwyer DJ, Kohanski MA, Hayete B, Collins JJ. 2007. Gyrase inhibitors induce an oxidative damage cellular death pathway in Escherichia coli. Molecular systems biology 3:91.

494. Foti JJ, Devadoss B, Winkler JA, Collins JJ, Walker GC. 2012. Oxidation of the guanine nucleotide pool underlies cell death by bactericidal antibiotics. Science 336:315-319.
495. Dias LP, Santos AL, Araújo NM, Silva RR, Santos MH, Roma RR, Rocha BA, Oliveira JT, Teixeira CS. 2020. Machaerium acutifolium lectin alters membrane structure and induces ROS production in Candida parapsilosis. International Journal of Biological Macromolecules 163:19-25.
496. Regente M, Taveira GB, Pinedo M, Elizalde MM, Ticchi AJ, Diz MS, Carvalho AO, de la Canal L, Gomes VM. 2014. A sunflower lectin with antifungal properties and putative medical mycology applications. Current microbiology 69:88-95.
497. Wilson D, Hebecker B, Moyes DL, Miramón P, Jablonowski N, Wisgott S, Allert S, Naglik JR, Hube B. 2013. Clotrimazole dampens vaginal inflammation and neutrophil infiltration in response to Candida albicans infection. Antimicrobial agents and chemotherapy 57:5178-5180.
498. Thapa D, Lee JS, Park S-Y, Bae Y-H, Bae S-K, Kwon JB, Kim K-J, Kwak M-K, Park Y-J, Choi HG. 2008. Clotrimazole ameliorates intestinal inflammation and abnormal angiogenesis by inhibiting interleukin-8 expression through a nuclear factor-κB-dependent manner. Journal of Pharmacology and Experimental Therapeutics 327:353-364.
499. Rosenberg AS, Sauna ZE. 2018. Immunogenicity assessment during the development of protein therapeutics. Journal of Pharmacy and Pharmacology 70:584-594.
500. Pratt KP. 2018. Anti-drug antibodies: emerging approaches to predict, reduce or reverse biotherapeutic immunogenicity. Antibodies 7:19.
501. Zhu A, Hurst R. 2002. Anti-N-glycolylneuraminic acid antibodies identified in healthy human serum. Xenotransplantation 9:376-381.
502. Basnet NB, Ide K, Tahara H, Tanaka Y, Ohdan H. 2010. Deficiency of N-glycolylneuraminic acid and Galα1-3Galβ1-4GlcNAc epitopes in xenogeneic cells attenuates cytotoxicity of human natural antibodies. Xenotransplantation 17:440-448.
503. Ponce R, Abad L, Amaravadi L, Gelzleichter T, Gore E, Green J, Gupta S, Herzyk D, Hurst C, Ivens IA. 2009. Immunogenicity of biologically-derived therapeutics: assessment and interpretation of nonclinical safety studies. Regulatory Toxicology and Pharmacology 54:164-182.
504. Ettinger RA, Liberman JA, Gunasekera D, Puranik K, James EA, Thompson AR, Pratt KP. 2018. FVIII proteins with a modified immunodominant T-cell epitope exhibit reduced immunogenicity and normal FVIII activity. Blood advances 2:309-322.
505. Benson-Mitchell R, Tolley N, Croft C, Gallimore A. 1994. Aspergillosis of the larynx. The Journal of Laryngology & Otology 108:883-885.
506. Myoken Y, Sugata T, Kyo T-I, Fujihara M. 1996. Pathologic features of invasive oral aspergillosis in patients with hematologic malignancies. Journal of oral and maxillofacial surgery 54:263-270.

507. Auluck A. 2007. Maxillary necrosis by mucormycosis: A case report and literature review. Medicina Oral, Patología Oral y Cirugía Bucal (Internet) 12:360-364.
508. Kiggundu R, Nabeta HW, Okia R, Rhein J, Lukande R. 2016. Unmasking histoplasmosis immune reconstitution inflammatory syndrome in a patient recently started on antiretroviral therapy. Autopsy & case reports 6:27.
509. Fontaine T, Simenel C, Dubreucq G, Adam O, Delepierre M, Lemoine J, Vorgias CE, Diaquin M, Latgé J-P. 2000. Molecular organization of the alkali-insoluble fraction ofAspergillus fumigatus cell wall. Journal of Biological Chemistry 275:27594-27607.
510. Wang ZA, Li LX, Doering TL. 2018. Unraveling synthesis of the cryptococcal cell wall and capsule. Glycobiology 28:719-730.
511. Bartnicki-Garcia S, Reyes E. 1964. Chemistry of spore wall differentiation in Mucor rouxii. Archives of biochemistry and biophysics 108:125-133.
512. Lange K, Buerger M, Stallmach A, Bruns T. 2016. Effects of antibiotics on gut microbiota. Digestive Diseases 34:260-268.
513. Palleja A, Mikkelsen KH, Forslund SK, Kashani A, Allin KH, Nielsen T, Hansen TH, Liang S, Feng Q, Zhang C. 2018. Recovery of gut microbiota of healthy adults following antibiotic exposure. Nature microbiology 3:1255-1265.
514. Seelig MS. 1966. Mechanisms by which antibiotics increase the incidence and severity of candidiasis and alter the immunological defenses. Bacteriological reviews 30:442-459.
515. Pappas PG, Rex JH, Sobel JD, Filler SG, Dismukes WE, Walsh TJ, Edwards JE. 2004. Guidelines for treatment of candidiasis. Clinical infectious diseases 38:161-189.
516. Belser JA, Gustin KM, Maines TR, Pantin-Jackwood MJ, Katz JM, Tumpey TM. 2012. Influenza virus respiratory infection and transmission following ocular inoculation in ferrets. PLoS Pathog 8:e1002569.
517. Belser JA, Rota PA, Tumpey TM. 2013. Ocular tropism of respiratory viruses. Microbiology and Molecular Biology Reviews 77:144-156.
518. Zhang X, Chen X, Chen L, Deng C, Zou X, Liu W, Yu H, Chen B, Sun X. 2020. The evidence of SARS-CoV-2 infection on ocular surface. Elsevier.

CURRICULUM VITAE

Henry Nabeta MBChB, MSc, MS, PhD.

CONTACT INFORMATION

Home address: 2803 Brookdale Avenue, Louisville, KY 40220

Work address: Lab of Kenneth E. Palmer Ph.D., 505 South Hancock Street, KCCTRB #442F, Louisville, KY 40202

Cell phone: 502-604-8663

E-mail: henry.nabeta@louisville.edu, hwnabeta@gmail.com

EDUCATION AND TRAINING

INSTITUTION AND LOCATION	DEGREE	MM / YY	FIELD OF STUDY
Makerere University, Uganda	MBChB	06/2008	Medicine and Surgery
Makerere University, Uganda	MSc	11/2014	Physiology
University of Louisville, Kentucky	MS	12/2018	Microbiology and Immunology
University of Louisville, Kentucky	PhD	09/2021	Microbiology and Immunology

ACADEMIC EXPERIENCE

2018-2021: Student Instructor, Department of Microbiology and Immunology, University of Louisville.

2012-2016: Assistant Lecturer, Department of Physiology, School of Biomedical Sciences, College of Health Sciences, Makerere University, Uganda.

2009-2012: Teaching Assistant, Department of Physiology, School of Biomedical Sciences, College of Health Sciences, Makerere University, Uganda.

ADDITIONAL TRAININGS COMPLETED

8/2018: Implementation Science Mini Course for HIV/ STIs, University of Washington, Seattle, Washington USA.

7/2018: 26th Annual Principles of STD/ HIV Research Course, University of Washington, Seattle, Washington, USA.

5/2018: Instructional Strategies in Science Education, University of Louisville, Louisville, Kentucky, USA.

5/2013: Global Health Course, in-person training; Clinical Tropical Medicine and Travelers' Health, University of Minnesota, Minneapolis, Minnesota, USA.

5/2012: Certificate in Good Clinical Practice at the Infectious Disease Institute, Kampala, Uganda.

9/2011: Advanced HIV Course, Aix en Provence, France.

9/2009: Protecting Human Research Participants; Web-based training course.

1/2009: Pediatric HIV/ AIDS for the Health Professional. Baylor International Pediatric AIDS Initiative/ Centers for Disease Control and Prevention. Kampala, Uganda.

6/2008: Communicating and counselling children living with or affected by HIV/ AIDS. Mildmay International, Kampala, Uganda.

6/2008: Comprehensive HIV/ AIDS Care. Mulago-Mbarara Teaching Hospitals' Joint AIDS Program, Kampala, Uganda.

2/2005: Effective Co-counselling. Faculty of Medicine, Makerere University, Kampala, Uganda.

2/2005: ART and latest developments in HIV/ AIDS Care. Makerere University, Kampala, Uganda.

AWARDS AND PROFESSIONAL HONORS

3/2020: Microbiology Society. Bursary to present poster at *Candida* and Candidiasis 2021 meeting, Montreal, Canada. March 2021. *Virtual meeting*.

11/2017: New Investigator Award to present poster at The Conference on Retroviruses and Opportunistic Infections (CROI) 2018, Boston MA, March 2018.

8/2016: Fulbright Scholarship Award to pursue doctoral studies at the University of Louisville, KY.

5/2014: Investigator award to attend the International Conference on Cryptococcus and Cryptococcosis, Amsterdam, The Netherlands.

10/2012: The International Investigator Award to attend Infectious Diseases Society of America (IDSA) Conference, San Diego, CA, USA.

9/2011: European AIDS Clinical Society, Scholarship to attend Advanced HIV Course, Aix en Provence, France.

8/2003: Government of Uganda Scholarship Award to study Bachelor of Medicine and Bachelor of Surgery at Makerere University, Kampala.

PROFESSIONAL MEMBERSHIPS AND ACTIVITIES

11/2019: Member, American Association for the Advancement of Science

4/2012: Member, Infectious Diseases Society of America

7/2008: Member, Uganda Medical & Dental Practitioners Council

6/2005: Member and student coordinator, Action Group for Health, Human Rights and HIV/ AIDS - Uganda

COURSES TAUGHT

- MBIO 610 Research Methods in Microbiology and Immunology at the University of Louisville, Ky.
- HMN1102 and HMN1202 Human Physiology for Bachelor of Human Nutrition students (taught and coordinated the Program) at Makerere University, Uganda.
- Physiology of body systems for Year I and II undergraduate and PGY1 postgraduate students at the School of Biomedical Sciences, Makerere University, Uganda.

SUPERVISION AND MENTORSHIP

- Peer-mentor at University of Louisville Department of Microbiology and Immunology graduate program.
- Clinical research mentor and supervisor for University of Minnesota medical students attached to the Infectious Diseases Institute, College of Health Sciences, Kampala, Uganda for their placement as part of the Global Health Pathway rotation. These included Emily Evans, Sruthi Velamakanni, Nathan Yueh, Wendy Fujita, Elissa Butler, Mahsa Abassi, and Maximilian von Hohenberg), 2010-2016.
- Research mentor and supervisor for at least 12 students annually at the College of Health Sciences, Makerere University in community-based education and research activities.

RESEARCH INTERESTS

- HIV/ AIDS-related opportunistic infections
- Vaccines development
- Tropical medicine
- Immunology of Infectious diseases

CLINICAL RESEARCH EXPERIENCE

2013-2016: Research Medical Officer. Study Title: Adjunctive Sertraline for the Treatment of HIV- Associated Cryptococcal meningitis. Clinical Trials.gov Reg Number: NCT01802385 Grand Challenges Canada Grant Number: S4 0296-01 David Meya, David Boulware (PI).

2012-2015: Study Medical Officer. Title: Operational Research for Cryptococcal Antigen screening. Trial No. U01 GH11005. Funded by CDC. PI Dr David Meya. Co-Investigators from University of Minnesota; Dr David Boulware, Dr Radha Rajasingham

2011-2013: PI. Title: Accuracy of non-invasive intraocular pressure or optic nerve sheath diameter measurement for prediction of elevated intracranial pressure in meningitis and cryptococcosis; Sub-study under the NIH NIAID U01 AI089244-0, Optimal ART timing trial. I developed the protocol that was funded under the main study grant.

2011-2013: PI. Title: Vitamin D status of children admitted with malnutrition in Mulago National Referral Hospital, Uganda.

2010-2015: Study Medical Officer. NIH NIAID U01 AI089244-01 Boulware (PI). Title: Trial for the Optimal Timing of HIV Therapy after Cryptococcal Meningitis. Implementation of a multisite, international randomized clinical trial in Africa to determine when to start HIV therapy after cryptococcal meningitis in order to maximize survival. Investigation of HIV IRIS and IRIS epidemiology was a secondary objective.

2010-2014: Study Coordinator and Medical officer. National Institutes of neurological disorders and stroke. Grant No. 1R21NS065713-01A1. Title: Neurology outcomes on Antiretroviral therapy: Impact of HIV and HIV therapy on the etiology and outcome of meningitis in Uganda. Investigators: Paul R Bohjanen, David R Boulware, Adam F Carpenter (University of Minnesota), David B Meya, Noeline Nakasujja (Makerere University, Kampala).

2008-2009: Intern Doctor and Research Assistant for one of the Internal Medicine residents. Title: The prevalence of hypercalcaemia in breast cancer patients in Mulago Hospital.

OTHER CLINICAL EXPERIENCE

5/2013: Observerships at Hennepin County Medical Centre, MN, USA, shadowing Stephen Dunlop MD. in the ER; Fairview Hospital & Delaware clinic, University of Minnesota; Shadowing Paul Bohjanen MD and at Abbott-Northwestern Hospital, Minneapolis and The Uptown ID Clinic, shadowing Frank Rhame MD.

10/2012: Observership at Hennepin County Medical Centre, MN, USA, shadowing Stephen Dunlop MD in the ER and at Fairview & Delaware clinic, University of Minnesota, Shadowing Paul Bohjanen MD.

2009-2011: Medical Officer, Uganda Heart Institute, Mulago Hospital, Kampala, Uganda.

2009-2010: Locum Medical Officer, Infectious Diseases Institute, Prevention, Care & Treatment Department, Kampala, Uganda.

2008-2009: Intern Doctor at Mulago National Referral Hospital, Kampala, Uganda.

RELEVANT CLINICAL SKILLS/ PROCEDURES GAINED

Performed over 3000 lumbar puncture procedures, inserted chest tubes and drainages, cardiocentesis, minor and major surgical procedures, delivered mothers both vaginally and performed caesarean sections among others.

RELEVANT LABORATORY SKILLS

Performed ELISA assays, cell cultures growth, RNA, DNA and protein extraction, electrophoresis, Flow cytometry analyses, PCR analysis, animal handling and experimental procedures, among others.

ORAL PRESENTATIONS

3/2014: Invited speaker, Case presentation at the Clinical Master Class, International Conference on Cryptococcus and Cryptococcosis (ICCC), Amsterdam, The Netherlands.

POSTER PRESENTATIONS

3/2021: Microbiology Society. *Candida* and Candidiasis 2021 meeting in Montreal, Canada. *Virtual meeting held March 21-27, 2021.* Title: Novel antifungal activity of Griffithsin-M78Q, a broad-spectrum antiviral lectin.

3/2018: Conference on Retroviruses and Opportunistic Infections (CROI), Boston, MA, 2018: Title: Activity of Griffithsin-M78Q, an HIV-entry Inhibitor, in the Rectal Environment.

8/2017: Research Louisville. Title: Activity and stability of Griffithsin-M78Q- an HIV entry inhibitor microbicide in the rectal environment.

5/2014: International Conference on Cryptococcus and Cryptococcosis (ICCC), Amsterdam, The Netherlands. Title: Non-invasive assessment of Intracranial pressure in cryptococcal meningitis using tonometry and ocular sonography.

106/2012: IDWeek 2012, a joint meeting by IDSA, SHEA, HIVMA and PIDS in San Diego, CA., USA. Title: Intraocular Pressure as a Non-Invasive Predictor for Increased Intracranial Pressure in Persons with Suspected or Confirmed Cryptococcal Meningitis.

PATENTS

1) Provisional patent filed with the United States Patent and Trademark Office for 'Anti-fungal Griffithsin compositions and methods of use'. U.S. Provisional application no. 63/226,234. Inventors: **Henry Nabeta**, Joseph C. Kouokam and Kenneth E. Palmer

RESEARCH FUNDING

Completed Research Support

1) University of Louisville/ National Institutes of Health (NIH), Expediting Commercialization, Innovation, Translation, and Entrepreneurship (ExCITE) Award. Title: Developing Griffithsin, an HIV microbicide, as an antifungal agent. Amount $75,000. PI: **Henry Nabeta MBCh.B, MSc, MS**, 8/1/2019-2/28/2020.
2) Next Generation of Academics in Africa (NGAA) Carnegie Research grant. MSc Physiology thesis. Title: Serum vitamin D status of children admitted to a national referral hospital in Uganda. Amount $12,000. PI: **Henry Nabeta MBChB, MSc, MS,** 11/1/2010-12/31/2012.

PEER REVIEWER

1. Scientific Reports -Nature
2. Canadian Journal of Infectious Diseases and Microbiology
3. Journal of Clinical Neuroscience

MEDICAL PRACTISE LICENSURE

1. Uganda

PUBLICATIONS

Manuscripts in preparation

1. **Henry W. Nabeta**, Amanda B. Lasnik, Joshua L. Fuqua, Kenneth E. Palmer. Efficacy of lectin Griffithsin-M78Q in an *in vivo* model of vaginal candidiasis. Manuscript in preparation.

2. **Henry W. Nabeta**, Maryam Zahin, Joshua L. Fuqua, Elizabeth D. Cash, Shesh N. Rai, Gerald W. Dryden, Kevin L. Potts and Kenneth E. Palmer. **PREVENT-COV: A Phase 1a study design to assess the safety, acceptability, and pharmacokinetics of Q-Griffithsin Intranasal spray for broad-spectrum coronavirus pre-exposure prophylaxis.** Manuscript in preparation.

3. Daniel Tuse, Nobuyuki Matoba, J. Calvin Kouokam, Amanda B. Lasnik, Milena Mazalovska, Krystal T. Hamosky, **Henry W. Nabeta**, Lin Wang, Charlene Dezutti, Urvi Parikh, Rhonda Brand, Ross D. Cranston, Ian McGowan, Patricia Guenthner, Janet McNicholl, James Bakke, Hanna Ng, Lisa C. Rohan, David Garber, Joshua L. fuqua and Kenneth Palmer. **Preclinical Safety and Efficacy of the Plant-Produced Griffithsin Analog Q-GRFT Supports its Clinical Evaluation in HIV Microbicides.** Manuscript in preparation.

4. **Henry W. Nabeta** and Kenneth E. Palmer. **Lectins in immunity and response to mucosal infections**. Manuscript in preparation.

Articles Published in Peer-Reviewed Journals: (*Corresponding author)

1. **Henry W. Nabeta**, Joseph C. Kouokam, Amanda B. Lasnik, Joshua L Fuqua, Kenneth E. Palmer. **Novel Antifungal activity of Q-Griffithsin, a broad-spectrum antiviral lectin**. Spectrum. 2021 Sep 8;e0095721. doi:10.1128/Spectrum.00957-21.
2. Okafor EC, Hullsiek KH, Williams DA, Scriven JE, Rhein J, **Nabeta HW**, Musubire AK, Rajasingham R, Muzoora C, Schutz C, Meintjes G, Meya DB, Boulware DR. **Correlation between Blood and CSF Compartment Cytokines and Chemokines in Subjects with Cryptococcal Meningitis.** Mediators Inflamm. 2020 Oct 29;2020:8818044. doi: 10.1155/2020/8818044. PMID: 33177951; PMCID: PMC7644322.
3. Sebatta DE, Siu G, **Nabeta HW**, Anguzu G, Walimbwa S, Lamorde M, Bukenya B, Kambugu A**. "You would not be in a hurry to go back home": patients' willingness to participate in HIV/AIDS clinical trials at a clinical and research facility in Kampala, Uganda**. BMC Med Ethics. 2020 Aug 24;21(1):77. doi: 10.1186/s12910-020-00516-z. PMID: 32831090; PMCID: PMC7446203.
4. Pullen MF, Hullsiek KH, Rhein J, Musubire AK, Tugume L, Nuwagira E, Abassi M, Ssebambulidde K, Mpoza E, Kiggundu R, Akampurira A, **Nabeta HW**, Schutz C,

Evans EE, Rajasingham R, Skipper CP, Pastick KA, Williams DA, Morawski BM, Bangdiwala AS, Meintjes G, Muzoora C, Meya DB, Boulware DR. **https://www.ncbi.nlm.nih.gov/pubmed/31912875/ fungicidal activity as a surrogate endpoint for cryptococcal meningitis survival in clinical trials.** Clin Infect Dis. 2020 Jan 8;. doi: 10.1093/cid/ciaa016. [Epub ahead of print] PubMed PMID: 31912875.

5. John D. Strickley, Jonathan L. Messerschmidt, Mary E. Awad, Tiancheng Li, Tatsuya Hasegawa, Dat Thinh Ha, **Henry W. Nabeta,** Paul A. Bevins, Kenneth H. Ngo, Maryam M. Asgari, Rosalynn M. Nazarian, Victor A. Neel, Alfred Bennett Jenson, Joongho Joh & Shadmehr Demehri. **Immunity to commensal papillomaviruses protects against skin cancer.** volume 575, pages 519–522(2019).
6. Skipper CP, Schleiss MR, Bangdiwala AS, Hernandez-Alvarado N, Taseera K, **Nabeta HW**, Musubire AK, Lofgren SM, Wiesner DL, Rhein J, Rajasingham R, Schutz C, Meintjes G, Muzoora C, Meya DB, Boulware DR. **Cytomegalovirus Viremia Associated With Increased Mortality in Cryptococcal Meningitis in Sub-Saharan Africa.** Clin Infect Dis. 2019 Sep 1;. doi: 10.1093/cid/ciz864. [Epub ahead of print] PubMed PMID: 31504335.
7. Bahr NC, Halupnick R, Linder G, Kiggundu R, **Nabeta HW**, Williams DA, Musubire AK, Morawski BM, Sreevatsan S, Meya DB, Rhein J, Boulware DR. **Delta-like 1 protein, vitamin D binding protein and fetuin for detection of Mycobacterium tuberculosis meningitis.** Biomark Med. 2018 Jul;12(7):707-716. doi: 10.2217/bmm-2017-0373. Epub 2018 Jun 1.
8. Sarah Lofgren, Kathy H. Hullsiek, Bozena M. Morawski, **Henry W. Nabeta,** Reuben Kiggundu, Kabanda Taseera, Abdu Musubire, Charlotte Schutz, Mahsa Abassi, Nathan C. Bahr, Lillian Tugume, Conrad Muzoora, Darlisha A. Williams, Melissa A. Rolfes, Sruti S. Velamakanni, Radha Rajasingham, Graeme Meintjes, Joshua Rhein, David B. Meya, David R. Boulware, and on behalf of the COAT and ASTRO-CM Trial Teams. **Differences in Immunologic Factors Among Patients Presenting with Altered Mental Status During Cryptococcal Meningitis**. 2017 Mar 1;215(5):693-697. doi: 10.1093/infdis/jix033.
9. Reuben Kiggundu, **Henry W Nabeta**, Richard Okia, Joshua Rhein, Robert Lukande. **Unmasking histoplasmosis immune reconstitution inflammatory syndrome in a patient recently started on antiretroviral therapy.** Autopsy Case Rep [Internet]. 2016;6(4):27-33.
10. Rhein J, Bahr NC, Hemmert AC, Cloud JL, Bellamkonda S, Oswald C, Lo E, **Nabeta H**, Kiggundu R, Akampurira A, Musubire A, Williams DA, Meya DB, Boulware DR; ASTRO-CM Team. **Diagnostic performance of a multiplex PCR assay for meningitis in an HIV-infected population in Uganda**. Diagn Microbiol Infect Dis. 2016 Mar;84(3):268-73. doi: 10.1016/j.diagmicrobio.2015.11.017. Epub 2015 Dec 1. PMID: 26711635; PMCID: PMC4764472.
11. Rhein J, Morawski BM, Hullsiek KH, **Nabeta HW**, Kiggundu R, Tugume L, Musubire A, Akampurira A, Smith KD, Alhadab A, Williams DA, Abassi M, Bahr NC, Velamakanni SS, Fisher J, Nielsen K, Meya DB, Boulware DR; ASTRO-CM Study Team. **Efficacy of adjunctive sertraline for the treatment of HIV-associated cryptococcal meningitis: an open-label dose-ranging study**. Lancet Infect Dis. 2016 Jul;16(7):809-818. doi: 10.1016/S1473- 3099(16)00074-8. Epub 2016 Mar 10. PMID: 26971081.
12. Melissa A. Rolfes, Joshua Rhein, Charlotte Schutz, Kabanda Taseera, **Henry W. Nabeta,** Kathy Huppler Hullsiek, Andrew Akampuira, Radha Rajasingham, Abdu Musubire, Darlisha A. Williams, Friedrich Thienemann, Paul R. Bohjanen, Conrad Muzoora, Graeme Meintjes, David B. Meya, and David R. Boulware**. Cerebrospinal**

Fluid Culture Positivity and Clinical Outcomes After Amphotericin-Based Induction Therapy for Cryptococcal Meningitis. Open Forum Infect Dis. 2015; Accepted 2015 Oct 19. doi: 10.1093/ofid/ofv157. http://ofid.oxfordjournals.org/content/2/4/ofv157.full.

13. **Henry W. Nabeta***, Josephine Kasolo, Reuben K. Kiggundu, Agnes N. Kiragga, and Sarah Kiguli. **Serum vitamin D status in children with protein-energy malnutrition admitted to a national referral hospital in Uganda.** BMC Res Notes. 2015; 8: 418. Published online 2015 Sep 7. doi: 10.1186/s13104-015-1395-2. http://link.springer.com/article/10.1186/s13104-015-1395-2
14. Kiggundu, Reuben, Morawski, Bozena , Bahr, Nathan C, Rhein, Joshua, Musubire, Abdu K, Williams, Darlisha A, Abassi, Mahsa, **Nabeta, Henry W**, Hullsiek, Kathy Huppler, Meya, David B ,Boulware, David R. **Effects of tenofovir and amphotericin B deoxycholate co-administration on kidney function in patients treated for cryptococcal meningitis.** JAIDS Journal of Acquired Immune Deficiency Syndromes. Accepted August 22, 2015. doi: 10.1097/QAI.0000000000000812. http://journals.lww.com/jaids/Abstract/publishahead/Effects_of_tenofovir_and_amphotericin_B.97442.aspx.
15. Nathan Bahr, MD, Grace Linder, Ryan Halupnick, Reuben Kiggundu, MBChB, Henry Nabeta, MBChB, Darlisha Williams, MPH, David Meya, MMed, Joshua Rhein, MD, and David Boulware, MD, MPH. **Delta-like 1 ligand (DLL) measurement in cerebrospinal fluid for detection of *Mycobacterium tuberculosis* meningitis.** Open Forum Infect Dis. 2014 Dec; 1(Suppl 1): S455-S456. Published online 2014 Dec. doi: 10.1093/ofid/ofu052.1249.
16. Rajasingham R, Rhein J, Klammer K, Musubire A, **Nabeta H**, Akampurira A, Mossel EC, Williams DA, Boxrud DJ, Crabtree MB, Miller BR, Rolfes MA, Tengsupakul S, Andama AO, Meya DB, Boulware DR. **Epidemiology of meningitis in an HIV-infected Ugandan cohort.** Am J Trop Med Hyg. 2015 Feb;92(2):274-9. doi: 10.4269/ajtmh.14-0452. Epub 2014 Nov 10. http://www.ncbi.nlm.nih.gov/pubmed/25385864.
17. **Henry W. Nabeta,** Nathan C. Bahr, Joshua Rhein, Nicholas Fossland, Agnes N. Kiragga, David B. Meya, Stephen J. Dunlop, and David R. Boulware. **Accuracy of Noninvasive Intraocular Pressure or Optic Nerve Sheath Diameter Measurements for Predicting Elevated Intracranial Pressure in Cryptococcal Meningitis.** Open Forum Infect Dis. 2014 Dec; 1(3): ofu093. Published online 2014 Oct 11. doi: 10.1093/ofid/ofu093. http://www.ncbi.nlm.nih.gov/pmc/articles/PMC4324219/.
18. J. Dyal, A. Akampurira, E. Butler, R. Kiggundu, **H. Nabeta**, A. Musubire, J. Rhein, D. Meya, D. Boulware. **Reproducibility of CSF quantitative culture methods for *Cryptococcus neoformans.*** International Journal of Infectious Diseases. DOI: http://dx.doi.org/10.1016/j.ijid.2014.03.1013.
19. Nathan C. Bahr; Melissa A. Rolfes; Abdu Musubire; **Henry Nabeta**; Darlisha Williams; Joshua Rhein; Andrew Kambugu; David B. Meya; David R. Boulware. **Standardized electrolyte supplementation and fluid management improves survival during amphotericin therapy for Cryptococcal meningitis in resource-limited settings.** *Open Forum Infectious Diseases 2014; doi: 10.1093/ofid/ofu070.*
20. Sruti S Velamakanni, Nathan C Bahr, Abdu K Musubire, David R Boulware, Joshua Rhein, **Henry W Nabeta**. **Central nervous system cryptococcoma in a Ugandan patient with Human immunodeficiency virus.** *Medical Mycology Case Reports*. http://dx.doi.org/10.1016/j.mmcr.2014.08.003.

21. Melissa A Rolfes, Kathy Huppler Hullsiek, Joshua Rhein, **Henry W Nabeta**, Kabanda Taseera, Charlotte Schutz, Musubire Abdu, Radha Rajasingham, Darlisha Williams, Friedrich Thienemann, Conrad Muzoora, Graeme Meintjes, David B Meya, David R Boulware**. The Effect of Therapeutic Lumbar Punctures on Acute Mortality from Cryptococcal Meningitis.** *Clin Infect Dis. (2014) doi: 10.1093/cid/ciu596.* http://cid.oxfordjournals.org/content/early/2014/07/23/cid.ciu596.
22. David R Boulware, David B Meya, Conrad Muzoora, Melissa A Rolfes, Kathy Huppler Hullsiek, Abdu Musubire, KabandaTaseera, **Henry W Nabeta**, Charlotte Schutz, Darlisha A Williams, Radha Rajasingham, Joshua Rhein, Friedrich Thienemann, Melanie W Lo, Kirsten Nielsen, Tracy L Bergemann, Andrew Kambugu, Yukari C Manabe, Edward N Janoff, Paul R Bohjanen, Graeme Meintjes, and the COAT Trial Team. **Timing of Antiretroviral Therapy after Diagnosis of Cryptococcal Meningitis**. *N Engl J Med2014; 370:2487-2498.*

List of Published Work in My Bibliography:
https://www.ncbi.nlm.nih.gov/myncbi/1HSPdwzo5j7AYT/bibliography/public/